

Polygenic risk score for persistent back pain

Frances MK Williams¹, Maxim B Freidin¹, Yakov A Tsepilov^{2,3}, Yurii S Aulchenko^{2,3}, Pradeep Suri^{4,5}

1. Department of Twin Research and Genetic Epidemiology, King's College London, London, United Kingdom

2. Institute of Cytology and Genetics, Novosibirsk, Russian Federation

3. PolyOmica, s'-Hertogenbosch, The Netherlands

4. Department of Rehabilitation Medicine, University of Washington, Seattle, Washington, USA

5. Division of Rehabilitation Care Services, VA Puget Sound Health Care System, Seattle, Washington, USA

Introduction

Persistent back pain (BP) is a common debilitating condition leading the list of disorders causing disability in much of the world. It leads to work absenteeism, job loss and long-term disability. In Europe, the costs of BP are estimated to amount to 1%-2% of GDP. Predicting the development of persistent BP may contribute to reducing its burden on society and healthcare by offering stratified clinical management early in the condition. The use of polygenic risk scores (PRS) is a promising approach to stratifying individuals into risk groups based on their genetic make-up across the whole genome. BP is heritable (30%-60%), therefore the use of PRS for this disorder may be fruitful as has been demonstrated in other common complex traits. In the current study we explored the utility of PRS for BP using UK Biobank and TwinsUK data.

Methods

We used summary statistics from our published UK Biobank genome-wide association study for BP in North Europeans (n = 450,000) to calculate a weighted PRS across multiple p-value thresholds. The PRS were tested for association with disabling and non-disabling BP in TwinsUK data (n = 1,812 and 4,135, respectively). We used the coefficient of determination (R^2) to select PRS with the highest predictive capacity and then calculated prevalence of BP phenotypes in various percentiles of the PRS. Based on the results we selected percentile thresholds to stratify individuals into high, medium and low risk groups followed by a comparison of prevalence of BP in high and low risk groups versus medium risk.

Results

The PRS with the highest R^2 ($R^2 = 0.01$) comprised 7,269 genetic variants with p-value < 1e-3 for association with BP in UK Biobank. We established that individuals with PRS below 20% and above 80% of the PRS distribution exhibit lower and higher prevalence of BP, respectively, compared to mean in TwinsUK. For both disabling and non-disabling BP there were statistically significant lower or higher odds of BP in respective percentile groups compared to medium risk group (Table).

Discussion

To the best of our knowledge, this is the first report considering PRS as a potential tool to predict the risk of BP. The results of the study suggest predictive capacity of PRS and warrant further research using a combination of PRS and available clinical tools, such as the STarT Back clinical tool which helps to match primary care patients to the most suitable treatment.

Acknowledgement

The use of UK Biobank data was approved under the project #18219.

Table – Odds ratios for disabling and non-disabling back pain for individuals with PRS-based low and high risks compared to medium risk in TwinsUK

Risk group	Percentiles of PRS to stratify individuals		
	0.2 vs 0.8	0.1 vs 0.9	0.05 vs 0.95
Disabling LBP			
Low	0.84 (0.64-1.09)	0.68 (0.47-0.98)	0.71 (0.41-1.18)
High	1.41 (1.10-1.82)	1.46 (1.04-2.04)	1.50 (0.91-2.43)
Non-disabling LBP			
Low	0.90 (0.75-1.08)	0.74 (0.57-0.94)	0.69 (0.48-0.97)
High	1.33 (1.11-1.57)	1.24 (0.99-1.56)	1.23 (0.89-1.67)

1. Freidin MB, et al. Insight into the genetic architecture of back pain and its risk factors from a study of 509,000 individuals. *Pain*. 2019 Jun;160(6):1361-1373. doi: 10.1097/j.pain.0000000000001514.

Intradiscal injection of platelet-rich plasma releasate for discogenic low back pain patients: a double-blind, randomized active-controlled trial

Koji Akeda¹, Norihiko Takegami¹, Takao Sudo¹, Junichi Yamada¹, Tatsuhiko Fujiwara¹, Akihiro Sudo¹

1. Orthopaedic Surgery, Mie University Graduate School of Medicine, Tsu, Mie, Japan

INTRODUCTION: Platelet-rich plasma (PRP) is an autologous blood concentrate containing a vast majority of bioactive proteins. PRP has been used for treatment of musculoskeletal pathologies, including muscle and tendon injuries and osteoarthritis. Recently, clinical application of PRP is also gaining popularity in treating degenerative disc disease. This study evaluated the efficacy and safety of PRP-releasate (PRPr) injection into degenerated discs of patients with discogenic low back pain (LBP).

METHODS: A randomized, double-blind, active-controlled clinical trial was conducted. Patients aged > 18 years who had LBP for more than three months with one or more lumbar discs (L3/L4 to L5/S1) with evidence of degeneration, as indicated by magnetic resonance imaging (MRI), and at least one symptomatic disc, confirmed using standardized provocative discography, were considered for inclusion. Sixteen patients (mean age: 32.2 ± 8.3 years old, 11 men, 5 women) with discogenic LBP were randomly assigned to receive an intradiscal injection of either autologous PRPr or corticosteroid (CS) (betamethasone sodium phosphate). Patients in both groups who wished to have PRPr treatment received an optional injection of PRPr eight weeks later. The primary outcome was change in visual analogue scale (VAS) from baseline at eight weeks post-injection. Secondary outcomes were pain, disability, quality of life (QOL), radiographic disc height, magnetic resonance imaging (MRI) grading of disc degeneration, the success rate of the treatment, and safety for up to 60 weeks.

RESULTS: VAS scores of both PRPr and CS groups decreased significantly over the observation period ($P < 0.01$) (Fig. 1). VAS change at eight weeks did not significantly differ between PRPr (-30.9 mm) and CS (-26.3 mm) groups ($P = 0.6$). Fifteen patients received the optional injection. Compared to the CS group, the PRPr group (PRPr double injection) had significantly improved disability score at 26 weeks (PRPr: -88.0%, CS: -42.1%, $P < 0.05$), and walking ability scores at four and eight weeks ($P < 0.05$, respectively). The mean change in radiographic disc height of the PRPr group tended to be higher than that of the CS group throughout, and a statistical significance was identified at week 60 ($P < 0.05$). MRI grading score was unchanged from baseline. PRPr caused no clinically important adverse events, except for injection pain.

DISCUSSION: The intradiscal injection of PRPr showed clinically significant improvements in LBP intensity in patients with discogenic LBP, like those injected with glucocorticoid at eight weeks post-injection. PRPr treatment was safe and maintained improvements in pain, disability, and QOL for 60 weeks follow-up.

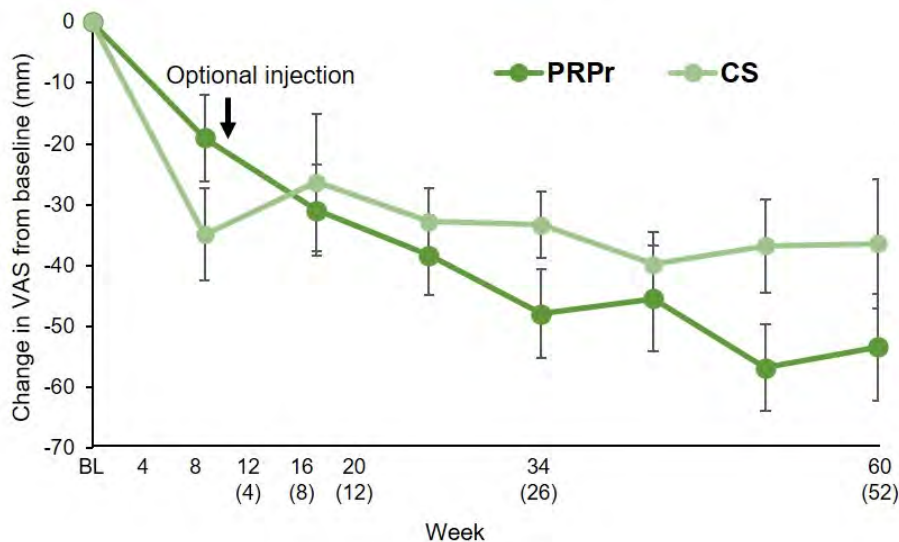


Fig. 1 Change in visual analogue scale (VAS). VAS was evaluated for 60 weeks after the injection of the releasate isolated from activated platelet-rich plasma (PRPr) or corticosteroid (CS).

Characteristics of sagittal spinopelvic alignment changes after symptom relief following simple lumbar decompression

Chang Hwa Ham¹, Dong Wook Kim¹, Woo-Keun Kwon¹, Joohan Kim¹, Youn-Kwan Park¹, Hong Joo Moon¹

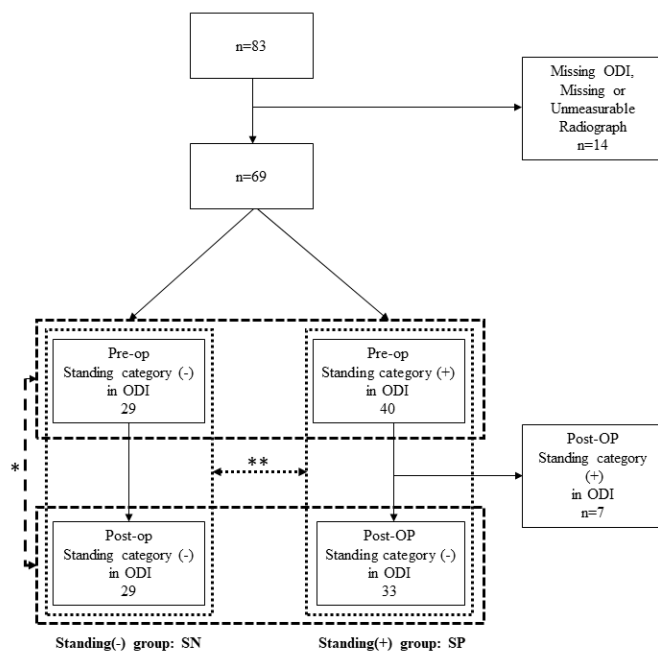
1. Korea University Guro Hospital, Seoul, SEOUL, Korea, Republic of

Introduction Sagittal spinopelvic alignment (SSPA) parameters are essential for the diagnosis of adult spinal deformities and their progression. Certain clinical symptoms that occur in patients with lumbar spinal stenosis (LSS) and herniated nucleus pulposus (HNP) may distort one's SSPA and mimic adult spinal deformities. Inaccurate measurements of SSPA may lead to unnecessary realignment surgeries, which is an enormous burden to both physicians and patients. In this study, we aimed to differentiate SSPA in symptomatic patients to those without symptoms in the standing position.

Methods This retrospective cohort study evaluated the changes in SSPA following simple lumbar decompression surgery in patients with LSS and HNP. Relative sagittal alignment (RSA), relative pelvic version, relative lumbar lordosis (RLL), lordosis distribution index (LDI), and global alignment and proportion (GAP) scores were calculated using the conventional Schwab classification method. First, the pre- and postoperative SSPA parameters were compared. Second, patients were sub-grouped into symptomatic (SP) and asymptomatic (SN) groups on standing position. Patients with pain that is evoked by standing for longer than 10 minutes were defined as symptomatic, which corresponds to 4 points or more on the ODI subcategory - 'standing'. SSPA parameter changes after symptom relief in SP group following simple lumbar decompression surgery were compared to those of SN group.

Results Sixty-three patients who underwent simple lumbar decompression between April 2019 and June 2021 were included in this study. Thirty-three and 29 patients were grouped into the SP and SN group, respectively. The mean age, BMI, male-to-female ratio, and diagnosis of lumbar pathology were not significantly different between the two groups ($p=.68$, $p=.82$, $p=.076$, and $p=.80$, respectively). In total, patients with lumbar pathology showed improvements in all SSPA parameters following surgery (RSA, RLL, and LDI values improved with $p=.002$, $p<.001$, and $p=.002$, respectively). However, after subgrouping, asymptomatic patients in the standing position did not show significant SSPA alterations except for LDI ($p=.035$), whereas symptomatic patients significantly improved in terms of their RSA, RLL, LDI, and GAP values ($p=.001$, $p<.001$, $p=0.032$, and $p=0.05$, respectively) following symptom relief from the surgery.

Discussion Our study demonstrated that patients with pain on standing within 10 minutes showed significant correction in RSA, RLL, and GAP values following simple lumbar decompression, whereas patients without pain on standing did not. Furthermore, SN group, scoring 3 or less on the ODI subcategory 'standing', scored higher VAS - leg and back - and total ODI compared to SP group. Therefore, misleading measurements of SSPA is more likely caused by the pain on standing position and not by other symptoms relating to LSS and HNP. Previous studies have reported that SSPA improvements were observed in LSS patients who have undergone simple lumbar decompression surgeries. Most presumed buckling of ligamentum flavum impinging on spinal nerves caused distortion of SSPA, as flexion of lumbar spine may release the impingement. However, these studies provided limited evidence on improvements of SSPA and showed various patterns of improvements. Based on our study, it is important to focus on clinical symptoms rather than disease entity itself.



The influence of psychosocial factors on chronic back pain: a bidirectional Mendelian randomisation study

Frances MK Williams¹, Elizaveta E Elgaeva², Maxim B Freidin¹, Olga O Zaytseva³, Yurii S Aulchenko⁴, Tsepilov A Yakov², Pradeep Suri⁵

1. King's College London, London, United Kingdom

2. Department of Natural Sciences, Novosibirsk State University, Novosibirsk, Russia

3. Genos Glycoscience Research Laboratory, Genos, Zagreb, Croatia

4. PolyOmica, 5237 PA 's-Hertogenbosch, The Netherlands

5. Division of Rehabilitation Care Services, VA Puget Sound Health Care System, Seattle, Washington, USA

INTRODUCTION

Risk factors for chronic back pain (CBP) include not only intervertebral disc degeneration but also psychological make-up and social influences (1). Our previous work suggested that such risk factors share genetic influence with CBP (2). Shared underlying genetic influence makes risk factors difficult to study using conventional epidemiological methods. New methods which use genetic factors as instruments or surrogate measures can overcome these difficulties to some extent. Using large, publicly available datasets we conducted a bi-directional Mendelian randomisation (MR) study to examine the causal effects of educational years, smoking, alcohol consumption, physical activity, sleep and depression on CBP and the causal effect of CBP on these same risk factors.

METHODS

Genetic instruments for risk factors and CBP were obtained from the largest published genome-wide association studies (GWAS) of risk factor traits conducted in individuals of European ancestry. To strengthen the confidence in our findings we used a combination of methods. We used inverse weighted variance meta-analysis (IVW), Causal Analysis Using Summary Effect (CAUSE) and sensitivity analyses to examine evidence for causal associations. We interpreted exposure-outcome associations as being consistent with a causal relationship if results with IVW or CAUSE were statistically significant after accounting for multiple statistical testing ($p < 0.003$), and if the direction and magnitude of effect estimates were concordant between IVW, CAUSE, and sensitivity analyses.

RESULTS

We found evidence for statistically significant causal associations between years of schooling (OR per 4.2 years = 0.54), ever smoking (OR = 1.27), greater alcohol consumption (OR = 1.29 per consumption category increase) and major depressive disorder (OR = 1.41) and the risk of CBP. Conversely, we found evidence for significant causal associations between CBP and greater alcohol consumption (OR = 1.19) and between CBP and smoking (OR = 1.21). Other relationships did not meet our pre-defined criteria for causal association.

CONCLUSION

Our work revealed that fewer years of schooling, smoking, greater alcohol consumption and major depressive disorder all increase the risk of CBP. Examination of the reverse direction showed that, unsurprisingly, CBP increases the risk of greater alcohol consumption and smoking. Our findings are robust to confounding because genetic instruments reduce this epidemiological limitation. This work suggests that public health measures childhood and early adulthood and the recognition and prompt treatment of depression may reduce the population burden of CBP. Randomised controlled clinical trials based on population samples should be explored.

REFERENCES

1. A. J. MacGregor, T. Andrew, P. N. Sambrook and T. D. Spector Structural, psychological, and genetic influences on low back and neck pain: a study of adult female twins. *Arthritis Rheum* 2004 Vol. 51 Issue 2 Pages 160-7
2. M. B. Freidin *et al.*, "Insight into the genetic architecture of back pain and its risk factors from a study of 509,000 individuals," *Pain*, vol. 160, no. 6, pp. 1361-1373

Terminal complement complex formation in C6-deficient and CD59-knockout mice during disc aging and degeneration

Cornelia Neidlinger-Wilke¹, Graciosa Q Teixeira¹, Yana Höpfner¹, Julian Ostertag¹, Jana Riegger², Anita Ignatius¹, Rolf Brenner²

1. Institute of Orthopaedic Research and Biomechanics, Ulm University, Ulm, Germany

2. Division for Biochemistry of Joint and Connective Tissue Diseases, Department of Orthopedics, Ulm University, Ulm, Germany

INTRODUCTION: In the intervertebral disc (IVD), several mechanisms are involved in higher proteolytic activity and activation of the immune system during degeneration. With the increase of the degree of disc degeneration, deposition of the terminal complement complex (TCC), an innate immune response activation product that contributes to cell lysis and inflammation, has been shown to be increased in human IVD tissues.¹ The present work focuses on understanding whether i) TCC deposition is involved in disc degeneration and ii) if mice deficient for C6 (a TCC component; C6-def group) and with deletion of CD59 (a TCC direct inhibitor; CD59-ko group) are suitable models for mechanistic investigations.

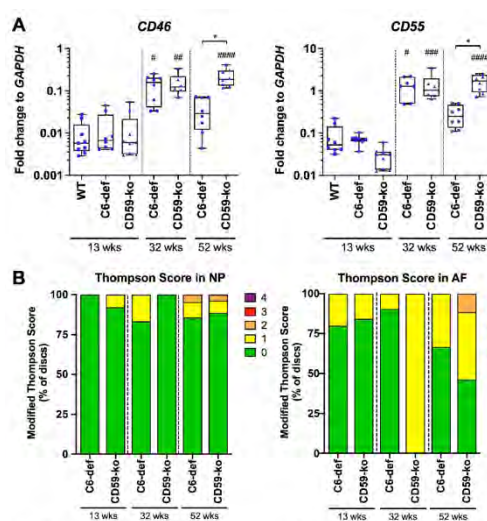


Figure 1. (A) Gene expression analysis of mouse IVD cells isolated from tail IVDs of 13-, 32- and 52-weeks old wild type (WT), C6-deficient (C6-def) and CD59-knockout (CD59-ko) mice. Relative mRNA expression of complement regulation molecules (*CD46* and *CD55*). Results were normalized to mRNA levels of glyceraldehyde 3-phosphate dehydrogenase (*GAPDH*). (B) Thompson Score in nucleus pulposus (NP) and annulus fibrosus (AF). n = 6–9, *p < 0.05, **p < 0.01, ***p < 0.001, ****p < 0.0001 (significant differences to 13 weeks old animals with the same deficiency); *p < 0.05 (significant differences between animals with the same age). Kruskal-Wallis test.

METHODS: IVDs were collected from lumbar spines and tails from male C6-def and CD59-ko mice and compared to wild type (WT) animals (n=6–9 mice/group), with ethical approval. Tail IVDs from 13-, 32- and 52-weeks old WT, C6-def and CD59-ko mice were directly prepared for gene expression analysis of TCC inhibitors *CD46* and *CD55*, as well as cell metabolism (*Bcl2*, *c-Fos*), inflammation (*IL6*), ECM composition (*COL1A1*, *COL2A1*) and matrix degradation (*MMP3*) markers. The lumbar spines were processed for safranin O/fast green histological staining and Thompson Score determination.² Moreover, lumbar spines from 13-weeks old WT, C6-def and CD59-ko mice were kept in organ culture for 8 days, and stimulated with 5% normal mouse serum (containing all the necessary components for TCC formation – C5, C6, C7, C8 and C9) and interleukin-1 β (IL-1 β) or cathepsin-D (CTSD).³ The described IVD evaluations were also performed after organ culture. Results were compared to unstimulated controls. Statistical analysis was performed with Kruskal-Wallis test.

RESULTS: IVD tissues from 52-weeks old CD59-def mice presented upregulated expression of *CD46*, *CD55* (Figure 1A), *Bcl2*, *c-Fos*, *IL6* and *MMP3* in comparison to 13-weeks old CD59-ko and to 52-weeks old C6-def mice (p<0.05), as well as slightly higher Thompson Score in the annulus fibrosus region, but not in the nucleus pulposus (Figure 1B). The organ culture data showed upregulation of *IL6* and *MMP3* by IVD cells from IL-1 β -treated spines of both C6-def and CD59-ko mice (p<0.05), whereas *Col1A1* and *COL2A1* were upregulated after CTSD treatment of C6-def mouse spines (p<0.05), but not affected in the CD59-ko samples. *CD45* and *CD55* gene expression was not altered.

DISCUSSION: Overall, IVDs from C6-def mice seem to present a different phenotype from CD59-ko mice, indicating a slightly accelerated IVD degeneration in CD59-ko compared to C6-def rodents with ageing, which is in agreement with previous results observed in osteoarthritic mice⁴. The findings also support our hypothesis that C6 deficiency may reduce the inflammatory response and thus protect the tissue from degeneration, while a CD59 knockout (leading to reduced inhibition of TCC formation) may contribute to accelerated disc degeneration. Therefore, TCC modulation may offer possible new therapeutic options to target IVD degeneration. **Acknowledgement:** ISSLS Research Grant 2020.

1. Teixeira, G.Q., et al. Terminal complement complex formation is associated with intervertebral disc degeneration. *Eur Spine J* 30, 217–226 (2021).
2. Choi, H., et al. A novel mouse model of intervertebral disc degeneration shows altered cell fate and matrix homeostasis. *Matrix Biol* 70, 102–122 (2018).
3. Teixeira, G.Q., et al. Interleukin-1 β and cathepsin D modulate formation of the terminal complement complex in cultured human disc tissue. *Eur Spine J* 30, 2247–2256 (2021).
4. Wang, Q., et al. Identification of a central role for complement in osteoarthritis. *Nat Med* 17, 1674–1679 (2011).

Irisin stimulates anabolism and matrix synthesis in human nucleopulpyocytes in vitro: new insights into a cross-talk between the muscle and the intervertebral disc.

Gianluca Vadalà¹, Luca Ambrosio¹, Giuseppina Di Giacomo¹, Claudia Cicione¹, Veronica Tilotta¹, Fabrizio Russo¹, Rocco Papalia¹, Vincenzo Denaro¹

1. Department of Orthopaedic and Trauma Surgery, Campus Bio-Medico University of Rome, Rome, N/A, Italy

INTRODUCTION

Physical activity favors weight loss and ameliorates pain and function in patients suffering from discogenic low back pain (LBP). Although there is currently no biologic evidence that the intervertebral disc (IVD) can respond to physical exercise in humans, a recent study has shown that chronic running exercise is associated with increased IVD hydration and hypertrophy¹. Irisin, a myokine released upon muscle contraction, has demonstrated to yield anabolic effects on different cell types, including chondrocytes². This study aimed to investigate the effect of irisin on human nucleopulpyocytes (hNPCs) in vitro. Our hypothesis was that irisin would improve hNPC metabolism and proliferation.

METHODS

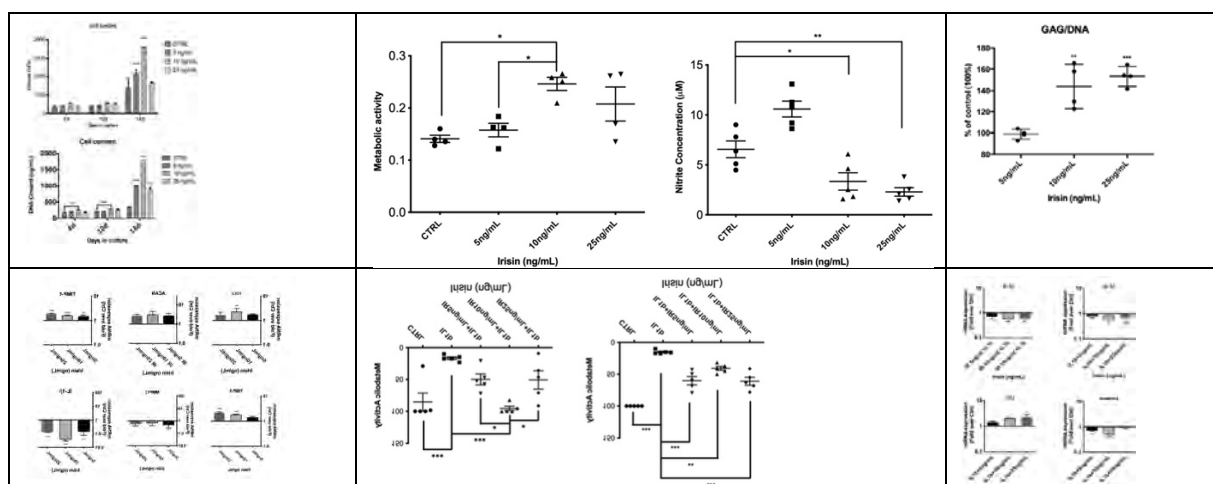
hNPCs were isolated from IVD samples obtained during spine surgery and cultured in alginate beads. hNPCs were then exposed to either phosphate-buffered saline (PBS) or human recombinant irisin (r-irisin) for 7 days at a concentration of 5, 10 and 25 ng/mL (n = 4). Each experiment was performed in triplicate. Cell proliferation was assessed with trypan blue staining-automated cell counting and PicoGreen assay at 4, 10 and 14 days of culture. Glycosaminoglycan (GAG) content was measured using the dimethylmethylene blue (DMMB) assay and normalized to the DNA ratio at 7 days of culture. Metabolic activity was assessed with the MTT assay and the Griess Reagent System at 4 days of culture. Gene expression of collagen type II (COL2), matrix metalloproteinase (MMP)-13, tissue inhibitor of matrix metalloproteinase (TIMP)-1 and -3, aggrecan, interleukin (IL)-1 β , a disintegrin and metalloproteinase with thrombospondin motifs (ADAMTS)-5 was measured by real time-polymerase chain reaction (RT-PCR) at 7 days of culture. In addition, MTT assay and ADAMTS-5, COL2, TIMP-1 and IL-1 β gene expression were evaluated following incubation with 5, 10 and 25 ng/mL r-irisin for 24 hours and subsequent culture with 10 ng/ml IL-1 β for 7 days and vice versa (incubation for 24 hours with IL-1 β and subsequent culture with r-irisin for 7 days).

RESULTS

Irisin increased hNPCs proliferation (Fig. 1, $p < 0.001$), metabolic activity (Fig. 2, $p < 0.05$), and GAG content (Fig. 3, $p < 0.01$), as well as COL2 ($p < 0.01$), ACAN ($p < 0.05$), TIMP-1 and -3 ($p < 0.01$) gene expression, while decreasing mRNA levels of MMP-13 ($p < 0.05$) and IL-1 β (Fig. 4, $p < 0.001$). r-irisin pretreatment of hNPCs cultured in pro-inflammatory conditions resulted in a rescue of metabolic activity (Fig. 5, $p < 0.001$), as well as a decrease of IL-1 β (Fig. 6, $p < 0.05$) levels. Similarly, incubation of hNPCs with IL-1 β and subsequent exposure to r-irisin led to an increment of hNPC metabolic activity ($p < 0.001$), COL2 gene expression ($p < 0.05$) and a reduction of IL-1 β ($p < 0.05$) and ADAMTS-5 levels (Fig. 6, $p < 0.01$).

DISCUSSION

The present study suggested that irisin may stimulate hNPC proliferation, metabolic activity, and anabolism by reducing the expression of IL-1 β and catabolic enzymes while promoting the synthesis of extracellular matrix components. Furthermore, such myokine was able to blunt the catabolic effect of in vitro inflammation. Our results indicate that irisin may be one of the mediators by which physical exercise and muscle tissues modulate IVD metabolism, thus suggesting the existence of a biological cross-talk mechanism between the muscle and the IVD.



1. Belavý DL, Quittner MJ, Ridgers N, Ling Y, Connell D, Rantalainen T. Running exercise strengthens the intervertebral disc. *Sci Rep.* 2017 Apr 19;7:45975. doi: 10.1038/srep45975.
2. Vadalà G, Di Giacomo G, Ambrosio L, Cannata F, Cicione C, Papalia R, Denaro V. Irisin Recovers Osteoarthritic Chondrocytes In Vitro. *Cells.* 2020 Jun 17;9(6):1478. doi: 10.3390/cells9061478.

Cell survival in the nucleus pulposus center is affected by loading

Elias Salzer¹, Vivian H.M. Mouser¹, Jurgen A. Bulsink¹, Marianna A. Tryfonidou², Keita Ito¹

1. Biomedical Engineering, Eindhoven University of Technology, Eindhoven, Netherlands

2. Veterinary Medicine, Utrecht University, Utrecht, Netherlands

INTRODUCTION: In the nucleus pulposus (NP) core, [glucose] is low, and, as anaerobic glycolysis leads to lactate production, the pH is low¹. It has been hypothesized that cells may be metabolically more active when they are loaded but it has not been determined if these changes in metabolism can affect cell survival by interacting with the nutrient/metabolite homeostasis (**Figure 1**).

METHODS: Bovine NP explants were cultured in a previously developed volume controllable chamber², which can be dynamically loaded in a novel axial compression bioreactor. Explants were cultured for 7 days in degenerative medium (DM, 1 mM glucose, pH 6.8) or healthy medium (HM, 3 mM glucose, pH 7.1) with either non dynamic loading (NDL) or simulated physiological loading (SPL) and compared to native tissue (n=6 for all groups). To determine changes of the extracellular matrix, the sulphated glycosaminoglycan-, hydroxyproline-, and water-content were measured, and the tissue was stained with Alcian blue. Glucose and lactate were measured in the medium supernatants and tissue. A lactate dehydrogenase staining was performed to determine the viable-cell density (VCD).

RESULTS: The histological appearance as well as tissue composition of NP explants did not change in any of the groups. There was no gradient formation of glucose or lactate in the tissue. Glucose levels in the tissue reached critical values for cell survival ($\leq 0.5 \text{ mM}^1$) in all groups. Generally, lactate in the medium was increased in the SPL compared to the NDL groups (**Figure 2**). The VCD in the periphery of the NPs was not reduced in any of the groups. However, the VCD in the central region of the NP was reduced in the SPL groups ($p \leq 0.01$, **Figure 3**), which led to a significant gradient formation of VCD in these groups ($p \leq 0.05$). Within the HM or DM groups, there were no differences in tissue lactate concentration, however, the concentration was significantly increased in the HM compared to the DM groups ($p \leq 0.001$).

DISCUSSION: Physiological loading is believed to be essential for homeostasis of the IVD³. Here, we demonstrated that such loading can affect cell metabolism so much so that it was associated with changes in cell viability leading to a new equilibrium in the tissue, in both DM and HM. Urban et al. (2004) described that an interplay between pH and glucose orchestrates cellular survival and that cellular survival between 0 to 0.5 mM glucose is pH-dependent^{1,4}. We hypothesize, that the formation of a VCD gradient was caused by critically low glucose levels in combination with increased lactate production, decreasing the pH locally. This might have created a temporal gradient of low nutrition and high pH in the central region, in which cell survival was no longer possible. However, at the timepoint of harvest, there was no gradient in lactate and glucose tissue levels, which we believe arose from fast equilibration once a new cell density was reached. Concluding, physiological levels of loading lead to metabolically more active cells, which is relevant for disc degeneration and regeneration.

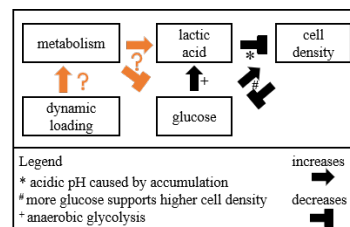


Figure 1: Cell nutrition equilibrium loop in the NP.

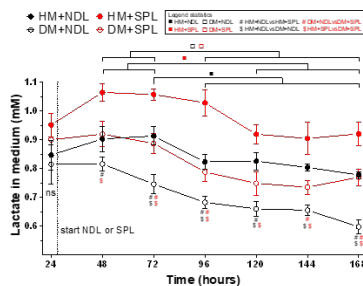


Figure 2: Lactate in medium is increased in SPL conditions.

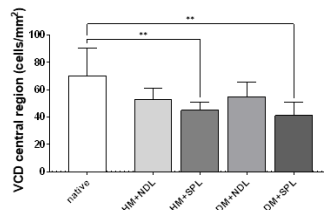


Figure 3: VCD in the NP center is reduced in SPL conditions.

ACKNOWLEDGEMENTS: EU Horizon 2020 (#825925, www.ipspine.eu).

1. Urban JPG et al., Spine, 2004
2. Salzer E et al., J. Orthop. Res., In Revision
3. Chan SCW et al., Eur. Spine J., 2011
4. Bibby SRS et al., Eur. Spine J., 2004

Does general exercise improve paraspinal myopathy, disc health and spinal alignment in sarcopenic TSC1mKO mice?

Wenhai Zhuo¹, Wing Moon Raymond Lam¹, Wenhai Zhuo¹, Xiaoyun Chloe Chan², Way Cherng Chen³, Simon Cool⁴, Elisa Marie Crombie⁵, Shih-Yin Tsai⁵, Hwee Weng Dennis Hey^{1,2}

1. Department of Orthopaedic Surgery, YLL School of Medicine, National University of Singapore, Singapore

2. Department of Orthopaedic Surgery, National University Health System, Singapore

3. Bruker Centre, SBIC, A*Star, Singapore

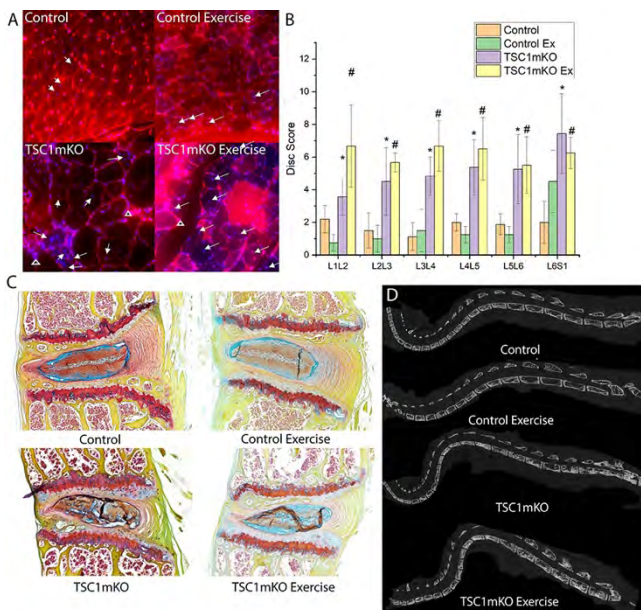
4. Institute of Molecular and Cell Biology, Agency for Science, Technology and Research, Singapore

5. Department of Physiology, YLL School of Medicine, National University of Singapore, Singapore

INTRODUCTION: TSC1mKO mice have muscle-specific knockout of the TSC1 inhibitor that leads to paraspinal myopathy-induced kyphosis and disc degeneration which is useful in the study of sarcopenia and the aging spine. Exercise has been commonly used for sarcopenia treatment, but its impact on spinal degeneration remains unclear. In this study, we examine general treadmill exercise on paraspinal muscle myopathy, intervertebral disc degeneration and kyphosis in female TSC1mKO mice.

METHODS: Twenty-five female mice were used for this study (TSC1mKO: n = 7, control: n = 7, TSC1mKO exercise (TSC1mKOEx): n=4, control exercise (ControlEx) n=7). Cobb angle, disc height was measured using high resolution microCT at 12 months. Exercise group mice were treated by uphill treadmill exercise 5 days/week between 8 and 12 months (2 stints of a 3-week exercise). At the end of treatment, time to exhaustion was measured. Myopathic changes in the paraspinal muscle were examined via Wheat Germ Agglutinin (WGA)/DAPI stain, and IVD was evaluated via FAST stain.

RESULTS: Similar to our previous study[1], TSC1mKO mice developed 1) accelerated myopathy representative of sarcopenia with histological sections showing presence of central nuclei and triangular fibres, 2) larger thoracolumbar kyphosis, and 3) faster intervertebral disc degeneration in terms of disc height loss and higher FAST staining disc scores at L3/4, L4/5 compared to controls.



White Arrow: Central Nucleus. White Triangle, Degenerated Triangular Fiber
* TSC1mKO mice vs Control p<0.05, # TSC1mKO Exercise vs Control p<0.05

After uphill treadmill exercise regime, the endurance performance of TSC1mKO exercise mice reached a level comparable to control sedentary mice level (>1000s) while TSC1mKO mice had reduced endurance of 750s. Exercise reduced the proportion of triangular degenerated fiber (TSC1mKOEx 2.9±0.1% vs TSC1mKO 6.3±4.8%, p= 0.07) in TSC1mKO mice. (Figure 1A)

In terms of disc health, exercise improved disc heights of control mice at L4/5 (ControlEx 294 ±33µm vs Control 247 ± 59µm, p=0.03) but not in TSC1mKO mice (TSC1mKOEx 164±42µm vs TSC1mKO 164 ±27µm, p=0.49), as well as the disc scores of control mice at L4/5 (ControlEx 1.25 ±0.50 vs control 2.0 ±0.53, p=0.025) but not in TSC1mKO mice (TSC1mKO 5.38 ±1.69 vs TSC1mKOEx 6.50±1.91, p= 0.18) (Figure 1B). Interestingly, exercise increased disc matrix/disc tissue area at L4/5 in TSC1mKO mice (TSC1mKOEx 59.4±17.3% vs TSC1mKO 37.4±13.1%, p=0.04) but not in control mice (ControlEx 61.9±19.3% vs Control 47.3±1.3%, p=0.14). (Figure 1C)

In spite of exercise, there were no changes in spinal kyphosis for both TSC1mKO mice (TSC1mKOEx 82.17±14.87° vs TSC1mKO 83.67±17.18°, p=0.44) (Figure 1D) and control mice (ControlEx 47.8±15.5° vs control 57.1±16.7°, p=0.17).

DISCUSSION: This study demonstrated that general treadmill exercise can improve overall TSC1mKO mice endurance and paraspinal myopathy. It fails to improve intervertebral disc health but increases disc matrix formation in TSC1mKO mice compared to control mice. Exercise has no impact on spinal alignment for all mice. This study supports further optimization of exercise regimes to be paraspinal muscle-specific, so as to treat the spinal degenerative process.

- Hey HWD, Lam WMR, Chan CX, Zhuo WH, Crombie EM, Tan TC, Chen WC, Cool S, Tsai SY. Paraspinal Myopathy-Induced Intervertebral Disc Degeneration and Thoracolumbar Kyphosis in TSC1mKO Mice Model - A Preliminary Study. Spine J. 2021 Oct 12:S1529-9430(21)00902-5.

Intensively loaded intervertebral disc enhances the spontaneous calcium oscillation in CGRP-negative dorsal root ganglion neurons

Sibylle Grad¹, Jan Gewiess¹, Janick Eglauf¹, Astrid Soubrier¹, Marianna Peroglio¹, Mauro Alini¹, Junxuan Ma¹

1. AO Research Institute Davos, Davos, Switzerland

Introduction

The intervertebral disc (IVD) is a frequent cause of low back pain (LBP), and severity of IVD degeneration correlates with LBP prevalence. Dorsal root ganglion (DRG) neurons are the first-order neurons that transduce nociceptive/pain signals. Particularly, the spontaneous activation of these DRG neurons in the absence of noxious stimuli is correlated with spontaneous pain. Aberrant spinal mechanical loading is frequently discussed as a potential risk for LBP, but whether the intensively loaded IVD can influence pain-associated sensory nerve sensitization remains unknown. We hypothesized that intensive loading of IVD induces an increased spontaneous activation of DRG neurons.

Methods

Whole organ cultures of bovine tail IVDs were mechanically loaded in a bioreactor. High static loading of 0.2 MPa for 24h/day was applied to the IVD for 7 days to represent 'long-term sitting and standing' compared with a low static loading maintaining the initial disc height. Furthermore, dynamic loading of high frequency and intensity represented the 'wear and tear' loading, whereas low frequency and intensity loading was applied to represent the 'physiological' loading condition (0.32~0.5 MPa at 5 Hz versus 0.02~0.2 MPa at 0.2 Hz, for 3 h/day for 5 days).

To investigate the influence of static loading on IVD biology, degeneration-associated gene expressions of the IVD cells were evaluated using real-time RT-PCR. Viability of the disc cells was analyzed using lactate dehydrogenase (LDH) and ethidium-homodimer-1 staining of IVD cryosections.

Conditioned media (CM) were collected to stimulate primary cultures of bovine DRG neurons. Calcium imaging with Fluo-4 was used to evaluate the spontaneous calcium oscillation in the DRG neurons. The phenotypes of DRG neurons were labelled using immunofluorescence following the calcium imaging. Calcium oscillation in calcitonin gene related peptide (CGRP)-positive and CGRP-negative neurons was evaluated separately.

Results

High static loading increased interleukin 6 (IL-6) and matrix metalloproteinase 13 (MMP-13) gene expression in nucleus pulposus (NP) cells by 43.7 (p=0.07) and 13.2 (p=0.05) fold, respectively. High static loading also induced higher cell death compared with low static loading in inner annulus fibrosus (AF) and NP regions. The proportion of dead cells was increased from 3.9% to 15.7% in inner AF (p=0.03) and from 14.3% to 18.5% in NP region.

CM of IVDs subjected to both forms of intensive loading enhanced the spontaneous calcium oscillation in CGRP(-) neurons compared with their control IVD CM. High static loading induced the spontaneous calcium signals in a larger proportion of CGRP(-) neurons (84.32% versus 69.62%, p<0.01). High frequency and intensity cyclic loading elevated the normalized spontaneous calcium fluorescent peak height ($\Delta F/F_0$) by 8.6% (p<0.05).

Discussion

The high static loading induced a degenerative-like change in the inner AF and NP region of the IVD. Likewise, consistent with our former studies, high frequency and intensity loading caused an upregulation of IVD degeneration-associated genes.

Both static and cyclic intensive loadings mediated an altered disc-nerve communication which may suggest a biological mechanism associated with discogenic pain. However, how this disc-nerve communication is associated with LBP should be validated using in vivo models and clinical studies in the future.

Decompression with or without Fusion in Degenerative Lumbar Spondylolisthesis

Christian Hellum¹, Ivar Austevoll², Erland Hermansen³, Morten Fagerland⁴, kjersti Storheim⁵, Jens Ivar Brox⁶, Tore Solberg⁷, Frode Rekeland², Eric Franssen⁸, Clemens Weber⁹, Helena Brisby¹⁰, Oliver Grundnes¹¹, knut Algaard¹², Tordis Bøker¹³, Hasan Banitalebi¹⁴, Kari Indrekvam²

1. Division of Orthopedic Surgery, Oslo University Hospital, Ullevål, Oslo, Norway
2. Kysthospitalet in Hagevik Orthopedic department, Haukeland University Hospital, Bergen, Norway
3. Orthopedic Department, Ålesund Hospital, Ålesund, Norway
4. Research Support Services, the Oslo Center for Biostatistics and Epidemiology, Oslo, Norway
5. the Research and Communication Unit for Musculoskeletal Health, Division of Clinical Neuroscience, oslo University Hospital, Oslo, Norway
6. the Department of Physical Medicine and Rehabilitation, Oslo University Hospital, Oslo, Norway
7. Department of Neurosurgery, University Hospital of North Norway, Tromsø, Tromsø, Norway
8. Orthopedic Department, Stavanger University Hospital, Stavanger, Norway
9. Department of Neurosurgery, Stavanger University Hospital, Stavanger, Norway
10. the Spine Surgery Team, Department of Orthopedics, Sahlgrenska Academy, University of Gothenburg, Gothenburg, Sweden, Gothenburg, Sweden
11. Orthopedic Department, Akershus University Hospital, Oslo, Norway
12. Radiology, Unilabs Radiology, Oslo, Norway
13. the Department of Radiology and Nuclear Medicine, oslo University Hospital, Oslo, Norway
14. the Institute of Clinical Medicine, University of Oslo, Akershus University Hospital, Oslo, Norway

INTRODUCTION

It remains uncertain whether decompression surgery is noninferior to decompression with instrumented fusion in patients with lumbar spinal stenosis and degenerative spondylolisthesis.

METHODS

In this open-label, multicenter, noninferiority trial, patients were randomly assigned to decompression or decompression with instrumented fusion. Patients were included with symptomatic lumbar stenosis that did not respond to conservative management for at least 3 months and 3 mm or greater single level spondylolisthesis, regardless of dynamic slippage of vertebral bodies. Patients with degenerative scoliosis more than 20 degrees, radicular pain related to an extensive foraminal stenosis, or previously operated at the level of spondylolisthesis were not included. The decompression group were operated with a midline-preserving decompression. The techniques used for decompression with instrumented fusion was at the discretion of operating surgeons.

The primary outcome was an improvement of at least 30% on the Oswestry Disability Index (ODI; ranging from 0 to 100, with higher scores indicating more impairment) from inclusion to 2-year follow-up. The noninferiority margin was a between-group difference of 15 percentage points in the primary outcome. To declare noninferiority for decompression, noninferiority was required in the modified intention-to-treat analysis and the per-protocol analysis. Secondary outcomes included mean improvements in the ODI, the Zurich Claudication Questionnaire, the Numerical Rating Scale for leg and back pain, duration of surgery and hospital stay, and reoperation within 2 years.

RESULTS

In total 267 patients were randomized; 134 to decompression alone (mean [SD] age 66.0 [7.4] years) and 133 to decompression and instrumented fusion (mean [SD] age 66.5 [7.9] years). In the modified intention-to-treat analysis with multiple imputation of missing data (n= 26), 95 of 133 patients (71.4%) in the decompression group and 94 of 129 patients (72.9%) in the instrumented fusion group met the primary outcome (difference 1.4 percentage points; 95% confidence interval [CI], -9.4 to 12.2). In the per-protocol-analysis 80/106 (75.5%) and 83/110 patients (75.5%) met the primary outcome (difference, 0.0; 95% CI -11.4 to 11.4). The both analyses demonstrated noninferiority. The mean between-group difference in ODI from baseline to 2-year follow-up was 0.7 (95% CI, -2.8 to 4.3). Decompression alone was associated with shorter operation time (104 vs 174 minutes; mean difference -70; 95% CI, -84 to -55) and shorter hospital stay (3.3 vs 5.0 days; mean difference -1.8; 95% CI, -2.4 to -1.2 days). The reoperation rate was 15 of 120 patients (12.5%) in the decompression group and 11 of 121 (9.1%) in the instrumentation group (mean difference, 3.4%-points; 95% CI, -4.6 to 11.5 %-points).

DISCUSSION

In this trial involving patients with primary surgery for single-level degenerative lumbar spondylolisthesis, without a deformity or an extensive foraminal stenosis, decompression alone was noninferior to decompression with instrumented fusion over 2 years.

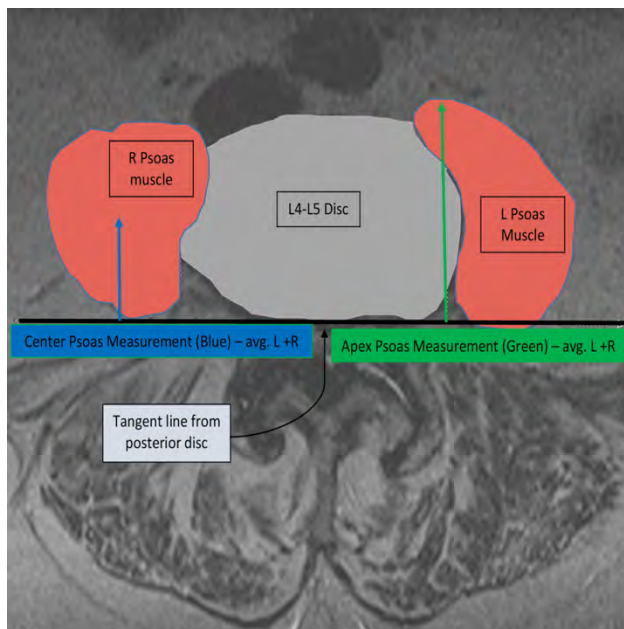
Tandem Spondylolisthesis and the Rising Psoas: The Danger of the Direct Lateral Trans-psoas Approach

Anthony A Oyekan¹, Dominic Ridolfi¹, Brandon K Couch¹, Aaron Zheng¹, Asher Mirvish¹, Jonathan F Dalton¹, Audrey Chang¹, Christopher M Gibbs¹, Jeremy D Shaw¹, William F Donaldson¹, Joon Y Lee¹

1. Department of Orthopaedic Surgery, University of Pittsburgh Medical Center, Pittsburgh, PA, United States

INTRODUCTION: The direct-lateral (trans-psoas) approach to the spine is a popular choice for interbody fusion procedures in the management of spondylolisthesis and degenerative disc disease. There are known risks of lumbar plexus and femoral nerve injury making preoperative planning essential. Previous investigators have described “the rising psoas sign” where the psoas muscle drifts anteriorly away from the vertebral column on advanced imaging axial views creating increased risk with the direct lateral approach. The purpose of the present study was to examine the association of sequential multilevel (tandem) spondylolisthesis and psoas position at the L4-L5 lumbar level.

METHODS: Subjects with lumbar spine MRIs and/or full-length spine films were identified and stratified into 3 age and gender-matched cohorts: 1) No spondylolisthesis, 2) Single level lumbar spondylolisthesis, & 3) sequential multilevel (tandem) lumbar spondylolisthesis. Medical records were retrospectively reviewed. The position of the psoas muscle (centrally and apically) relative to a tangent line at the posterior aspect of the L4-5 disc was measured. Spinopelvic parameters were recorded in all patients with full-length spinal films. Chi-square analysis was used to determine differences in gender. Two-tailed unpaired t-tests were used to identify differences in continuous variable demographics and radiographic measurements. $p < 0.05$ was considered statistically significant.



RESULTS: Two hundred and one subjects (75 M, 126 F; age 63 ± 13 years) were identified. No spondylolisthesis patients ($n=52$, 20 M, 32 F, age 61 ± 19 , BMI 30.80 ± 7.03 , aCCI 3 ± 2), single-level spondylolisthesis patients ($n=110$, 41 M, 69 F, age 63 ± 12 , BMI 31.44 ± 6.95 , aCCI 3 ± 2), and tandem spondylolisthesis patients ($n=39$, 14 M, 25 F, age 65 ± 8 , BMI 30.66 ± 7.29 , aCCI 3 ± 2) had no differences in demographics ($p > 0.1$). The center (C) psoas and apical (A) psoas position was more ventral in patients with tandem spondylolisthesis ($n=39$) (C: $28.9 \text{ mm} \pm 10.1 \text{ mm}$ & A: 50.9 mm) as compared to patients with single-level spondylolisthesis ($n=110$) (C: $24.3 \text{ mm} \pm 7.3 \text{ mm}$; $p = 0.012$ & A: 46.7 mm ; $p = 0.041$) and no spondylolisthesis ($n=52$) (C: $23.4 \text{ mm} \pm 8.0 \text{ mm}$; $p = 0.007$ & A: $45.3 \text{ mm} \pm 9.9 \text{ mm}$; $p = 0.019$). Tandem spondylolisthesis was associated with increased pelvic tilt ($27^\circ \pm 11^\circ$) vs. single-level spondylolisthesis ($21^\circ \pm 11^\circ$; $p = 0.002$) and no spondylolisthesis ($17^\circ \pm 12^\circ$; $p < 0.001$). Pelvic incidence was increased in subjects with tandem spondylolisthesis ($65^\circ \pm 19^\circ$; $p = 0.001$) and single-level spondylolisthesis ($61^\circ \pm 23^\circ$; $p = 0.026$) compared to patients with no spondylolisthesis ($54^\circ \pm 25^\circ$). Tandem spondylolisthesis was also associated with increased pelvic incidence-lumbar lordosis mismatch ($18^\circ \pm 16^\circ$) vs. single-level spondylolisthesis ($7^\circ \pm 13^\circ$; $p < 0.001$) vs. no spondylolisthesis ($11^\circ \pm 19^\circ$; $p = 0.059$). There were no significant differences

for the tandem spondylolisthesis group in lumbar lordosis angle, sacral slope, or sagittal vertical axis angle ($p > 0.1$). Single level spondylolisthesis was associated with increased lumbar lordosis ($52^\circ \pm 17^\circ$ vs. $43^\circ \pm 20^\circ$; $p = 0.003$) compared to patients with no spondylolisthesis.

DISCUSSION: Tandem spondylolisthesis is associated with a more ventrally positioned psoas muscle which poses a danger in trans-psoas approaches to the lumbar spine. Careful pre-operative planning with attention to the psoas position for lateral interbody fusion candidates is recommended.

1. Kepler, C. K., Bogner, E. A., Herzog, R. J., & Huang, R. C. (2011). Anatomy of the psoas muscle and lumbar plexus with respect to the surgical approach for lateral transpsoas interbody fusion. *European spine journal : official publication of the European Spine Society, the European Spinal Deformity Society, and the European Section of the Cervical Spine Research Society*, 20(4), 550–556. <https://doi.org/10.1007/s00586-010-1593-5>
2. Tanida, S., Fujibayashi, S., Otsuki, B., Masamoto, K., & Matsuda, S. (2017). Influence of spinopelvic alignment and morphology on deviation in the course of the psoas major muscle. *Journal of orthopaedic science : official journal of the Japanese Orthopaedic Association*, 22(6), 1001–1008. <https://doi.org/10.1016/j.jos.2017.08.002>
3. Voyadzis, J. M., Felbaum, D., & Rhee, J. (2014). The rising psoas sign: an analysis of preoperative imaging characteristics of aborted minimally invasive lateral interbody fusions at L4-5. *Journal of neurosurgery. Spine*, 20(5), 531–537. <https://doi.org/10.3171/2014.1.SPINE13153>

Assessment of Lumbar Motion and Patient Reported Outcomes after Decompression and use of Paraspinous Tension Band for Degenerative Spondylolisthesis: Results from 24-month FDA Study

Michael P Stauff¹, Rick C Sasso², Serena Hu³, Alan T Villavicencio⁴, Tim Yoon⁵, William Lavelle⁶, Kee D Kim⁷, Sandhu Harvinder⁸, Hyun Bae⁹, Harel Deutsch¹⁰, Khalid Sethi¹¹, Jeffrey S Fischgrund¹², Mick Perez-Cruet¹², Elizabeth Yu¹³, Sigurd H Berven¹⁴, Matthew Mermer¹⁵, Reginald J Davis¹⁶, Ravi S Bains¹⁷, Calvin C Kuo¹⁷, W Zach Ray¹⁸, Todd F Alamin³, Louie Fielding¹⁹, William C Welch²⁰

1. UMass Memorial Medical Center/University of Massachusetts Medical School, Worcester, MASSACHUSETTS, United States

2. Indiana Spine Group, Carmel, Indiana, United States

3. Stanford University, Stanford, CA

4. Boulder Neurosurgical Associates, Boulder, CO

5. Emory University, Atlanta, GA

6. SUNY Upstate Medical University, Syracuse, NY

7. University of California Davis, Sacramento, CA

8. Hospital for Special Surgery, New York, NY

9. Cedars Sinai, Los Angeles, CA

10. Rush University, Chicago, IL

11. UHS Neurosurgery, Johnson City, NY

12. Beaumont Hospital, Royal Oak, MI

13. Ohio State University Wexner Medical Center, Columbus, OH

14. University of California, San Francisco, San Francisco, CA

15. Kaiser Permanente, Roseville, CA

16. BioSpine Institute, Tampa, FL

17. Kaiser Permanente, Oakland, CA

18. Washington University, St Louis, MO

19. Empirical Spine, San Carlos, CA

20. University of Pennsylvania, Philadelphia, PA

Introduction: Durable outcome for degenerative spondylolisthesis (DS) often requires decompression and fusion. Fusion, however, places greater stress at adjacent levels that can lead to progressive adjacent segment disease. A novel interspinous tension band is proposed for segmental stabilization after decompression for DS, as an alternative to fusion. An FDA IDE study (NCT03115983) compares decompression and stabilization with the paraspinous tension band (PTB, treatment group) to decompression and instrumented fusion (control group) for symptomatic DS.

Methods: Prospectively enrolled IDE study subjects with 24 months postoperative radiographic follow-up were included in this analysis. X-rays obtained during the follow-up period for both the treatment (n=75) and control (n=52) groups were reviewed by an independent Core Laboratory for flexion/extension range of motion (ROM) and translation at the index, supradjacent and subjacent levels. Enrolled patients reported clinical outcomes (VAS back/leg, ODI) at baseline, 6 weeks, 3, 6, 12 months, and 24 months. Clinical success was defined as an ODI improvement of 15 points. Paired t-test was used to assess differences in outcomes.

Results: For the PTB group, pre-op to 24-month post-operative ROM was reduced 33% ($p<0.01$) and translation was reduced 29% ($p<0.01$). The fusion group as expected showed a significantly greater decrease in ROM (68%, $p<0.01$) and translation (77%, $p<0.01$) at the index level. Neither group had a statistically significant change in ROM/translation at supradjacent and subjacent levels. When assessing lumbar segmental range of motion at 24 months, adjacent segments accounted for 73% of motion in the treatment group and 87% in the control group. The patient reported outcomes were strong in both the PTB (mean VAS leg improvement 56.1, mean VAS back improvement 47.1, mean ODI improvement 39.4) and fusion (mean VAS leg improvement 51.0, mean VAS back improvement 57.4, mean ODI improvement 31.9) patients with no significant difference between groups. Clinical success, defined by ODI improvement of 15 points, was achieved in 88% in the PTB cohort and 76% in the fusion cohort, with no significant difference between groups.

Conclusion: Unlike fusion, PTB for DS maintained both stability and the anatomic range of motion and translation at the index levels out to 24 months. This maintained motion could lead to less progressive adjacent segment disease when DS is treated with PTB as opposed to fusion. The patient-reported clinical outcomes at 24 months post-operatively were similarly strong for both groups. These results should be confirmed with a longer follow-up including clinical outcomes in propensity score-matched patients.

A Canadian Spine Outcomes and Research Network Study of Functional Outcomes After Surgery for Lumbar Degenerative Spondylolisthesis

Patrick Thornley¹, Y. Raja Rampersaud², Raymond Andrew Glennie³, Charles Fisher⁴, Jennifer Urquhart⁵, Chris Bailey¹

1. London Health Sciences Centre, London, ON, Canada

2. Department of Surgery, Division of Orthopaedic Surgery, The Schroeder Arthritis Research Institute, Krembil Research Institute, University Health Network, Toronto, ON, Canada

3. Department of Surgery, Division of Orthopaedic Surgery, Dalhousie University, Halifax, Nova Scotia, Canada

4. Combined Neurosurgical and Orthopaedic Spine Program, University of British Columbia, Vancouver, British Columbia, Canada

5. Lawson Health Research Institute, Western University, London, ON, Canada

Introduction: Degenerative lumbar spondylolisthesis (DLS) is a debilitating condition associated with poor preoperative functional status. Surgical intervention has been shown to improve outcomes in this population though the nature of the most appropriate surgical intervention is controversial. The importance of maintaining and/or improving sagittal and pelvic spinal balance parameters has faced increasing emphasis in the DLS surgical population. However, little is known about the radiographic parameters most associated with improved functional outcomes among patients undergoing surgery for DLS. Thus, the objective of this study was to identify the radiographic parameters that correlate with functional outcomes after DLS surgery.

Methods: Retrospective analysis of the prospectively collected cohort of consecutively enrolled patients in the Canadian Spine Outcomes and Research Network (CSORN) database was performed. All enrolled study patients had a DLS diagnosis and underwent decompression in isolation or with posterolateral or interbody fusion. Patients reported their baseline and one-year post-operative leg and back pain on a 10-point logarithmic scale of severity in addition to completing the Oswestry Disability Index (ODI). Furthermore, multiple global and regional alignment parameters were documented at baseline and one-year postoperative including sagittal vertical axis (SVA), pelvic incidence (PI) and lumbar lordosis (LL).

Results: Two-hundred forty-one patients were available for analysis. Among participants, the mean age was 66 with 63% (152/241) female and a primary surgical indication of neurogenic claudication in 188/241 (78%) of patients. By Pearson correlation coefficient, worsened PI-LL mismatch >9cm was correlated with increased one-year postoperative ODI (.134, $p=0.05$), leg pain (.143, $p=0.05$) and back pain (0.189, $p=0.01$). A multiple linear regression was performed adjusting for baseline patient age, BMI, gender and preoperative presence of depression. From this regression analysis, worsening of a PI-LL mismatch was associated with a higher one-year postoperative ODI score R^2 0.179 (95% CI 0.080, 0.415, $p=0.004$), back pain R^2 0.152 (95% CI 0.021, 0.070, $p < 0.001$) and leg pain R^2 0.059 (95% CI 0.008, 0.066, $p=0.014$) score. Likewise, reduction of LL was associated with a higher ODI score R^2 0.168 (-0.387, -0.024, $p=0.027$) and back pain R^2 0.135 (95% CI -0.064, -0.010, $p=0.007$). Interestingly, worsened SVA >5cm was not statistically significant for worse one-year post-operative ODI, leg pain nor back pain scores.

Discussion: In our longitudinal multi-centre cohort study worsening of sagittal balance and loss of lumbar lordosis with lumbar degenerative spondylolisthesis correlates with worse postoperative outcomes. Accordingly, preoperative emphasis on regional and global spinal alignment parameters must be considered in order to optimize surgical procedure indication and functional outcome in lumbar degenerative spondylolisthesis treatment.

A Prospective Study of Lumbar Facet Arthroplasty in the Treatment of Degenerative Spondylolisthesis and Stenosis: Results from the Total Posterior Spine System (TOPS) IDE Study

Zachariah W Pinter¹, Harold Salmons¹, Brett A Freedman¹, Ahmad N Nassr¹, Arjun S Sebastian¹, Domagoj Coric², William C Welch³, Michael P Steinmetz⁴, Stephen E Robbins⁵, Yossi Smorgick⁶, Yoram Anekstein⁶

1. Mayo Clinic, Rochester, MINNESOTA, United States
2. Carolinas Neurosurgery & Spine Associates, Charlotte, North Carolina
3. University of Pennsylvania, Philadelphia, Pennsylvania
4. Cleveland Clinic Foundation, Cleveland, Ohio
5. Wisconsin Bone & Joint, Milwaukee, Wisconsin
6. Shamir Medical Center, Zerifin, Israel

Introduction

Lumbar facet arthroplasty is a method of dynamic stabilization used to treat Grade 1 spondylolisthesis with stenosis. There are currently no FDA-approved devices for facet arthroplasty. The purpose of the present study is to report the 1-year clinical and radiographic outcomes as well as safety profile of patients who underwent lumbar facet arthroplasty via implantation of the TOPS device as part of a prospective Investigational Device Exemption (IDE) trial.

Methods

We reviewed the prospectively collected clinical and radiographic outcomes of patients who underwent facet arthroplasty via implantation of the TOPS device in the investigational arm of a multicenter, prospective, randomized, controlled Food and Drug Administration (FDA) IDE trial. Standard demographic information was collected for each patient, including surgical variables. Radiographic parameters and patient reported outcome measures (PROMs) including ODI, VAS back and leg, and ZCQ were assessed preoperatively and at 6 weeks, 3 months, 6 months, and 12 months postoperatively. Adverse event, complication, and reoperation data were also collected for each patient.

Results

At the time of this study, 153 patients had undergone implantation of the TOPS device as part of this ongoing clinical trial and were included in this study. The mean surgical time was 187.8 minutes and mean estimated blood loss was 205.7cc. The mean length of hospital stay was 3.0 days. Mean ODI, VAS leg and back, and ZCQ scores improved significantly at all postoperative time points ($P > 0.001$). Greater than 79% of patients achieved MCID in all patient reported outcome measures at all postoperative time points. There were no clinically significant changes in radiographic parameters, and all operative segments remained mobile at 1-year follow-up without evidence of worsening sagittal translation. Postoperative complications occurred in 11 patients out of the 153 patients (7.2%) who underwent implantation of the TOPS device, including two new neurological deficits, two dural tears, two retained drains, one misplaced pedicle screw, one screw loosening, one infection, one seroma, and one hematoma. Nine patients (5.9%) underwent a total of 13 reoperations, eight for surgical complications (5.3%) and one (0.6%) of which was for device-related failure due to bilateral L4 pedicle screw loosening.

Discussion

Lumbar facet arthroplasty with the TOPS device demonstrated a statistically significant improvement in all PROMs and the ability to maintain motion at the index level while limiting sagittal translation with a low complication rate. The complication rates and improved postoperative PROMs are similar to those reported in the literature following single-level TLIF.

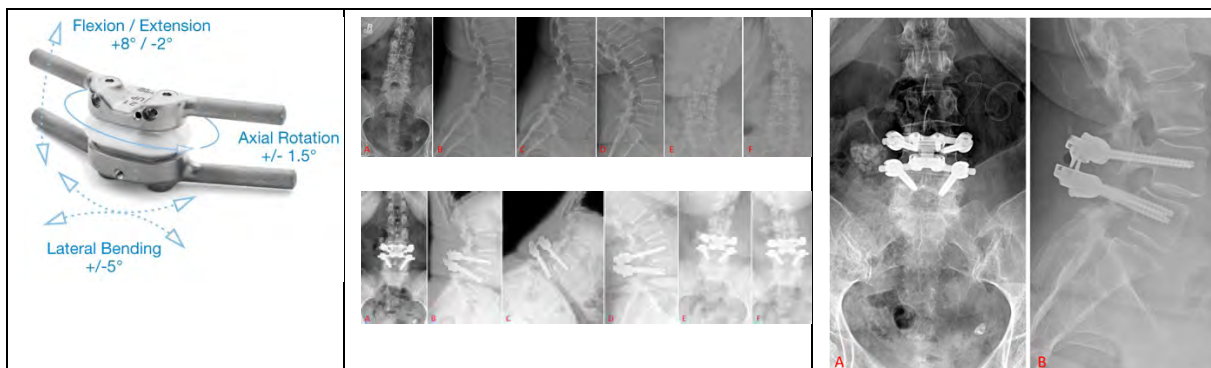


Table 2: Surgical Variables		n=153	
Time in Surgery (mins)	187.8 ± 62.4		
Length of Stay (days)	3.0 ± 4.1		
EBL (cc)	205.7 ± 154.3		
Estimated Blood Loss			
<100 cc	28 (18.3%)		
100 - <250 cc	75 (49.0%)		
250 - <400 cc	31 (20.3%)		
>=400 cc	19 (12.4%)		
Abbreviations: Estimated Blood Loss (EBL) Continuous variables are displayed as mean ± standard deviation. Categorical variables are displayed as number (percent).			

Table 3: Complications			n=153	
Complication	# of Patients	✓	✗	%
New Neurologic Deficits	2			1.3%
Dural Tear	2			1.3%
Infection	1			0.7%
Seroma	1			0.7%
Hematoma	1			0.7%
Implant loosening	1			0.7%
Misplaced instrumentation	1			0.7%
Retained drains	2			1.3%
Reoperation	9			5.9%

Table 5: Patient Reported Outcomes										n=105		
	ODI		VAS - Low Back Pain		VAS - Worst Leg Pain		ZCQ - Symptom Score		ZCQ - Physical Score		ZCQ - Satisfaction	
	Mean	MCID	Mean	MCID	Mean	MCID	Mean	MCID	Mean	MCID	Mean	≤ < 2
Preoperative	56.9 ± 12.4	-	67.2 ± 24.4	-	83.9 ± 13.2	-	3.76 ± 0.64	-	2.95 ± 0.40	-	-	-
Week 6	22.1 ± 17.0	83.7%	15.9 ± 16.7	79.6%	12.0 ± 20.4	91.3%	1.99 ± 0.63	94.2%	1.84 ± 0.59	85.6%	1.42 ± 0.49	96.2%
Month 3	14.3 ± 16.2	92.2%	13.4 ± 19.8	79.6%	12.4 ± 21.3	94.1%	1.66 ± 0.74	95.1%	1.45 ± 0.62	90.3%	1.43 ± 0.61	91.3%
Month 6	14.0 ± 17.5	89.3%	15.1 ± 23.4	80.6%	13.3 ± 23.4	90.3%	1.78 ± 0.71	94.2%	1.43 ± 0.64	89.3%	1.40 ± 0.65	91.3%
Month 12	11.5 ± 14.9	93.2%	12.7 ± 21.8	83.5%	11.5 ± 22.7	94.2%	1.74 ± 0.74	93.2%	1.39 ± 0.56	93.2%	1.34 ± 0.64	91.3%
P Value	<0.001		<0.001		<0.001		<0.001		<0.001		-	-
Abbreviations: Oswestry Disability Index (ODI), Visual Analog Score (VAS), Zurich Claudication Questionnaire (ZCQ), Minimum Clinically Important Difference (MCID)												

Table 6: Radiographic Parameters					n=153			
Parameters Assessed on Static Radiographs*					Preoperative	Postoperative	Δ	P Value
Disc Angle								
Inlet	7.8 ± 4.5	8.8 ± 4.2	0.8 ± 2.9	0.004				
Outlet	10.2 ± 3.1	11.2 ± 2.1	-0.8 ± 1.7	0.006				
Spine Index					33.3 ± 6.4	35.1 ± 5.1	-1.8 ± 3.2	<0.001
Disc Height								
Preval	10.0 ± 3.0	10.5 ± 2.8	-0.5 ± 1.2	<0.001				
Posterior	9.2 ± 1.5	9.7 ± 1.7	-0.5 ± 1.0	<0.001				
Posterior	7.9 ± 1.9	8.0 ± 2.0	-0.1 ± 0.8	<0.001				
Global Lordosis (L1-S3)					40.1 ± 9.3	39.3 ± 8.2	-0.3 ± 0.8	<0.001
Spondylolisthesis (mm†)								
Inlet	-4.1 ± 2.5	-1.1 ± 2.6	3.0 ± 1.8	<0.001				
Outlet	3.4 ± 1.5	3.4 ± 1.5	0.0 ± 0.6	0.51				
Outlet	2.2 ± 1.8	1.3 ± 1.6	0.9 ± 0.8	0.04				
Parameters Assessed on Dynamic Radiographs*					Preoperative	12 Months	Δ	P Value
Flexion ROM								
Inlet	3.8 ± 2.9	4.7 ± 3.0	-0.2 ± 1.4	0.05				
Outlet	3.2 ± 2.0	3.6 ± 2.5	0.6 ± 2.4	0.12				
Outlet	5.4 ± 3.6	5.3 ± 4.1	-0.4 ± 1.1	<0.001				
Flexion Translation								
Inlet	1.0 ± 0.6	0.9 ± 0.6	-0.3 ± 1.1	0.001				
Outlet	0.8 ± 0.7	0.8 ± 0.7	0.1 ± 0.8	0.04				
Outlet	0.4 ± 0.4	0.3 ± 0.5	0.2 ± 0.5	0.01				
Neutral ROM					3.2 ± 2.7	3.6 ± 3.0	-0.4 ± 1.2	0.14

Abbreviations: ROM=range of motion
*Standard deviations reported as a positive value. An increase in values represents an increase in the parameter.
†Mean lordosis refers to a more anterior lordosis. An increase in values represents an increase in the lordosis.
‡Radiographs were obtained 12 months postoperatively.

1. Martin BI, Mirza SK, Spina N, Spiker WR, Lawrence B, Brodke DS. Trends in Lumbar Fusion Procedure Rates and Associated Hospital Costs for Degenerative Spinal Diseases in the United States, 2004 to 2015. Spine (Phila Pa 1976). 2019;44(5):369-376.
2. Cheh G, Bridwell KH, Lenke LG, et al. Adjacent segment disease following lumbar/thoracolumbar fusion with pedicle screw instrumentation: a minimum 5-year follow-up. Spine (Phila Pa 1976). 2007;32(20):2253-2257.
3. Eck JC, Humphreys SC, Hodges SD. Adjacent-segment degeneration after lumbar fusion: a review of clinical, biomechanical, and radiologic studies. Am J Orthop (Belle Mead NJ). 1999;28(6):336-340.
4. Kim TH, Lee BH, Moon SH, Lee SH, Lee HM. Comparison of adjacent segment degeneration after successful posterolateral fusion with unilateral or bilateral pedicle screw instrumentation: a minimum 10-year follow-up. Spine J. 2013;13(10):1208-1216.
5. Schlegel JD, Smith JA, Schleusener RL. Lumbar motion segment pathology adjacent to thoracolumbar, lumbar, and lumbosacral fusions. Spine (Phila Pa 1976). 1996;21(8):970-981.
6. Mulholland RC, Sengupta DK. Rationale, principles and experimental evaluation of the concept of soft stabilization. Eur Spine J. 2002;11 Suppl 2(Suppl 2):S198-205.
7. Heuer F, Schmidt H, Käfer W, Graf N, Wilke HJ. Posterior motion preserving implants evaluated by means of intervertebral disc bulging and annular fiber strains. Clin Biomech (Bristol, Avon). 2012;27(3):218-225.
8. Meyers K, Tauber M, Sudin Y, et al. Use of instrumented pedicle screws to evaluate load sharing in posterior dynamic stabilization systems. Spine J. 2008;8(6):926-932.
9. Wilke HJ, Schmidt H, Werner K, Schmölz W, Drumm J. Biomechanical evaluation of a new total posterior-element replacement system. Spine (Phila Pa 1976). 2006;31(24):2790-2796; discussion 2797.
10. Stoll TM, Dubois G, Schwarzenbach O. The dynamic neutralization system for the spine: a multi-center study of a novel non-fusion system. Eur Spine J. 2002;11 Suppl 2(Suppl 2):S170-178.

Cell-Laden Injectable High-Modulus Biomaterial Composites Repair Intervertebral Discs Under Physiological Loading

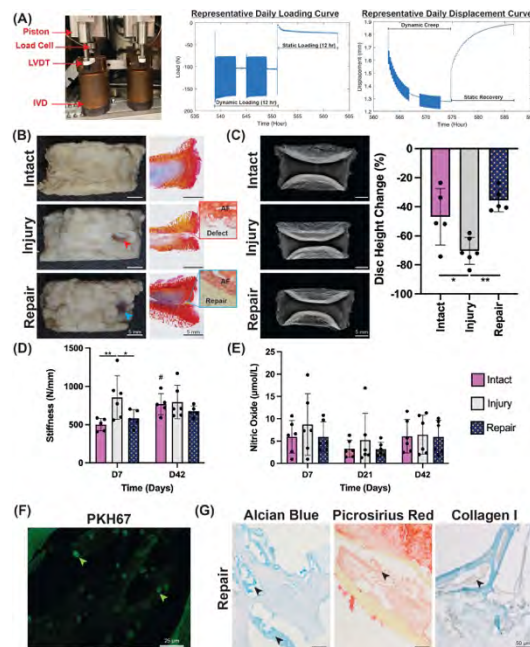
Christopher J Panebianco¹, Sanjna Rao², Warren W Hom¹, Andrew C Hecht¹, Jennifer R Weiser², James Iatridis¹

1. Icahn School of Medicine at Mount Sinai, New York, NY, United States

2. Chemical Engineering, The Cooper Union for the Advancement of Science and Art, New York, NY, United States

INTRODUCTION: Cell therapies have potential to slow the progression of painful intervertebral disc (IVD) degeneration,¹ which costs \$134.5 billion in domestic healthcare spending.² To support cell-mediated healing, injectable cell delivery biomaterials may be used as a platform to retain cells in the IVD.³ Engineering annulus fibrosus (AF) cell delivery biomaterials is challenging because of the need to balance biomechanical and biological performance.⁴ To overcome this challenge, we developed a novel composite biomaterial for AF repair. It uses cell-laden, degradable oxidized alginate (OxAlg) microbeads (MBs) to deliver AF cells within high-modulus genipin-crosslinked fibrin (FibGen) hydrogels (FibGen+MB composites). This study evaluates the long-term biomechanical and biological performance of FibGen+MB composites in an *ex vivo* bovine organ culture model.

METHODS: Intact, Injury and Repair IVDs [N=5-6 per group] were cultured for 42 days using a custom Loading system for Disc Organ Culture (LODOC),⁵ which simulates physiologic loading (Fig. 1A). Herniation risk [Gross morphology & Histology], disc height changes [X-rays & LODOC] and stiffness [LODOC] were measured to assess biomechanical repair. Biological repair was assessed using culture viability [Nitric oxide], cell tracking [PKH67] and extracellular matrix (ECM) synthesis [Alcian blue, Picrosirius red and Collagen I]. Two-way ANOVA with Bonferroni [Biomechanics & Nitric Oxide] and one-way ANOVA with Tukey's post-hoc [Disc Height Change] tests found significant differences ($p < 0.05$).



RESULTS: Morphological and histological assessments showed that composites remained within defects at culture day (D) 42 with high adhesion, suggesting FibGen+MB composites have very low herniation risk under cyclic compressive loading (Fig. 1B). Repair IVDs had significantly less disc height loss when compared to Injury IVDs, and no differences between Intact and Repair IVDs were detected (Fig. 1C). Repair also prevented injury-induced IVD stiffening at D7, but by D42 there were no significant differences between groups (Fig. 1D). This is likely due to mechanical compaction in all groups from approximately 96,000 loading cycles over the 42-day culture. All IVDs remained viable with constant, low nitric oxide levels throughout culture (Fig. 1E). Delivered AF cells were present within the degraded OxAlg MB space of composites at D42, suggesting successful cell delivery and retention (Fig. 1F). Delivered AF cells synthesized ECM as OxAlg MBs degraded within FibGen+MB composites, as shown by positive staining for Alcian blue, picrosirius red and collagen I in the interstitial space between cells (Fig. 1G).

DISCUSSION: FibGen+MB composites restored IVD height and improved the biomechanical properties of injured IVDs, while delivering AF cells capable of ECM synthesis. FibGen+MB composites did not herniate after approximately 96,000 cycles of compression *in situ*, which is a very rigorous challenge for an experimental IVD repair biomaterial.⁶ Importantly, composites also restored disc height loss to intact levels, which is one of the most sensitive measurements of IVD repair.⁷ Lastly, delivered AF cells synthesized ECM within composites,

suggesting this composite strategy shows promise for long-term tissue synthesis and IVD repair. Overall, we demonstrated a proof-of-concept for this composite repair strategy as a next-generation AF repair method that balances biomechanical and biological repair.

- [1] Sakai, D. & Andersson, G. B. J. Stem cell therapy for intervertebral disc regeneration: obstacles and solutions. *Nat. Rev. Rheumatol.* 11, 243–256 (2015).
- [2] Dieleman, J. L. et al. US Health Care Spending by Payer and Health Condition, 1996-2016. *JAMA* 323, 863–884 (2020).
- [3] Burdick, J. A., Mauck, R. L. & Gerecht, S. To Serve and Protect: Hydrogels to Improve Stem Cell-Based Therapies. *Cell Stem Cell* 18, 13–15 (2016).
- [4] Panebianco, C. J., Meyers, J. H., Gansau, J., Hom, W. W. & Iatridis, J. C. Balancing biological and biomechanical performance in intervertebral disc repair: a systematic review of injectable cell delivery biomaterials. *eCM* 40, 239–258 (2020).
- [5] Walter, B. A., Illien-Jünger, S., Nasser, P. R., Hecht, A. C. & Iatridis, J. C. Development and validation of a bioreactor system for dynamic loading and mechanical characterization of whole human intervertebral discs in organ culture. *J. Biomech.* 47, 2095–2101 (2014).
- [6] Dixon, A. R., Warren, J. P., Culbert, M. P., Mengoni, M. & Wilcox, R. K. Review of *in vitro* mechanical testing for intervertebral disc injectable biomaterials. *J Mech Behav Biomed Mater* 123, 104703 (2021).
- [7] Iatridis, J. C., Nicoll, S. B., Michalek, A. J., Walter, B. A. & Gupta, M. S. Role of biomechanics in intervertebral disc degeneration and regenerative therapies: what needs repairing in the disc and what are promising biomaterials for its repair? *Spine J.* 13, 243–262 (2013).

Infectious and autoinflammatory etiologies of Modic type 1 change have different cytokine profiles

Irina Heggli¹, Regula Schüpbach², Nadja Farshad-Amacker³, Michael Betz⁴, José Spirig⁴, Florian Wanivenhaus⁴, Christoph Laux⁴, Florian Brunner⁵, Mazda Farshad⁴, Oliver Distler¹, **Stefan Dudli¹**

1. Center of Experimental Rheumatology, University of Zurich, Zurich, Switzerland

2. Unit of Clinical and Applied Research, Balgrist University Hospital, Zurich, Switzerland

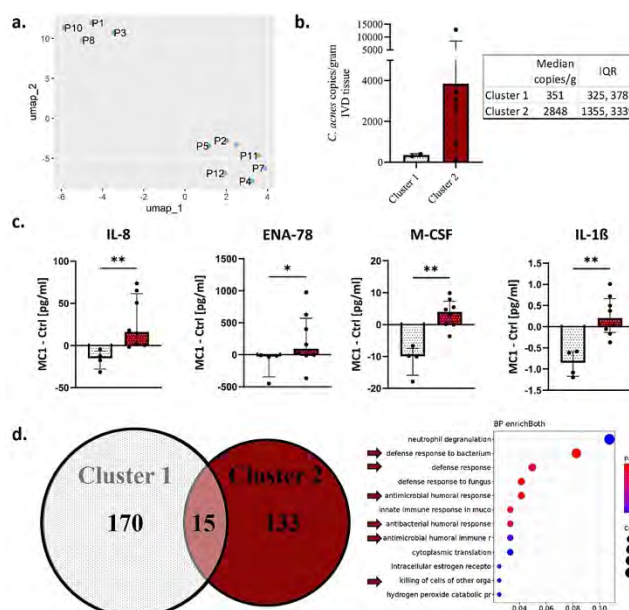
3. Department of Radiology, Balgrist University Hospital, Zurich, Switzerland

4. Department of Orthopedic Surgery, Balgrist University Hospital, Zurich, Switzerland

5. Department of Physical Medicine and Rheumatology, Balgrist University Hospital, Zurich, Switzerland

INTRODUCTION Modic type 1 changes (MC1) are an inflammation of the vertebral bone marrow and an independent source of low back pain. Two etiologies have been described: (i) an autoinflammatory reaction of the bone marrow against disc cells and matrix and (ii) infection of the disc with bacteria, mainly with *Cutibacterium acnes* (*C. acnes*). The different etiologies require different treatments. Therefore, we need to be able to diagnostically distinguish the two etiologies and understand the etiology-specific pathomechanisms. The aim of this study was to identify etiology-specific pathomechanisms that could serve as basis for etiology-specific biomarkers.

METHODS This study was approved by the local Ethics Commission and performed in accordance with the Declaration of Helsinki. Bone marrow aspirates were obtained from MC1 patients undergoing spinal fusion. Aspirates were taken prior to screw insertion through the pedicle screw trajectory. From each patient, a MC1 and an intra-patient control aspiration from the adjacent vertebral level was collected in K2-EDTA tubes. Plasma and cell fraction were separated and collected by centrifugation. Plasma (n=12+12) was analyzed for interleukin-1 β (IL-1 β), granulocyte-macrophage colony-stimulating factor (GM-CSF), epithelial-derived neutrophil-activating peptide 78 (ENA-78), tumor necrosis factor alpha (TNF- α), colony stimulating factor 1 (M-CSF), chemokine C-C motif ligand 2 (CCL2), interleukin-4 (IL-4), IL-6, IL-8, and IL-13 using MesoScale U-Plex. Different cytokine profiles were identified with Uniform-Manifold-Approximation-Projection (UMAP) analysis. Protein concentrations between two clusters were compared with t-tests. Neutrophils (n=8+8) were isolated from the cell fraction (StemCell neutrophile kit), RNA isolated (Qiagen RNeasy Kit) and sequenced (Novaseq). Differentially expressed genes (DEG; p-value < 0.01, log₂fc > \pm 0.5) in MC1 were compared to control bone marrow and analyzed with gene ontology (GO) enrichment in R (GOseq). Discs adjacent to MC1 (n=8) were tested with anaerobic bacterial culture and 16S qPCR for the presence of *C. acnes*.



RESULTS UMAP dimensionality reduction identified two cytokine clusters (Figure a). IVDs of patients in cluster 2 had higher *C. acnes* genome copies (n = 6, median = 2848 copies/g) than IVDs in cluster 1 (n = 2, median = 351 copies/g) (Figure b). This suggests that patients of cluster 1 have an autoinflammatory etiology and patients of cluster 2 an infectious etiology. There was no difference in cytokine concentrations between MC1 and control. However, when stratifying by clusters, IL-8, ENA-78, M-CSF, and IL-1 β were significantly higher in cluster 2 than in cluster 1 (Figure c). Since IL-8 and ENA-78 are potent neutrophil chemoattractants and activators, we compared the neutrophile transcriptome in MC1 bone marrow of cluster 1 and 2. Only 15 DEGs overlapped between cluster 1 (185 DEG) and cluster 2 (165 DEG) suggesting different pathomechanisms (Figure d). Six of the top 12 enriched biological processes in cluster 2 related to bacterial defense response. None of them were present in cluster 1.

DISCUSSION Autoinflammatory (cluster 1) and infectious etiologies (cluster 2) of MC1 have different cytokine profiles and neutrophile activation profiles indicating different pathomechanisms. It is clinically relevant to be able to distinguish the two etiologies, because different pathomechanisms require different treatments.

Progression of spinal degenerative changes in a group of chronic low back pain patients and patients 11-14 years after discography evaluation

Hanna Hebelka^{2,1}, Kerstin Lagerstrand^{1,3}, Veronica Gunterberg^{1,4}, Helena Brisby^{1,5}

1. Institute of Clinical Sciences, Sahlgrenska Academy, University of Gothenburg,, Gothenburg

2. Department of Radiology, Sahlgrenska University Hospital, Gothenburg, Sweden

3. Dept. of Medical Physics and Techniques, Sahlgrenska University Hospital, , Gothenburg, Sweden

4. Department of ortopaedics, Borås Hospital, Borås, Sweden

5. Dept of Orthopaedics, Sahlgrenska University Hospital, Gothenburg, Sweden

Introduction: Low back pain (LBP) is associated with intervertebral disc (IVD) degeneration, however there is still poor understanding of the exact relationship between IVD degeneration and LBP [1]. The development of degenerative changes over time for individuals, as well as for specific spinal motion segments, is difficult to predict and more knowledge is needed. Discography has been demonstrated to accelerate degenerative changes in injected IVDs [2]. Even if discography today is rarely used, long-term follow up of individuals previously obtaining discography can serve as an in-vivo human model for other annular injuries and might thus provide information regarding the association between annular injury and the degenerative process.

The aim of the current study was to investigate the longitudinal MRI appearance in LBP patients, in whom discography had been performed as diagnostic guidance.

Methods: 30 LBP patients, prospectively enrolled year 2007-2010 in a comparative discography-MRI study (1.5T, sagittal T2/T1-weighted) were asked to participate in this long-term follow-up. The reason for discography at inclusion was LBP (>6 months), severe enough to consider surgery. Those accepting to participate in the follow-up performed MRI of the lumbar spine during year 2021. The MRIs were evaluated, blinded, according to Pfirrmann classification, Endplate Classification Score (EPS) and HIZ for 6 IVD's per individual at baseline and follow-up (Th12/L1- L5/S1). At baseline discography of 2-4 discs in each individual had been performed and data on which discs that had been injected or not were used here.

Figure 1. Example of pairs of sagittal MRI at baseline (left) and 11-14 year follow-up (right) for some of the individuals who had not undergone surgery during the follow-up period with injected IVDs highlighted with a circle



Results: 17 patients (6 male/mean 58.5 years;range 49-72), accepted participation, at this 11-14 year follow-up. Reasons for not participating were; 2 deceased, 5 unreachable, 1 had obtained a non-MR compatible device and 5 declined participation. Between baseline and follow-up, 10 (27 IVDs) of the 17 included patients had undergone fusion surgery. These fused IVD segments omitted adequate longitudinal evaluation and were therefore excluded. Out of the 75 non-

fused IVDs, 30 were injected (discography) at baseline. Comparing groups of injected and non-injected IVDs significant differences were found at both baseline and follow-up regarding Pfirrmann grade and HIZ, and at follow-up also for EPS, with higher degeneration grade respectively EPS for injected IVDs (Table 1). However, in terms of morphological changes over time, no significant differences between the groups of injected and non-injected IVD's were detected (Table 1).

Table 1: MRI parameters at baseline and follow-up for groups of injected respectively non-injected IVDs

	Baseline			Follow-up			Change from baseline		
	non-injected n=48	injected n=30	p-value	non-injected n=48	injected n=30	p-value	non-injected n=48	injected n=30	p-value
Pfirrmann									
1	33 (73.3%)	6 (20.0%)		20 (41.4%)	1 (3.3%)		-4	2 (6.4%)	3 (10.0%)
2	7 (15.6%)	16 (53.3%)		11 (24.4%)	13 (43.3%)		0	26 (67.6%)	12 (40.0%)
3	2 (4.4%)	5 (16.7%)	0.0010	10 (22.2%)	12 (40.0%)	0.0010	-1	10 (22.2%)	13 (43.3%)
4	3 (6.7%)	3 (10.0%)		4 (8.9%)	4 (13.3%)		2	6 (15.3%)	2 (6.7%)
5							3	1 (2.2%)	0 (0.0%)
Endplate score (EPS)									
1	23 (51.1%)	4 (13.3%)		9 (20.0%)	0 (0.0%)		-2	0 (0.0%)	1 (3.3%)
2	7 (15.6%)	10 (33.3%)		10 (22.2%)	1 (3.3%)		-4	4 (8.9%)	2 (6.7%)
3	3 (6.7%)	6 (20.0%)	0.001	9 (20.0%)	12 (40.0%)	0.0001	0	10 (22.2%)	5 (20.0%)
4	7 (15.6%)	5 (16.7%)		9 (20.0%)	7 (23.3%)		1	11 (24.4%)	11 (36.7%)
5	2 (4.4%)	3 (10.0%)		4 (8.9%)	7 (23.3%)		2	8 (17.8%)	8 (26.7%)
6	3 (6.7%)	2 (6.7%)		4 (8.9%)	3 (10.0%)		3	2 (4.4%)	1 (3.3%)
							4	0 (0.0%)	1 (3.3%)
							5	1 (2.2%)	0 (0.0%)
HIZ									
no HIZ	39 (86.7%)	15 (50.0%)	0.0014	42 (88.3%)	22 (73.3%)	0.040	-8	4 (8.9%)	8 (26.7%)
HIZ	6 (13.3%)	15 (50.0%)		3 (6.7%)	8 (26.7%)		6	40 (83.3%)	21 (70.0%)
							1	1 (2.2%)	1 (3.3%)

Discussion: When comparing discography-injected and non-injected IVDs over more than 10 years, no significant differences in progression of degenerative changes between the groups were detected, with reservation for inherent limitations being a case study. This long-term follow-up could thus not confirm previous findings that a needle-puncture of the disc (annular injury) induce excessive degenerative progression of the IVD. This study highlights how sometimes surprisingly little progress of degenerative changes, on an individual level, may be seen over a decade in spite of needle puncture and chronic LBP (Figure 1). The findings support the concept of high complexity regarding annular injury and the progression of disc degeneration and suggest that other factors than limited annular injuries may be of larger importance in development of spinal degeneration.

- 1 Urban JP, Fairbank JC (2020) Current perspectives on the role of biomechanical loading and genetics in development of disc degeneration and low back pain; a narrative review. Journal of biomechanics 102:109573
- 2 Carragee EJ, Don AS, Hurwitz EL, Cuellar JM, Carrino J, Herzog R (2009) 2009 ISSLS Prize Winner: does discography cause accelerated progression of degeneration changes in the lumbar disc: a ten-year matched cohort study. Spine 34:2338-2345

A systematic review of Clinical Practice Guidelines for persons with non-specific low back pain with and without radiculopathy: Identification of best evidence for rehabilitation to develop the WHO's Package of Interventions for Rehabilitation

Fabio Zaina¹, Pierre Coté², Carolina Cancelliere², Francesca Di Felice¹, Sabrina Donzelli¹, Alexandra Rauch³, Leslie Verville², Stefano Negrini^{1,4,5}, Margareta Nordin⁶

1. ISICO (Italian Scientific Spine Institute), Milan, MI, Italy

2. Faculty of Health Sciences, Ontario Tech University, Oshawa, Ontario, Canada

3. Department of Management of Noncommunicable Diseases, Disability, Violence and Injury Prevention, World Health Organization, Geneva, Switzerland

4. "La Statale" University, Milan, Italy

5. IRCCS Istituto Ortopedico Galeazzi, Milan, Italy

6. Departments of Orthopedic Surgery and Environmental Medicine, New York University, New York, USA

Background. The identification of evidence-based interventions for rehabilitation for persons with non-specific low back pain (LBP) is a crucial step for the development of the World Health Organization's (WHO) Package of Interventions for Rehabilitation (PIR). Our objective was to conduct a systematic review of clinical practice guidelines (CPGs) about the management of persons with non-specific LBP with and without radiculopathy and synthesize the recommendations to inform the WHO PIR.

Methods. This paper is part of a "Best Evidence for Rehabilitation" (be4rehab) series, developed according to the methodology by the WHO Rehabilitation Program and Cochrane Rehabilitation under the guidance of WHO's Guideline Review Committee Secretariat. Eligible guidelines were published between 2009 and 2019 in English, French, Italian, or Swedish; included adults or children with non-specific LBP with or without radiculopathy; assessed the benefits of interventions for rehabilitation on functioning. We searched electronic databases (MEDLINE, EMBASE, CINAHL, the Canadian Medical Association CPG Infobase, International Guidelines Network, and American College of Physicians Clinical Guidelines and Recommendations) and the grey literature from January 1, 2009 to March 17, 2019. Pairs of independent reviewers assessed the quality of the CPGs using AGREE II. Relevant data were extracted, and the findings were synthesized narratively.

Results: Our search yielded 3,049 articles. We removed 236 duplicates and screened 2,813 articles. Of those, 12 CPGs were eligible for critical appraisal and 4 CPGs fulfilled the quality criteria and were included in our synthesis. One of the included guidelines was about the conservative treatment of LBP and sciatica inpatients ≥ 16 years of age, one was about manual therapy and other rehabilitation treatments for adults (≥ 18 years) with LBP, one included interventional therapies, surgery and interdisciplinary rehabilitation for adults with LBP, and the last included pharmacological, educational and rehabilitation treatments for adults with acute and chronic LBP. Recommended interventions included: 1) education about recovery expectations, self-management strategies, and continuance of usual activities; 2) multimodal approaches incorporating education, exercise and spinal manipulation; 3) NSAIDs in the acute stage with education; and 4) for those with persistent pain, intensive interdisciplinary rehabilitation based on exercise with a cognitive/behavioral approach.

Discussion: Many CPGs for LBP are available, but their quality varies. According to our systematic search and evaluation, most of the retrieved CPGs didn't fulfil the minimum quality criteria to be included in the present review and there is a lack of high-quality clinical practice guidelines for people below 18 years. Our review summarizes recommendations from high-quality CPGs for the rehabilitation of adults with LBP with or without radiculopathy. Overall, the recommendations highlight the benefits of education, exercise and multimodal care that includes manual therapies. However, the use of most passive modalities is not recommended. The collected recommendations were consistent among the guidelines. Implementation strategies are needed to implement the recommendations and evaluation of these strategies to see if there's improvement in patients' outcomes and costs.

1. Rauch A, Negrini S, Cieza A. Toward Strengthening Rehabilitation in Health Systems: Methods Used to Develop a WHO Package of Rehabilitation Interventions. *Arch Phys Med Rehabil* 2019;100(11):2205–11.
2. Zaina F, Balagué F, Battié M, Karppinen J, Negrini S. Low Back Pain in 2020: new frontiers and old limits of our understanding. An overview of the state of the art from a rehabilitation perspective. *Eur J Phys Rehabil Med* 2020
3. National Guideline Centre (UK). Low Back Pain and Sciatica in Over 16s: Assessment and Management [Internet]. London: National Institute for Health and Care Excellence (UK); 2016 [cited 2020 Nov 1]. Available from: <http://www.ncbi.nlm.nih.gov/books/NBK401577/>
4. Thorson D, Campbell, Robb, Massey, Michael, et al. Low Back Pain, Adult Acute and Subacute [Internet]. ICSI. 2018 [cited 2020 Nov 4]; Available from: <https://www.icsi.org/guideline/low-back-pain/>
5. Bussi eres AE, Stewart G, Al-Zoubi F, et al. Spinal Manipulative Therapy and Other Conservative Treatments for Low Back Pain: A Guideline From the Canadian Chiropractic Guideline Initiative. *J Manipulative Physiol Ther* 2018;41(4):265–93.
6. Chou R, Loeser JD, Owens DK, et al. Interventional therapies, surgery, and interdisciplinary rehabilitation for low back pain: an evidence-based clinical practice guideline from the American Pain Society. *Spine (Phila Pa 1976)* 2009;34(10):1066–77.

Lumbar Total Disc Replacement Removals/Revisions during a 20 Year Experience with 1,775 Patients

Richard Guyer¹, Scott L Blumenthal¹, Jack E Zigler¹, Jessica L Shellock¹, Donna D Ohnmeiss²

1. *Center for Disc Replacement at the Texas Back Institute, Plano, TX, USA*

2. *Texas Back Institute Research Foundation, Plano, TX, United States*

INTRODUCTION: A concern expressed about lumbar total disc replacement (TDR) has been safety. One measure of safety is the need for subsequent surgery for implant removal or revision. This may be of particular importance considering TDR removal/revision generally requires re-operation through the anterior approach with the corresponding increased risk of vascular injury. The purpose of this study was to analyze the incidence of, and reasons for, lumbar TDR removal/revision.

METHODS: Data were collected from a multi-site spine specialty practice. A consecutive series of 1,775 lumbar TDR patients, beginning with the first case experience in 2000, was reviewed to identify those undergoing re-operation for TDR removal or revision. Only patients who were at least 2 years postoperative were included. Contact by mail and/or telephone phone calls to collect current data was conducted for patients who did not have a recent office visit. The mean follow-up was 85.9 months with a median of 73 months and maximum of 251 months. For each case of device removal/revision, the reason, duration from index surgery, and procedure performed were recorded.

RESULTS: In the series of 1,775 patients, 26 (1.46%) underwent TDR removal or revision. Removal was performed in 23 patients (1.29%) and 3 patients underwent TDR revision (0.17%). Based on the total number of 2,082 TDRs implanted in the 1,775 patients, rates of removals and revisions were 1.15% and 0.14%, respectively. Removals included: 10 for migration and/or loosening, 3 developed problems after a trauma, 3 had ongoing pain, 2 developed lymphocytic reaction to device materials, and there was one each of: TDR was too large and replaced with smaller device, vertebral body fractures (osteoporosis), developed a lytic lesion, device subsidence and facet arthrosis, and infection seeded from a chest infection at 146 month post-TDR. The 3 revisions were: Repositioning the core (technique error), repositioning device after displacement, and core replacement due to wear/failure. With respect to timing, 34.6% of removals/revisions occurred within one month after the index implantation. Of note, 42.3% of revisions/removals occurred in the first 25 TDR cases performed by individual surgeons. Vascular complication during TDR removal occurred in one patient with an iliac vein tear whose TDR was removed due to trauma including spinal fracture. Removal/revision status was verified by office visit or mailing/telephone in 227 patients with a minimum of 15-year follow-up data. Only one patient underwent removal/revision surgery more than 15 years post-TDR. This was the patient who underwent TDR removal due to trauma-related spinal fracture.

DISCUSSION: In this large consecutive patient series, 1.5% of lumbar TDRs were removed/revised. Only one revision was related to device failure or wear. Many of the removals/revisions were performed within a month of implantation. Also of note, many occurred within the first 25 TDR cases for individual surgeons, suggesting a learning curve. The low rate of removal/revision in this large institutional experience over a 20 year period provides support for the safety of these devices.

Comparative plasma proteomics analysis between clinically mild and severe participants from two independent pilot samples of Lumbar Spinal Stenosis and Chronic Low Back Pain.

Valerio TonelliEnrico¹, Michael Schneider¹, Nam Vo¹, Nathan Yates¹, Gwendolyn Sowa¹

1. University of Pittsburgh, Pittsburgh, PA, United States

Introduction Lumbar Spinal Stenosis (LSS) and Chronic Low Back Pain (CLBP) are two serious conditions affecting the lumbar spine, both often resulting in significant pain, decreased function, and poor treatment outcomes. There is growing consensus that plasma biomarkers could become clinically useful to better understand and treat these conditions. Nonetheless, the literature on plasma proteomics for these two conditions is lacking, and so is the understanding of what could be common pathways and shared contributing factors. This pilot comparative study used plasma proteomics analysis on two independent populations (one with LSS and one with CLBP) to explore significant similarities and differences in circulatory proteins.

Methods Two independent sample cohorts were used (LSS; n=259 and CLBP; n=186) to select high clinically severe (HCS) subjects to compare against the less clinically severe (LCS) subjects. The comparison was done among the 2 groups within each cohort, and significant results were then compared between cohorts to highlight possible common proteins. Subjects were chosen based on VAS and ODI score

In the LSS population, participants in the LCS group (n=10) had a mean pain score (VAS) of 1.2 and Oswestry Disability Index (ODI) of 17.4. The HCS group (n=10) consisted of subjects with mean VAS=8.4 and ODI= 57.8. For the CLBP population, participants in the LCS group (n=18) had a mean pain score of 2.7 and an ODI mean of 13.6, while those in the HCS group (n=19) had a mean pain score of 7.7 and ODI mean of 49.4.

Differential Mass Spectrometry was performed on collected plasma. 385 plasma proteins were detected and quantified and compared between the two groups of the LSS population, while 377 proteins were quantified and compared between the two groups of the CLBP population. The relative abundance of these proteins was assessed using student's t-test (Log2 transformed) with a p-value cut-off of 0.02.

Results In the LSS samples, 11 plasma proteins were significantly elevated in the HCS group. In the CLBP sample, 31 plasma proteins were significantly elevated and 2 were significantly decreased in the HCS group. The only protein that was found to be significantly different in both populations (LSS and CLBP) was Factor 5 (F5), which was increased in the HCS group for both cohorts.

Discussion Our finding is thought-provoking and unexpected. Interestingly, in addition to its role in the coagulation system, F5 is implicated in platelet degranulation, which is known to play a role in inflammatory responses and immune modulation. While there is an established body of evidence highlighting the relevance of inflammation in CLBP and LSS, research on F5 as an inflammatory mediator in these two conditions is lacking.

In conclusion, our study highlights a possible novel area of research to explore the potential role of F5 in LSS and CLBP both as a biomarker for clinical severity and as a potential shared mechanism. Confirming the finding in larger cohorts and in association with other mediators of inflammation will be important to determine the significance of this finding.

Spatial distribution of fat infiltration within the paraspinal muscles: implications for chronic low back pain

Karim Khattab¹, Lucas K Dziesinski¹, Rebecca Crawford², Alex Ballatori¹, Priya Nyayapati¹, Roland Krug³, Aaron Fields¹, Conor W O'Neill¹, Jeffrey C Lotz¹, Jeannie F Bailey¹

1. Department of Orthopaedic Surgery, University of California San Francisco, San Francisco, CA, United States

2. Body Urbanist, Hünenberg See, Zug, Switzerland

3. Department of Radiology, University of California San Francisco, San Francisco, CA, United States

INTRODUCTION MRI-based characterization of paraspinal muscle (PSM) composition by quantifying fat infiltration (FI) is a popular approach for assessing muscle quality for spine conditions. However, the relationship between PSM FI and chronic low back pain (cLBP) is not straightforward. Inconsistencies in associations among clinical studies are most notably due to the natural degenerative cascade as a result of aging. Despite advances in quantifying PSM FI and degenerative intervertebral disc (IVD) pathology, their mechanistic structure-function relationship in cLBP remains poorly understood. PSM FI is most commonly quantified using conventional summary measurements of overall mean FI% within a muscle cross-sectional area or volumetric region. However, summary measurements for PSM FI lack granularity as they do not capture specific locations of fat accumulation in the muscle. Identifying specific spatial patterns of muscle FI may better reflect the complex morphology and biomechanical function both between and within individual PSMs, most notably for multifidus (MF). We hypothesized that PSM fat-mapping would reveal distinct FI distribution patterns in relation to cLBP symptoms and proximity to symptomatic IVD degeneration.

METHODS From advanced-sequence water-fat MRI of 40 axial cLBP patients and 21 controls, we examined the spatial distribution of PSM FI in relation to the center of rotation at the L4L5 disc. Cartilage endplate pathology (CEP) was measured based on presence and absence of defects in the cartilage using high-resolution 3D ultrashort echo time. Modic changes (MC) were graded using T1 and T2 standard clinical sequences. Disc degeneration was scored using Pfirrmann Grade (PG). Using statistical parametric mapping (SPM) t-tests, we compared FI patterns for Multifidus (MF), Erector Spinae (ES), and Psoas between patients and controls, and to the presence and severity of adjacent degenerative IVD pathology.

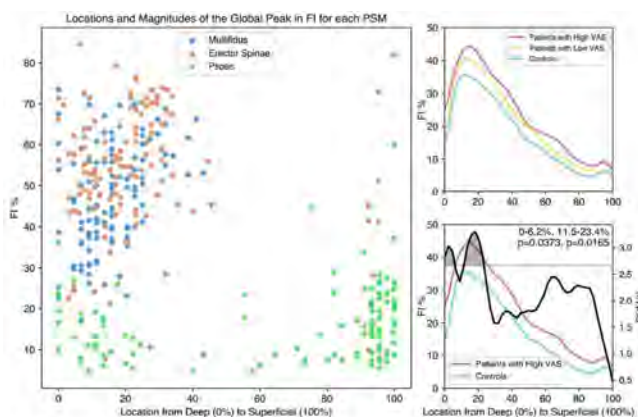


Figure 1. Stratifying subjects into three groups using subject reported pain severity (VAS) shows a shift in MF FI between groups, focused near the peak of the FI distribution in the deep MF Left: The location of the MF and ES global peak in FI consistently falls in the deep region of the muscle, whereas there is more variability in peak location in the Psoas. Only the MF global peak magnitude is significantly different between patients and controls. Right: SPM analysis shows significant differences in FI distribution at the global peak in MF FI between patients with high VAS and controls (bottom). Patients with low VAS scores were not different from controls, showing a pain-associated shift in FI localized at the deep MF. Differences in FI were deemed significant between groups if the SPM(t) (solid black line) for a given region surpassed the critical threshold (dashed black line). Regions of significance (clusters) are shaded for visualization. The shaded area of a given cluster is associated with the strength of significance.

RESULTS The spatial distribution of PSM FI differs between PSMs and according to symptoms and the adjacent degenerative IVD pathology. We identified specific regions with higher FI% in patients versus controls, specifically in the deep MF and intermediate to superficial Psoas ($p < .05$ - $p < .001$) but not in the ES. There was also a significant difference in FI% distribution related to degenerative IVD pathology (CEP, PG, MC) concentrated in the deep to intermediate regions of the MF ($p < .05$ - $p < .001$) and the intermediate to superficial regions of the ES ($p < .05$ - $p < .001$) and Psoas ($p < .05$ - $p < .001$). The location and magnitude of the global peak in FI differed between PSMs (Figure 1; Left). The magnitude of the global peak in MF FI was 6.5 percent points higher for patients ($49.3\% \pm 12.8\%$) compared to controls ($42.8\% \pm 14.8\%$). Furthermore, the region of MF closest to the disc center of rotation appears most susceptible to FI in the presence of symptomatic IVD degeneration (Figure 1).

DISCUSSION Our study identified spatial distribution patterns of FI in the PSMs, particularly in the deep regions of the MF, as a potential diagnostic biomarker that may also provide granular mechanistic insights into spine biomechanics related to cLBP, as well as advancing the use of prior summary measures limited to overall muscle FI.

ACKNOWLEDGEMENTS Supported by NIH HEAL Initiative award numbers R01AR63705, U19 AR076737-01 and UH3 AR076719.

Automated analysis of the lumbar paravertebral muscles in MRI: an accurate tool for large-scale clinical studies

Frank Niemeyer¹, Annika Zanker¹, René Jonas¹, Youping Tao¹, Fabio Galbusera^{3,2}, Hans-Joachim Wilke¹

1. Ulm University, Ulm

2. Schulthess Clinic, Zurich, Switzerland

3. IRCCS Istituto Ortopedico Galeazzi, Milan

Introduction. The scientific study of sarcopenia gained high attention in recent years and is nowadays one of the most discussed issues in the field of the health of ageing subjects. Imaging studies about sarcopenia and its relationship with spinal disorders require the segmentation of the muscles in the images, which is very labour-intensive if performed manually and poses a practical limit to the number of investigated subjects. This study aimed at developing a deep learning-based tool able to fully automatically perform an accurate segmentation of the lumbar muscles in axial MRI scans, and at validating the new tool on an external dataset of prospectively acquired images of a group of healthy volunteers.

Methods. A set of 60 axial MRI images of the lumbar spine was retrospectively collected from a clinical database. Psoas major, quadratus lumborum, erector spinae, and multifidus were manually segmented by an expert operator in all available slices, using a published method as a reference. The dataset was used to train and validate a deep neural network able to segment muscles automatically, with an architecture derived from the U-Net and incorporating several modifications. Subsequently, the network was externally validated on images purposely acquired from 22 healthy volunteers.

Results. The neural network provided excellent outputs from a qualitative point of view when employed on the external validation set (Figure). A three-dimensional reconstruction of the shape of the paravertebral muscles showed realistic anatomies from a perceptual point of view, with smooth surfaces and limited artefacts (Figure). The Jaccard index for the individual paravertebral muscles calculated for the 22 subjects of the external validation set ranged between 0.862 and 0.935 with respect to the manual segmentations performed by an expert operator, demonstrating a generally excellent performance of the network. Cross-sectional area and fat fraction of the muscles were in agreement with published data; the male subjects showed generally higher cross-sectional areas of all muscles with respect to females, while the fat fraction was larger in females than in males and generally increased with age.

Conclusions. The externally validated deep neural network was able to perform the segmentation of the paravertebral muscles in axial MRI scans in an accurate and fully automated manner, and is therefore a suitable tool to perform large-scale studies in the field of spinal disorders and sarcopenia, overcoming the limitations of non-automated methods.

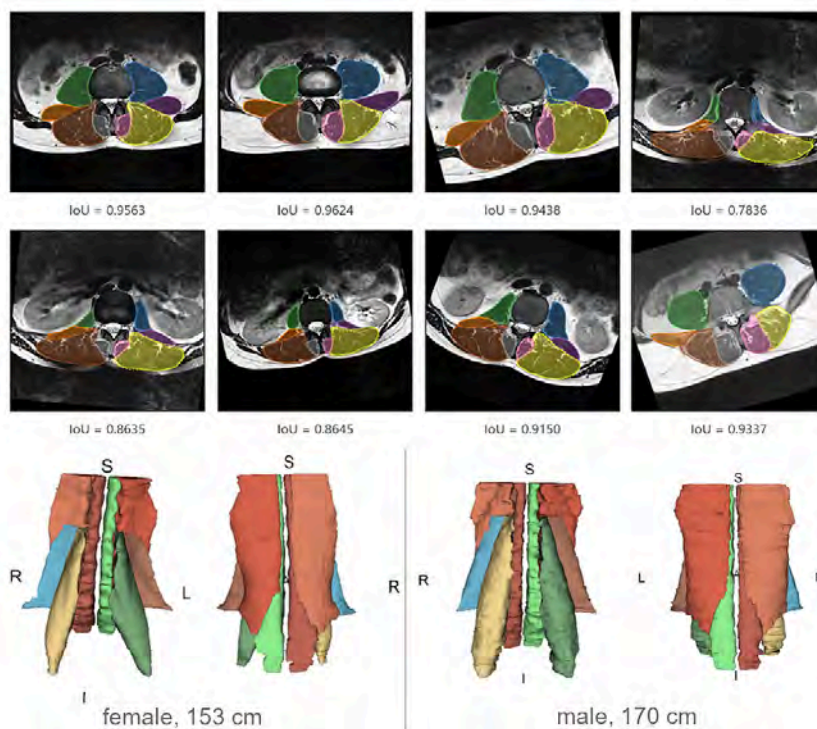


Figure caption. Exemplary segmentations performed on axial T2-weighted slices of the lumbar spine showing the relative Jaccard index ("IoU") (top). Exemplary three-dimensional reconstructions of the paravertebral muscles of two healthy volunteers (bottom).

The Impact of Frailty on Postoperative Complications in Geriatric Patients Undergoing Multi-Level Lumbar Fusion Surgery

Andy Ton¹, Shane Shahrestani¹, Nima Saboori¹, Xiao Chen¹, Allexander Ballatori¹, Jeffrey C Wang¹, Zorica Buser¹

1. Keck School of Medicine, University of Southern California, Los Angeles, CA, United States

Introduction: Increased age is a well-established risk factor for perioperative complications. Using age, however, may lead to crude generalizations given that patients present with varying degrees of comorbidities, cognition, and physical capabilities across all ages. Frailty, alternatively, utilizes a wide array of physical and mental assessments and better reflects physiological age than chronological age. With such a large proportion of lumbar fusions indicated for degenerative disorders amongst geriatric patients, it is important to stratify risk using an indicator that incorporates both age and functional capacity rather than using age alone. Despite the high incidence of degenerative spine conditions in elderly patients, efforts to better understand the impact of frailty in spine surgery have only recently emerged. To address this paucity within the literature, this study evaluates the impact of frailty status on postoperative complications in patients undergoing multi-level lumbar fusions.

Methods: The Nationwide Readmission Database (NRD) was retrospectively queried between 2016 and 2017 for patients receiving multi-level lumbar fusions. Demographics, frailty status, and relevant complications were queried at index admission and readmission intervals. Nearest-neighbor propensity score matching 1:1 cohorts was implemented to identify 3,544 patients in each frail and non-frail cohorts with similar demographic characteristics, diagnoses, and procedures. Patients under age 65, with spinal neoplasms, or spinal trauma were excluded. Primary outcome measures included perioperative complications and 30-, 90, and 180-day complication and readmission rates. Perioperative complications of interest were infection, urinary tract infection (UTI), and posthemorrhagic anemia and only pertain to complications occurring between index procedure and discharge. Complications assessed at 30- and 90-days included infection, acute kidney failure (AKI), thromboembolism, wound dehiscence, hardware failure, neurological injury, and mortality. At 180-days, complications of interest were hardware failure and mortality. Secondary outcome measures included inpatient length of stay (LOS), adjusted all-payer costs, and discharge disposition. The analysis used nonparametric Mann-Whitney U testing and odds ratios.

Results: Frail patients encountered higher rates of perioperative complications including posthemorrhagic anemia (OR: 1.73, 95%CI: 1.50-2.00, $p < 0.0001$), infection (OR: 2.94, 95%CI: 2.04-4.36, $p < 0.0001$), UTI (OR: 2.57, 95%CI: 2.04-3.26, $p < 0.0001$), and higher rates of non-routine discharge (OR: 2.07, 95%CI: 1.80-2.38, $p < 0.0001$). Frail patients had significantly greater LOS and total all-payer inpatient costs compared to non-frail patients ($p < 0.0001$). Frailty was associated with significantly higher rates of 90-day (OR: 1.43, 95%CI: 1.18-1.74, $p = 0.0003$) and 180-day (OR: 1.28, 95%CI: 1.03-1.60, $p = 0.02$) readmissions and higher rates of wound dehiscence at 90 days (OR: 2.21, 95%CI: 1.17-4.44, $p = 0.02$).

Discussion: Patient frailty status functions as a meaningful, independent predictor of postoperative outcomes in patients undergoing multi-level lumbar fusion. The present study observed significantly increased rates of all perioperative complications in frail patients. Frail patients were also significantly more likely to be readmitted at 90- and 180-days and demonstrated higher rates of wound dehiscence at 90-day readmission. Finally, frailty was associated with significantly greater LOS, total all-payer inpatient costs, and non-routine discharges. These findings highlight the importance of frailty status, particularly in multi-level lumbar fusions, and provide implications for its substantive role in determining surgical candidacy, perioperative management, and postoperative follow-up planning.

Appropriate Telemedicine Utilization in Spine Surgery: Results From a Delphi Study

Sravisht Iyer¹, Patawat Bovonratwet¹, Dino Samartzis², Andrew J. Schoenfeld³, Howard S. An², Waleed Awwad⁴, Scott L. Blumenthal⁵, Jason P.Y. Cheung⁶, Peter B. Derman⁵, Mohammad El-Sharkawi⁷, Brett A. Freedman⁸, Roger Hartl⁹, James D. Kang³, Han Jo Kim¹, Philip K. Louie¹⁰, Steven C. Ludwig¹¹, Marko H. Neva¹², Martin H. Pham¹³, Frank M. Phillips², Sheeraz A. Qureshi¹, Kris E. Radcliff¹⁴, K. Daniel Riew¹⁵, Harvinder S. Sandhu¹, Daniel M. Sciubba¹⁶, Rajiv K. Sethi¹⁷, Marcelo Valacco¹⁸, Hasan A. Zaidi³, Corinna C. Zygourakis¹⁹, Melvin C. Makhni³

1. Hospital for Special Surgery/Cornell Medical Center Program - New York, NY, New York, NY, United States
2. Department of Orthopedic Surgery, Rush University Medical Center, Chicago, Illinois, United States
3. Department of Orthopaedic Surgery, Brigham and Women's Hospital, Boston, MA, USA
4. Department of Orthopaedic Surgery, King Saud University, Riyadh, Saudi Arabia
5. Department of Orthopaedic Surgery, Texas Back Institute, Dallas, TX, USA
6. Department of Orthopaedic Surgery, The University of Hong Kong, Queen Mary Hospital, Hong Kong
7. Department of Orthopaedic Surgery, Assiut University Medical School, Assiut, Egypt
8. Department of Orthopaedic Surgery, Mayo Clinic, Rochester, MN, USA
9. Department of Neurosurgery, Weill Cornell Brain and Spine Center, Weill Cornell Medicine, New York Presbyterian Hospital, New York, NY, USA
10. Virginia Mason Medical Center, Neuroscience Institute, Seattle, WA, USA
11. Department of Orthopaedic Surgery, University of Maryland School of Medicine, Baltimore, MD, USA
12. Department of Orthopaedic Surgery, Tampere University Hospital, Tampere, Finland
13. Department of Neurosurgery, University of California San Diego School of Medicine, San Diego, CA, USA
14. Department of Orthopaedic Surgery, Thomas Jefferson University, Rothman Institute, Township, NJ, USA
15. Department of Orthopaedic Surgery, Columbia University Medical Center, The Spine Hospital at NewYork-Presbyterian, New York, NY, USA
16. Department of Neurosurgery, Zucker School of Medicine at Hofstra, Long Island Jewish Medical Center and North Shore University Hospital, Northwell Health, Manhasset, NY, USA
17. Virginia Mason Medical Center and University of Washington, Seattle, WA, USA
18. Hospital Churruca Visca, Buenos Aires, Argentina
19. Department of Neurosurgery, Stanford University, Palo Alto, CA, USA

Introduction: Several studies have shown high patient satisfaction associated with telemedicine during the COVID-19 peak pandemic period as well as after easing of restrictions. As this technology will most likely continue to be employed, there is a need to define appropriate utilization. Therefore, the objective of the current study were to obtain expert consensus on best practices for appropriate telemedicine utilization in spine surgery.

Methods: An expert panel consisting of 27 spine surgeons from various countries was assembled in February 2021. A two-round consensus-based Delphi method was used to generate consensus statements on various aspects of telemedicine (separated as video visits or audio visits) including themes, such as patient location and impact of patient diagnosis, on assessment of new patients. Topics with $\geq 75\%$ agreement were categorized as having achieved a consensus.

Results: The expert panel reviewed a total of 59 statements. Of these, 32 achieved consensus. The panel had consensus that video visits could be utilized regardless of patient location and that video visits are appropriate for evaluating as well as indicating for surgery multiple common spine pathologies, such as lumbar stenosis, lumbar radiculopathy, and cervical radiculopathy. Finally, the panel had consensus that video visits could be appropriate for a variety of visit types including early, mid-term, longer-term post-operative follow-up, follow-up for imaging review, and follow-up after an intervention (i.e. physical therapy, injection).

Conclusions: This is the first study, to our knowledge, to provide expert consensus on best practices for appropriate telemedicine utilization in spine surgery. To summarize, there was consensus that video-based telemedicine could be utilized regardless of patient location, is sufficient for evaluation and indication of surgery for multiple common spine pathologies, such as lumbar stenosis, lumbar radiculopathy, as well as cervical radiculopathy, and could be appropriate for various visit types. The results of the current study help elaborate optimal conditions and criteria for implementation of telemedicine in the evaluation of patients with spine conditions.

Figure 1: Summary of Select Consensus Statements

Location	Can provide safe and appropriate care to patients located in a different state and country using video-based telemedicine .
Diagnosis	Can adequately evaluate and indicate for surgery new patients using video-based telemedicine for lumbar stenosis, lumbar radiculopathy, and cervical radiculopathy.
Physical Exam	Can adequately assess gait abnormalities but not special tests for cervical myelopathy through video-based telemedicine .
Need for in person visit	In-person visit prior to surgery is necessary after initial video-based telemedicine visit for cervical myelopathy and deformity.
Visit Types	Both video-based and audio-based telemedicine are appropriate for early, mid-, longer-term follow-up, follow-up for imaging review, and follow-up after intervention.

Table 1. Expert panel characteristics.

CHARACTERISTIC	TOTAL = 27
Specialty	
Orthopaedic Surgeon	22
Neurosurgeon	5
Academic Rank	
Full Professor	12
Associate Professor	6
Assistant Professor	6
Not Applicable	3
Average Years in Practice	14.7 years
Practicing Country	
United States	22
Saudi Arabia	1
Argentina	1
Finland	1
Hong Kong	1
Egypt	1

Table 2. Impact of patients' location on ability to provide safe and appropriate care via video and audio based telemedicine.

IMPACT OF PATIENT LOCATION ON TELEMEDICINE	Yes	No	Maybe
CONSENSUS (>=75%):			
Can provide safe and appropriate care to patients located in a different state using video-based telemedicine	89.29%	3.57%	7.14%
Can provide safe and appropriate care to patients located in a different country using video-based telemedicine	82.14%	7.14%	10.71%
STRONG AGREEMENT (>=66%):			
Patients' physical location does NOT affect ability to provide care using telemedicine platforms	66.67%	29.63%	3.70%
NO CONSENSUS:			
Can provide safe and appropriate care to patients located in a different state using audio-based telemedicine	55.56%	33.33%	11.11%
Can provide safe and appropriate care to patients located in a different country using audio-based telemedicine	48.15%	33.33%	18.52%

Table 3. Diagnoses where a positive or negative consensus was reached regarding telemedicine for video- and audio-based visits.

	Video-based telemedicine visit		Audio-based telemedicine visit	
	Adequately evaluate new patients	Indicate new patients for surgery	Adequately evaluate new patients	Indicate new patients for surgery
Lumbar stenosis	✓	✓	SA	
Lumbar radiculopathy	✓	✓		
Cervical myelopathy			X	X
Cervical radiculopathy	✓	✓		
Deformity	SA		X	X

✓ (Check mark) = positive consensus (i.e., >=75% AGREE that video based visits allow for adequate evaluation of patients with lumbar stenosis); x = negative consensus (i.e., >=75% DISAGREE that audio-based visits are sufficient to evaluate patients with cervical myelopathy); SA = Strong agreement (66% <= AGREE <= 75%); Blank = no consensus reached

Table 4. Consensus for physical exam maneuvers performed through video-based visits.

Using a telemedicine video conferencing visit, do you feel you can adequately assess:	Yes	No	Undecided
Upper extremity strength	37.04%	51.85%	11.11%
Lower extremity strength	55.56%	44.44%	0%
Neurologic deficits	37.04%	48.15%	14.81%
Gait abnormalities	75.00%	17.86%	7.14%
Special tests for cervical myelopathy	7.14%	75.00%	17.86%
Special tests for lumbar stenosis	37.04%	51.85%	11.11%
Special tests for lumbar radiculopathy	37.04%	55.56%	7.41%
Special tests for cervical radiculopathy	48.15%	37.04%	14.81%
Special tests for deformity	40.74%	40.74%	18.52%

Table 5. Diagnoses where a positive or negative consensus was reached regarding whether an in person visit prior to surgery was considered "best practice" or necessary.

	In-person visit prior to surgery is best practice after initial video telemedicine evaluation	In-person visit prior to surgery is necessary after initial video telemedicine evaluation
Lumbar Stenosis	SA	
Lumbar Radiculopathy	SA	
Cervical Myelopathy	✓	✓
Cervical Radiculopathy	✓	SA
Deformity	✓	✓

✓ (Check mark) = positive consensus (i.e., >=75% AGREE that it is best practice to see patients with cervical myelopathy in person prior to surgery); SA = Strong agreement (66% <= AGREE <= 75%); Blank = no consensus reached

Table 6. Visit types where audio- and video-based visits may be appropriate.

	Video-based telemedicine visit	Audio-based telemedicine visit
Early post-operative visit (2-6 weeks)	✓	✓
Mid-term post-operative visit (3-6 month)	✓	✓
Longer term post-operative visit (>6 month)	✓	✓
Post-operative wound issues	SA	X
Follow up visit for imaging review	✓	✓
Follow up visit after an intervention (e.g., injection or physical therapy)	✓	✓

✓ (Check mark) = positive consensus (i.e., >=75% AGREE that a video visit is adequate for a longer-term post-operative visit); x = negative consensus (i.e., >=75% DISAGREE that audio-based visits are adequate for evaluation of post-operative wound issues); SA = Strong agreement (66% <= AGREE <= 75%); Blank = no consensus reached

Social Vulnerability is an Important Contributor to Racial Disparities in the Safety of Spine Surgery

Ian D Engler^{2,1}, Kinjal D Vasavada², Megan E Vanneman³, Andrew J Schoenfeld⁴, Brook I Martin³

1. University of Pittsburgh, Pittsburgh, PA

2. Tufts University, Boston, MA, USA

3. University of Utah, Salt Lake City, UT, United States

4. Brigham & Women's Hospital, Boston, MA, USA

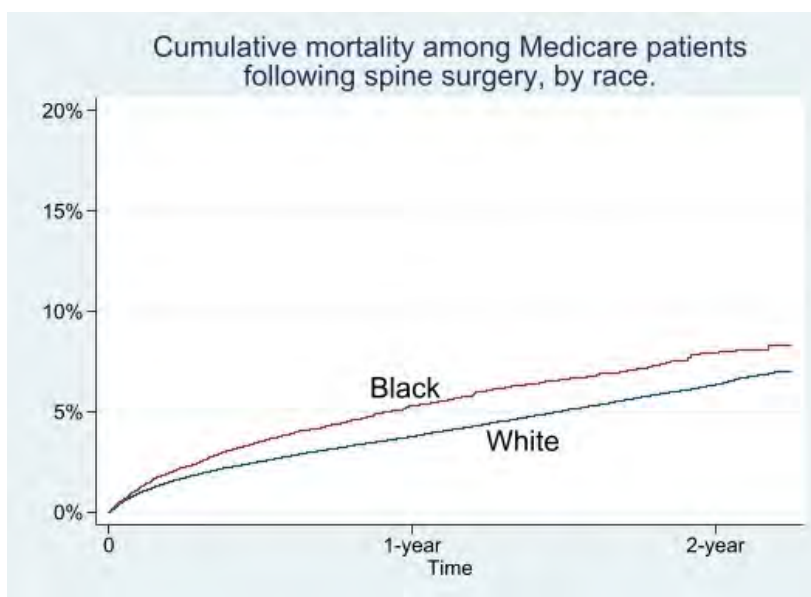
Introduction: People of color in the United States have an increased risk for delayed surgery, complications, readmissions, and mortality following spine surgery. Social determinants of health represent the complex conditions of an individual's lived environment, including the social structure and economic systems that affect health. The contribution of the Center for Disease Control's community-level Social Vulnerability Index (SVI) as a social determinant of racial disparities in the safety of spine surgery is unknown.

Methods: We performed a retrospective analysis of Medicare claims from 2015-2017 to identify racial differences in the rates of mortality, readmission, and complications among patients undergoing spine surgery. We included fee-for-service beneficiaries aged 65 or older with a hospital Diagnosis Related Group (DRG) code for spinal surgery as defined by Medicare, including cohorts labeled as "cervical fusion", "fusion, except cervical", "anterior-posterior combined fusion", "complex fusion", and "back or neck surgery, except fusion". Our primary independent variable was race, which was coded as "black" (Black or African American), "white" (white or Caucasian), and a combined "other" (includes other, Asian, Hispanic Ethnicity, and North American Native). The SVI reflects community disadvantage at the U.S. Census Tract level in socioeconomic (poverty, work, education, income), household composition and disability, minority and language, and housing and transportation domains. Logistic regression and propensity-matched analyses adjusted for age, sex, comorbidities, and spine cohort were used to calculate the percentage of disparities between black and white patients explained by SVI.

Results: A total of 209,137 eligible Medicare beneficiaries met inclusion criteria for this analysis. The majority of the population (89.8%) was white, with 5.6% black. Unadjusted rates of surgical safety measures among black and white patients, respectively, were 2.3% and 1.7% for mortality, 17.1% and 14.4% for readmission, 22.3% and 18.6% for complications without associated readmission, and 27.2% and 25.1% for complications with readmission. Logistic regression and propensity-matched analyses without factoring in SVI showed significantly increased rates of mortality, readmission, and complications in black patients compared to white patients. Adding SVI into the models explained 9.4-28.6% of the difference in safety measures between black and white patients, depending on the measure. Most notably, SVI explained 20.0-28.6% of the disparity in mortality rates between black and white patients.

Discussion: Social vulnerability explains up to nearly 30% of the racial health disparities in safety measures between black and white Medicare beneficiaries following spine surgery. This finding is consistent with an Institute of Medicine report that showed socioeconomic status, racism, and culture each explain roughly one-third of disparities encountered in the United States. Focused policies to support vulnerable communities may lead to a meaningful reduction in racial health disparities.

Figure 1: Unadjusted cumulative mortality rate following spine surgery among Medicare beneficiaries, by race.



Healthcare Resource Utilization and Costs Two Years Pre and Post Lumbar Spine Surgery for Stenosis: A National Claims Cohort Study of 22,182 Cases

Jayme CB Koltsov¹, Todd F Alamin¹, Kirkham B Wood¹, Ivan Cheng², Serena S Hu¹

1. Stanford University School of Medicine, Redwood City, CALIFORNIA, United States

2. St. David's Healthcare, Austin, TX

Introduction: Improved understanding of the pre and postoperative trends in costs and healthcare resource utilization (HCRU) is needed to better inform patient expectations and aid in the development of strategies to minimize the significant healthcare burden associated with lumbar spine surgery. The purpose of this study was to examine the time course of costs and HCRU surrounding lumbar spine surgery in a national claims cohort.

Methods: Longitudinal analyses of adult patients undergoing elective primary single-level lumbar surgery for stenosis from the IBM® MarketScan® Research Databases 2007—2015 were performed. Patients were required to have continuous health plan enrollment 2 years pre- and postoperatively. Outcomes included monthly rates of HCRU (15 categories) and monthly gross covered payments (2015 US dollars) overall, by HCRU category, and by whether they were spine versus non-spine-related. All available patients were utilized for analysis of HCRU. For analysis of payments, patients on non-capitated health plans providing accurate financial information were analyzed. Trends in payments and HCRU were plotted on a monthly basis pre- and post-surgery and assessed with regression models. Relationships with demographics, surgical factors, and comorbidities were assessed with repeated measures generalized estimating equations.

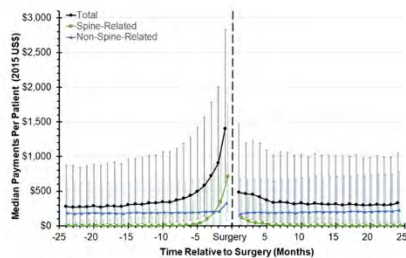


Figure 1. Median monthly healthcare payments for the 2 years pre and post lumbar spine surgery for stenosis. Error bars denote interquartile ranges.

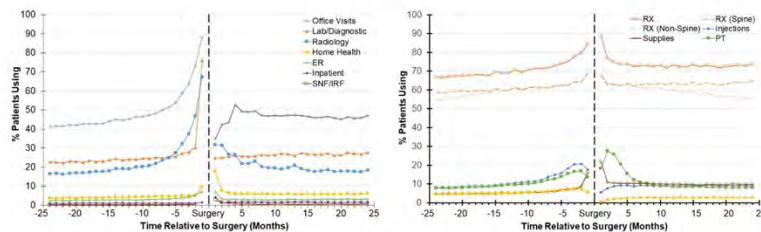


Figure 2. Trends in the percent of patients using each HCRU category for 2 years pre- and postoperatively (split into 2 panels for readability).

Results: The final cohort included 22,182 patients (age 58 ± 13 years, 48.9% female). 27.1% of cases involved a fusion. Payments rose steeply 6 months prior to surgery, reaching a peak of \$1,402 (\$634, \$2,827) 1 month prior to surgery (Figure 1). This was driven by an increase in radiology, office visits, PT, injections, prescription medications, ER encounters, and inpatient admissions (Figure 2). In the first month postoperatively, payments achieved levels lower than 5 months preoperatively. The median monthly payments continued to decline gradually over the 2 years postoperatively primarily due to a decrease in non-spine-related payments. Most HCRU categories remained elevated 2 years postoperatively relative to 2 years preoperatively; however, patients aged 4 years over the course of follow up. Patients with a fusion component to their surgeries had higher payments and HCRU preoperatively, and this did not

resolve postoperatively. Variations in payments and HCRU were evident among plan types, with patients on employer-sponsored supplemental Medicare coverage utilizing more inpatient, ER, and inpatient rehabilitation & skilled nursing facilities. Patients on high-deductible plans had fewer payments and HCRU across all categories; however, we are unable to distinguish whether this was due to using fewer services or due to payment out of pocket. By 2 years postoperatively, 54% of patients had lower median monthly healthcare payments relative to 2 years preoperatively, and when looking at spine-related care, specifically, 68% had lower payments

Discussion: This is the first study to characterize time trends in direct healthcare payments and HCRU over an extended period preceding and following spine surgery. Despite patients aging 4 years over the course of longitudinal follow up, half lower overall median monthly healthcare payments and nearly 7 in 10 had lower spine-related healthcare payments 2 years postoperatively relative to 2 years preoperatively. Differences among plan types potentially highlight disparities in access to care and plan-related financial mediators of patients' healthcare resource utilization.

THE INFLUENCE OF PATIENT PERCEPTIONS ON THE DECISION TO UNDERGO SURGERY FOR LUMBAR SPINAL STENOSIS

Alaa El Chamaa¹, Jacquelyn Marsh¹, Rick Hu², Chris Bailey¹, Michele C. Battie¹

1. Western University, London, ON, Canada

2. The University of Calgary, Calgary, Alberta, Canada

Introduction: Lumbar spinal stenosis (LSS) is primarily a degenerative condition among older adults associated with narrowing of the spinal canal affecting the neurovascular structures contained within. LSS is the most common diagnosis associated with spine surgery in adults over 65 and the decision to undergo elective spine surgery may be the most consequential decision patients with this condition make. The aim of this study was to examine patient-related factors that may affect surgical treatment decision-making for LSS.

Methods: We used data from the Alberta Lumbar Spinal Stenosis Study, a prospective cohort study on prognostic factors and outcomes in LSS, to investigate the association between baseline factors and subsequent spine surgery for LSS within two years. Participants of the inception cohort, formed at the time of clinical imaging, completed a structured interview at baseline. Measures included the Swiss Spinal Stenosis (SSS) Physical Function and Symptom Severity subscales, the Oswestry Disability Index (ODI), the Health Utilities Index (HUI3) for health-related quality of life, number of comorbidities, and a series of questions on participants' beliefs about spine surgery benefits and risks, and satisfaction with prior care and continuing life with current symptoms. Surgery was determined from self-report during interviews and administrative health data through two years of follow-up. Data analysis included univariate and multivariable logistic regression.

Results: Of the 245 participants from the original cohort with the diagnosis of LSS, 225 (92%, mean age 65.6+11.7) were included in the present study. Within two years of baseline interviews, 56 underwent spine surgery (mean age 63.9/SD 10.8) and 169 did not (mean age 66.2/SD 11.9). In the univariate logistic regression analyses, the ODI, HUI3, SSS Physical Function and Symptom Severity subscales, level of satisfaction with continuing life with current symptoms (negatively correlated), belief that surgery would help their current condition, and satisfaction with prior care (negatively correlated) were all significantly associated with the decision to undergo spine surgery within two years. In the multivariable analysis, the only factors that remained significantly associated with the decision to undergo spine surgery were *level of satisfaction with continuing life with current symptoms* (7-point ordinal scale) with a regression coefficient of -0.413 (-0.816, -0.01, $p < 0.001$) and *patients' beliefs that surgery would help their current condition* (4-point ordinal scale) with a regression coefficient of 1.157 (0.693, 1.621, $p = 0.035$).

Discussion: We found that patients' level of dissatisfaction living with their current symptoms, and beliefs about the benefits of surgery, were more predictive of the decision to undergo spine surgery for lumbar spinal stenosis than perceptions of the risks of surgery, which were similarly high for both surgical and non-surgical groups, or level of LSS-related pain and disability, sex or age. This finding emphasizes the importance of providing patients with evidence-informed, realistic expectations about surgical outcomes.

Full-endoscopic Transforaminal Discectomy is Non-inferior and Cost-effective compared to Microdiscectomy for Sciatica: Two-year results of a randomized controlled trial

Pravesh Gadhradi¹, Sidney Rubinstein², Maurits van Tulder², Biswadji Sanjay Harhangi³

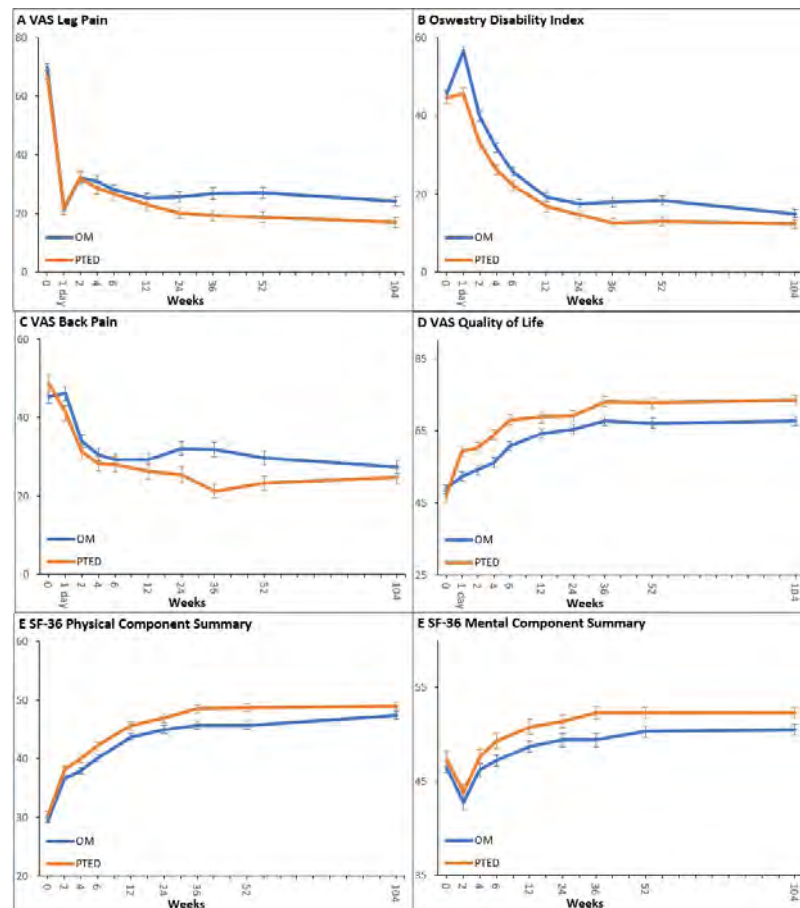
1. Weill Cornell Medicine, Rotterdam, ZUID-HOLLAND, Netherlands

2. Health Sciences, Vu University, Amsterdam

3. Neurosurgery, Erasmus MC, Rotterdam

Introduction Open microdiscectomy (OM) is the current standard procedure to treat sciatica caused by lumbar disk herniation. Percutaneous transforaminal endoscopic discectomy (PTED) is an alternative procedure which is performed under local anesthesia. It is uncertain whether if PTED is non-inferior in treating sciatica compared to OM.

Methods A pragmatic, multicenter, non-inferiority, randomized controlled trial was conducted in which patients were randomized between PTED or OM in a 1:1 ratio. Patients between 18-70 years of age with at least 6 weeks of excessive radiating pain were recruited from 4 participating centers. The primary outcome is self-reported leg pain measured by the 0-100 Visual Analogue Scale (VAS) with a non-inferiority margin of 5. Secondary outcomes include self-reported ODI, back pain, costs, QALYs, health-related quality of life and self-perceived recovery. Outcomes were measured the day following surgery, at 2, 4, and 6 weeks, and at 3, 6, 9, and 12, 24 months. Data were longitudinally analyzed according to the intention-to-treat principle.



Results A total of 613 were randomized to either PTED (n=304) or OM (n=309). At 24 months, 92% of the patients had follow-up data available. At 24 months, the adjusted between group difference of the VAS leg pain was 7.3 in favor of PTED (17.0 ± 22.4 vs. 24.3 ± 26.5). Back pain was less in the PTED-group during the first 12 months but showed no differences at 24 months compared to the OM group. All other secondary patient-reported outcomes such as the ODI, VAS quality of life, SF-36 physical and mental component summary, QALYs, self-perceived recovery of symptoms and satisfaction with treatment, showed small but statistically more favorable results for the PTED-group. Complications rates appear similar between both groups, while estimated perioperative blood loss and length of hospital stay was smaller in the PTED-group. Rate of repeated surgery at 24 months was similar between both groups.

Except for costs of the surgery itself, all other costs were lower for PTED than OM. Cost-effectiveness acceptability curves indicated that the probability of PTED being cost-effective compared with OM was almost 100% for leg pain and QALYs, regardless of the willingness-to-pay.

MCIDs. Furthermore, PTED is cost-effective compared to OM in treating sciatica. Therefore, based on these study results, implementation of PTED as an invasive treatment option for sciatica is warranted.

Discussion PTED is non-inferior to OM in the treatment of sciatica at 24 months of follow-up and clinical outcomes appear to be more favorable for PTED albeit not exceeding established

Clinical Outcome of Lumbar Hybrid Surgery in a Consecutive Series of Patients with Long-term Follow-up

Richard Guyer¹, Scott L Blumenthal¹, Jessica L Shellock¹, Jack E Zigler¹, Donna D Ohnmeiss²

1. Center for Disc Replacement at the Texas Back Institute, Plano, TX, USA

2. Texas Back Institute Research Foundation, Plano, TX, United States

INTRODUCTION: Many patients with symptomatic lumbar degenerative disc disease (DDD) are affected at more than one level. When non-operative treatment fails to provide adequate relief, multilevel surgery may be considered. Lumbar total disc replacement (TDR) was introduced as an option to fusion. Some disc levels are not amenable to TDR and fusion is preferable at that level. Hybrid surgery, involving TDR at one level and fusion at the adjacent segment, has been introduced as an option to fusing multiple levels. The purpose of this study was to investigate the long-term clinical outcome of patients undergoing lumbar hybrid surgery for treating symptomatic lumbar DDD at more than one level.

METHODS: A consecutive series of 296 patients undergoing lumbar hybrid surgery was identified beginning with the first case experience in 2005. Operative data and clinical outcome data including visual analog scales (VAS) assessing back and leg pain as well as Oswestry Disability Index (ODI) scores were recorded from charts and previous study records. Current data were collected from charts, mailings, and telephone calls. Data on re-operations were also collected from charts and patient contact. All patients were at least 2 years post-operative. The mean follow-up duration was 67.9 months with a maximum of 196 months. A total of 647 levels were operated with TDR implanted in 319 levels and 328 levels undergoing either stand-alone ALIF or combined anterior/posterior fusion. The most common combination for hybrid surgery was TDR at L4-5 and fusion at L5-S1.

RESULTS: The mean blood loss was 100.7 ml. There were statistically significant improvements ($p < 0.001$) in the mean values of all three clinical outcome measures: VAS back pain scores improved from 6.7 to 3.2; VAS leg pain scores improved from 4.3 to 2.0; and ODI scores improved from 45.6 to 25.0. There was no significant differences in the pain and function scores for patients with minimum 10-year follow-up vs. those with shorter follow-up duration. Re-operation occurred in 16.2 % of patients (see table). The majority of these were for the removal of painful posterior instrumentation at the fusion level (6.1%). Re-operations directly involving the TDR level occurred in 9 patients (3.0%). One patient reported multiple re-operations on the returned mailing, but insufficient detail was provided to determine the procedure(s) performed.

Re-op	TDR level	Fusion level	Both levels	Neither level
Posterior instrumentation removal	NA	18	0	0
TDR migration	3	NA	0	0
Posterior fusion for facet joint arthrosis	1	0	0	0
Decompression	0	0	4	0
Superficial wound infection	0	0	2	0
Approach related	0	0	1	0
Multilevel deformity	0	0	1	0
Sacroiliac joint fusion	0	0	0	5
Spinal cord stimulator	0	0	0	7
Adjacent segment degeneration	0	0	0	5
Other: 1 patient reported multiple re-operations on returned mailing, insufficient detail provided				

DISCUSSION: The results of this study support that for many patients with symptomatic DDD arising from more than one disc, hybrid surgery is a viable surgical option. Significant improvement was demonstrated in pain and function scores with no difference in scores among patients with more than 10 year follow-up. The most commonly occurring re-operation was removal of painful posterior fixation, unrelated to the TDR.

Comparison of Value Per Operative Time Between Anterior Lumbar Interbody Fusion and Lumbar Disc Arthroplasty: A Propensity Score-Matched Analysis

Junho Song^{2,1}, **Austen Katz**¹, **Terence Ng**¹, **Eric Neufeld**¹, **Nipun Sodhi**¹, **Jeff Silber**¹, **David Essig**¹, **Sheeraz Qureshi**², **Sohrab Virk**¹

1. Northwell Health Long Island Jewish Medical Center, New Hyde Park, NY, United States

2. Hospital for Special Surgery, New York, NY, United States

Introduction: Fusion procedures, such as anterior lumbar interbody fusion (ALIF), have been the standard for surgical management of lumbar degenerative disc disease¹. Lumbar disc arthroplasty (LDA) is a more novel technique which has been shown to be a highly effective alternative to fusion^{2,3}. It has been suggested that the motion-preserving nature of disc arthroplasty provides a unique benefit of reduction in adjacent segment disease⁴. Despite the growing evidence demonstrating its effectiveness, LDA rates have not increased significantly in recent years^{5,6}. A likely contributing factor is insurers' denial of coverage due to fear of late complications, reoperations, and unknown secondary costs^{7,8}. Although the cost analyses of LDA have been performed, no prior study has compared the physician reimbursement rates of lumbar fusion and LDA⁹. Therefore, the aim of this study was to compare the relative value units (RVUs) per minute of ALIF and LDA.

Methods: This retrospective cohort study utilizes data obtained from the American College of Surgeons National Surgical Quality Improvement Program database. Patients who underwent ALIF or LDA between 2011 and 2019 were identified and included based on Current Procedural Terminology (CPT) codes 22558 and 22857, respectively. Exclusion criteria included multilevel, revision, emergency, non-elective, deformity procedures, intraspinal lesion, concomitant cervical procedures, laminectomy, laminotomy, and other posterior procedures. Patients with missing operation time, reoperation, and readmission data were also removed to prevent biases in the results. Statistical analysis was performed using SPSS software (version 28, IBM, Armonk, New York). Propensity score matching analysis was performed with a match tolerance of 0.01 according to demographic characteristics, comorbidities, and preoperative laboratory values. Matched groups were compared via Fisher's exact test and independent t-test for categorical and continuous variables, respectively.

Results: The total cohort prior to matching consisted of 6,722 patients. 502 patients who underwent ALIF were matched with 591 patients who underwent LDA via propensity score matching. There were no differences in sex, race, and ethnicity between the matched groups, but patients in the ALIF group were significantly older on average (48.4 years vs. 43.8 years, $p<0.001$). Hypertension requiring medication (33.9% vs. 25.4%, $p=0.003$), chronic steroid use (2.0% vs. 0.3%, $p=0.032$), and ASA class of 3 or greater (26.7% vs. 21.0%, $p=0.032$) were more common in the ALIF group compared to LDA group (Table 1). Mean RVUs per minute was significantly higher for ALIF compared to LDA (0.431 vs. 0.302, $p<0.001$). In addition, LDA was associated with significantly higher readmission (3.4% vs. 0.0%, $p<0.001$) and reoperation (2.0% vs. 0.4%, $p=0.027$) rates, while morbidity rates were statistically similar (3.6% vs. 2.8%, $p=0.496$). No differences in rates of individual complications were observed (Table 2).

Conclusion: ALIF was associated with significantly higher RVUs per minute compared to LDA. LDA was associated with higher 30-day readmission and reoperation rates. These findings provide valuable evidence for assessing the physician reimbursement and outcomes of surgical treatment options for lumbar degenerative disc disease.

1. Teng I, Han J, Phan K, Mobbs R. A meta-analysis comparing ALIF, PLIF, TLIF and LLIF. *J Clin Neurosci*. Oct 2017;44:11-17. doi:10.1016/j.jocn.2017.06.013
2. Gornet MF, Burkus JK, Dryer RF, Pelozo JH, Schranck FW, Copay AG. Lumbar disc arthroplasty versus anterior lumbar interbody fusion: 5-year outcomes for patients in the Maverick disc investigational device exemption study. *J Neurosurg Spine*. May 17 2019;31(3):347-356. doi:10.3171/2019.2.Spine181037
3. Shultz BN, Wilson AT, Ondeck NT, et al. Total Disc Arthroplasty Versus Anterior Interbody Fusion in the Lumbar Spine Have Relatively a Few Differences in Readmission and Short-term Adverse Events. *Spine (Phila Pa 1976)*. Jan 1 2018;43(1):E52-e59. doi:10.1097/brs.0000000000002337
4. Xu S, Liang Y, Zhu Z, Qian Y, Liu H. Adjacent segment degeneration or disease after cervical total disc replacement: a meta-analysis of randomized controlled trials. *J Orthop Surg Res*. Oct 3 2018;13(1):244. doi:10.1186/s13018-018-0940-9
5. Yoshihara H, Yoneoka D. National trends in the surgical treatment for lumbar degenerative disc disease: United States, 2000 to 2009. *Spine J*. Feb 1 2015;15(2):265-71. doi:10.1016/j.spinee.2014.09.026
6. Salzmann SN, Plais N, Shue J, Girardi FP. Lumbar disc replacement surgery-successes and obstacles to widespread adoption. *Curr Rev Musculoskelet Med*. Jun 2017;10(2):153-159. doi:10.1007/s12178-017-9397-4
7. Heider FC, Mayer HM, Siepe CJ. Lumbar disc replacement: update. *J Neurosurg Sci*. Jun 2015;59(2):169-80.
8. Siepe CJ, Heider F, Wiechert K, Hitzl W, Ishak B, Mayer MH. Mid- to long-term results of total lumbar disc replacement: a prospective analysis with 5- to 10-year follow-up. *Spine J*. Aug 1 2014;14(8):1417-31. doi:10.1016/j.spinee.2013.08.028
9. Stubig T, Ahmed M, Ghasemi A, Nasto LA, Grevitt M. Total Disc Replacement Versus Anterior-Posterior Interbody Fusion in the Lumbar Spine and Lumbosacral Junction: A Cost Analysis. *Global Spine J*. Apr 2018;8(2):129-136. doi:10.1177/2192568217713009

Clinical outcome in decompression-alone versus decompression and instrumented fusion in patients with isthmic spondylolisthesis: a prospective cohort study.

Kayoumars Azizpour¹, Pieter J Schutte^{2,3}, Mark P Arts², Willem Pondaag^{1,3}, Gerrit J Bouma⁴, Maarten H Coppes⁵, Ewout W Steyerberg⁶, Wilco C Peul^{1,2,3}, Carmen L.A. Vleggeert-Lankamp^{1,2,7}

1. Leiden University Medical Center, 's-gravenhage, ZUID-HOLLAND, Netherlands

2. Neurosurgery, Haaglanden Medical Center, 's-gravenhage, Zuid-Holland, Nederland

3. Neurosurgery, Alrijne Hospital, Leiden & Leiderdorp, Zuid-Holland, Netherlands

4. Neurosurgery, OLVG, Amsterdam, Noord-Holland, Netherlands

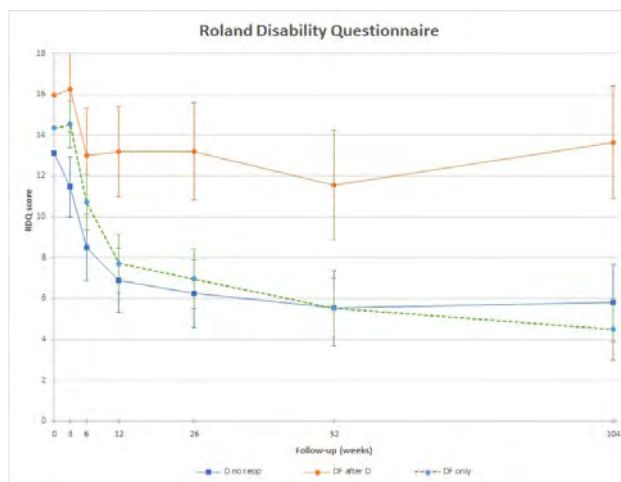
5. Neurosurgery, University Medical Center Groningen, Groningen, Netherlands

6. Biostatistics, Leiden University Medical Center, 's-gravenhage, Zuid-Holland, Nederland

7. Neurosurgery, Spaarne Gasthuis, Haarlem/Hoofddorp, Noord-Holland, Netherlands

Introduction: In the surgical treatment of neurogenic claudication and/or radiculopathy in isthmic spondylolisthesis it is debatable whether instrumented fusion (DF) has to be added to decompression (D). To that end a randomized controlled trial was performed randomizing patients to both treatment options, and the two year analysis demonstrated a superior outcome for DF. Eligible patients that declined randomization were included in an observational cohort study. The objective of the current study is to analyze this larger population, to assess a possible difference in outcome between randomized and patient-preferred treatment, and to evaluate whether a subgroup of patients would benefit more of a particular treatment strategy.

Methods: Between 2008–2017, 172 patients with low-graded isthmic spondylolisthesis enrolled in this study (84 in RCT) and were followed up for 2 years. Primary outcome measures were Roland Disability Questionnaire and patient's perceived recovery. Visual-analogue scale (VAS) for back pain and for leg pain, and the proportion of reoperated patients were evaluated as secondary outcome measures through Kaplan-Meier analyses. Repeated-measurement analysis of variance was performed. Subgroup analyses were performed for gender, age, BMI, smoking, patient preference, and DF after D.



Results: 85 patients received decompression-alone (D), and 87 patients received decompression-and-fusion (DF). Both groups were similar at baseline. At 12-week follow-up, improvement of Roland Disability Questionnaire scores were comparable (D: 5.1 points 95% CI [3.7 to 6.5] and DF: 6.6 points 95% CI [5.3 to 8.0], $p = 0.38$). In contrast, both VAS back pain (25.5 points 95% CI [18.6 to 32.3] in D versus 35.9 points 95% CI [29.1 to 42.6], $p = 0.034$) and leg pain (23.5 points 95% CI [13.3 to 33.7] in D versus 34.0 points 95% CI [24.1 to 43.8], $p = 0.04$) improved significantly more in the DF-group.

At 2-year follow-up, DF-group showed 4.1 points more improvement in RDQ scores (9.8 95% CI [8.3 to 11.4] versus 5.7 95% CI [4.1 to 7.3], ($p < 0.001$), and more improvement in VAS-back pain (-17.4 (95% CI [-27.2 to -7.5] $p = 0.001$). VAS-leg pain did not differ between both groups ($p = 0.1$). Perceived recovery was comparable in both groups at 12-week follow-up (37% (D) versus 58.3% (DF; $p = 0.08$), but superior for DF (74% versus 47.1%; $p < 0.001$) at 2-year follow-up. None of the subgroup analysis demonstrated a

superior outcome for mere decompression. During the 2-year follow-up period, cumulative probability of reoperation was 38.6% in the D-group and 6.2% in the DF-group ($p < 0.001$). RDQ score was significantly worse in patients that were submitted to DF after D (Figure 1).

Discussion: In patients with isthmic spondylolisthesis, decompression and instrumented fusion showed superior functional outcome and perceived recovery compared to decompression-alone at two-year follow-up. Additionally, decompression and fusion resulted in less reoperations, and adding fusion to decompression in second stage led to inferior functional outcome. No subgroups could be discerned to have a better outcome with mere decompression. Therefore, we recommend decompression and instrumented fusion over decompression-alone as a primary surgical treatment option in isthmic spondylolisthesis.

A Canadian Spine Outcomes and Research Network study of radiographic alignment outcomes with different surgery type for degenerative lumbar spondylolisthesis

Patrick Thornley¹, Jennifer Urquhart², Raymond Andrew Glennie³, Y. Raja Rampersaud⁴, Charles Fisher⁵, Chris Bailey¹

1. London Health Sciences Centre, London, ON, Canada

2. Lawson Health Research Institute, Western University, London, ON, Canada

3. Department of Surgery, Division of Orthopaedic Surgery, Dalhousie University, Halifax, Nova Scotia, Canada

4. Department of Surgery, Division of Orthopaedic Surgery, The Schroeder Arthritis Research Institute, Krembil Research Institute, University Health Network, Toronto, ON, Canada

5. Combined Neurosurgical and Orthopaedic Spine Program, University of British Columbia, Vancouver, British Columbia, Canada

Introduction: The importance of sagittal balance and pelvic parameters as they pertain to overall spinal balance are well-established for the deformity and isthmic spondylolisthesis population. The overall effect of differing surgical intervention type for patients undergoing interventions for degenerative lumbar spondylolisthesis (DLS) is not known. Furthermore, the magnitude of postoperative alignment effects based on a particular surgical intervention for DLS is not established. The objective of this investigation was to assess the effect of decompression versus posterolateral fusion versus interbody fusion on spinal alignment among patients undergoing surgery for DLS.

Methods: Retrospective analysis of the Canadian Spine Outcomes and Research Network (CSORN) prospective study on the assessment and management of DLS was performed. Patients who had decompression alone (D), posterolateral fusion (PLF) or interbody fusion (IB) between 2015 and 2020 and were one-year postoperative were included. Sagittal vertical axis (SVA), lumbar lordosis (LL) and pelvic incidence (PI) were measured preoperatively and one-year postoperatively. Patients were divided into two groups based on whether their one-year postoperative spinal alignment improved/stayed the same or deteriorated by subtracting the one-year measure from baseline. The proportion of patients and the magnitude of the change was compared among surgery types.

Results: Two-hundred forty-eight patients had LL (D=69, IB=147, PLF=32), 192 patients had SVA (D=52, IB=114, PLF=26) and 243 patients had PI-LL (D=71, IB=137, PLF=32) measures at one-year. The majority of patients saw an improvement in alignment and the proportion of patients that improved was similar among surgery groups (SVA: 50%, 35%, 41%, $P=0.148$; PI-LL: 64%, 66%, 56%, $P=0.617$; LL: 62%, 71%, 63% $P=0.385$ for D, IB and PLF respectively). LL deteriorated an average of $6.1\pm 5.7^\circ$ and was similar among surgery types. Patients undergoing decompression only saw a smaller improvement in LL compared to IB ($P=0.039$; D= $6.5\pm 6.0^\circ$, IB= $9.7\pm 7.6^\circ$, PLF= $9.1\pm 7.0^\circ$). SVA deteriorated an average of 14 ± 18 mm and was similar among surgery types. PLF saw the greatest improvement in SVA (48 ± 51 mm vs D, 24 ± 39 mm ($P=0.002$) vs IB 18.1 ± 23 ($P=0.003$)). PI-LL deteriorated an average of 7.1 ± 6.0 mm and improved an average of 11.1 ± 9.2 mm and did not differ among surgery types.

Discussion: Overall spinal alignment either remains the same or improves with the vast majority of patients undergoing surgery for DLS regardless of surgical intervention. In this large, longitudinally followed multi-centre patient cohort, more invasive surgical intervention in the form of interbody or posterolateral fusion for DLS was not associated with a statistically significant between group alignment improvement compared to decompression alone.

Comparing osteostimulative bone graft substitutes in interbody fusion – is there a difference?

Paul Licina¹, Emma Johnston¹, Chelsea Lehmann¹

1. Brisbane Private Hospital Research Group, Brisbane, QLD, Australia

INTRODUCTION:

A number of bone graft substitutes that claim to be both osteoconductive and bioactive (sometimes termed 'osteostimulative') are now available. They purport to combine the advantages of osteoconductive and osteoinductive graft substitutes without the associated drawbacks and complications. The aim of this study was to evaluate the clinical and radiological effectiveness of three such bone graft substitutes used in patients undergoing single level lumbar fusion.

METHODS:

A consecutive series of patients undergoing primary single level transforaminal lumbar interbody fusion (TLIF) for degenerative lumbar conditions were allocated either BonAlive® putty MIS (BonAlive® Biomaterials Ltd., Turku, Finland) (n=20) or NanoBone® SBX putty (Artoss GmbH, Rostock, Germany) (n=19) bone graft substitute and prospectively studied. The graft was used alone (without autologous supplementation) in the cage, in the disc space and in the lateral gutters. This data was then compared with a historical cohort comprised of patients who had previously undergone primary single level TLIF using Actifuse (Baxter, Unterschleißheim, Germany) bone graft substitute in a similar fashion (n=63). Fusion rate was assessed at 12 months postoperatively using computed tomography (CT) by an independent radiologist blinded to bone graft type. Radiological parameters included bone growth through the cage, bone growth around the cage, new end-plate cyst formation and new end-plate sclerosis. Patient reported outcome measures were assessed via the Oswestry Disability Index (ODI), and the Back and Leg Visual Analog Scale (VAS) preoperatively and at 6 weeks, 6 months, and 12 months postoperatively.

RESULTS:

There was no statistical difference in fusion rates between groups, with BonAlive® achieving a rate of 80%, NanoBone® a rate of 84% and Actifuse a rate of 87% at 12 months. The presence of new endplate sclerosis was significantly lower ($p=0.016$) with Actifuse (24%) than with BonAlive® and NanoBone® (55% and 42%). There was no significant difference in new endplate cyst formation; BonAlive® 30%, NanoBone® 32% and Actifuse 17%. There were no significant differences for ODI, back VAS and leg VAS between the groups at any of the postoperative timepoints. At 12 months BonAlive® patients had an improvement in ODI of 58%, NanoBone® patients an improvement in ODI of 59% and Actifuse an improvement in ODI of 66%, compared with baseline. Four patients did not reach minimally clinically important difference in ODI and VAS improvement: 2 in the BonAlive® group, 1 in the NanoBone® group and 1 in the Actifuse group. There were no significant graft-related complications. There were no reoperations.

DISCUSSION:

All three bone graft materials exhibited similar radiological results and patient reported outcomes. Results were comparable with other materials and techniques to the point that these bone graft substitutes could be considered as satisfactory replacements for autologous bone graft.

Asymmetry in lumbar trunk muscle activation in adolescent idiopathic scoliosis during forward flexion: A computational study based on musculoskeletal modelling approach

Tito Bassani¹, Matteo Panico^{1,2}, Dominika Ignasiak³, Fabio Galbusera¹

1. IRCCS Istituto Ortopedico Galeazzi, Milan, Italy

2. Department of Chemistry, Materials and Chemical Engineering "Giulio Natta", Politecnico di Milano, Milan, Italy

3. Institute for Biomechanics, ETH Zurich, Zurich, Switzerland

Introduction: Adolescent idiopathic scoliosis (AIS) is a three-dimensional deformity of the spine occurring in the general population with prevalence between 2 and 3%, the aetiology and pathogenesis of which are poorly understood¹. Investigating the relationship between scoliosis and biomechanical measures such as trunk muscle activation would provide valuable information for the understanding of the pathomechanics of the AIS spine. Unfortunately, this measure is difficult to be acquired *in vivo* due to the invasiveness of the measurement procedure, and few data (from surface EMG) are available from the literature^{2,3}. An alternative strategy is represented by computational simulation based on musculoskeletal modelling approach, which allows calculating muscle activation in assigned postures and movements by means of inverse dynamic analysis. In this regard, a thoracolumbar model with articulated ribcage, developed in AnyBody software⁴ (AnyBody Technology, Denmark), has been recently adapted to replicate the spine alignment in AIS^{5,6}. The present study exploits the available model to replicate the subject-specific spine alignment in a dataset of 66 AIS subjects with scoliotic curve with apex in the thoracolumbar/lumbar region (Lenke type 3, 5, and 6) and Cobb angle of the curve ranging from 10° to 45°. Movement of trunk forward flexion from 0° (relaxed standing) to 45° is simulated (distributed from T12 to the fixed sacrum, Fig. 1e). The asymmetry in erector spinae (ES) and multifidus (MF) muscle activation in the lumbar region (T12-L5) is calculated between the convex and concave side of the scoliotic curve, and distinguished between mild scoliosis (Cobb 10°-25°, 32 subjects) and moderate (Cobb 25°-45°, 34).

Methods: The exploited dataset was acquired by our group in a previous clinical study⁷. The subjects underwent radiological examination in orthostatic position by EOS system (EOS Imaging, France), providing the simultaneous acquisition of the frontal and lateral plane images (Fig. 1a,b). The 3D spine alignment was replicated in the musculoskeletal model (Fig. 1c,d) and scaling by subject's weight and height was performed³. The asymmetry in ES and MF muscle activation was evaluated as (convex - concave)/(convex + concave) side of the scoliotic curve, providing zero value in case of balanced activation, and positive and negative values (from 0 to ±1) for larger activation in the convex and concave side, respectively.

Results: During flexion, the asymmetry of ES and MF activation showed decreasing and increasing trend, respectively, both for mild and moderate scoliosis (Fig. 2a,b and d,e). Compared to relaxed standing, ES activation was found more negative at maximum flexion (Fig. 2c,f), with mean±sd equal to 0.02±0.11 and -0.09±0.21 (mild scoliosis), and -0.01±0.15 and -0.11±0.25 (moderate), respectively. Conversely, MF exhibited larger positive values: 0.03±0.19 and 0.29±0.14 (mild), and -0.02±0.18 and 0.29±0.13 (moderate).

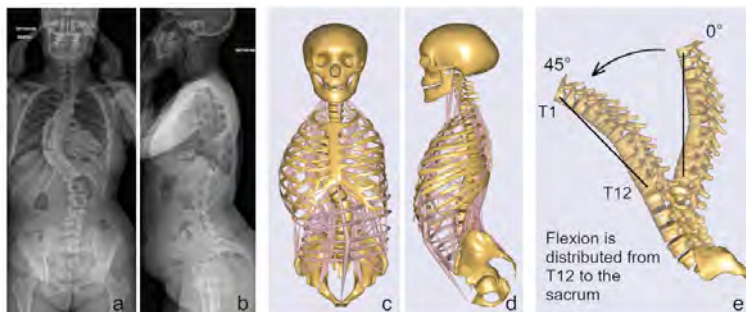


Figure 1. Frontal and lateral radiographic images of one subject (a,b) and corresponding musculoskeletal model in AnyBody software (c,d). Right panel (e): spine in relaxed standing (0°) and at maximum of trunk flexion (45°), with muscles and ribcage not shown to better illustrate the spine alignment.

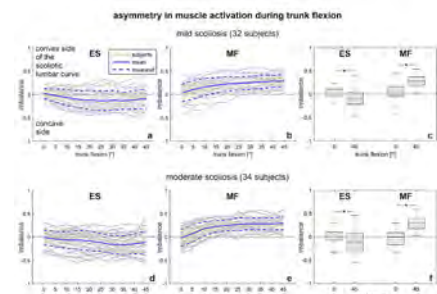


Figure 2. Asymmetry in ES and MF muscle activation in the lumbar section (from T12 to L5) during the trunk flexion movement in case of mild and moderate scoliosis (19,8) and (24), respectively). Right column: box and whiskers plot of muscle activation at minimum (0°) and maximum (45°) level of trunk flexion (c,d), with * indicating statistical difference with $p < 0.05$.

Discussion: The results pointed out concurrent opposite activation of ES and MF muscle in the lumbar region during forward flexion. This novel finding, based on computational simulation, suggests the presence of muscle synergy between ES (more involved to straighten the trunk) and MF (stabilizing the motion segments) in presence of scoliosis. Larger datasets and the simulation of additional movements in the other planes are needed to provide deeper understanding

- de Sèze M, Cugy E. Pathogenesis of idiopathic scoliosis: a review. *Ann Phys Rehabil Med.* 2012 Mar;55(2):128-38. English, French. doi: 10.1016/j.rehab.2012.01.003. Epub 2012 Jan 27. PMID: 22321868.
- Kwok G, Yip J, Cheung MC, Yick KL. Evaluation of Myoelectric Activity of Paraspinal Muscles in Adolescents with Idiopathic Scoliosis during Habitual Standing and Sitting. 2015 *BioMed Research International* 958450.
- Cheung J, Halbertsma JP, Veldhuizen AG, Sluiter WJ, Maurits NM, Cool JC, van Horn J. A preliminary study on electromyographic analysis of the paraspinal musculature in idiopathic scoliosis. 2005 *European Spine Journal: Official Publication of the European Spine Society, the European Spinal Deformity Society, and the European Section of the Cervical Spine Research Society* 14, 130–137.
- Ignasiak D, Dendorfer S, Ferguson SJ. Thoracolumbar spine model with articulated ribcage for the prediction of dynamic spinal loading. *J Biomech.* 2016 Apr 11;49(6):959-966. doi: 10.1016/j.jbiomech.2015.10.010. Epub 2015 Nov 30. PMID: 26684431.

5. Barba N, Ignasiak D, Villa TMT, Galbusera F, Bassani T. Assessment of trunk muscle activation and intervertebral load in adolescent idiopathic scoliosis by musculoskeletal modelling approach. *J Biomech*. 2021 Jan 4;114:110154. doi: 10.1016/j.jbiomech.2020.110154. Epub 2020 Nov 27.
6. Bassani T, Cina A, Ignasiak D, Barba N, Galbusera F. Accounting for Biomechanical Measures from Musculoskeletal Simulation of Upright Posture Does Not Enhance the Prediction of Curve Progression in Adolescent Idiopathic Scoliosis. *Front Bioeng Biotechnol*. 2021 Sep 10;9:703144. doi: 10.3389/fbioe.2021.703144. eCollection 2021.
7. Bassani T, Stucovitz E, Galbusera F, Brayda-Bruno M. Is rasterstereography a valid noninvasive method for the screening of juvenile and adolescent idiopathic scoliosis? *Eur Spine J*. 2019 Mar;28(3):526-535. doi: 10.1007/s00586-018-05876-0. Epub 2019 Jan 7. PMID: 30617835.

Comparison of Relative Value Units and 30-Day Outcomes Between Primary and Revision Pediatric Spinal Deformity Surgery

Junho Song¹, Austen Katz¹, David Essig¹, Sohrab Virk¹

1. Northwell Health Long Island Jewish Medical Center, New Hyde Park, NY, United States

Introduction: Spinal deformity in the pediatric population can pose a significant detriment to quality of life and development¹. Spinal deformity surgery can be performed to correct coronal and sagittal deformities such as scoliosis and kyphosis. Unfortunately, pediatric spinal deformity surgery is frequently complicated by the need for reoperation, with a revision rate of nearly 10%². However, there is limited literature on outcomes following primary vs. revision deformity surgery in the pediatric population. In addition, no prior study has evaluated for a difference in physician reimbursement rates between primary and revision pediatric spinal deformity surgery. The purpose of this study is to compare the relative value units (RVUs) per minute and 30-day outcomes between primary and revision pediatric spinal deformity surgery.

Methods: This study was performed using data obtained from the American College of Surgeons National Surgical Quality Improvement Program Pediatric database. Patients between 10 and 18 years of age who underwent posterior spinal deformity surgery between 2012 and 2019 were identified using Current Procedural Terminology codes 22800, 22802, and 22804. Patients undergoing anterior-only or concurrent anterior-posterior fusions were excluded to ensure patient cohort homogeneity. Exclusion criteria also included missing demographic or clinical data, malignancy, active infection, and emergent procedure.

Univariate analysis was performed using Pearson Chi-square tests to compare baseline demographic and clinical characteristics. Univariate and multivariate regression models were used to assess the independent impact of revision surgery on RVUs and postoperative outcomes. Backwards stepwise regression model was utilized to account for all baseline differences in demographics and comorbidities, with entry at $p=0.05$ and removal at $p=0.1$.

Results: The study cohort included 15,055 patients with 358 patients who underwent revision pediatric spinal deformity surgery. Patients in the revision group were most likely to be younger (13.7 vs. 14.3 years, $p<0.001$) and male sex (38.0% vs. 30.4%, $p=0.002$). Multiple comorbidities were more common in the revision group as detailed in Table 1. Revision surgery more commonly required osteotomy (13.7% vs. 8.3%, $p=0.002$). All variables included in Table 1 were adjusted for in the subsequent regression models.

Univariate analysis revealed higher total RVUs (71.09 vs. 60.51, $p<0.001$), RVUs per minute (0.27 vs. 0.23, $p<0.001$), readmission rate (6.7% vs. 4.0%, $p=0.012$), and reoperation rate (7.5% vs. 3.3%, $p<0.001$) for the revision surgery group. Morbidity rates were found to be statistically similar between revision and primary surgery (65.3% vs. 69.3%, $p=0.108$). In addition, deep surgical site infection (2.2% vs. 0.9%, $p=0.010$), pulmonary embolism (0.3% vs. <0.1%, $p=0.010$), and urinary tract infection (1.7% vs. 0.7%, $p=0.038$) were more common in the revision group (Table 2). After multivariate regression, the differences in total RVUs, RVUs per minute, reoperation rate, and rate of pulmonary embolism between primary and revision surgery remained statistically significant (Table 3).

Conclusion: Revision pediatric spinal deformity surgery was found to be assigned appropriately higher mean total RVUs and RVUs per minute corresponding to the higher operative complexity compared to primary surgery. Revision surgery was also associated with poorer 30-day outcomes, including higher frequencies of reoperation and pulmonary embolism.

Table 1. Baseline demographic and clinical characteristics

	Primary N (%)	Revision N (%)	p-value
N of subjects	14,697	358	
Age (years), mean±SD	14.3±1.9	13.7±2.1	<0.001*
Female sex	10,223 (69.6%)	222 (62.0%)	0.002*
Black race	2,655 (18.1%)	57 (15.9%)	0.297
Hispanic ethnicity	1,166 (7.9%)	22 (6.1%)	0.215
Comorbidities			
BMI (kg/m ²), mean±SD	22.3±19.2	21.4±6.8	0.190
Ventilator dependence	368 (2.5%)	19 (5.3%)	0.003*
Chronic lung disease	541 (3.7%)	37 (10.3%)	<0.001*
Oxygen support	216 (1.5%)	13 (3.6%)	0.003*
Tracheostomy	194 (1.3%)	10 (2.8%)	0.031
Structural pulmonary abnormality	723 (4.9%)	48 (13.4%)	<0.001*
Esophageal/gastric/intestinal disease	1,420 (9.7%)	54 (15.1%)	0.001*
Developmental delay	3,007 (20.5%)	134 (37.4%)	<0.001*
Seizure disorder	1,448 (9.9%)	42 (11.7%)	0.243
Cerebral palsy	1,483 (10.1%)	50 (14.0%)	0.019*
Structural CNS abnormality	1,911 (13.0%)	84 (23.5%)	<0.001*
Neuromuscular disorder	3,149 (21.4%)	135 (37.7%)	<0.001*
Nutritional support	1,038 (7.1%)	43 (12.0%)	<0.001*
Hematologic disorder	307 (2.1%)	10 (2.8%)	0.348
Inotropic support	268 (1.8%)	3 (0.8%)	0.224
ASA class ≥3	4,262 (29.0%)	199 (55.6%)	<0.001*
Preoperative laboratory values			
Elevated creatinine	20 (0.1%)	1 (0.3%)	0.397
Elevated white blood cells	935 (6.4%)	30 (8.4%)	0.122
Low hematocrit	1,198 (8.2%)	42 (11.7%)	0.016*
Low platelet count	345 (2.3%)	8 (2.2%)	1.000
Operative data			
Operative time, mean±SD	289.08±111.86	296.77±123.37	0.100
Osteotomy	1,121 (8.3%)	43 (13.7%)	0.002*

Fisher's exact test performed for categorical variables; independent t-test performed for continuous variables.

*Statistically significant (p<0.05). SD, standard deviation. BMI, body mass index. CNS, central nervous system. ASA, American Society of Anesthesiologists.

Table 2. Unadjusted RVUs and 30-day outcomes between primary vs. revision surgery

	Primary N (%)	Revision N (%)	p-value
N of subjects	14,697	358	
Total RVUs, mean±SD	60.51±26.73	71.09±26.50	<0.001*
RVUs per minute, mean±SD	0.23±0.14	0.27±0.13	<0.001*
30-day outcomes			
Readmission	593 (4.0%)	24 (6.7%)	0.012*
Reoperation	485 (3.3%)	27 (7.5%)	<0.001*
Morbidity	10,189 (69.3%)	234 (65.3%)	0.108
Complications			
Superficial SSI	115 (0.8%)	6 (1.7%)	0.061
Deep SSI	133 (0.9%)	8 (2.2%)	0.010*
Organ/Space SSI	39 (0.3%)	2 (0.6%)	0.293
Wound dehiscence	91 (0.6%)	1 (0.3%)	0.389
Pneumonia	157 (1.1%)	4 (1.1%)	0.929
Pulmonary embolism	4 (<0.1%)	1 (0.3%)	0.010*
Unplanned intubation	116 (0.8%)	6 (1.7%)	0.064
Renal insufficiency	10 (<0.1%)	1 (0.3%)	0.144
Urinary tract infection	106 (0.7%)	6 (1.7%)	0.038*
Stroke	5 (<0.1%)	0 (0.0%)	0.727
Nerve injury	48 (0.3%)	1 (0.3%)	0.877
Bleeding requiring transfusion	10,039 (68.3%)	229 (64.0%)	0.081
Venous thromboembolism	16 (0.1%)	1 (0.3%)	0.343
Sepsis	109 (0.7%)	4 (1.1%)	0.416
Central line infection	3 (<0.1%)	0 (0.0%)	0.787

Fisher's exact test performed for categorical variables; independent t-test performed for continuous variables. *Statistically significant (p<0.05). RVUs, relative value units. SD, standard deviation. SSI, surgical site infection.

Table 3. Multivariate analysis of impact of revision surgery on RVUs and 30-day outcomes

	Adjusted OR (95% CI)	p-value
RVUs per minute, mean±SD	0.034 (0.017 - 0.056)	<0.001*
30-day outcomes		
Readmission	0.899 (0.510 - 1.585)	0.713
Reoperation	2.066 (1.191 - 3.584)	0.010*
Complications		
Deep SSI	1.257 (0.498 - 3.173)	0.628
Pulmonary embolism	9.890 (1.018 - 96.061)	0.048*
Urinary tract infection	1.143 (0.439 - 2.976)	0.785

*Statistically significant (p<0.05). RVUs, relative value units. SD, standard deviation. SSI, surgical site infection.

- Weinstein SL, Dolan LA, Spratt KF, Peterson KK, Spoonamore MJ, Ponseti IV. Health and function of patients with untreated idiopathic scoliosis: a 50-year natural history study. *JAMA*. 2003 Feb 5;289(5):559-67. doi: 10.1001/jama.289.5.559. PMID: 12578488.
- Kim HJ, Cunningham ME, Boachie-Adjei O. Revision spine surgery to manage pediatric deformity. *J Am Acad Orthop Surg*. 2010 Dec;18(12):739-48. doi: 10.5435/00124635-201012000-00004. PMID: 21119140.

Using a Convolutional Neural Network (CNN) model to quantify longitudinal changes in MRI readings of the lumbar spine.

Amir Jamaludin¹, Jill Urban², Timor Kadir¹, Andrew Zisserman¹, Frances MK Williams³, Jeremy Fairbank^{4,5}

1. Engineering Science, University of Oxford, Oxford, United Kingdom

2. DPAG, University of Oxford, Oxford, United Kingdom

3. Kings College, London, United Kingdom

4. Oxford Spine Group, Banbury, UNITED KINGDOM, United Kingdom

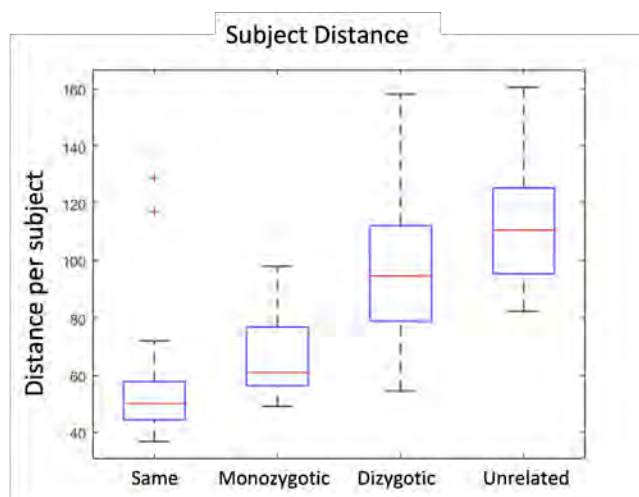
5. NDORMS, University of Oxford, Oxford, United Kingdom

Introduction: Automated MRI systems such as SpineNet¹ enable rapid re-annotation of cohort intervertebral disc traits onto the same objective scale¹, independent of the original MRI annotation systems², and hence allow direct comparisons of degenerative disc gradings between cohorts. Here, we aimed to increase the predictive capability of SpineNet, a Convolutional Neural Network (CNN) model, by training it to examine differences in morphology in images of the same individual taken 10 years apart, and in differences in morphology between individuals. To assess the sensitivity of the system we examined differences between vertebral bodies (volumes) of middle-aged subjects, assuming they were less likely to change morphologically than the intervertebral discs.

Methods: The MRI dataset comprised 920 consented subjects (6327discs) from Twins UK (<https://twinsuk.ac.uk/>). 423 of these subjects have follow-up scans 10-12 years after baseline imaging; these scans were used to examine intra-individual spinal differences.

A model was trained solely on pairs of 3D vertebral body (VB) volumes at each level of the lumbar area (T12 to L5); "same" pairs are pairs sampled from the same individual at different timepoints while "different" pairs are pairs sampled from different individuals ignoring timepoint information. Monozygotic/dizygotic twin pairs were omitted during training. The model was trained to produce a measure of distance (i.e. difference) between the morphology of two VBs, such that the lower the distance, the more similar were the two vertebrae. While distances were calculated per VB pair, here we show the distances summed to give a measure of the distance between two spines i.e. subjects.

Results: This model was sufficiently sensitive to detect differences in morphology of paired vertebrae. The distances for all spine pairings in our dataset, is shown in Figure 1. MR images of the same individual taken 10-12 years apart, had the smallest distance between them, i.e. were most similar. For scans taken at the same time point, as expected, the distance between monozygotic twins, was smaller than between dizygotic twins, with the distance between unrelated individuals, noticeably larger than that between any of their twin pairs.



Conclusions: This study shows a deep learning model can be trained to detect and quantify morphological differences of spinal features such as vertebral bodies in terms of image 'distance'. Here we showed it can be used to detect 'distances' between individuals, and 'distances' between the same individual, imaged at different times. This latter capability would be of particular benefit in longitudinal imaging studies, as it would enable quantitative assessment of morphological changes in the spine.

References:

1. Jamaludin et al; 2017. doi.org/10.1007/s00586-017-4956-3
2. Sambrook et al, 1999, Arthritis Rheum 1999;42:366–372

CD90-positive bone marrow stromal cells in Modic changes associate with bone marrow fibrosis and edema

Stefan Dudli¹, Luca Guidici², Agnieszka Karol³, Christoph Germann⁴, Nadja Farshad-Amacker⁴, Christoph Laux⁵, Michael Betz⁵, Jose Spirig⁵, Florian Wanivenhaus⁵, Florian Brunner⁶, Mazda Farshad⁵, Oliver Distler¹

1. Center of Experimental Rheumatology, University of Zurich, Zurich, Switzerland

2. Institute of Pathology and Molecular Pathology, University Hospital Zurich, Zurich, Switzerland

3. Department of Molecular Mechanisms of Disease, University of Zurich, Zurich, ZURICH, Switzerland

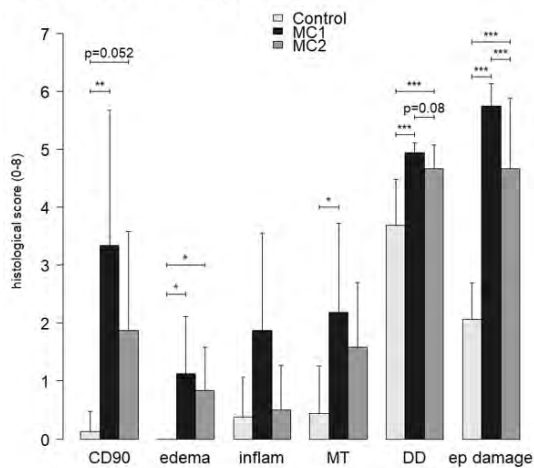
4. Department of Radiology, Balgrist University Hospital, Zurich, Switzerland

5. Department of Orthopedic Surgery, Balgrist University Hospital, Zurich, Switzerland

6. Department of Physical Medicine and Rheumatology, Balgrist University Hospital, Zurich, Switzerland

INTRODUCTION Vertebral bone marrow lesions known as Modic changes are specific for axial low back pain. Fibrosis, inflammation, and enhanced myelopoiesis have been described as hallmarks of Modic changes. CD90-positive bone marrow stromal cells (BMSC) regulate inflammatory myelopoiesis and drive fibrosis of the bone marrow in primary myelofibrosis. However, the role of CD90-positive BMSC in Modic change pathophysiology is unknown. In this study, we investigated CD90-positive BMSC in biopsies from MC and their association with inflammatory and fibrotic markers. We hypothesized that presence of CD90-positive BMSC correlates with bone marrow fibrosis and edema.

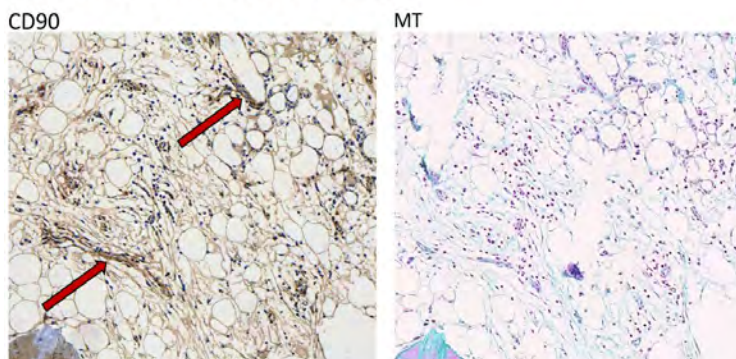
Fig.1 – Histology scores



METHODS This study was approved by the local Ethics Commission and conducted in accordance with the Declaration of Helsinki. From fourteen patients undergoing lumbar spinal fusion twenty-two bone marrow biopsies were taken through the pedicle screw trajectory before screw insertion. Collected patient demographics included age, sex, size, weight, height, BMI, smoker, 10-point visual analogue score (VAS) for back and leg pain (VAS.back, VAS.leg), and Oswestry-Disability-Index (ODI). Two experienced radiologists independently classified MC main type (Control, MC1, MC2), graded disc degeneration (DD)(Pfirman grade 0-5), and endplate damage (Rajasekaran grade 0-6). Biopsies were processed for histology and thin sections were stained with hematoxylin/eosin (HE), Masson trichrome (MT) and analysed with immunohistochemistry for alpha-smooth-muscle-actin (αSMA), type I collagen (COL1), type III collagen (COL3), cellular fibronectin (FN), Thy-1-membran-glykoprotein (CD90), and endoglin (CD105). Two pathologists independently scored immunopositivity (0-8) of αSMA, COL1, COL3, FN, CD90, and CD105, and scored inflammatory infiltrates and edema (=interstitial water) on HE slides (0-8). Scores were compared between MC types with Kruskal Wallis test with Bonferroni correction. Scores were (i) correlated to patient demographics and clinical data and (ii) to each other using Kendall-Tau correlation.

RESULTS There was no difference in patient demographics between MC1, MC2, and control. CD90-positive BMSC were more frequent in MC1 (3.34 ± 2.33 , $p=0.001$) and MC2 (1.88 ± 1.70 , $p=0.052$) compared to control (0.13 ± 0.35) (Fig.1). Edema was not found in control bone marrow but frequently in MC1 (1.13 ± 0.99 , $p=0.015$) and MC2 (0.83 ± 0.75 , $p=0.044$). Scores for inflammatory cell infiltrates above 1.5 were exclusively found in MC1 (1.88 ± 1.69 vs. control 0.38 ± 0.69 , $p=0.081$). Connective tissue in the bone marrow (measured with MT) was increased in MC1 (2.19 ± 1.53 , $p=0.027$) compared to control (0.44 ± 0.82). The discs adjacent to MC1 and MC2 were stronger degenerated, and endplates were more damaged than control discs and endplates (all $p < 0.001$). CD90 correlated with hallmarks of MC1, e.g. edema ($\tau=0.69$, $p < 0.001$), endplate damage ($\tau=0.65$, $p < 0.001$), and DD ($\tau=0.56$, $p=0.002$). CD90 also correlated with the pro-fibrotic markers MT ($\tau=0.48$, $p=0.006$) (Fig.2), COL1 ($\tau=0.44$, $p=0.011$), and FN ($\tau=0.48$, $p=0.006$). Importantly, correlation of MT with VAS.back ($\tau=0.51$, $p=0.068$) suggests that bone marrow fibrosis is linked to back pain in Modic changes.

Fig.2 – Fibrosis in Modic type 1 change



DISCUSSION Correlation of CD90-positive BMSC with pro-fibrotic markers and edema points at a key role of CD90-positive BMSC in MC pathomechanisms. CD90-positive BMSC might be responsible for bone marrow fibrosis in Modic changes similar as in primary myelofibrosis. Inhibiting proliferation and activation of CD90-positive BMSC could become a novel interesting treatment target for MC-related low back pain.

DISCUSSION Correlation of CD90-positive BMSC with pro-fibrotic markers and edema points at a key role of CD90-positive BMSC in MC pathomechanisms. CD90-positive BMSC might be responsible for bone marrow fibrosis in Modic changes similar as in primary myelofibrosis. Inhibiting proliferation and activation of CD90-positive BMSC could become a novel interesting treatment target for MC-related low back pain.

THE NATURAL HISTORY OF MODIC CHANGES - A 5- AND 15-YEAR FOLLOW-UP STUDY

Parnian Saremi^{2,1}, Andrew Leung², Michele C.Battié^{2,1,3}

1. Faculty of Health Science, London

2. Western university, London, ON, Canada

3. Western's Bone and Joint Institute, Lonodn, Ontario, Canada

Introduction

In recent years there has been growing interest in Modic changes (MCs), defined as bone marrow lesions adjacent to the vertebral endplate seen on MRI. There are different types of MCs, with different histopathological correlates. However, the natural history of these lesions, which this study aims to examine, is not well established.

Methods

The community-based study sample comprised 110 men (mean age of 48±8 years) from the Twin Spine Study, shown to be highly representative of the corresponding Finnish population, with baseline, 5-year, and 15-year follow-up MRIs. T1- and T2-weighted sagittal lumbar scans were analyzed at the three time points for all participants. Following training and reliability testing, 1320 endplates (T12-S1) were evaluated for MC presence, type (MC1, MC2, or Mixed MC), and dimensions (anteroposterior, transverse and vertical height) at each time point. To better understand the total changes in size of an MC at follow-up, a Sum of Changes variable was used, which was the sum of changes in size of the three dimensions of an MC. Negative values represented a reduction in size, and positive represented an increase in size.

Results

Intra-rater agreement was found to be almost perfect for classification of MCs ($k=0.81-0.91$). MC2 was the most common type (88% of MCs at baseline, and 89% and 83% at 5- and 15-year follow-up, respectively), with approximately half located at the two lowest disc levels (48-52%). However, MC1s were distributed almost similarly across the lumbar region. The presence of an MC on one endplate, was significantly associated with the presence of an MC on the adjacent endplate ($p<0.001$).

At baseline, MC1s were present on 16(1%) endplates in 12(10%) participants. Five MC1s persisted at 5-year follow-up, however, all MC1s from baseline had converted to other types by the 15-year follow-up. At 5-year follow-up, there were 8 new MC1s on previously normal endplates (6 in the anterior aspect of the endplate). Out of 16 MC1s in baseline, at 5-year follow-up, one resolved completely and 10 converted to either MC2 or Mixed (all Mixed ones converted to MC2 at 15-year follow-up). There were 40 new MC1s at the 15-year follow-up, with 35(88%) arising from normal endplates and five converting from MC2s. Of the new MC1s at 15-year follow-up, 13(32%) covered the entire endplate and 18(45%) were located anteriorly.

Of the MCs that remained as MC2s throughout the study, the mean Sum of Changes in size over follow-up was 1.05 ± 1.05 (on a -9 to 9 scale), suggesting a modest overall increase, but more than 55% had the same transverse, AP and vertical size.

Discussion

This longitudinal study confirmed that MC2 is the most common MC type in men, with MC2, but not other types, mainly located at the lower lumbar endplates. Also, MC1 appears to be a transient phase, with no MC1s at baseline persisting to 15-year follow-up. New MCs mostly occurred in the anterior aspect of the endplate, which may provide clues related to pathogenesis. Complete resolution of MCs can occur, but it is very uncommon.

Lumbar endplate microfracture induces Modic-like changes and pain-related behaviors in rats in-vivo

Dalin Wang^{1,2}, Alon Lai¹, Jennifer Gansau¹, Alan C Seifert³, Yunsoo Lee¹, Jazz Munitz³, Philip Nasser¹, Damien M Laudier¹, Andrew Hecht¹, James C Iatridis¹

1. Leni and Peter W. May Department of Orthopaedics, Icahn School of Medicine at Mount Sinai, New York, NEW YORK, United States

2. Department of Orthopaedics, Nanjing First Hospital, Nanjing Medical University, Nanjing, Jiangsu, China

3. Biomedical Engineering and Imaging Institute, Department of Radiology, Icahn School of Medicine at Mount Sinai, New York, United States

Introduction

Increasing attention has been paid to endplate (EP) injury as having a crucial role in the etiopathogenesis of painful intervertebral disc (IVD) degeneration due to associations of Modic changes (MCs) and pain in clinical^[1]. EP injuries are described to occur through peripheral or central accumulating microfracture, and accumulation of EP microfractures are involved in all types of EP injury^[2]. Models of EP microfracture that progresses to painful conditions are highly needed to better understand pathophysiological mechanisms and screen therapeutics. This study established an EP microfracture model and characterized associated IVD degeneration, vertebral remodeling, and pain-related behaviors.

Methods

Male Sprague-Dawley rats (5 months of age) were randomly divided into 3 groups: Sham (n=6), EP injury+PBS (n=6), EP injury+TNF α (n=7). For the EP injury groups, the proximal EPs of L4-5 and L5-6 were punctured obliquely through the vertebral body using a 0.6 mm K-wire (Fig. 1A). A total of 2.5 ul of PBS or TNF α (0.25 ng in 2.5 ul) were then injected into each IVD following the EP injury. IVD height was quantified using radiography pre-operatively, and at 8 weeks. Behavioral tests (i.e. hind paw von Frey and forepaw grip test) were performed biweekly. Lumbar spines were dissected for MRI and μ CT analyses.

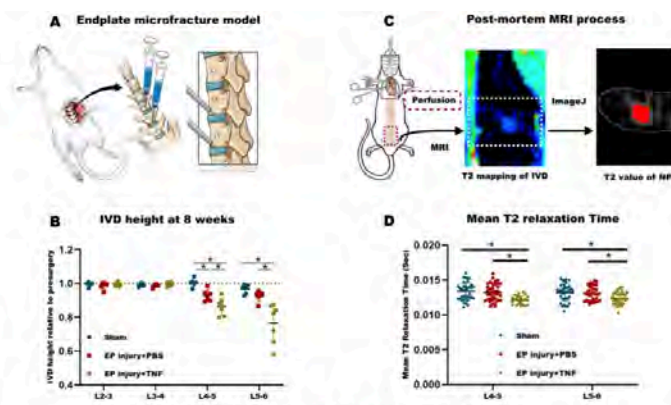


Fig. 1 X-ray&Quantified MRI indicates IVD degeneration * P<0.05

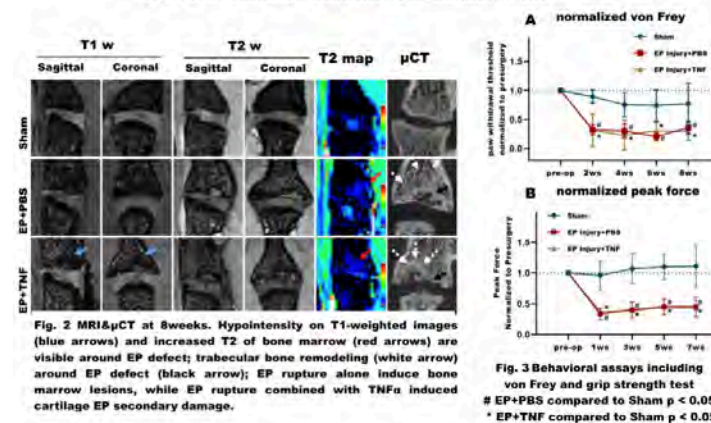


Fig. 2 MRI& μ CT at 8weeks. Hypointensity on T1-weighted images (blue arrows) and increased T2 of bone marrow (red arrows) are visible around EP defect; trabecular bone remodeling (white arrow) around EP defect (black arrow); EP rupture alone induce bone marrow lesions, while EP rupture combined with TNF α induced cartilage EP secondary damage.

Fig. 3 Behavioral assays including von Frey and grip strength test # EP+PBS compared to Sham p < 0.05 * EP+TNF compared to Sham p < 0.05

Results

EP injuries induced IVD degeneration with decreased IVD height and MRI T2 values compared to Sham (Fig. 1B, D). EP injury showed MC type1-like changes around the EP defects on MRI with hypointensity on T1-weighted images and increased T2 of bone marrow being visible in the EP+TNF α group. EP microfracture similarly showed trabecular bone remodeling on μ CT, and EP+TNF α further showed secondary damage in cartilage EP adjacent to the injury (Fig. 2). EP injuries caused significantly decreased paw withdrawal threshold & reduced grip forces (Fig.3), suggesting increased pain sensitivity.

Discussion

Decreased grip force and paw withdrawal threshold following EP microfracture suggest increased pain-like behaviors consistent with axial mechanical pain. EP-driven axial pain is consistent with our biomechanical findings that EP microfracture cause axial instability^[3]. Interestingly, we created an EP injury with size of only ~2% of the average rat lumbar EP surface area^[4], yet this minimal injury appears sufficient to induce axial pain since two injuries groups had identical behavioral results. Most importantly, this EP microfracture model induced Modic-like changes and the EP+ TNF α group appeared to amplify bone marrow/IVD crosstalk to stimulate MC type1-like changes, and these results are consistent with Dudli et al. who found proinflammatory stimulus was critical to induce MC1-like changes^[1]. This EP injury model might therefore be a clinically relevant model involving IVD pro-inflammatory conditions and EP

microfracture accumulation to better understand and screen EP pathophysiology. Further studies will associate pain-related behaviors with signal intensity of MC1-like bone marrow changes to further compare with the human condition, and will assess nervous system changes to inform pain pathomechanisms.

References:

[1]. Dudli+The Spine Journal, 2018 [2]. Lotz +Global Spine, 2013 [3]. Wang+ORS, Poster1432, 2020 [4]. Jaumard+Spine,2015

Acknowledgment: Funded by NIH grants R01AR057397, R01AR078857, and R01EB019980.

Spinal cord sensitization following lumbar endplate microfracture – An In Vivo Rat Model

Alon Lai¹, Kashaf Zaheer^{1,2}, Dalin Wang^{1,3}, Damien M Laudier¹, Venetia Zachariou⁴, James C Iatridis¹

1. Icahn School of Medicine at Mount Sinai, New York, NY, United States

2. Vassar College, Poughkeepsie, NY

3. Department of Spine Surgery, Nanjing First Hospital, Nanjing Medical University, Nanjing, Jiangsu, China

4. Nash Family Department of Neuroscience, and Friedman Brain Institute, Icahn School of Medicine at Mount Sinai, New York, NY, United States

Introduction

Intervertebral disc (IVD) degeneration is highly associated with chronic back pain. Dorsal-root-ganglia (DRG) of peripheral nervous system are reported to be sensitized with upregulation of neuropeptides and pro-inflammatory cytokines from IVD degeneration [1-4]. Animal models are needed to better understand pathophysiological transition from acute spinal injury to chronic pain, and to screen therapeutics. This study identified cross-talk between IVD degeneration and spinal cord by measuring substance P (SubP), a common neurotransmitter in the nervous system, following endplate (EP) microfracture injury-induced IVD degeneration in an in-vivo rat model.

Method

Procedures were IACUC approved. Nineteen male five-month-old Sprague-Dawley rats underwent sham (n=6) or EP injury surgery (n=13). In EP injury groups, L4-5 and L5-6 IVDs were punctured obliquely through their proximal vertebral body using K-wire, and injected with either tumor necrosis factor-alpha (TNF α) (n=7) or PBS (n=6). Back pain-related behaviors (i.e. hindpaw mechanical allodynia and forepaw grip force) were tested biweekly. At 8-weeks after injury, all rats were euthanized after taking radiograph for IVD height measurement. Lumbar spinal cord (corresponding to vertebral level T12-L1) was isolated, and stained for substance P (SubP) using immunohistochemistry with Nissl stain to visualize spinal cord neurons. SubP-immunoreactivity (SubP-ir) area relative to spinal dorsal horn compared between groups.

Results

SubP was found in laminae I-II of spinal cord (Fig1A). SubP-ir area in tended to be higher in both EP injury groups compared to Sham (Fig1B). SubP-ir area was significantly correlated with pain-like behaviors including the peak and average grip force, and had statistical trends in association with von Frey hindpaw withdrawal threshold, and IVD height (Fig1C).

Discussion

This is the first study to demonstrates that EP-injury driven IVD degeneration results in spinal cord sensitization with increased SubP in the dorsal horn of spinal cord in rats 8 weeks after EP injury. The SubP in the spinal cord were mainly localized to laminae I and II where terminations of nociceptive A-delta and C nerve fibers occur [5]. Increased spinal cord SubP was previously reported in animal models of neuropathic pain and inflammation [6-9], suggesting that EP-injury in this study may involve a combination of inflammatory and neuropathic conditions needing further characterization. SubP-ir was significantly correlated with pain-like behaviors as well as IVD height loss in this model suggesting cross-talk between spinal cord and IVD following EP injury, that results in increased pain-like behaviors. These multiple associations across tissues and behaviors observed in this study have clinical implications suggesting that treatment strategies for chronic discogenic pain may require interventions targeting both IVD and neural pathologies.

Acknowledgements: Funded by NIH grants R01AR057397, R01AR078857, and R01EB019980.

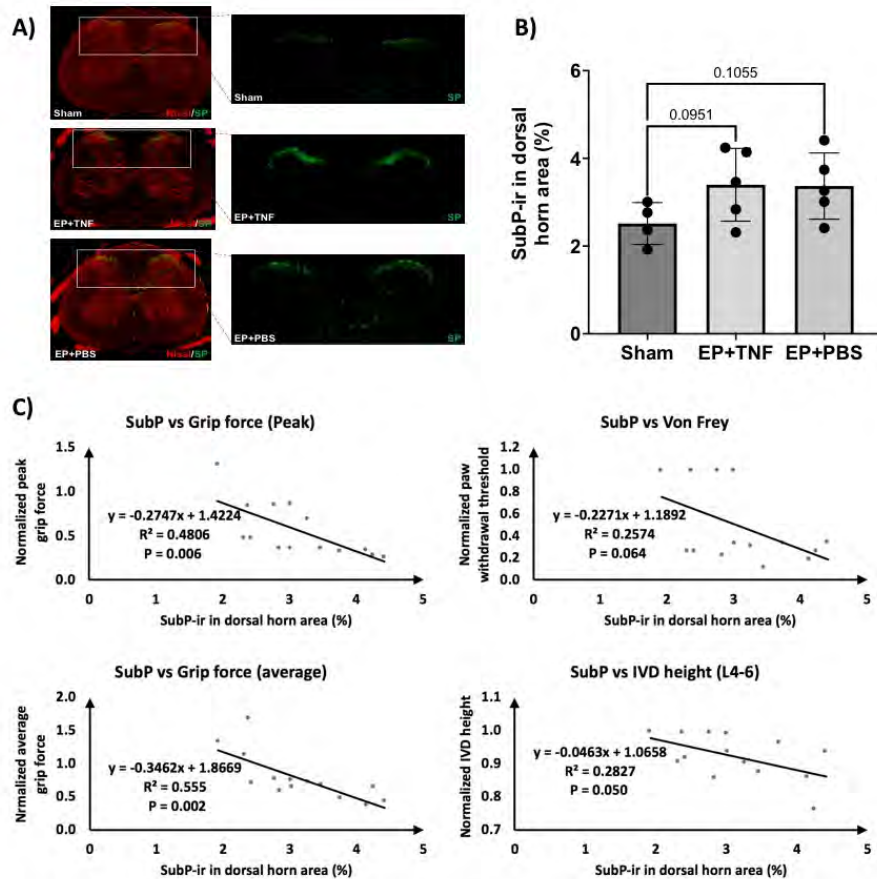


Fig 1. EP injuries induced spinal cord sensitization. (A) Representative images of spinal cord SubP and Nissl staining. (B) Percentage of SubP-ir area in dorsal horn. (C) Correlation analyses for percentage SubP-ir area vs grip force (peak & average), hindpaw withdrawal threshold and IVD height.

- Lai A, Ho L, Evashwick-Rogler TW, Watanabe H, Salandra J, Winkelstein BA, Laudier D, Hecht AC, Pasinetti GM, Iatridis JC. Dietary polyphenols as a safe and novel intervention for modulating pain associated with intervertebral disc degeneration in an in-vivo rat model. *PLoS One*. 2019;14(10):e0223435. Epub 2019/10/03. doi: 10.1371/journal.pone.0223435. PubMed PMID: 31577822; PMCID: PMC6774529.
- Lai A, Moon A, Purmessur D, Skovrlj B, Laudier DM, Winkelstein BA, Cho SK, Hecht AC, Iatridis JC. Annular puncture with tumor necrosis factor-alpha injection enhances painful behavior with disc degeneration in vivo. *Spine J*. 2016;16(3):420-31. Epub 2015/11/28. doi: 10.1016/j.spinee.2015.11.019. PubMed PMID: 26610672; PMCID: PMC4913353.
- Makino H, Seki S, Yahara Y, Shiozawa S, Aikawa Y, Motomura H, Nogami M, Watanabe K, Sainoh T, Ito H, Tsumaki N, Kawaguchi Y, Yamazaki M, Kimura T. A selective inhibition of c-Fos/activator protein-1 as a potential therapeutic target for intervertebral disc degeneration and associated pain. *Sci Rep*. 2017;7(1):16983. Epub 2017/12/07. doi: 10.1038/s41598-017-17289-y. PubMed PMID: 29208967; PMCID: PMC5717052.
- Zhang J, Li Z, Chen F, Liu H, Wang H, Li X, Liu X, Wang J, Zheng Z. TGF- β 1 suppresses CCL3/4 expression through the ERK signaling pathway and inhibits intervertebral disc degeneration and inflammation-related pain in a rat model. *Exp Mol Med*. 2017;49(9):e379. Epub 2017/09/25. doi: 10.1038/emmm.2017.136. PubMed PMID: 28935976; PMCID: PMC5628275.
- Merighi A, Carmignoto G, Gobbo S, Lossi L, Salio C, Vergnano AM, Zonta M. Neurotrophins in spinal cord nociceptive pathways. *Prog Brain Res*. 2004;146:291-321. Epub 2004/01/01. doi: 10.1016/s0079-6123(03)46019-6. PubMed PMID: 14699971.
- Zucoloto AZ, Manchope MF, Borghi SM, Dos Santos TS, Fattori V, Badaro-Garcia S, Camilios-Neto D, Casagrande R, Verri WA, Jr. Probenecol Ameliorates Complete Freund's Adjuvant-Induced Hyperalgesia by Targeting Peripheral and Spinal Cord Inflammation. *Inflammation*. 2019;42(4):1474-90. Epub 2019/04/24. doi: 10.1007/s10753-019-01011-3. PubMed PMID: 31011926.
- Kim KT, Kim HJ, Cho DC, Bae JS, Park SW. Substance P stimulates proliferation of spinal neural stem cells in spinal cord injury via the mitogen-activated protein kinase signaling pathway. *Spine J*. 2015;15(9):2055-65. Epub 2015/04/30. doi: 10.1016/j.spinee.2015.04.032. PubMed PMID: 25921821.
- Zachariou V, Goldstein BD. Dynorphin-(1-8) inhibits the release of substance P-like immunoreactivity in the spinal cord of rats following a noxious mechanical stimulus. *Eur J Pharmacol*. 1997;323(2-3):159-65. Epub 1997/04/04. doi: 10.1016/s0014-2999(97)00038-1. PubMed PMID: 9128834.
- Wan FP, Bai Y, Kou ZZ, Zhang T, Li H, Wang YY, Li YQ. Endomorphin-2 Inhibition of Substance P Signaling within Lamina I of the Spinal Cord Is Impaired in Diabetic Neuropathic Pain Rats. *Front Mol Neurosci*. 2016;9:167. Epub 2017/01/26. doi: 10.3389/fnmol.2016.00167. PubMed PMID: 28119567; PMCID: PMC5223733.

Are Modic changes 'Primary infective endplateitis'?- A study by multimodal imaging

Shanmuganathan Rajasekaran¹, Pushpa B T¹, Sri Vijay Anand K S¹, S Dilip Chand Raja¹, Chandhan Murugan¹, Ajoy Shetty¹, Rishi Kanna¹

1. Ganga hospital, Coimbatore, TAMIL NADU, India

Introduction: The etiopathogenesis of Modic changes is unresolved. Two proposed theories implicate trauma and sub-clinical infection. Traditionally, Modic changes have been defined and studied using magnetic resonance imaging alone. Being a pathology of subchondral bone, it is only natural that a CT scan will be reflective of bone changes better than MRI. With this in the background, we did a study to probe the pathophysiological basis of Modic change (MC) by multimodal imaging rather than by MRI alone.

Materials & Methods: The study was done in three steps. In Step 1, radiological signs found in documented mild infections and traumatic endplate fractures were identified by MRI and CT, and by careful elimination, three signs unique to infection and trauma were distilled. In step 2, by ranking Z score, appropriate positive values for infection and negative for trauma were assigned, and an 'Infection Probability Score' (IPS) was developed. The score's ability to differentiate infection and traumatic endplate changes (EPC) was validated in further 30 patients (15 infections and 15 trauma). In step 3, the score was applied to 80 non-specific low back pain patients (NSLBP), and the probability of EPC as a result of infection was assessed.

Results: The three unique signs for infection and scores were: involvement of end plates at both sides of the disc(+3), typical CT erosion patterns of the subchondral bone associated with infection(+2), and extensive reactive sclerosis(+1). Involvement of superior EP only(-3), single vertebral body edema(-2), and none or only rim sclerosis(-1) were the pure signs for traumatic EP changes. The confidence interval pointing towards infection was 65% for score 4, 79% for score 5, and 89% for score 6. The mean IPS score for the 80 patients with MCs was 4.5. None of the patients with an MC had a negative score, thus excluding trauma as an etiology of MC.

Conclusion: Inclusion of CT in evaluating MC helped to identify signs indicating a high probability of infective process for MC. Contrary to the traditional belief that MCs are secondary inflammatory changes, the study findings indicated that blood-borne primary infective endplateitis might, in fact, be the cause of MC.

Disability in patients with endplate bone marrow lesions (Modic changes) is associated with continuous measures of lesion composition assessed using water-fat MRI

Noah B. Bonnheim¹, Ann A. Lazar², Jiamin Zhou³, Ravi Chachad³, Nico Sollmann^{4,3,5,6}, Xiaojie Guo¹, Conor O'Neill¹, Jeffery C. Lotz¹, Thomas M. Link³, Roland Krug³, Aaron J. Fields¹

1. Department of Orthopaedic Surgery, University of California, San Francisco, San Francisco, CA, USA

2. Department of Epidemiology and Biostatistics, University of California, San Francisco, San Francisco, CA, USA

3. Department of Radiology and Biomedical Imaging, University of California, San Francisco, San Francisco, CA, USA

4. Department of Diagnostic and Interventional Neuroradiology, Technical University of Munich, Munich, Germany

5. Department of Diagnostic and Interventional Radiology, University Hospital Ulm, Ulm, Germany

6. TUM-Neuroimaging Center, Klinikum rechts der Isar, Technical University of Munich, Munich, Germany

Introduction: Vertebral endplate bone marrow lesions (BML), also referred to as 'Modic changes' (MC), are associated with endplate damage, neoinnervation, and chronic low back pain (cLBP). Histology studies show that BMLs represent a continuum of marrow changes reflecting a complex pathological process. Yet, diagnostic classification of BML is binary, based on MC presence/absence on T₁- and T₂-weighted MRI. Advances in quantitative MRI enable measurement of BML composition. The premise of this work is that quantitative assessment of BML composition using water-fat MRI can reveal characteristics of painful BMLs, providing insight into BML pathology and helping to identify phenotypes of cLBP.

Methods: Eighty four patients with cLBP (>3 month duration) were prospectively recruited for this study. 3T MRI of the lumbar spine included sagittal T₁- and T₂-weighted, and chemical shift encoding-based water-fat sequences. MC type was graded on sagittal T₁- and T₂-weighted images for L1–S1 levels. In those vertebrae with MC, BML severity was quantified by calculating the difference in bone marrow fat fraction (BMFF) between regions affected and unaffected by the BML. To do this, BMFF was averaged for five circular ROIs (10 mm² area each) manually placed inside the trabecular bone encompassed by the BML (Fig 1). Five equivalently-sized ROIs were placed in the unaffected adjacent bone marrow. The mean difference in BMFF between affected minus unaffected marrow was calculated for each BML. In the subset of patients with multiple BMLs, the lesion with the largest absolute difference in BMFF between affected and unaffected marrow was used in the analysis. Linear regression was used to test associations between ODI and BML severity, adjusted for age, sex, and BMI. An additional model was tested replacing BML severity with MC type (I, II, or III).

Results: MCs of any type were present in 48% of patients (40/84; 31 male, 9 female; mean±SD age=48.4±13.7 years; ODI=22.7±15.0; VAS=6.4±2.3) and 10% of lumbar endplates (91/924). ODI was significantly associated with the mean difference in BMFF between affected and unaffected marrow ($p=0.001$, whole-model $R^2=0.36$, Fig 2a): large negative differences were associated with higher ODI scores, whereas smaller negative changes transitioning to positive changes were associated with lower ODI scores. MC type was also significantly associated with ODI (mean ODI=27.6 [95% CI: 21.2, 34.1] versus 16.1 [9.0, 23.2] for MC type I versus II, respectively, $p=0.011$, whole-model $R^2=0.28$, Fig 2b).

Discussion: These results indicate that disability in patients with endplate BMLs is related to BML composition assessed along a continuum of marrow changes. BMLs with more severe fibrovascular changes—presenting as greater negative differences in BMFF between affected and unaffected regions—were associated with greater ODI scores. Binary classification of MC type explained less variance (lower R^2) with less statistical significance (higher p -value) than the continuous measures from water-fat MRI. This new assessment methodology may help identify characteristics of painful BML, visualize BMLs to their maximum extent (Fig 1 c–d), and improve cLBP phenotyping over the legacy clinical classification system.

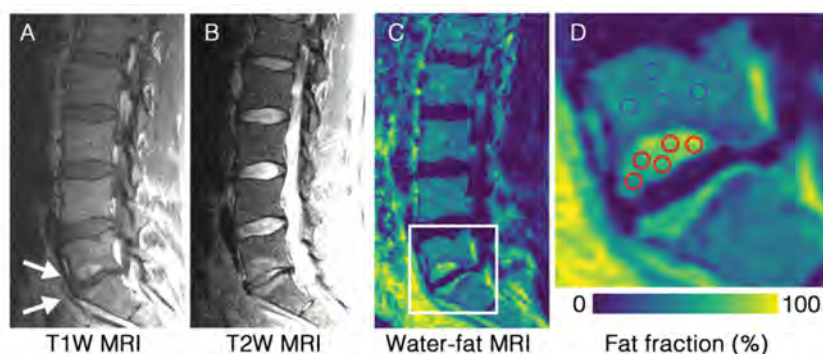


Figure 1 Mid-sagittal images show BMLs (primarily MC II) at L5/S1 on (a) T₁-weighted, (b) fat-saturated T₂-weighted, and (c) water-fat MRI. (d) Inset from water-fat MRI showing ROIs placed in the affected (red) and unaffected (blue) bone marrow. Images from a 37-year-old male patient.

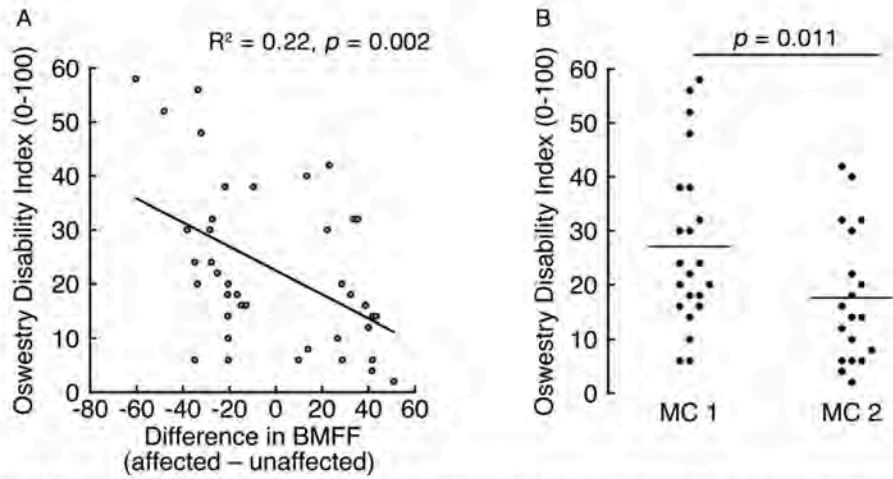


Figure 2 ODI was significantly associated with (a) the difference in bone marrow fat fraction (BMFF; $R^2 = 0.22, p = 0.002$ as shown; $p = 0.001$ after adjusting for age, sex, and BMI with whole-model $R^2 = 0.36$) between affected minus unaffected marrow regions and (b) MC type ($p = 0.011$). The horizontal bars in (b) represent the group mean.

Chronic Low Back Pain Subpopulations with Higher Probabilities for Continued Opioid Use have Higher Self-Reported Pain Scores at Initial Visit

Ayesha Firdous¹, Petr Pancoska¹, Gwendolyn A Sowa¹

1. University of Pittsburgh, Pittsburgh, PA, United States

Introduction Chronic low back pain (CLBP) is one of the leading causes of disability and chronic pain among adults. Despite evidence against effectiveness in CLBP, opioids are often prescribed. It has been shown that approximately 20% of individuals receiving long-term opioid therapy develop an opioid use disorder. Given the prevalence of CLBP in the United States and the debilitating effects of opioid dependency, it is important to identify individuals who will benefit from opioid therapy and those who may not. We used the novel network phenotyping strategy (NPS) to identify unique CLBP subpopulations with characteristic probabilities for continued opioid use at follow-up. We then determined how self reported pain scores at the initial visit were distributed among the CLBP subpopulations to gain further insight into which individuals may benefit from opioid therapy.

Methods

We used a UPMC database with 100 clinical variables from 20,000 CLBP patients prescribed opioids at the initial visit as input for NPS which is an explainable artificial intelligence approach. NPS gave us NPS-X and NPS-Y which are related to probabilities for continued opioid use and discontinued opioid use at 60-day follow-up respectively.

Self-reported pain scores ranged from 0-10 and were not included in the input list of 100 variables used to make NPS predictions. Pain-scores at initial visit for each patient were superimposed back onto each patient's NPS-X and NPS-Y predictions for further analyses.

Results

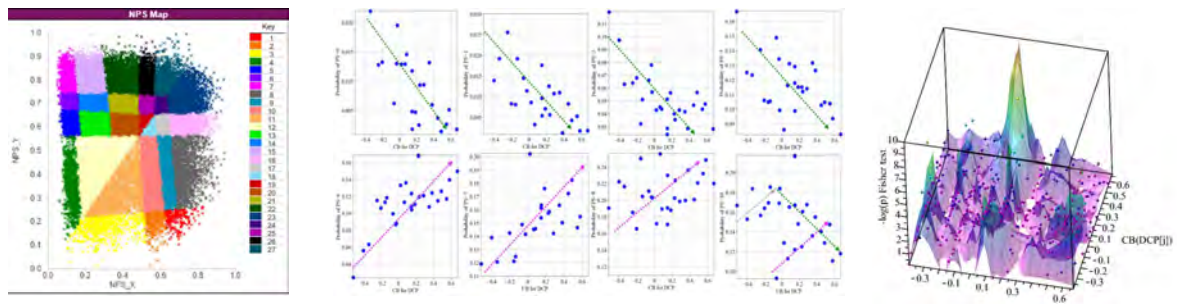
NPS classified patients with CLBP into 27 unique subpopulations with characteristic probabilities for opioid use (Fig1). In the map, each patient is a point defined by their NPS-X and NPS-Y descriptors. Patients with higher value of X have higher probability of discontinuing opioids and those with higher Y have higher risk of staying on opioids.

Clinical burden is the difference between probabilities for continued opioid use and stopped opioid use at follow-up. We determined that clinical burden and probability for a particular pain score are negatively correlated for pain scores between 0 and 5 at index visit. For pain score 6 to 10 at index visit, the clinical burden and probability for pain score were positively correlated (Fig 2).

For each subpopulation, we categorized pain scores at index visit into 2 groups - above 5 and below or equal to 5. We then compared 2 of the 27 subpopulations at a time using a fisher test to determine whether there was any difference in the distribution of pain scores above and below 5. We found that several subpopulation-subpopulation comparisons (48 out of 351 comparisons) were statistically significant ($p < 0.01$) demonstrating there was a significant difference between distribution of pain scores above 5 vs. below 5 among subpopulations with characteristic probabilities for opioid use (Fig3).

Discussion

Subpopulations with higher probabilities for continued opioid use have fewer pain scores in the range of 0-5 and more pain scores in the range of 6-10. Thus, patients with higher self-reported pain scores may need to be given more attention clinically and provided with alternatives to opioid therapy when possible.



Prediction of Lumbar Disc Herniation Resorption and Self-Healing in Symptomatic Patients: a Prospective, Multi-Imaging and Clinical Phenotype Study

Alexander J. Hornung¹, J. Nicolas Barajas¹, Samuel S Rudisill¹, Alexander Butler¹, Grant J Park¹, Garrett Harada¹, Skylar F Leonard², Ashley C Roberts¹, Howard S An¹, Anton Epinof³, Hanne B Albert⁴, Alexander Tkachev³, Dino Samartzis¹

1. Department of Orthopaedic Surgery, Rush University Medical Center, Chicago, IL, USA

2. International Spine Research and Innovation Initiative, Rush University Medical Center, Chicago, IL, USA

3. Tkachev and Epifanov Clinic, Volgograd, Russia

4. The Modic Clinic, Odense, Denmark

Introduction: Symptomatic lumbar disc herniations (LDH) are very common. However, LDH resorption is a “self-healing” phenomenon that may develop yet remains not well understood. By most guidelines, if LDH remains symptomatic after 3 months and conservative management fails, surgical intervention may be an option. The following prospective study aimed to identify determinants that may predict early versus late LDH resorption.

Methods: A one-year prospective study was conducted of consecutive patients diagnosed with acute symptomatic LDH. All patients were managed similarly. Baseline entailed assessment of patient demographics (e.g., smoking status, height, weight, etc.), herniation characteristics (e.g., the initial level of herniation, the direction of herniation, prevalence of multiple herniations, etc.) and MRI phenotypes (e.g Modic changes, endplate abnormalities, disc degeneration, vertebral body dimensions, etc.) were collected for further analysis. MRIs were performed approximately every 3 months from time of enrolment to assess disc integrity. LDH resorption was classified as early (<3 months) or late (>3 months) (**Figure 1**). A prediction model of pretreatment factors was constructed.

Results: 90 patients were included (n=23-early-resorption, n=67-late-resorption groups) with a mean age of 48.7±11.9 years. A greater percent reduction of disc herniation between MRI-0 (baseline) to MRI-1 (p=0.043), greater reduction of herniation size for total study duration (p=0.007) and increased percent resorption per day was noted in the early LDH resorption group (p<0.001). Multivariate modeling yielded greater L4 posterior vertebral height (coeff:14.58), sacral slope (coeff:0.12), and herniated disc volume (coeff:0.013) at baseline as most predictive of early resorption (p<0.05).

Discussion: This is the first comprehensive imaging and clinical phenotypic prospective study, to our knowledge, that has identified distinct determinants for early LDH resorption. Early resorption can occur in 24.7% of LDH patients. The “vertebral body profile,” is the strongest predictor for disc resorption and represents a paradigm shift as to how such pathologies can occur that can eventually lead to disc “self-healing.” A risk profile is proposed that will aid clinical decision-making and manage patient expectations.

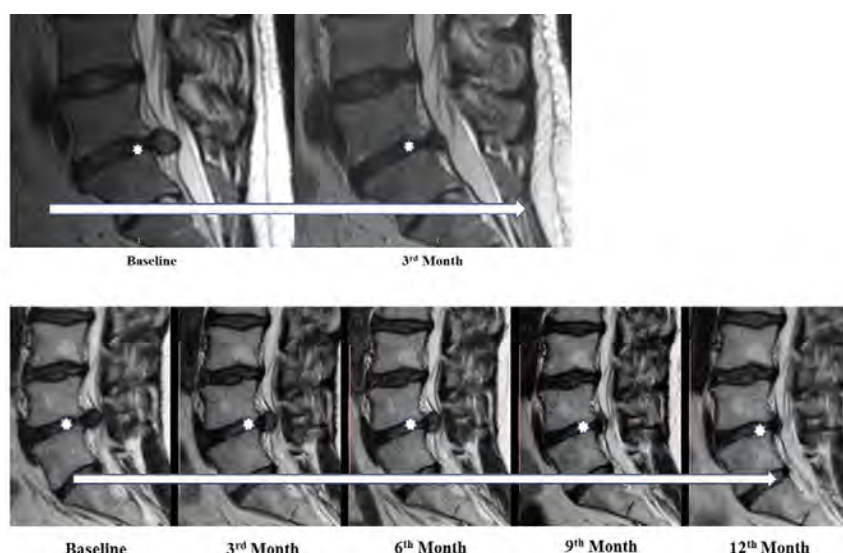


FIGURE 1. Sagittal T2-weighted MRIs of the lumbar spine noting (**top**) early disc herniation resorption in a 41-year-old male and (**bottom**) late resorption in a 36-year-old female. Asterisk denotes level of the disc herniation. The arrow depicts the progression of the imaging from earliest (left) to latest follow-up (right). Note, first MRI was taken at baseline and each subsequent MRI at each 3-month follow-up interval until asymptomatic.

Clinical and Radiographic Differences Between Single- and Multi-Level Lumbar Disc Herniations and Resorption: a *Prospective Multi-Imaging and Clinical Phenotype Study*

Alexander L Hornnung¹, Samuel S Rudisill¹, J. Nicolas Barajas¹, Garrett Harada¹, Ashlyn Fitch¹, Skylar F Leonard¹, Ashley C Roberts², Howard S An¹, Anton Epifanov³, Hanne B Albert⁴, Alexander Tkachev³, Dino Samartzis¹

1. Department of Orthopaedic Surgery, Rush University Medical Center, Chicago, IL, USA

2. International Spine Research and Innovation Initiative, Rush University Medical Center, Chicago, IL, USA

3. Tkachev and Epifanov Clinic, Volgograd, Russia

4. The Modic Clinic, Odense, Denmark

Introduction: Lumbar disc herniations (LDH) are amongst the most common spinal pathologies worldwide. As part of a “self-healing” phenomenon, patients often undergo spontaneous LDH resorption. However, the mechanism of this process remains poorly understood, particularly in the context of multiple herniations. The current study therefore aimed to identify specific patient characteristics, MRI findings, and resorption features associated multiple herniations and LDH resorption. We hypothesized patients with multiple LDH herniations will (1) demonstrate distinct patient characteristics, (2) exhibit discrete MRI findings, and (3) experience longer resorption times compared to those with a single herniation.

Methods: A one-year prospective study was conducted of patients presenting with acute symptomatic LDH. All patients were managed by a single clinician between 2017 and 2019. All included patients (1) were >18 years of age, (2) exhibited MRI findings of acute LDH, and (3) had symptomatic radiculopathy. Baseline assessment encompassed patient demographics, herniation characteristics (e.g., herniation location), and MRI phenotypes (e.g., disc degeneration, endplate abnormalities, vertebral body dimensions). Treatment consisted of gabapentin, acupuncture, and avoidance of inflammatory-modulating medications in all patients. MRIs were performed approximately every 3 months after initial evaluation to assess disc integrity. P-values <0.05 were deemed statistically significant.

Results: Ninety patients were included (n=73 single herniation, n=17 multi-herniation) with a mean age of 48.7±11.9 years. Baseline demographics did not differ between single- and multi-herniation groups apart from body mass index (BMI), as the multi-herniation group consisted of patients with higher BMI (p<0.001). Moreover, the frequency of multiple herniations was similar between males (9 of 44, 20.5%) and females (8 of 46, 17.4%). Those with multiple herniations were more likely to have greater initial disc size (axially) compared to those with only a single herniation (p=0.012). No other baseline herniation characteristics differed between groups (e.g., initial size of herniation, location of herniation, or sagittal maximal measurement), nor did vertebral dimensions, Cobb angle (CA), sacral slope (SS) or CA:SS. Patients with multiple herniations were more like to have L3/L4 inferior endplate changes (p=0.001), L4/L5 superior endplate changes (p=0.012) and L4/L5 inferior endplate changes (p=0.020). No other differences in MRI phenotypes (e.g., Modic changes, osteophytes, etc.) existed between groups. Furthermore, no differences in resorption rate or time to resolution were observed between those with single and multiple herniations.

Discussion: In the first study of its kind, compared to those with single-level LDH, patients with multiple herniations are more likely to have a higher BMI, greater initial axial measurements, and endplate changes at the inferior L3/L4, superior L4/L5, and inferior L4/L5 levels. Patients of both groups, all managed conservatively, experienced similar rates of resorption and times to symptom resolution. Taken together, these results indicate conservative management represents an effective strategy for managing patients with LDH regardless of the number of affected levels, and they may assist clinicians in prognosticating recovery within this specific patient population.

Risk factors for postoperative complaints in patients following lumbar decompression and fusion: analyses focusing on preoperative symptoms

SANGYUN 1 SEOK¹, Jae Hwan 2 Cho²

1. Daejeon Eulji University hospital, Seo-gu Dunsanseo-ro 95, DAEJEON, Korea, Republic of

2. Seoul Asan Medical Center, Seoul

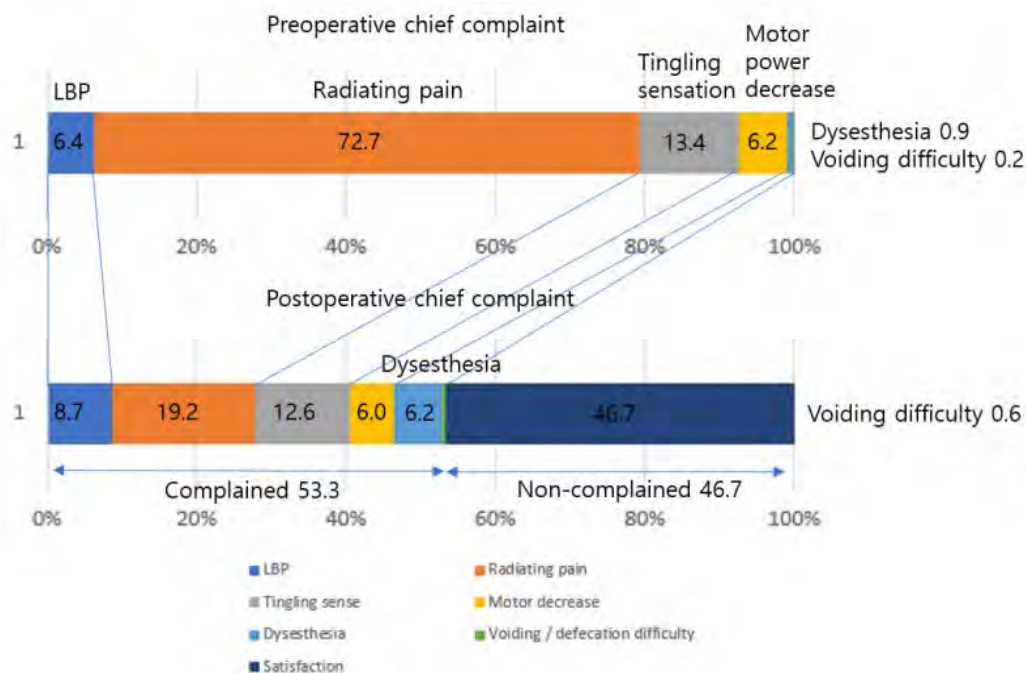
Introduction: Many patients complained of residual symptoms following lumbar decompressive surgery. However, few studies analyze this dissatisfaction by focusing on preoperative patients' symptoms. Therefore, we designed this study to determine the factors that could predict the patients' postoperative complaints by focusing on their preoperative symptoms.

Methods: Four hundred and sixty-nine consecutive patients who underwent lumbar decompression and fusion surgery for lumbar degenerative disease (LDD) were included. Postoperative complaint was defined by at least twice same complaint during the outpatient follow-up of 3,6,12, and 24 months after surgery. A comparative analysis was performed between complaint group (group C, n = 250) and non-complaint group (group NC, n = 219). Preoperative and postoperative chief complaints were analyzed through chart review. Demographic, operative, symptomatic, and clinical factors were compared between the groups by univariate and multivariate analyses.

Results: Most common postoperative complaint was residual radiating pain (36.0%, n = 90) followed by tingling sensation (23.6%, n = 59). The presence of psychotic disease (odds ratio [OR], 4.666; p = 0.019), longer pain duration (OR, 1.021; p < 0.001), pain to below the knee (OR, 2.326; p = 0.001), preoperative tingling sensation (OR, 2.631; p < 0.001), preoperative sensory and motor power decrease (OR, 2.152 and 1.678; p = 0.047 and 0.007, respectively) were significantly correlated with postoperative patients' complaints in multivariate analysis.

Conclusions: Base on the current study, the postoperative patients' complaints could be predicted and explained in advance by checking the preoperative characteristics of patients' symptoms, including the duration and site carefully. This could be helpful to enhance the understanding of the surgical results preoperatively, which could control the anticipation of the patients.

Figure: Comparisons of preoperative and postoperative patients' chief complaints



1. Jang HD, Lee JC, Choi SW, Shin BJ. Risk Factors for Postsurgical Foot Complaints One Year Following Degenerative Lumbar Spinal Surgery. *Spine* 2019;45(9):E533-541.
2. Crawford CH 3rd, Carreon LY, Bydon M, et al. Impact of preoperative diagnosis on patient satisfaction following lumbar spine surgery. *J Neurosurg Spine* 2017;26(6):709-715.
3. Katz JN, Lipson SJ, Brick GW, et al. Clinical correlates of patient satisfaction after laminectomy for degenerative lumbar spinal stenosis. *Spine* 1995;20(10):1155-1160.

10-year prediction of adjacent-level degeneration and disease after lumbar total disc replacement and fusion: A post hoc analysis of 7-year data from a prospective clinical trial

Anton Jorgensen¹, Dom Coric², Peter Derman³, Ernest Braxton⁴, Kris Radcliff⁵, Glenn Buttermann⁶, Aaron Situ⁷, Nicole Ferko⁷, Jack Zigler³

1. Ortho San Antonio, San Antonio, Tx

2. Carolina Neurosurgery and Spine Associates, Charlotte, NC

3. Texas Back Institute, Plano, Tx

4. Vail Health Vail Summit Orthopaedics and Neurosurgery, Vail, CO

5. Rothman Orthopedic Institute, Philadelphia, PA

6. Midwest Spine & Brain Institute, Stillwater, MN

7. CRG-EVERSANA Canada, Burlington, ON, Canada

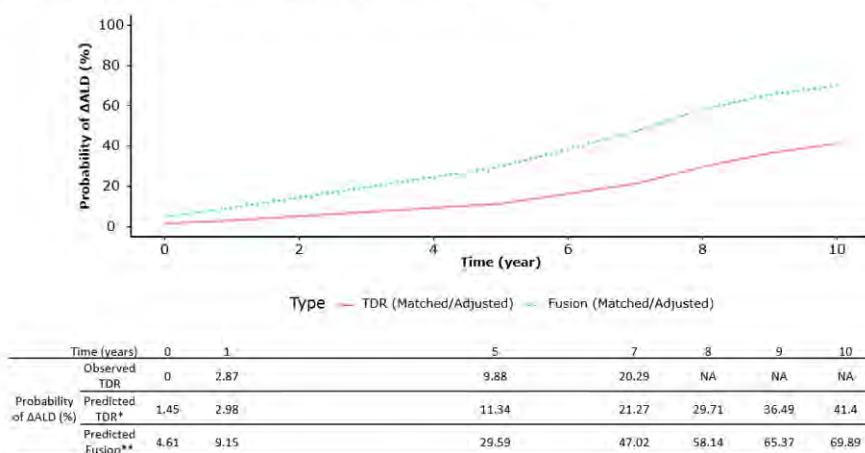
Objectives: To estimate the probability of adjacent-level degeneration (ALDeg) and adjacent-level disease (ALDis), and progression of ALDeg (Δ ALDeg) beyond 7 years after TDR and to compare Δ ALDeg between TDR and fusion using the final, 7-year follow-up data from the prospective activL IDE trial.

Methods: Patients with single-level, symptomatic lumbar disc degeneration who were unresponsive to at least 6 months of nonoperative care who received activL or ProDisc-L and had radiographs available were analyzed for the incidence for ALDeg, incidence of ALDis, and progression of ALDeg (Δ ALDeg). Prediction of the probability of ALDeg, ALDis, and Δ ALDeg with TDR to 10 years was conducted using logistic regression modelling. To predict the Δ ALDeg with fusion, an unanchored MAIC was conducted to mitigate differences between the TDR and fusion patient cohorts and derive a five-year odds ratio (OR) that was applied. A sensitivity analysis using an unadjusted TDR cohort and five-year OR published by Zigler et al., 2018.

Results: The predicted probability of ALDeg after lumbar TDR was 18.8% by one year, 27.2% by five years, 35.0% by seven years, and 53.9% by 10 years. In contrast, the predicted probability of clinical ALDis was 4.2% by 10 years. These probabilities were similar to those observed in the activL trial during the seven-year follow-up. After matching and adjusting, TDR had significantly lower odds of Δ ALDeg than fusion at five-years (OR 0.32 ;95% CI, 0.13-0.72). The probability of Δ ALDeg was predicted to be lower with TDR than with fusion to 10 years (TDR vs. fusion: 1 year, 3.0% vs. 9.1%; 5 years, 11.3% vs. 29.6%; 7 years, 21.3% vs. 47.0%; 10 years, 41.4% vs. 70.0%) (Figure). Similar results were observed in sensitivity analysis (TDR vs. fusion: 1 year, 2.0% vs. 6.8%; 5 years, 10.4% vs. 29.3%; 7 years, 21.1% vs. 48.9%; 10 years, 43.2% vs. 73.1%).

Conclusions: Predicted probability of ALDeg and ALDis to 10 years is low with TDR. Progression of ALDeg is anticipated to be substantially lower with TDR than with fusion over 10 years.

Figure: Prediction of Δ ALDeg (% of patients) with TDR compared with spinal fusion through 10 years, primary analysis (matched and adjusted activL cohort)



Note: The probabilities of Δ ALDeg for TDR and the 5-year OR for Δ ALDeg with TDR versus fusion were derived using the matched and adjusted activL cohort deriving from MAIC comparing activL to fusion cohort in Zigler et al. (2012). The probabilities of Δ ALDeg for fusion were calculated using the derived probabilities of Δ ALDeg for TDR and the 5-year OR for Δ ALDeg with TDR versus fusion.

* Estimated using matched and adjusted activL cohort derived from MAIC

** Estimated using the matched & adjusted activL cohort derived from MAIC and the odds ratio results for Δ ALD for TDR vs. fusion in Zigler et al. (2012)

Abbreviations: ALDeg = radiographic adjacent-level degeneration; ALDis = clinical/symptomatic adjacent-level disease; NA = not applicable; TDR = total disc replacement.

- Zigler JE, Glenn J, Delamarter RB (2012) Five-year adjacent-level degenerative changes in patients with single-level disease treated using lumbar total disc replacement with ProDisc-L versus circumferential fusion. J Neurosurg Spine 17 (6): 504-511.

MRI Quantification of Intervertebral Disc Between Physiological and Experimental States

Harrah R Newman¹, Natalie A Thurlow², Kyle D Meadows¹, Adriana Barba³, Thomas P Schaer³, Edward J Vresilovic¹, Dawn M Elliott¹

1. University of Delaware, Newark, DE, United States

2. University of Florida, Gainesville, FL, United States

3. School of Veterinary Medicine, University of Pennsylvania, Kennett Square, PA, United States

Introduction

Numerous studies have quantified cadaveric intervertebral disc structure, composition, and mechanical behavior and interpreted results in the context of *in vivo* disc; however, there are substantial differences between *in vivo* and *ex vivo* discs. In many *ex vivo* studies, segments are pre-loaded and hydrated, to mimic the physiological *in vivo* condition. However, the differences between the physiological and experimental conditions are unknown, limiting interpretation of cadaveric study outcomes. The objective of this study is to assess geometric and hydration differences between physiological and experimental conditions using repeated magnetic resonance imaging (MRI) in the porcine spine.

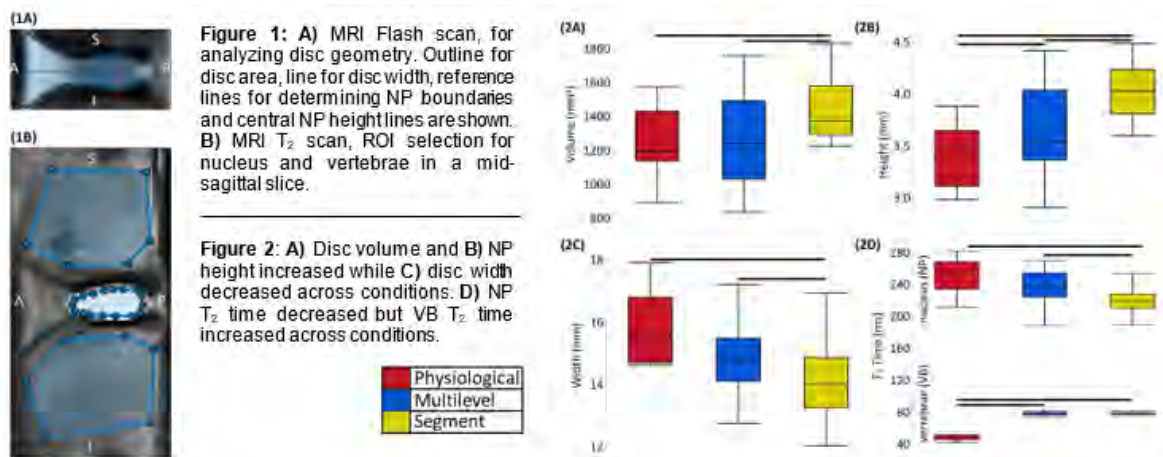
Methods

Repeat 3T MRI were acquired on 3 lumbar discs from Yucatan minipigs in 3 conditions: **physiological** (intact torso <2 hours since sacrifice, n=4 pigs, 12 discs), **multilevel** (fresh-frozen intact excised spine, n=8 pigs, 24 discs), and **segment** (fresh-frozen vertebra-disc-vertebra motion segment, n=8 pigs, 24 discs). Each sample was in PBS-soaked gauze during thawing, imaging, and freezing. The physiological condition was reasonably represented by the fresh torso because *in vivo* animal MRI is performed under anesthesia in supine position which minimizes axial load and eliminates active muscle contractions [1].

Two MRI sequences were used, a T₁-weighted FLASH sequence for geometry and a T₂-weighted CPMG sequence for T₂ relaxation time. Disc volume was calculated from T₁ image segmentations using ITK-SNAP and mid-sagittal height, width, and area were calculated using custom MATLAB code (Fig 1A). T₂ times, positively correlated with hydration, were evaluated in the nucleus pulposus (NP) and adjacent vertebral bodies by fitting the intensity in the regions of interest to noise-corrected exponentials [2] (Fig 1B). Mixed model fits with fixed effect of condition, random effect of specimen, and post-hoc pair-wise Tukey honest significance tests were conducted with p < 0.05.

Results and Discussion

Physiological *in vivo* spines are constrained and loaded by surrounding tissues and body forces that are progressively removed when spines are dissected for *ex vivo* testing. This study showed that dissection altered disc geometry with increased disc volume, increased height, and reduced width (Fig 2A-C). While area was not significantly changed, the increased volume is likely due to the increased height, assuming soft tissue dissection reduced physiological constraints mostly in the axial direction. The reduced width could be related to release of annulus fibrosus circumferential pre-strain. The decrease in NP T₂ indicates reduced water content in the analyzed region: this has two potential causes, 1) water redistribution within the larger volume disc and/or 2) water loss to the vertebral bodies, which had increased T₂ time (Fig 2D). Importantly, these geometric and hydration changes will alter segment mechanical behaviors. While the effects of spinal dissection have been preliminarily quantified here, further work to evaluate the differences in physical constraints and boundary conditions between *in vivo* and *ex vivo* states is ongoing, with the ultimate goal of restoring cadaveric spinal segments to the *in vivo* physiologic state for testing and modeling.



- [1] Wilke et. al. J Biomech, 1996.
- [2] Meadows et. al. JOR Spine, 2020.
- [3] Newell et al. J Mech Behav Biomed Mater, 2017.

Accelerated disc degeneration after pubertal growth spurt differentiates adults with low back pain from their asymptomatic peers

Anni Aavikko¹, Martina Lohman¹, Leena Ristolainen², Hannu Kautiainen³, K Östermam², Dietrich Schlenzka², Teija Lund¹

1. Helsinki University Hospital, Helsinki, FINLAND, Finland

2. Orton Research Institute, Helsinki, FINLAND, Finland

3. Medcare Oy, Espoo, FINLAND, Finland

Introduction Findings of disc degeneration (DD) on magnetic resonance imaging (MRI) are frequently seen in asymptomatic individuals with increasing prevalence with age. DD developing in early adulthood seems to predispose the individual for a more rapid progression of degeneration. Although disc degeneration, protrusion, bulge, and extrusion have been associated with LBP, the value of MRI findings in predicting future LBP has proven low.

Our knowledge on the natural history of the intervertebral disc (IVD) is insufficient to differentiate age-related changes from possible pathologic findings. The few long-term studies including MRI published to date either lack clinical information or report on specific populations or older subjects. In the present study, our objective was 1) to describe the natural history of lumbar IVDs from childhood to adulthood, and 2) to investigate whether findings of DD were associated with LBP.

Methods Ninety-four healthy school children were randomly recruited in 1994 to a longitudinal study including a semi-structured interview, a clinical examination and lumbar spine MRI at the age of 8, 11 and 18. In January 2021, all those subjects who could be reached (n=89) were invited to take part in this long-term follow-up including a semi-structured interview, a clinical examination and a lumbar spine MRI (high-field 1.5T MRI with a dedicated spine coil). Three lowest IVDs were assessed using a Pfirmann summary score, and the ratio of signal intensity of the disc to signal intensity of the adjacent cerebrospinal fluid (SINDL). The association of disc changes at any age with self-reported LBP at the age of 34 was analyzed.

Results Forty-eight subjects consented to this long-term follow-up at the mean age of 34.2 years (SD 0.6). Thirty-five of them reported LBP without specific trauma. The Pfirmann summary score significantly increased with age ($p<0.001$). Subjects reporting LBP at the age of 34 demonstrated statistically significantly higher summary scores both at the age of 18 and 34 compared to asymptomatic subjects ($p=0.004$ at age 18, and $p=0.039$ at age 34). SINDL significantly decreased with age ($p<0.001$ for all levels separately), but no significant differences between subjects with or without LBP at the age of 34 were observed.

Discussion Our main finding was that subjects who reported LBP at the age of 34 had statistically significantly higher Pfirmann summary scores already at the age of 18. The difference remained statistically significant at the age of 34, although progression of DD was seen in the asymptomatic subjects alike (Figure, error bars for 95% confidence intervals.). Hence, more severe DD in single IVD or more extensive DD in multiple IVDs after pubertal growth spurt may be associated with LBP in adulthood. When SINDL was calculated for each level separately, no statistically significant differences emerged between subjects with or without LBP at the age of 34 suggesting that changes in a single IVD may not be as consequential as more widespread DD. In conclusion, subjects with LBP at the age of 34 had more wide-spread or severe DD already at the age of 18 compared to asymptomatic subjects.

Epidemiology, Risk Factors and Clinical Impact of Juvenile Modic Changes in Pediatric Patients with Low Back Pain

G. Michael Mallow¹, David Zepeda¹, Timothy G Kuzel¹, J. Nicolas Barajas¹, Khaled Aboushaala¹, Michael T Nolte¹, Alejandro Espinoza-Orias², Chundo Oh¹, Matthew Colman¹, Monica Kogan¹, Frank M Phillips¹, Howard S An¹, Dino Samartzis¹

1. Department of Orthopaedic Surgery, Rush University Medical Center, Chicago, IL, USA

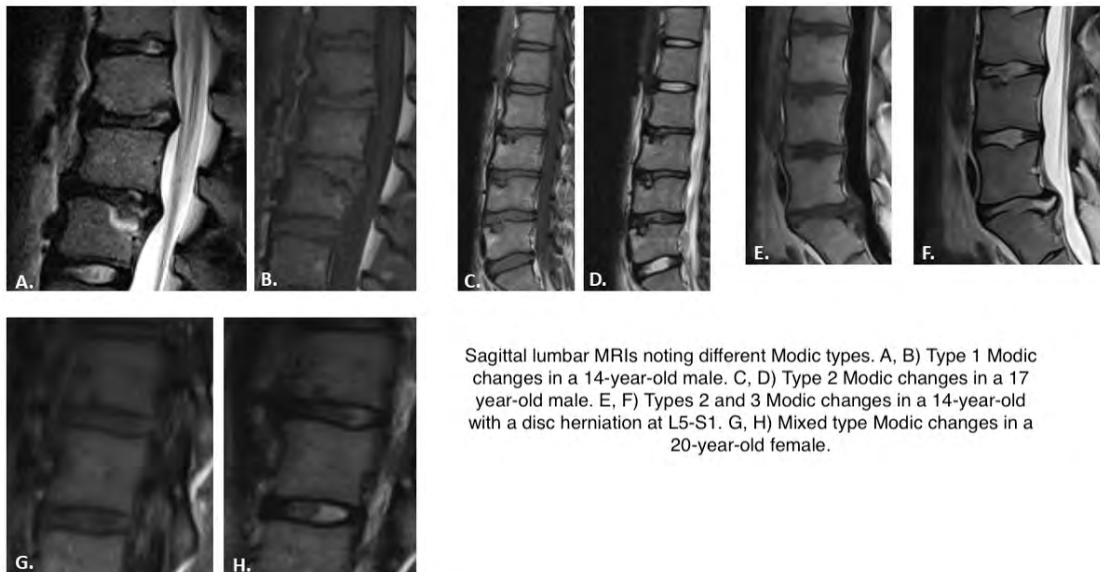
2. International Spine Research and Innovation Initiative, Rush University Medical Center, Chicago, IL, USA

Introduction: Modic changes of the lumbar spine have been abundantly reported in the adult population and are highly associated with low back pain(1). It has been a long-held belief that Modic changes occur in older age, following the progression of disc degeneration. However, little is known regarding the development of Modic changes in the pediatric population. As such, the following study addressed the occurrence of Modic changes in younger patients, and reported on their epidemiology, risk factors and clinical relevance. In addition, the study aimed to raise awareness of the "juvenile" variant of Modic changes.

Methods: 207 consecutive patients that sought medical consultation for low back pain at a single center from 2009 to 2018 that had no history of deformities, neoplasms, trauma, or infections were included in this ambispective study. Sagittal T1- and T2-weighted 1.5T MRIs of L1-S1 were assessed for Modic changes as well as other spinal degenerative phenotypes (e.g. disc degeneration, herniated disc, high intensity zones (HIZs), endplate abnormalities, osteophytes). The presence of Modic types 1, 2, 3, and mixed types were assessed. Measurements were performed independently by two raters, whereby good to excellent reliability was noted. Subject demographics were assessed. Clinical characteristics collected included duration of symptoms in months, total office visits, types of conservative management utilized (physical therapy, NSAIDs, opioids, injections), and if later underwent spine surgery. Univariate and multivariate analyses were performed. Significance for all analyses was set at a $p < 0.05$.

Results: The mean age was 16.5 years old (46.9% males), 14% had MCs and they occurred throughout the spine. Subject baseline demographics were similar between MCs and non-MCs patients ($p > 0.05$). Modic type 2 (50%) was the most common type (type 1:27.1%; type 3:18.8%; mixed:4.7%). Multivariate analyses noted that endplate damage (OR: 11.36), disc degeneration (OR: 5.81), disc space narrowing (OR: 5.77), Schmorl's nodes (OR: 4.30) and spondylolisthesis (OR: 3.55) to be significantly associated with MCs ($p < 0.05$). No significant differences in conservative management were noted between Modic and non-MCs patients ($p > 0.05$). Among surgery patients ($n=44$), 21% also had MCs ($p=0.134$). Symptom-duration was significantly greater in MC patients ($p=0.049$).

Discussion: To our knowledge, this is the first study to address Modic changes, multiple subtypes and their clinical relevance in a pediatric population with low back pain. "Juvenile" Modic changes can occur in pediatric patients who experience low back pain with a prevalence rate of 14% and were noted at every lumbar disc space level. Modic type 2 is the most common sub-type, followed by types 1 and 3. Determinants of Juvenile Modic changes consisted of specific disc and endplate phenotypes. Juvenile MCs have prolonged symptoms and related to specific structural spine phenotypes. Modic changes were also found to be commonly noted in surgery patients. Additional studies are needed to further validate our findings in the young population. Our study further warrants a refined classification of Modic changes for the juvenile variant, and its implications in the lifespan.



Sagittal lumbar MRIs noting different Modic types. A, B) Type 1 Modic changes in a 14-year-old male. C, D) Type 2 Modic changes in a 17 year-old male. E, F) Types 2 and 3 Modic changes in a 14-year-old with a disc herniation at L5-S1. G, H) Mixed type Modic changes in a 20-year-old female.

- 1) Thompson KJ, Dagher AP, Eckel TS, Clark M, Reinig JW. Modic changes on MR images as studied with provocative diskography: clinical relevance--a retrospective study of 2457 disks. *Radiology* 2009; 250(3): 849-55

Repeated Cyclic Loading Induces Intervertebral Disc Regeneration

Elizabeth A Capogna^{1,2}, Emma Brown^{1,2}, Evan Walrath^{1,2}, William Furst^{1,2}, Chao-Ming Zhou³, Qing Dong³, Sarah Gullbrand⁴, Gwendolyn Sowa³, Nam Vo³, Eric Ledet^{1,2,5}

1. Rensselaer Polytechnic Institute, Troy, NY, United States

2. Rehabilitation R&D, Stratton VA Medical Center, Albany, NY, United States

3. PM&R, University of Pittsburgh Medical Center, Pittsburgh, PA, United States

4. Orthopedic Surgery, University of Pennsylvania, Philadelphia, PA, United States

5. Research & Development, Center for Disability Services, Albany, NY, United States

INTRODUCTION: The intervertebral disc has a poor propensity for regeneration. This may be due to the disc's avascularity and limited nutrient supply. Small molecules must undergo trans-endplate transport from subchondral capillaries to metabolically active cells as far away as the central nucleus pulposus.¹ Increased biosynthesis in the disc in response to degeneration leads to increased metabolic activity and increase in demand for nutrients. If transport cannot meet demand, rapid depletion of nutrients and further degeneration can result.¹ Recently, low rate cyclic axial loading has been shown to increase transport of small molecules to and from a healthy disc via convective transport (bulk flow).² If transport can be augmented similarly in a degenerated disc, then an increase in nutrient supply could promote biosynthesis and regeneration. The purpose of this study was to determine if repeated cyclic loading could slow, arrest, or reverse the progression of disc degeneration in the rabbit lumbar spine.

METHODS: After IACUC approval, 56 New Zealand White rabbits were assigned to one of four treatment groups: (i) Control (no degeneration, n=19), (ii) 8 weeks degeneration ("8D", n=14), (iii) 16 weeks degeneration ("16D", n=10), or (iv) 8 weeks degeneration + 8 weeks therapy ("Therapy", n=13). All animals underwent surgery to instrument the spine for cyclic loading of the L4/5 intervertebral disc.² All animals other than the controls underwent disc puncture to induce degeneration. Animals in the 8D and 16D groups were allowed to degenerate for 8 or 16 weeks, respectively. Animals in the Therapy group were first allowed to degenerate for 8 weeks, then underwent a cyclic loading regimen (0.5Hz, 3mm/s) for 2 hours a day, 5 days per week, for the next 8 weeks. T2-weighted MRI and histologic analysis were performed. Nucleus volume, T2 relaxation times, Pfirrmann, and modified Pfirrmann scales were used to assess disc health. Histology was evaluated using the ORS Spine Section grading system. Indicators of biosynthesis, inflammation, and matrix degradation were analyzed via gene expression. Data were analyzed via one-way ANOVA with Games Howell *post-hoc* analysis or Kruskal-Wallis Test with a Mann-Whitney *post-hoc* analysis.

RESULTS: Animals tolerated the surgery and daily loading well with no signs of distress or discomfort during loading. T2 relaxation times, nucleus volumes, Pfirrmann, modified Pfirrmann, ORS Spine Section histo score, and gene expression are summarized in Figure 1. Data demonstrate that punctured discs progressively degenerate from week 0 to week 16. In contrast, discs that were allowed to degenerate for 8 weeks and then underwent cyclic loading therapy for 8 weeks showed improvements that suggest disc regeneration.

DISCUSSION: We have demonstrated for the first time, the ability of a degenerated intervertebral disc to regenerate in response to a non-invasive, non-pharmacologic treatment regimen. As a result of the treatment, data from every metric indicate that disc health, disc volume, and disc organization improved as a result of cyclic loading. Discs appeared to reverse the extent of degeneration and data suggest that discs regenerated back to an earlier stage of degeneration and in some animals resembled normal healthy discs.

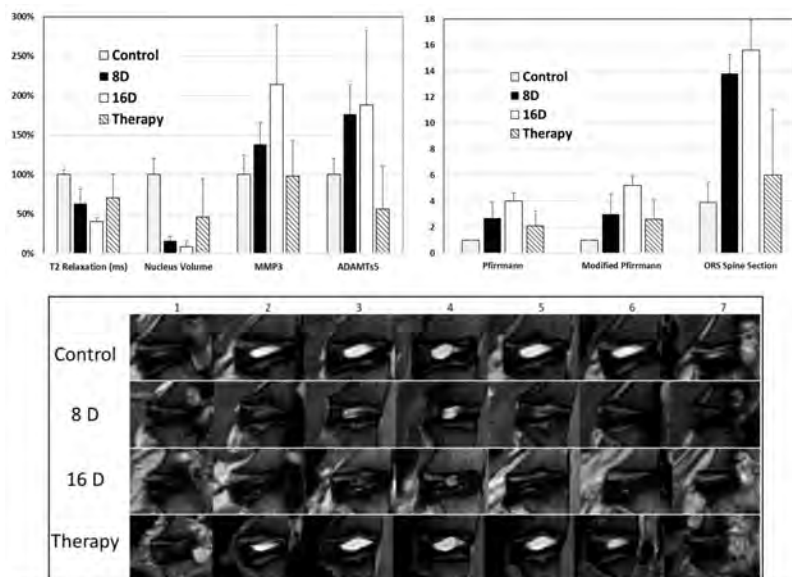


Figure 1: Continuous (upper left) and categorical (upper right) data show that the values for Therapy discs in all assessments demonstrated regeneration. T2 weighted MRI images (bottom) show regeneration in the nucleus in the Therapy group. (Image 1 = left, Image 4 = mid-sagittal, Image 7 = right.)

- [1] Urban et al. Clin Orthop Relat Res. 1982;170:296-302.
- [2] Gullbrand et al. Spine. 2015;40(15):1158-1164.

Torque- and Muscle-Driven Flexion Provoke Disparate Herniation Risk

Minhao Zhou¹, Reece D Huff¹, Grace D O'Connell¹

1. University of California -- Berkeley, Berkeley, CALIFORNIA, United States

Introduction: Lumbar disc herniation is a common cause of lower back pain, resulting in significant socioeconomic burdens. Unfortunately, herniation etiology is not well understood, partially due to challenges in provoking herniation *in vitro* [1]. Previous studies suggested that flexion increased herniation risk. Thus, the objective of this study was to use a finite element modeling approach to evaluate herniation risk under torque-driven flexion, which represents most *in vitro* setups, and the more physiologically representative muscle-driven flexion.

Methods: Triphasic bovine caudal disc motion segment finite element models were created based on our recently validated multiscale structure-based model, with model parameters defined from our previous work [2]. Models were developed to represent torque-driven flexion with the instantaneous center of rotation (ICR) located on the disc, and muscle-driven flexion with the ICR located anterior of the disc; ten cases were investigated (**Figure 1A**). All models were loaded in three steps: 1) free swelling in 0.15 M phosphate-buffered solution until equilibrium, 2) 0.5 MPa axial compression, and 3) 5° flexion. Model predictions of herniation were based on AF mechanics data in the literature. Specifically, effective strain and fiber stretch were analyzed in the posterolateral AF. Bulk disc deformation and intradiscal stress-strain distributions were also evaluated.

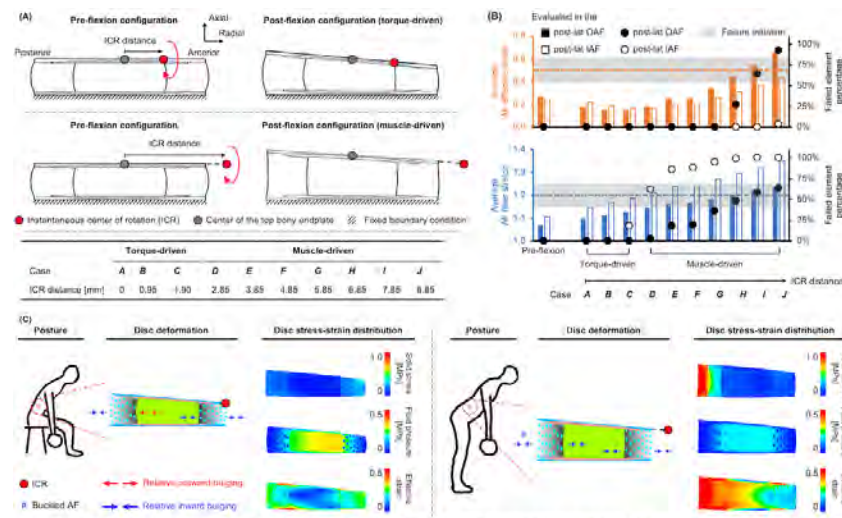


Figure 1: (A) Disc frontal cross sections demonstrating the schematics of torque-driven flexion, where the instantaneous center of rotation (ICR) is located on disc, and the schematics of muscle-driven flexion, where the ICR is located on the same anatomical transverse plane, but away from the disc. The ICR location for the 10 cases investigated is also summarized. (B) The average effective strain and fiber stretch with the corresponding failed element percentage evaluated in the posterolateral (post-lat) inner and outer annulus fibrosus (AF). The gray boxes represent the range where tissue failure was expected to initiate. The failed element percentage was calculated using the failure threshold highlighted by the horizontal dashed lines, above which tissue failure was highly expected. (C) Disc deformation and stress-strain distribution under two physiological flexion postures. The instantaneous center of rotation is located close to the body (left), and away from the body (right).

threshold. For the outer AF, the average fiber stretch did not reach the threshold until Case **H**, where ~50% of the elements failed (**Figure 1B** – bottom). Overall, failure was predicted in the inner AF before the outer AF based on the average fiber stretch criterion.

Discussion: Simulating flexion under a range of ICR locations helps understand intradiscal mechanics under various physiological activities (**Figure 1C**). Torque- and muscle-driven flexion resulted in distinct disc mechanics, resulting in disparate predictions for AF failure, a widely acknowledged precursor for disc herniation. Particularly, torque-driven flexion did not induce herniation, agreeing with the limited success reported in the literature in provoking herniation through *in vitro* experiments. However, muscle-driven flexion greatly increased the likelihood of *in vitro* herniation through the posterolateral AF, agreeing with the AF failure location observed for herniations. In conclusion, this study provided a computational framework for designing *in vitro* testing protocols that can advance the assessment of disc failure behavior.

Results: The average effective strain in the posterolateral inner and outer AF was 0.25 and 0.26 before flexion, with no elements exceeding the failure threshold. Torque-driven flexion did not affect the effective strain. By contrast, as the ICR moved anteriorly with muscle-driven flexion, the effective strain in the posterolateral AF increased, and failure was predicted for Cases **H–J** (**Figure 1B** – top). Overall, failure was predicted in the outer AF before the inner AF based on the effective strain criterion.

Average fiber stretch in the posterolateral inner and outer AF was 1.11 and 1.07 before flexion and increased pseudo-linearly with ICR distance; no elements exceeded the failure threshold pre-flexion. For the inner AF, average fiber stretch was 1.21 in Case **D**, resulting in >60% of the elements exceeding the failure

- [1] Wilke HJ, Kienle A, Maile S, Rasche V, Berger-Roscher N. A new dynamic six degrees of freedom disc-loading simulator allows to provoke disc damage and herniation. *Eur Spine J*. 2016 May;25(5):1363-1372.
- [2] Zhou M, Lim S, O'Connell GD. A Robust Multiscale and multiphase structure-based modeling framework for the intervertebral disc. *Frontiers – In Press*, 05/2021.

How to treat lumbar disc herniations in order to prevent a reherniation?

Laura Zengerle¹, Lena Zöllner¹, Jan Ulrich Jansen¹, Youping Tao¹, Hans-Joachim Wilke¹

1. Ulm University, Ulm, DEUTSCHLAND, Germany

Introduction: Clinical papers have discussed the outcome of different treatments after lumbar disc herniations, namely sequestrectomy versus (partial) nucleotomy. While in one study, the partial nucleotomy was superior to the sequestrectomy with respect to reherniations (Carragee 2006), another study showed the opposite result (Thomé 2005). The aim of this in vitro study was to use a standardized in vitro disc herniation model in order to enlighten this complex issue.

Methods: First a disc herniation was provoked in 6 cadaveric lumbar motion segments (L2/3, L3/4, L4/5, L5/S1) from four different human donors (age: 19–53 years; sex: 3 male/1 unknown) with low disc degeneration (Pfirrmann 1–2). This herniation was provoked by setting a standardized round annular defect of Ø4 mm, then the segments were dynamically loaded simulating physiological activities such as bending forward or lifting heavy boxes, according a recently developed test method (Zengerle 2021). After the herniation different treatments were performed. In a first step, a sequestrectomy was carried out and the specimens were loaded again in the same way as above. In a second step, independently whether a reherniation occurred or not, the remaining nucleus material within the annular defect was removed (anulotomy) and the segments were tested and loaded again. Finally, a partial nucleotomy was cautiously performed, again followed by dynamical loading simulating physiological activities. Disc height, range of motion (ROM) and intradiscal pressure (IDP) were evaluated between all test steps and analysed statistically using a Friedman-Test with Bonferroni Post-Hoc correction ($\alpha \leq 0.05$).

Results: In all specimens, the round 4 mm defect led to a herniation using the physiological loading protocol. After removing only the sequester with an amount of 0.06g (0.02g – 0.11g), no reherniation could be provoked. However, after the anulotomy (additional removal of 0.05g (0.02g – 0.12g) nucleus material), one reherniation could be observed. After performing a partial nucleotomy with dissection of significantly more nucleus material (0.38g (0.27g – 0.67g)), two discs reherniated (Fig. 1). This partial nucleotomy also led to a significant increase of ROM of about 1° ($p = 0.044$) and decrease of the IDP of 0.14MPa ($p = 0.035$), but only in lateral bending (Fig. 1). Disc height decreased remarkable only after the initial herniation, and not gradually after performing the surgical treatments, whereas ROM and IDP did not change remarkably subsequent to the (re-)herniation (Fig. 1).

Discussion: In this study, the outcome of different surgical procedures for the treatment of lumbar disc herniations regarding reherniation risk could be investigated under realistic dynamic conditions simulating physiological worst case scenarios such as lifting heavy weights completely bent forward. The results of this study may support the clinical findings, that the risk of reherniation may be lower when only performing a sequestrectomy compared to a partial nucleotomy. However, it is known from former studies that the initial herniation risk also depends on other parameters, such as size or shape of the annular defect. Hence, those parameters should be considered as potential risk factors for reherniations, as well.

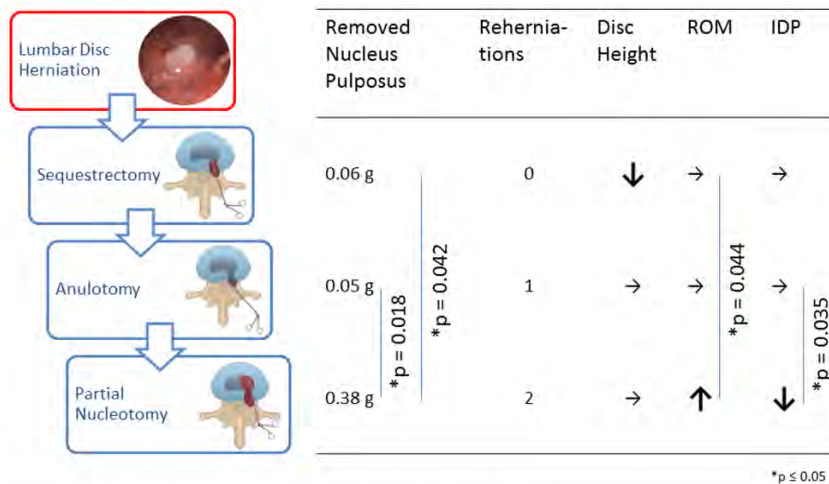


Fig. 1: Provoked reherniations and effect of the removal of nucleus pulposus on the biomechanical parameters disc height, range of motion (ROM) and intradiscal pressure (IDP) after treating the index lumbar disc herniation with a sequestrectomy, anulotomy and partial nucleotomy, * $p \leq 0.05$.

1. Thomé C, Barth M, Scharf J, Schmiedek P. Outcome after lumbar sequestrectomy compared with microdiscectomy: a prospective randomized study. *J Neurosurg Spine*. 2005 Mar;2(3):271-8. doi: 10.3171/spi.2005.2.3.0271. PMID: 15796351.
2. Carragee EJ, Spinnickie AO, Alamin TF, Paragioudakis S. A prospective controlled study of limited versus subtotal posterior discectomy: short-term outcomes in patients with herniated lumbar intervertebral discs and large posterior annular defect. *Spine (Phila Pa 1976)*. 2006 Mar 15;31(6):653-7. doi: 10.1097/01.brs.0000203714.76250.68. PMID: 16540869.
3. Zengerle L, Debout E, Kluger B, Zöllner L, Wilke H-J. In Vitro Model for Lumbar Disc Herniation to Investigate Regenerative Tissue Repair Approaches. *Applied Sciences*. 2021; 11(6):2847. <https://doi.org/10.3390/app11062847>

An In Vivo Biomechanical Analysis of Neuromuscular Recovery of Dynamic Lumbar Spinal Stiffness Following Joint Injury

Christopher J Colloca¹, Robert Gunzburg², Marek Szpalski³, Mostafa A Hegazy⁴, Brian JC Freeman⁵

1. International Spine Research Foundation, Chandler, AZ, United States

2. Department of Orthopaedic Surgery, Edith Cavell Clinic, Brussels, Belgium

3. Department of Orthopaedics, Centre Hospitalier Molière Longchamp, Brussels, Belgium

4. Kinesiology, Associate Professor, Southwest Minnesota State University, Marshall, MN, USA

5. Faculty of Health Sciences, School of Medicine, University of Adelaide, Australia, Adelaide, SA, USA

Introduction. Although the stabilizing role of the lumbar musculature is appreciated, the muscles ability to recover ligamentous injury or instability are less understood. The purpose of this experimental study was to quantify the effects of ligament injury and muscle activation on the *in vivo* dynamic dorsoventral (DV) lumbar spine stiffness.

Methods. Two pairs of electrical stimulating electrodes were placed in the multifidus at L3-L4 in fifteen anesthetized prone laying Merino sheep. Dynamic DV spine stiffness was assessed at L3 using a computer-controlled testing apparatus oscillating from 0.5 to 20 Hz. Five randomized trials were conducted at rest and during four 20 Hz supramaximal stimulation voltages (6, 8, 15, and 20 volts). Five randomized trials were repeated following progressive injury to the interspinous/supraspinous ligament (ISL/SSL), and again following facetectomy. The secant stiffness ($k_y = DV \text{ force}/L3 \text{ displacement}$, N/mm) were determined across 44 mechanical testing frequencies and normal and injured spine states. Descriptive statistics were computed and within group comparisons evaluated with a series of repeated measures ANOVAs with post-hoc Bonferroni correction, and condition differences were assessed using a paired-observations t-tests (two-tailed POTT).

Results. The dynamic stiffness varied nearly 4-fold over the 0.5 to 20 Hz frequency range consistent with the viscoelastic nature of the ovine spine. In the intact spine, muscle stimulation provided significant up to two-fold increases in k_y at 43 of 44 mechanical testing frequencies examined ($p < 0.034$). Likewise, a significant graded increase in k_y was observed for submaximal contractions for most mechanical excitation frequencies when compared to rest ($p < 0.048$). Injury to the ISL/SSL caused a significant loss in spinal stiffness ($p < 0.05$) that was able to be recovered by submaximal (8V, 15V) and maximal (20V) muscle stimulations at most mechanical excitation frequencies ($p < 0.05$). Facetectomy, however, caused a significant loss ($P < 0.05$) of dynamic spinal stiffness at all mechanical excitation frequencies which was only able to be recovered with maximal (20 V) muscle stimulation.

Discussion. Dynamic lumbar spine stiffness is dependent upon mechanical testing frequency and is appreciably decreased with ligament and joint injuries. Certain levels of muscle stimulation can recover stiffness in ISL/SSL injury but only maximal multifidus stimulation can recover stability in conditions of facetectomy. Quantifying the passive and active contributions of the lumbar spine musculature to lumbar spine stiffness contributes to biomechanical modeling, surgical, and rehabilitative considerations in instability.

Dysfunctional Paraspinal Muscles in Adult Spinal Deformity Patients Lead to Increased Spinal Loading

Masoud Malakoutian^{1,2}, Alex M. Noonan³, Iraj Dehghan-Hamani^{1,2}, Shun Yamamoto⁴, Sidney Fels⁵, David Wilson⁶, Majid Doroudi⁷, Peter Schutz⁸, Stephen Lewis⁹, Tamir Ailon^{6,2}, John Street^{6,2}, Stephen H.M. Brown³, Thomas R. Oxland^{1,6,2}

1. Mechanical Engineering, University of British Columbia, Vancouver, British Columbia, Canada

2. ICORD, University of British Columbia, Vancouver, British Columbia, Canada

3. Human Health and Nutritional Sciences, University of Guelph, Guelph, Ontario, Canada

4. Orthopaedics, Jikei University, Tokyo, Japan

5. Electrical and Computer Engineering, University of British Columbia, Vancouver, British Columbia, Canada

6. Orthopaedics, University of British Columbia, Vancouver, British Columbia, Canada

7. Cellular & Physiological Sciences, University of British Columbia, Vancouver, British Columbia, Canada

8. Pathology and Laboratory Medicine, University of British Columbia, Vancouver, British Columbia, Canada

9. Surgery, University of Toronto, Toronto, Ontario, Canada

Introduction: Decreased spinal extensor muscle strength in adult spinal deformity (ASD) patients is well-known but poorly understood. Whether this decreased strength results from altered muscle properties due to fibrosis, fatty infiltration, or other causes, is unknown. Thus, this study aimed to investigate the biomechanical and histopathological properties of paraspinal muscles from ASD patients and predict the effect of altered biomechanical properties on spine loading.

Methods: 68 muscle biopsies were collected from nine ASD patients (66±8 years old; five males and four females) at L4-L5 (bilateral multifidus and longissimus sampled). The ASD patients comprised group I (four patients) with no sagittal imbalance (SI) and no usage of compensatory mechanisms (CMs); group II (three patients) with no SI through usage of CMs; and group III (two patients) with SI despite usage of CMs. The biopsies were tested for muscle fiber and fiber bundle biomechanical properties (i.e. passive elastic modulus, active specific force, in situ and slack sarcomere lengths) and histopathology. The small sample size (due to Covid-19) precluded formal statistical analysis, but the properties were compared to literature data. Changes in spinal loading due to the measured properties were predicted by a lumbar spine musculoskeletal model.

Results: Single fiber passive elastic moduli were similar to literature values, but in contrast, the fiber bundle moduli exhibited a wide range beyond literature values, with 22% of 171 fiber bundles exhibiting very high stiffness, up to 20 times greater than has been reported previously (Figure 1). Active contractile specific force was consistently less than literature values (Figure 2), with notably 24% of samples exhibiting no contractile ability. Both in situ and slack sarcomere lengths presented a large variation, with in situ sarcomere length exceeding literature data in most cases (Figure 3). Histological analysis of 28 biopsies revealed frequent fibro-fatty replacement with a range of muscle fiber abnormalities (Figures 4 and 5). In general, the degree of abnormality was more severe in patients with greater deformity. Biomechanical modelling predicted that high muscle stiffness could increase the compressive loads in the spine by over 500%, particularly in flexed postures (Figure 6).

Discussion: The histopathological observations suggest diverse mechanisms of potential functional impairment. The large variations observed in muscle biomechanical properties can have a dramatic influence on spinal forces. These early findings highlight the potential key role of the paraspinal muscle in ASD.

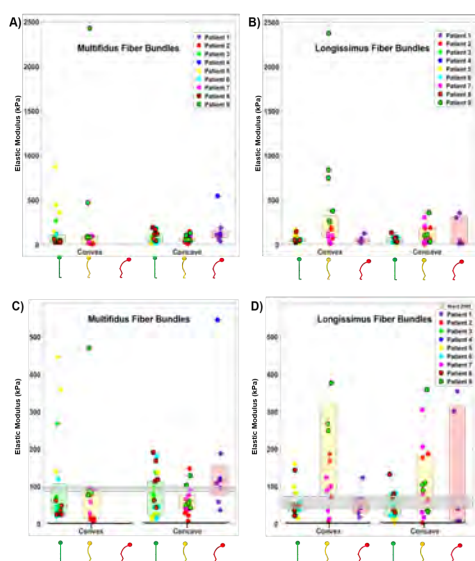


Figure 1. Passive elastic modulus of fiber bundles represented by boxplots for each patient group. (A) and (B) are the same plots as (C) and (D) but with a larger scale on the y-axis to encompass all data points. The red lines denote the medians, the heights of the boxes indicate the interquartile ranges and each dot represents the elastic modulus value for a tested fiber. Green, yellow, and red icons along the x-axis represent patient groups I, II, and III, respectively. The gray box represents the mean±standard error of the elastic modulus reported in the single study that measured this from live human biopsies.

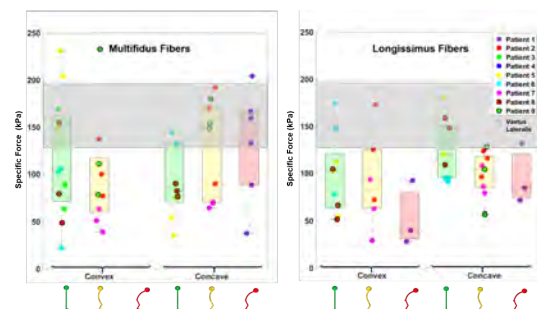


Figure 2. Specific force values of type I single muscle fibers from the multifidus and longissimus represented by box and whisker plots for each patient. The red lines represent the median, while the height of the boxes indicate the 25th to 75th percentiles, the whiskers represent the minimum and maximum values, and each dot represents the specific force value for a single muscle fiber. Green, yellow, and red icons along the x-axis represent patient groups I, II, and III, respectively. The gray box represents the mean±standard deviation of the average specific forces reported for elderly human vastus lateralis (65-85 years old) in the literature.

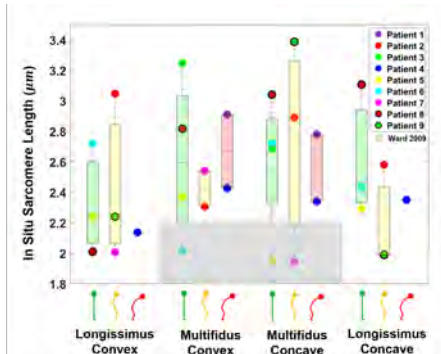


Figure 3. In-situ sarcomere length represented by boxplots for each patient group. The red lines denote the medians, the heights of the boxes indicate the interquartile ranges and each dot is the average of three measurements for each biopsy (the three measurements were quite consistent for almost all biopsies). Green, yellow, and red icons along x-axis represent patient groups I, II, and III, respectively. The gray box represents the mean±standard error of in-situ sarcomere length reported in the single study that has measured it in multifidus only.

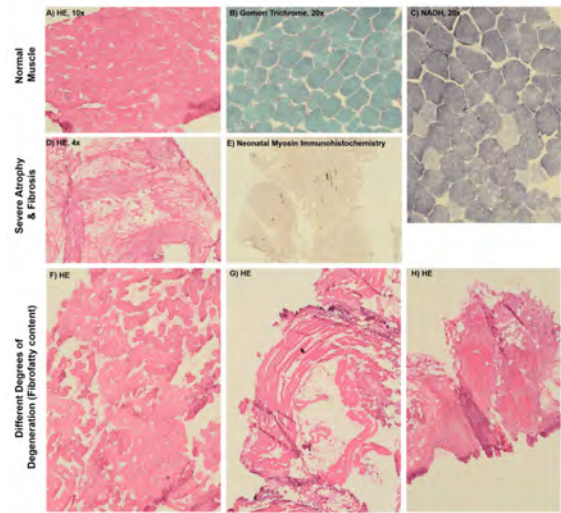


Figure 4. Illustration of variable degrees of fibro-fatty replacement in paraspinal muscle biopsies from ASD patients. A-C) Fairly normal biopsy with regular internal architecture of muscle fibers. D-E) Severe fibrosis. Scarce remaining muscle fibers are only identified on immunohistochemical stain for neonatal myosin. F-H) Variable degrees of fibro-fatty replacement on H&E stained sections with scattered fat cells in F, increasing and regional fatty replacement and fibrosis in G, and significant fibrosis with increased size variability of remaining fibers in H.

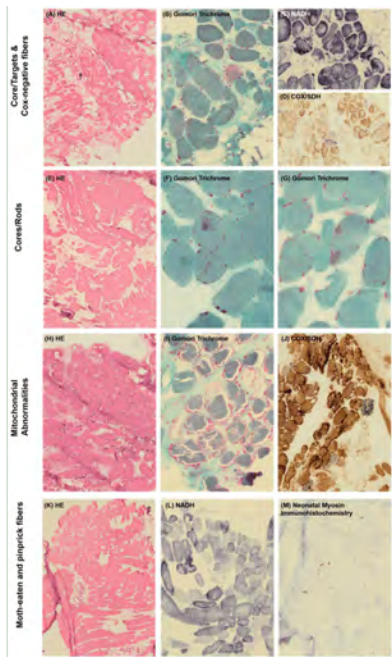


Figure 5. Illustration of muscle fiber abnormalities found in paraspinal muscle biopsies from ASD patients. A-D) Biopsy showing core/target fibers on the NADH stain (C), mitochondrial abnormalities on B, and Cox negative fibers on the combined COX/SDH stain D. E-G) Biopsy showed rod like structures on the Gomori Trichrome stain, central deposits consistent with cores, and cytoplasmic bodies. H-J) Biopsy showed significant mitochondrial abnormalities with subsarcolemmal accumulation apparent on the trichrome stain and Cox-negative fibers on the COX/SDH stain. K-M) Milder fiber pathology exemplified by moth-eaten changes to the internal architecture on the NADH stain and presence of highly atrophic, neonatal-myosin positive fibers ("pin-prick fibers") on immunohistochemistry.

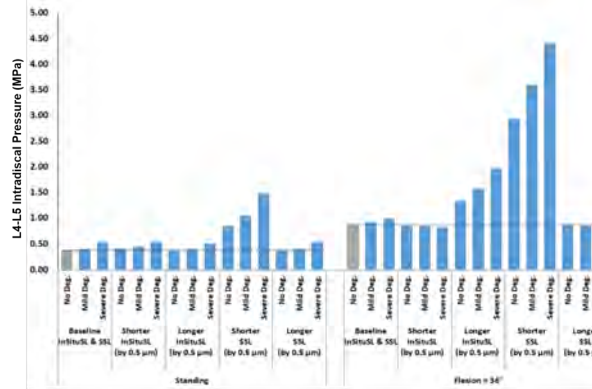


Figure 6. Predicted L4-L5 intradiscal pressure by the musculoskeletal model for three different conditions: no muscle degeneration, mild muscle degeneration, and severe muscle degeneration. In-situ sarcomere lengths and slack sarcomere lengths were also varied, as was posture (upright standing compared to standing with 36° spine flexion).

INVESTIGATING THE ACTIVE CONTRACTILE FUNCTION OF THE RAT PARASPINAL MUSCLES REVEALS UNIQUE CROSSBRIDGE KINETICS IN THE MULTIFIDUS

Alex M. Noonan¹, Thomas R. Oxland², Stephen H. M. Brown¹

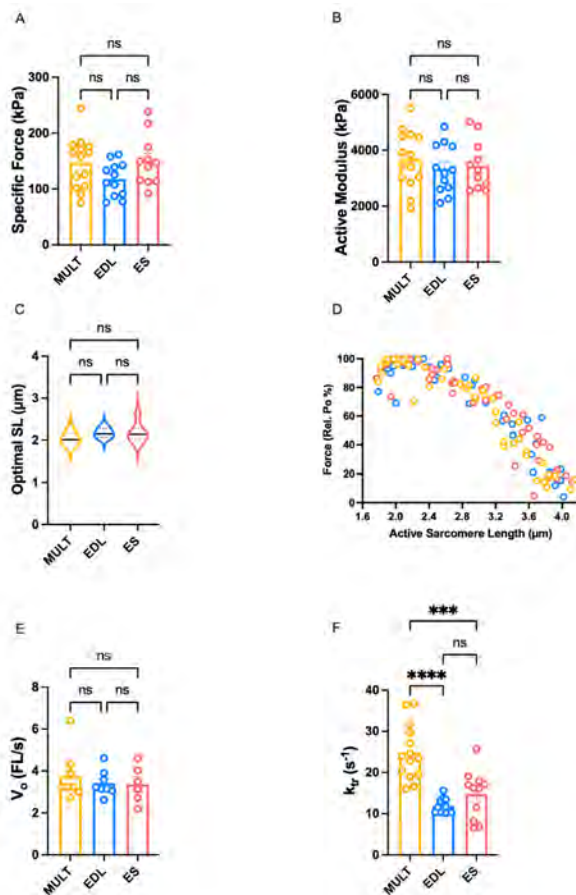
1. University of Guelph, Guelph, Ontario, Canada

2. University of British Columbia, Vancouver, British Columbia, Canada

INTRODUCTION: The paraspinal muscles are responsible for moving and stabilizing the spinal column. There have been debates regarding the functional roles of the different paraspinal muscles, in particular the multifidus and erector spinae (combined longissimus and iliocostalis). While various aspects of paraspinal muscle anatomy, biology, and histology have been studied, information on paraspinal muscle contractile function is almost non-existent, thus hindering functional interpretation of these muscles in healthy individuals and those with low back disorders. The aim of this study was to measure and compare the contractile function and force-sarcomere length properties of muscle fibres from the multifidus (MULT) and erector spinae (ES) as well as a commonly studied lower limb muscle (extensor digitorum longus (EDL)) in the rat.

METHODS: Single muscle fibres (n = 77 total from 6 animals) were isolated from each of the muscles, chemically permeabilized, activated by immersing them in a chamber containing a high-Ca²⁺ activating solution (pCa 4.2) to elicit maximal force and tested to determine their active contractile function; all fibres used in the analyses were type IIB.

RESULTS: There were no significant differences between muscles for specific force (sF₀) (p = 0.11), active modulus (stiffness) (p = 0.63), average optimal sarcomere length (p = 0.27) or unloaded shortening velocity (V₀) (p = 0.69) (Figure 1A-E). However, there was a significant difference in the rate of force redevelopment (k_{tr}) between muscles (p = <0.0001), with MULT being significantly faster than both the EDL (p = <0.0001) and ES (p = 0.0001) and no difference between the EDL and ES (p = 0.41) (Figure 1F).



DISCUSSION: Rate of force redevelopment (k_{tr}) is a proxy measure of the transition from non-force bearing to force bearing cross-bridge states (i.e., weakly to strongly bound states). The present finding suggests that multifidus has faster crossbridge turnover kinetics when compared to other muscles (ES and EDL) when matched for fibre type. Since Ca²⁺ is the driver of muscle contraction, changes in the way the contractile apparatus handles Ca²⁺ could affect muscle contractile performance at the single fibre level and is therefore one possible mechanism that could explain the difference in k_{tr} between muscles; future efforts will aim to determine if the MULT handles calcium in a "unique" way, compared to other muscles. Whether the faster crossbridge kinetics translate to a functionally significant difference in whole muscle performance needs to be studied further.

Figure Caption: Multifidus (MULT), extensor digitorum longus (EDL) and erector spinae (ES) data, shown in yellow, blue and red, respectively, for A) specific force, B) active modulus (stiffness), C) optimal sarcomere length, D) force-sarcomere length relationship, E) unloaded shortening velocity, F) rate of force redevelopment (k_{tr}). MULT had significantly faster k_{tr} than both EDL and ES.

3D internal strain analysis of intervertebral disc at three stages of nucleus replacement surgery

Tamanna Rahman¹, Saman Tavana¹, Nicoleta Baxan¹, Axel Moore¹, Jonathan Bull², Nigel Smith³, Nicolas Newell¹

1. Imperial College London, London, United Kingdom

2. BARTS Health NHS Trust, London, United Kingdom

3. University College London, London, United Kingdom

Introduction

Nucleus-replacement is an alternative surgical treatment for patients with symptomatic early-stage disc degeneration. The surgery involves removing degenerated nucleus material (nucleotomy) from the intervertebral disc to make space for a replacement device aiming to restore physiological function. Uptake of this surgery has been slow, predominantly due to poor performance in clinical trials¹. Clinical performance could be improved if the interaction between device and internal components of the disc is better understood. Therefore, this study aims to non-invasively analyse internal disc interactions using 9.4T-MRI combined with digital volume correlation (DVC), a technique that quantifies 3D tissue deformations². Interactions will be assessed at three stages through the surgery: intact, post-nucleotomy, and post-nucleus replacement.

Methods

Seven human (42 ± 15 years) vertebra-disc-vertebra lumbar specimens (Pfirrmann: 3 ± 1^3) underwent nucleotomy followed by nucleus replacement. 9.4T-MRIs were acquired when the samples were intact, post-nucleotomy, and post-nucleus replacement, both in unloaded and loaded to 1kN states. Average disc heights were manually measured from MRIs and disc stiffness was measured at each stage through axial compression tests (5 cycles to 1kN, 1Hz). Finally, a preliminary DVC analysis was conducted on a single sample to compare internal 3D strains.

Results

From manual calculations, intact disc average axial annulus strains were higher compared to axial nucleus strains (12.34% vs 8.31%). Following nucleotomy, axial nucleus strains reduced to 6.69%, whilst axial annulus strains were similar to those at the intact stage. The nucleus replacement reduced average axial annulus and nucleus strains compared to the intact stage (strains of 10.20% and 7.32%, respectively). Compared to the unloaded intact disc, the average post-nucleotomy heights were 12.27% and 10.13% lower in the annulus and nucleus, respectively. Post-nucleus replacement, disc height increased to values 7.32% and 3.20% higher than the average intact stage in the annulus and nucleus, respectively. In terms of stiffness, nucleotomy caused an average elastic-region stiffness drop (16.93% lower than the intact stiffness). After nucleus replacement the average elastic-region stiffness was within 9.53% of the intact stiffness. In the toe-region of the stiffness curves, the nucleus replacement did not restore stiffness back to the intact state (stiffness was 41.56% of the intact value). DVC-analysis identified peak minimum principal strains in mid-annulus regions of the intact discs. These regions shifted towards the inner-annulus when denucleated, and then back to the mid-annulus post-nucleotomy (Figure 1).

Discussion

This is the first study to capture ultra-high-field MRIs of intervertebral discs in intact, post-nucleotomy and post-nucleus replacement states. Nucleotomy leads to a reduction in disc height, stiffness and altered internal strain distributions. The nucleus replacement device used in this study restored stiffness to intact levels at higher loads (500N-1kN), and internal 3D strain patterns, but failed to restore toe-region stiffnesses. Therefore, future development of devices that are able to capture the full physiological behaviour of healthy, intact discs across all loads is recommended. Additionally, this study has shown that DVC has great potential to non-invasively assess internal interactions between nucleus replacement devices and surrounding tissue.

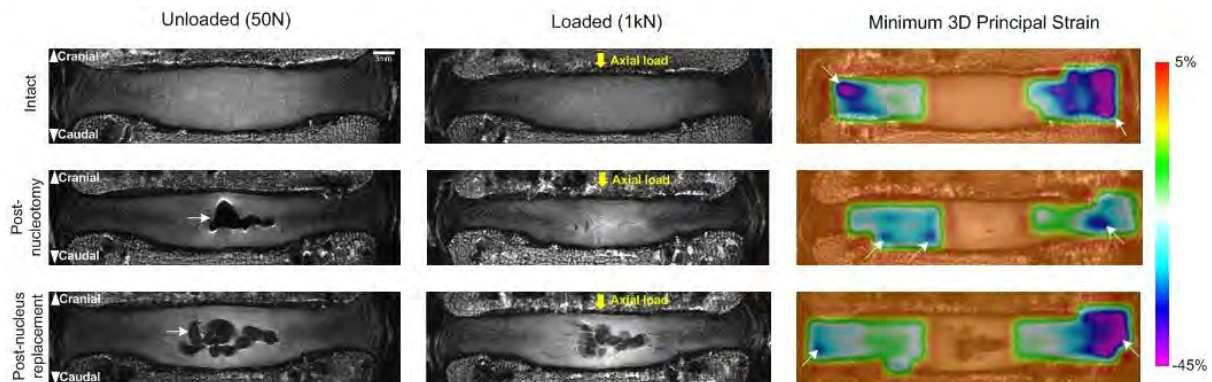


Figure 1: 9.4T MRI coronal plane view of intervertebral disc in intact, post-nucleotomy and post-nucleus replacement in both unloaded and loaded conditions along with the minimum 3D principal strain maps. The arrow in the unloaded post-nucleotomy MRI indicates the cavity formed in the disc after nucleus removal. The arrow in the bottom left unloaded state MRI indicates the nucleus replacement device. The arrows on the strain maps indicate location of peak strain.

1. Coric et al., Neurosurg. Spine-8, 115–120 (2008)
2. Tavana et al., J. Biomech.-102, 109604 (2020)
3. Pfirrmann et al., Spine-26, 1873–1878 (2001).

Improved sagittal spinal alignment and standing body balance by a “locomotion training” rehabilitation program in patients with “locomotive syndrome”

Yutaro Kanda¹, Takashi Yurube¹, Toru Takeoka², Nobuyoshi Watanabe³, Hideyo Inaoka², Ryu Tsujimoto¹, Kunihiko Miyazaki¹, Hiroki Ohnishi¹, Tomoya Matsuo¹, Masao Ryu¹, Yoshiki Takeoka¹, Yuji Kakiuchi¹, Zhongying Zhang¹, Ryosuke Kuroda¹, Kenichiro Kakutani¹

1. Orthopaedic Surgery, Kobe University Graduate School of Medicine, Kobe, Hyogo, Japan

2. Rehabilitation, Kyoto Kujo Hospital, Kyoto, Japan

3. Orthopaedic Surgery, Kyoto Kujo Hospital, Kyoto, Japan

INTRODUCTION: “Locomotive syndrome” is a degenerative condition of reduced mobility due to the impaired musculoskeletal system, which has gained increasing attention as a Japan’s health policy target. The Japanese Orthopaedic Association (JOA) recommends “locomotion training” exercises (basically squatting and single-leg standing) to be effective in preventing “locomotive syndrome”. However, the extent to which “locomotion training” affects body function is unknown. Therefore, a cohort study was designed. Our objective was to clarify effects of a “locomotion training”-based rehabilitation program on the sagittal spinal alignment and standing body balance.

METHODS: Patients who fulfilled the JOA criteria for “locomotive syndrome” were enrolled and prospectively followed in our outpatient clinic ($n = 106$: age, 76.1 ± 5.9 years; male:female = 12:94). While 44 patients accepted and completed our “locomotion training”-based rehabilitation program once per week for 6 months (20-min stretching and self-exercise achievement evaluation), 41 patients denied the exercise participation but received medicinal treatment (NSAIDs, pregabalin, duloxetine, and/or tramadol). Standing whole-spine radiographs for the spine-pelvis-lower extremity axis, ODI and SF-36 questionnaires for QOL, and piezoelectric force-plate measurements for postural stability were taken at baseline and >6 months. The chi-squared test or Student’s *t*-test was used.

RESULTS: [Exercise-intervention analysis] While there were no obvious differences in baseline sagittal vertical axis (SVA), >6-month changes were significantly different (exercise, -5.5 ± 20.0 mm; control, $+5.2 \pm 22.6$ mm: $P = 0.02$). In other radiographic parameters, >6-month changes were more remarkable in the lumbar lordosis (LL) (exercise, $+1.5 \pm 8.1^\circ$; control, $-1.3 \pm 9.1^\circ$: $P = 0.14$), thoracic kyphosis between T5 and T12 (exercise, $-0.05 \pm 5.5^\circ$; control, $+1.8 \pm 6.0^\circ$: $P = 0.13$), and T1 slope (exercise, $-0.4 \pm 6.3^\circ$; control, $+1.6 \pm 5.8^\circ$: $P = 0.14$). Questionnaires of ODI and SF-36 did not reach statistical significance ($P = 0.08$). However, in force-plate examination, the center-of-pressure area (exercise, -0.4 ± 1.8 cm²; control, $+0.2 \pm 1.6$ cm²: $P = 0.07$), speed (exercise, -0.1 ± 0.4 cm/s; +0.1 \pm 0.4 cm/s: $P = 0.03$), and distance (exercise, -5.1 ± 24.3 cm; control, $+6.5 \pm 23.3$ cm: $P = 0.03$) decreased after >6-month rehabilitation. [SVA analysis] Of 40 patients with baseline SVA ≥ 40 mm, endpoint SVA improvement to <40 mm was observed in 12 (30.0%). In the comparison between 12 patients with and 28 without improved SVA, baseline SVA ($+51.6 \pm 10.2$ mm; $+79.5 \pm 34.0$ mm: $P < 0.01$), C2–C7 angle ($+10.9 \pm 6.0^\circ$; $+19.6 \pm 13.0^\circ$: $P = 0.03$), and hip-flexion angle ($+8.1 \pm 2.4^\circ$; $+11.2 \pm 4.0^\circ$: $P = 0.02$) were significantly different. Then, >6-month changes were relatively obvious in LL ($+4.6 \pm 9.0^\circ$; $-0.6 \pm 8.1^\circ$: $P = 0.08$). In force-plate examination, >6-month changes were marked in the area (-1.6 ± 5.3 cm²; $+0.2 \pm 1.7$ cm²: $P < 0.01$).

DISCUSSION: This is the first study to demonstrate that “locomotion training” protects against “locomotive syndrome”-associated positive SVA shift and improves the standing spinal balance. However, rehabilitation-induced SVA improvement is limited in patients with advanced baseline SVA positive shift, C2–C7 hyperlordosis, and hip contracture.

Home-Based Functional Outcome Measurements: Validation and Feasibility Study of Low-Cost Wearable Sensor for Spine Patients

Ram Haddas¹, Yair Barzilay²

1. Texas Back Institute, Plano, TX, United States

2. Shaare Zedek Medical Center, Jerusalem, Israel

Introduction: Functional outcome measurements (FOMs) have been shown to be effective tools in diagnosing, planning treatments, and tracking outcomes in several subspecialties of medicine. FOMs often produce large volumes of complex data that require sophisticated collection, storage, and analytic techniques to generate functional measures of domains such as gait performance, postural stability, neuromuscular activity, and movement strategies. These complexities pose particular challenges for the application of FOMs in the clinical setting where the primary focus is on patient care. Unfortunately, there are capital and support costs associated with running and maintaining FOMs labs which pose additional hurdles that may inhibit otherwise interested surgeons. As interest in and use of clinically-derived functional evaluations of spine patients grow, so will the need for simple, objective measures that summarize complex data sets to create clinically-meaningful and actionable information. Therefore, the purpose of this study was to develop and validate low-cost FOMs generated from a wearable sensor that quantifies common movement in a home-based environment.

Methods: Twelve Lumbar Degenerative surgical candidates (LD; Age: 59.6, Height: 1.68 m, Weight: 71.5 kg) and 12 healthy controls (C; Age: 46.1, Height: 1.74 m, Weight: 80.1 kg) participated in this study. Controls wear a small sensor (30 x 44 x 8mm, weight: 12 grams) with a patch on T1 in addition to traditional Gait Lab sensors. Validation of the proposed sensor and common FOMs outcomes out of a gait lab were compared. Furthermore, subjects wore the wearable sensor for additional 24 hours. The sensor detected different types of activities during the day (i.e. standing, walking, sitting, etc.) and also capture the patient's level of activity in the home-based environment (Figure 1).

Results: In comparison to a gold standard human motion capture, the wearable sensor was able to reliably measure all trunk kinematic during standing, walking, and transition from sitting ($p>0.05$). Based on the sensor detection and algorithm, patients with degenerative lumbar spinal pathologies presented with a lower level of activity (Walking:4.7%, Standing: 11.6%, Sitting: 25.3%) in comparison to controls (Walking:7.9%, Standing: 21.7%, Sitting: 17.1%; Figure 1). Balance effort and the Cone of Economy dimensions were found to be significantly larger in LD patients (sagittal: 7.9°, coronal: 7.2°) compared to controls (sagittal: 5.8°, coronal: 3.2°; $p<0.035$; Figure 2).

Discussion: The underlying purpose of this study was to validate and prove the feasibility of home-based functional outcome measurements, which can provide relevant details in a digestible format that conveys the functional status of the patient and raises flags for areas of concern. Such insights may lead to changes in assessments of disability, treatment strategies, or modifications of rehabilitation regimens. Several benefits are anticipated from a wearable quantitative tool to assist with preoperative planning for patient-specific alignment objectives, which may assist in choosing the right surgical procedure for the right patient, recognition of red flags, leading to avoidance of surgery where it is not going to help, and also recovery monitoring, early detection of perioperative complications, prognostic information, and treatment data.

Figure 1. Activity Detection by the Proposed Sensor of a Representative Spine Patient and Healthy Con

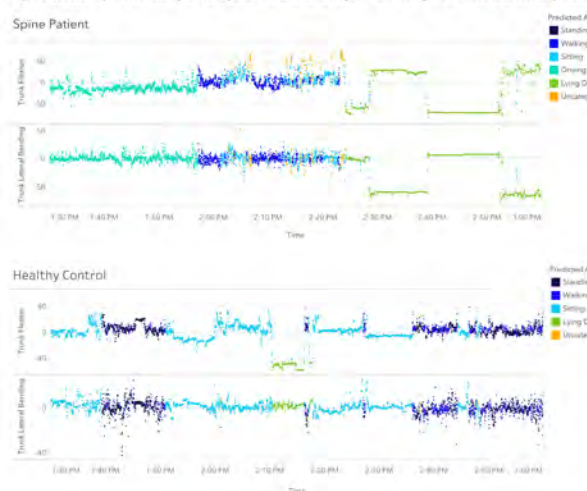
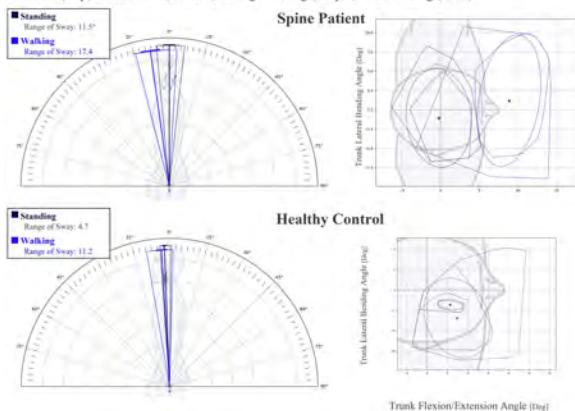


Figure 2. Cone of Economy Dimensions of a side (Left) and top (Right) Views for Representative Spine Patients (Top) and Control (Bottom) during Walking (Purple) and Standing (Blue)



Regenerative potential of moderately degenerated human nucleus pulposus cells subjected to changes in physicochemical stresses mimicking daily spinal motion

Yutaro Kanda¹, Yoshiaki Takeoka¹, James Kang¹, Shuichi Mizuno¹

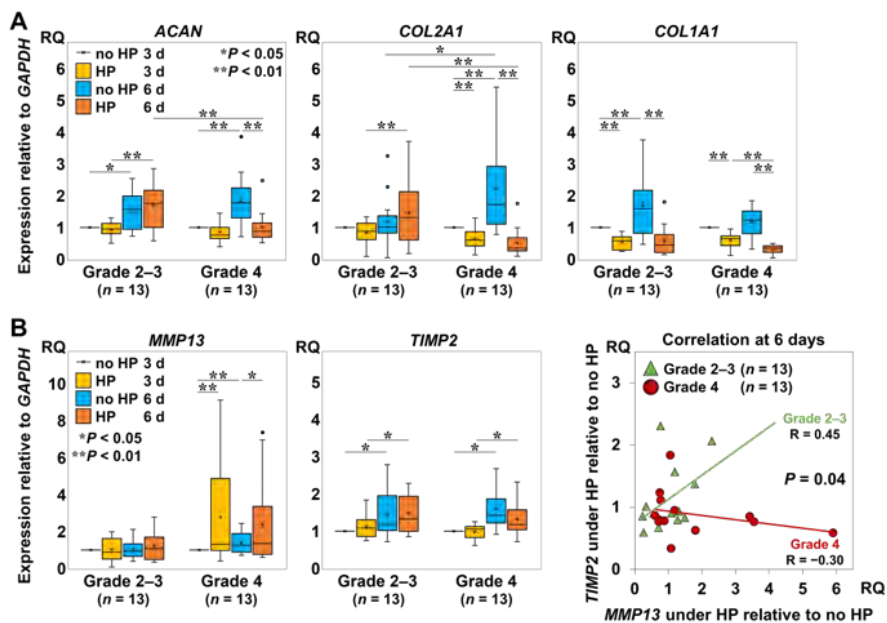
¹. Brigham and Women's Hospital, Boston, MA, United States

Introduction: To develop regenerative strategies to treat intervertebral disc (IVD) degeneration, it is necessary to understand the metabolic characteristics of the resident cells in degenerated IVDs. Nucleus pulposus (NP) cells are exposed to changes in hydrostatic pressure (HP) at high osmotic pressure (OP) due to compressive spinal motion and negatively charged extracellular matrix (ECM). Our studies using bovine NP cells indicated that repetitive changes in HP at high OP stimulated the production of NP-specific ECM. We hypothesized that human NP (hNP) cells in moderately degenerated IVDs (defined with Pfirrmann grades) express anabolic turnover under the same regimen of HP in high OP as used for bovine NP cells. We assessed metabolic turnover in hNP cells isolated from tissue with Pfirrmann grades 2-3 or 4 under HP at high osmolality using gene expression assay and immunohistology.

Methods: All experiments were performed under IRB approval. We measured the amounts of DNA, RNA, and sulfated glycosaminoglycan (SGAG) in hNP tissues from subjects who underwent surgery (n=10: age 47.4±16.8 [21–69]) and then evaluated the correlation with Pfirrmann grades. We thereafter divided hNP tissues into 2 groups according to Pfirrmann grade: grade 2–3 (n=13: age 46.7±14.0 [22–71]), and grade 4 (n=13: age 53.0±11.5 [37–75]). NP cells/clusters were isolated and incubated within semi-permeable membrane pouches under 2 different conditions: no HP, in which pouches were placed in culture medium; and HP, in which cyclic HP (0.2–0.7 MPa, 0.5 Hz) was applied for 2 days followed by constant HP (0.3 MPa) for 1 day, repeated twice over 6 days. The OP of medium was set at 450 mOsm/kg H₂O with NaCl. The pouches were harvested at 3 and 6 days. The gene expression of collagen types I (*COL1*) and II (*COL2*), aggrecan (*ACAN*), and matrix metalloproteinase 13 (*MMP13*) were measured. Immunohistology for *MMP13* and *TIMP2* were also performed. Three-way repeated-measures ANOVA with the Bonferroni post hoc test was used with significance at $P < 0.05$. Linear regression analysis was also performed to assess the correlation between the expression of *MMP13* and *TIMP2*.

Results: SGAG contents / DNA amounts had a negative correlation with Pfirrmann grade ($R=0.69$) (Grade 3, 295.8±276.0 mg/mg; Grade 4, 32.3±21.4 mg/mg), whereas RNA amounts had no correlation with Pfirrmann grade. *ACAN* and *COL2* were significantly upregulated under HP in grade 2–3 compared to grade 4 (both, $P < 0.01$). *COL1* was significantly lower in both grades under HP than under no HP at 3 and 6 days (all, $P < 0.01$) (Figure A). Linear regression analysis showed a positive correlation between *MMP13* and *TIMP2* expression in grade 2–3 under HP, but a negative correlation in grade 4 ($P=0.04$) (Figure B). Immunohistology for *MMP13* and *TIMP2* showed a similar trend. These results reflect the difference in inhibition capacity for catabolic upregulation under HP between the two groups.

Discussion: Remnant hNP cells of Pfirrmann grade 2–3 under physiological stresses including HP and OP will be capable of to regenerate by reactivating anabolic turnover in hNP cells and suppressing catabolic turnover compared to those of Pfirrmann grade 4.



Is pelvic incidence constant value?: Minimum 13 year longitudinal follow-up of pelvic incidence

Chang-Hoon Jeon¹, Nam-Su Chung¹, Han-Dong Lee¹, Hee-Woong Chung¹, Ki-Hoon Park¹, Ha-Seung Yoon¹

1. Ajou University School of Medicine, Suwon, Kyonggi, South Korea

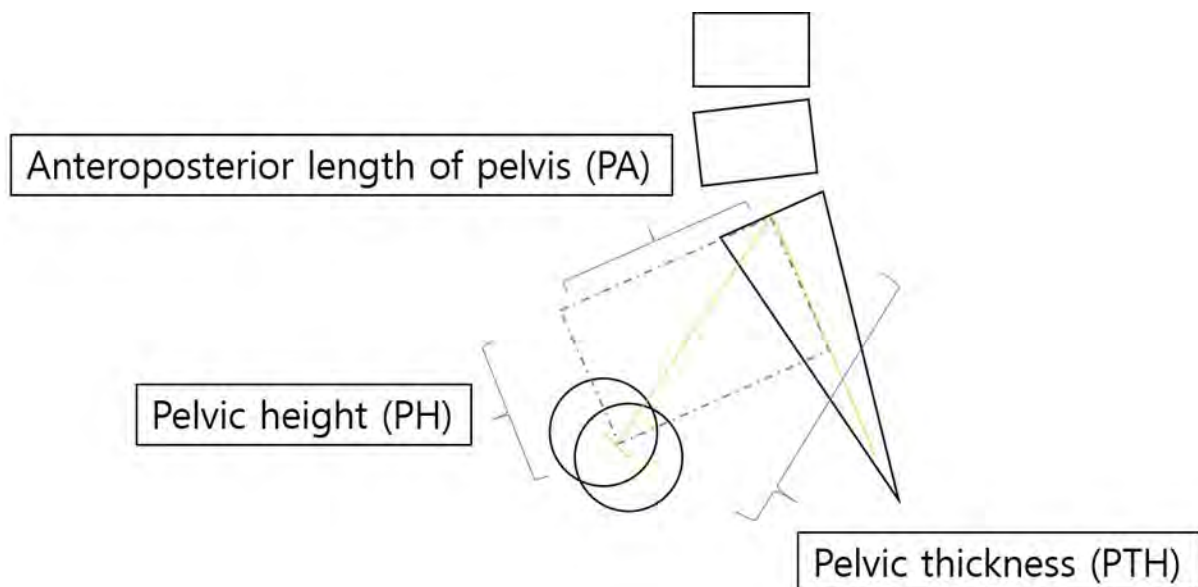
Introduction: Pelvic incidence (PI) is a sagittal anatomical parameter of the pelvis and is known to remain unchanged. However, recent studies found PI increase with age. No studies have been conducted evaluating longitudinal changes in PI. Our objective of this study was to evaluate the longitudinal change of PI and related demographic and radiological factors.

Methods: We analyzed 84 individuals who did not undergone spinal instrumentation and were followed more than 13 years in our institute (the mean duration of follow-up length was 14.2 ± 0.8 years). Standing lumbar radiographs were taken at the initial visit and at the final follow-up. PI, pelvic tilt (PT), sacral slope (SS), L1-S1 lumbar lordosis (LL), L4-S1 lower lumbar lordosis (LLL), anteroposterior length of S1 upper endplate (S1UE), and pelvic thickness (PTH) were measured on both radiographs. Pelvic height (PH) and anteroposterior pelvic length (PA) were also measured (Figure 1). All baseline and follow-up parameters were compared using the paired t-test. Study subjects were divided into PI change group (PI increase more than 5° during follow-up, $n=21$) and the control group ($n=63$) and the reference parameters were compared between groups using the t-test. Among PI change group, changes in PTH, PH and PA (normalized by S1UE) were analyzed.

Results: The mean age at the initial visit was 49.9 ± 14.6 years (range: 19-82 years). There were 27 men and 57 women. Baseline PI, PT, SS, LL, LLL, S1, and PTH were $50.5 \pm 10.0^\circ$, $15.7 \pm 7.7^\circ$, $34.7 \pm 10.7^\circ$, $45.4 \pm 13.2^\circ$, $33.9 \pm 8.5^\circ$, $41.4 \pm 3.8\text{mm}$, and $132.0 \pm 10.8\text{mm}$, respectively. PI and LLL were not significantly different between initial and follow-up images. PT increased, LL decreased during follow-up (all $P < 0.05$). Between PI change group and the control group, age and gender were not significantly different. In PI change group, the baseline LL ($40.3 \pm 15.0^\circ$ vs. $47.0 \pm 12.3^\circ$, $P=0.041$) and the LLL ($30.8 \pm 7.8^\circ$ vs. $35.0 \pm 8.5^\circ$, $P=0.046$) were lower. Among the PI change group, PA increased (2.4 ± 0.4 to 2.6 ± 0.4 , $P < 0.001$) and PH decreased (2.2 ± 0.4 to 1.8 ± 0.5 , $P < 0.001$) without significant changes in PTH (3.3 ± 0.4 to 3.2 ± 0.3 , $P=0.500$)

Discussion: PI did not change significantly changed in a minimum follow-up of 13 years. However, PI increased more than 5 degrees in 25% of cases. There was no difference in age between the group with and without PI, and there was a difference in LL and LLL. This implies that sagittal imbalance has more influence on PI change than age itself. In the cases where the PI was changed, the distance between the sacrum center and the femoral head center did not change, but changed in the form of increasing PA and decreasing PH. A larger number of study on PI changes are additionally needed to confirm to change of PI, and biomechanical study on PI changes are also needed to understand the change of PI.

Figure 1. Anteroposterior length of pelvis and pelvic height



Detection and Characterization of Vertebral Endplate Structural Defects on Clinical Imaging and Micro-CT: A Diagnostic Test Validity Study

Michele C. Battié¹, Aliyu Lawan¹, Andrew Leung², Stephanie Leung²

1. Faculty of Health Sciences and Western's Bone & Joint Institute, University of Western Ontario, London, Ontario, Canada

2. Department of Medical Imaging, Victoria Hospital, London Health Sciences Centre, London, Ontario, Canada

Introduction: Studies of endplate structural defects (EPSD) may further the understanding of pathoanatomical mechanisms underlying back pain. However, with CT, as with MRI, the common measurement methods used to document EPSD have not been validated, leaving uncertainty about what the observations represent or how accurately they capture the presence or absence of EPSDs. This study aims to compare and determine the reliability and validity of two common EPSD assessment methods using clinical-CT, with micro-CT as the reference standard.

Methods: Using an evaluation manual, 418 endplates on sagittal slices of clinical-CT obtained from 19 embalmed cadavers (9 men and 10 women, aged 62-91 years) were independently assessed by three raters (two experienced radiologists and a novice) for EPSD using two methods (Brayda-Bruno: wavy/irregular, notched, Schmorl's nodes and fracture; and Feng: focal, corner, and erosive defects), with two-week intervals between each assessment, blinded to all prior assessments. A Nominal Group Technique was followed to resolve discordance and achieve consensus. The corresponding micro-CT from the harvested T7-S1 spines were assessed by another independent rater with excellent intra-rater agreement (Kappa=0.955, 95%CI: 0.912–0.998). All data were analyzed descriptively and inferentially for reliability and validity, including sensitivity and specificity, on SPSS version 22. The study was prospectively registered at ClinicalTrials.gov (NCT04808960).

Results: Inter-rater agreement between each pair of raters was good (Kappa=0.60-0.69) for assessing the presence of EPSD using both Brayda-Bruno and Feng assessments. However, poor agreement was observed for the assessment of specific EPSD phenotypes according to Brayda-Bruno (Kappa=0.43) and Feng (Kappa=0.58). All normal endplates according to Brayda-Bruno (n=151) were classified as normal using Feng. However, 26% (n=58) of normal endplates by Feng corresponded to wavy/irregular endplates in the Brayda-Bruno system for which a category did not exist in Feng. Similarly, erosion, for which Brayda-Bruno lacked a category, was mainly (82.8%) classified as wavy/irregular. While the majority of notched defects (n=15, 46.9%) and Schmorl's nodes (n=45, 79%) using Brayda-Bruno's classification were recorded as focal defects using Feng's. *When compared to micro-CT*, fractures (n=53) and corner defects (n=28) were routinely missed on clinical-CT. Endplates classified as wavy/irregular on clinical CT corresponded to erosion (n=29, 21.2%), jagged defects (n=21, 15.3%) and calcification (n=19, 13.9%) on micro-CT. Schmorl's nodes assessed on clinical CT often represented erosion (n=16, 32%) on micro-CT and focal defects represented endplate fractures (n=21, 27.6%). Overall, there was a sensitivity of 70.9% and specificity of 79.1% for Feng's method, and 79.5% and 57.5%, respectively, using Brayda-Bruno's. Schmorl's nodes (60%) and Focal defects (52%) had the highest sensitivity. All EPSD clinical-CT and micro-CT dimensions significantly correlated ($p < 0.001$), except defect depth.

Discussion: There is good reliability and support for the validity of assessing the presence of EPSD with the two classification methods using clinical CT. However, neither method contained sufficient EPSD phenotypes to provide the needed specificity. The Brayda-Bruno system lacked a category for erosion, and Feng lacked a category for wavy/irregular defects. A standardized, combined method, with a publicly available measurement atlas, is needed to improve reliability and improve specificity of EPSD presence and interpretation.

1. Brayda-Bruno M, Albano D, Cannella G, et al (2018) Endplate lesions in the lumbar spine: a novel MRI-based classification scheme and epidemiology in low back pain patients. *Eur Spine J* 27:2854–2861. <https://doi.org/10.1007/s00586-018-5787-6>
2. Feng Z, Liu Y, Yang G, et al (2018) Lumbar Vertebral Endplate Defects on Magnetic Resonance Images. *Spine (Phila Pa 1976)* 43:919–927. <https://doi.org/10.1097/brs.0000000000002450>

Extending the straight leg raise test for improved clinical evaluation of sciatica

Janne Pesonen^{2,1}, **Michael Shacklock**^{3,1}, **Juha-Sampo Suomalainen**⁴, **Lauri Karttunen**^{2,1}, **Jussi Mäki**^{2,1}, **Olavi Ariaksinen**^{2,1}, **Marinko Rade**^{5,1,6}

1. *Department of Rehabilitation, Kuopio University Hospital, Kuopio, Finland*

2. *Department of Surgery, Institute of Clinical Medicine, University of Eastern Finland, Kuopio, Itä-Suomen lääni, Finland*

3. *Neurodynamic Solutions, Adelaide, South Australia, Australia*

4. *Department of Radiology, Kuopio University Hospital, Kuopio, Itä-Suomen lääni, Finland*

5. *Josip Juraj Strossmayer University of Osijek, Faculty of Medicine, Orthopaedic and Rehabilitation Hospital "Prim. dr. Martin Horvat", Rovinj, Croatia*

6. *Department of Natural and Health Studies, Juraj Dobrila University of Pula, Pula, Croatia*

INTRODUCTION: The straight leg raise test (SLR) is one of the most utilized and studied physical tests in patients with low back pain for the detection of lumbar disc herniation (LDH), showing high sensitivity and heterogeneous or low specificity. Based on in-depth knowledge from previous studies on neural movement during the SLR on subjects with or without pathology, we were able to add location-specific structural differentiation movements to the traditional SLR for it to better discern neural symptoms from musculoskeletal. Hence, the test was named the extended straight leg raise test (ESLR). The differentiating movements were ankle dorsiflexion for proximally reproduced symptoms (buttock/hamstring), and hip internal rotation for distally (below the knee) emerged responses. The hip flexion angle was not limited to any specific angle. Having previously found that the ESLR is both repeatable and reliable to detect sciatic patients from low back pain patients, we wanted to assess how the ESLR predicted pathology seen on the MRI.

METHODS: 40 subjects comprised the study population, 20 in sciatic group and 20 in control group. The study controller allocated the patients to these groups. The ESLR was performed 'blinded' to the subjects by two independent examiners and judged positive/negative. After the ESLR testing, each subject's lumbar MRI was evaluated. The MRIs were analyzed independently by 2 senior radiologists and a spine specialist. Cohen's Kappa was calculated for the agreement of the test result. To obtain the odds ratio (OR) for positive ESLR result for LDH or nerve root compression (NC), a binary logistic regression analysis with subjects' age, gender, height and weight was performed. ESLR's validity was assessed by combination of interrater agreement (Cohen's Kappa) of independent examiners and percentage prevalence of both LDH and NC.

RESULTS: The extended straight leg raise test (ESLR) showed almost perfect interrater reliability between examiners and ability to detect sciatic patients: Cohen's Kappa was 0.85 between blinded examiners, and 0.90 and 0.95 when compared to group allocation, respectively. In the MRI scans, 85% of sciatic (ESLR+) patients had LDH and 75% NC in the MRI. Not surprisingly, MRI showed a very high incidence of 'false-positive'/pathologic/asymptomatic findings with the ESLR negative group. A positive result in the ESLR was found to be highly predictive for both LDH and NC: the OR was 8.0 ($p = 0.028$) and 5.6 ($p = 0.041$), respectively.

DISCUSSION: The ESLR showed high repeatability, reliability and validity in detecting neural symptoms and pathology seen in the MRI when judged positive. It is noteworthy that these results were obtained when the ESLR was performed to the patients blindly, and its performance should even improve in detecting patients experiencing sciatic symptoms when its combined to the normal patient history and clinical examination.

The severity of disc degeneration associates with poor cartilage endplate composition but not with deficits in vertebral bone marrow composition

Noah B. Bonnheim¹, Linshanshan Wang¹, Ann A. Lazar², Jiamin Zhou³, Ravi Chachad³, Nico Sollmann^{3,4,5,6}, Xiaojie Guo¹, Claudia Iriondo³, Conor O'Neill¹, Jeffery C. Lotz¹, Thomas M. Link³, Roland Krug³, Aaron J. Fields¹

1. Department of Orthopaedic Surgery, University of California, San Francisco, San Francisco, CA, USA

2. Department of Epidemiology and Biostatistics, University of California, San Francisco, San Francisco, CA, USA

3. Department of Radiology and Biomedical Imaging, University of California, San Francisco, San Francisco, CA, USA

4. Department of Diagnostic and Interventional Radiology, University Hospital Ulm, Ulm, Germany

5. Department of Diagnostic and Interventional Neuroradiology, Klinikum rechts der Isar, Technical University of Munich, Munich, Germany

6. TUM-Neuroimaging Center, Klinikum rechts der Isar, Technical University of Munich, Munich, Germany

Introduction: Nutrients that nourish cells in the avascular disc diffuse from the vertebral capillaries, across the cartilage endplate (CEP), and into the nucleus pulposus (NP). Thus, the composition of CEP tissue and subchondral bone marrow may play important roles in disc health by influencing nutrient diffusion and vertebral perfusion. However, the relative roles of these factors in disc degeneration have not been quantified. The goal of this study was to use biomarkers of tissue composition derived from quantitative MRI to establish how CEP composition (surrogate for permeability) and vertebral bone marrow fat fraction (BMFF, surrogate for perfusion) contribute to disc degeneration in humans. This knowledge could help clarify the etiology of disc degeneration and identify factors impacting the efficacy of regenerative intradiscal biologic therapies.

Methods: MRI data from 77 patients were included in this study. Sixty subjects had chronic low back pain (cLBP; >3 month duration; age=40.0±11.9 years, 19–65 [mean±SD, min–max]; 28 female, 32 male; ODI=26.1±14.6; VAS=6.5±2.4,) and 17 were asymptomatic controls (age=41.4±10.9 years, 23–67; 9 female, 8 male). Ultra-short echo-time (UTE) MRI was used to calculate CEP T2* relaxation times (reflecting biochemical composition and permeability), chemical shift encoding-based water-fat MRI was used to calculate vertebral BMFF (proportional to the amount of hematopoietic marrow and providing a proxy for perfusion), and T1ρ MRI was used to calculate T1ρ relaxation times in the NP (NP T1ρ, reflecting proteoglycan content and degenerative grade). A combination of neural network-generated and manually-generated segmentations for levels L4–S1 were used for biomarker analysis (**Fig. 1**). Univariate linear regression was used to assess the independent effects of CEP T2* and vertebral BMFF on NP T1ρ. Mixed effects linear regression accounting for spinal level, age, and sex were used to assess combined relationships.

Results: CEP T2* and vertebral BMFF were independently associated with NP T1ρ ($p=0.014$ and 0.0001 , respectively). After adjusting for age, sex, and spinal level, NP T1ρ remained significantly associated with CEP T2* ($p=0.004$, **Table 1**) but not vertebral BMFF ($p=0.40$). The relationship between disc degeneration and CEP composition was similar in cLBP and asymptomatic cohorts ($p=0.59$ for the interaction between cohort and CEP T2*). In this age-adjusted model, the severity of disc degeneration was also similar between cohorts (mean NP T1ρ=64.2 ms [95% CI: 59.7, 68.6] versus 71.8 ms [63.8, 79.7], cLBP versus control, $p=0.09$).

Discussion: These results provide the first evidence that lumbar disc degeneration severity associates with compositional deficits in the CEP. We found that CEPs with lower T2* values—reflecting lower CEP hydration, lower GAG content, a higher ratio of collagen-to-GAG, and lower permeability—were associated with more severe disc degeneration. Unlike vertebral BMFF, CEP composition was a significant predictor of disc health after accounting for co-variates, demonstrating the relative importance of CEP composition in disc degeneration in humans both with and without cLBP and with and without deficits in vertebral perfusion. The UTE-derived CEP T2* biomarker may be a promising diagnostic measurement to help select patients with adequate CEP composition to support intradiscal biologic therapies, which inherently increase nutrient demands.

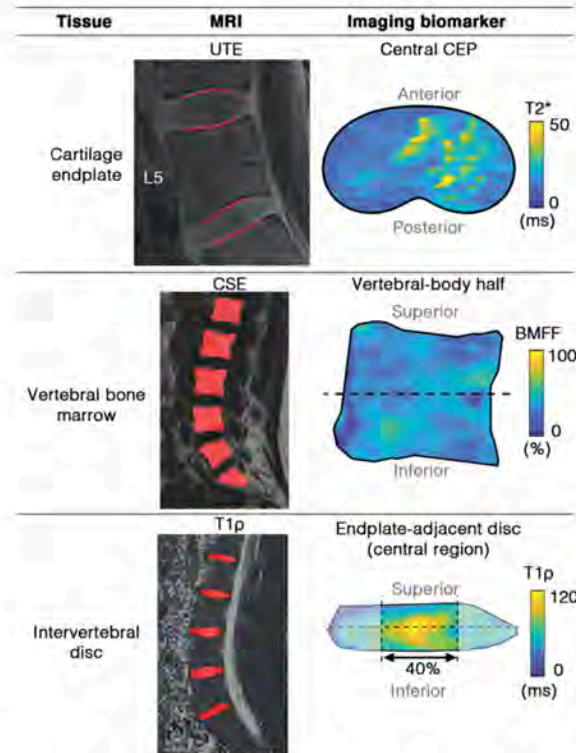


Figure 1 Tissue segmentations and biomarker visualization for the CEP (top row), vertebral bone marrow (middle row), and intervertebral disc (bottom row). Biomarkers were defined as the mean T2* value in the central CEP, the mean BMFF value in the hemi-vertebral region adjacent to each endplate, and the mean T1 ρ in the central (NP) region of the disc adjacent to each endplate. CEP = cartilage endplate, BMFF = bone marrow fat fraction, NP = nucleus pulposus, UTE = ultra-short echo-time MRI, CSE = chemical shift encoding-based water-fat MRI.

Table 1 Parameter estimates and 95% CI from a mixed effects linear regression model predicting NP T1 ρ . * $p < 0.05$ (two-sided).

Term	β_i estimate	Lower 95%	Upper 95%	p -value
CEP T2*	0.80	0.26	1.33	0.004*
Level	3.50	1.41	5.59	0.001*
CEP T2* \times Level	0.64	0.16	1.11	0.009*
Age	-0.53	-0.90	-0.17	0.005*
Vertebral BMFF	-0.14	-0.48	0.19	0.40
Sex	1.83	-1.90	5.56	0.33

How to mimic disc degeneration for in vitro experiments to test regenerative approaches? Usage of chondroitinase versus papain

Jan Ulrich Jansen¹, Graciosa Q Teixeira¹, Andrea Vernengo², Sibylle Grad², Karin Benz³, Cornelia Neidlinger-Wilke¹, Hans-Joachim Wilke¹

1. Institute of Orthopaedic Research and Biomechanics, Ulm University Hospital, Ulm, Germany

2. AO Research Institute Davos, Davos, Switzerland

3. TETEC Tissue Engineering Technologies AG, Reutlingen, BW, Germany

Introduction: Hydrogels are playing an increasingly important role in the development of regenerative approaches for the intervertebral disc (IVD)^{1,2}. Since there is limited availability of native human discs for research and often animal models do not mimic human disc degeneration, testing the biomechanical performance of a hydrogel after implantation remains difficult. The objective of the present study was to adapt and optimize an in vitro model of bovine tail discs for biomechanical testing. Discs were artificially degenerated with different enzymes and the distribution of a hydrogel after injection was investigated.

Methods: In total, four groups of motion segments (CY3/4, n=6/group) were prepared from 24 fresh bovine tails and embedded in PMMA. Each group was injected with 0.25 or 5 U/mL chondroitinase ABC (ChABC), 65 U/mL papain or PBS (sham control), and cultured for 7 days (6% O₂, 37°C). Complex loading was applied to diminish the swelling of the discs after culture. As much as possible of a radiopaque albumin/hyaluronan hydrogel (Albugel) was injected and the injected volume quantified. μ CT scans were performed after injection to view the material distribution within the discs. After each step, the biomechanical behavior of the motion segments namely range of motion (ROM) and disc height were determined. Statistics: Shapiro-Wilk, Mann-Whitney-U, Friedman, Bonferroni-post-hoc ($p \leq 0.05$).

Results: At day 7, all specimens digested with papain developed a cavity in the nucleus, in all other three groups the nucleus seemed macroscopically intact. After incubation, the ROM for papain remained unaltered in comparison to intact specimens ($p=1.000$), whereas PBS and ChABC groups became stiffer, i.e. ROM decreased ($p \leq 0.250$). Only following complex loading, the ROM significantly increased in all groups versus intact, with the most prominent increase for papain in axial rotation ($p \leq 0.028$). More hydrogel could be injected into the papain group (1.3 ± 0.3 mL) than into ChABC-5U-digested discs (0.7 ± 0.25 mL). μ CT reconstruction of the IVDs showed one large bubble for papain and a more inhomogeneous fluffy-cloud-like distribution of the hydrogel in ChABC-5U-digested specimens (Fig. 1). The hydrogel decreased the ROM in both digested groups compared to the intact condition, more strongly in the ChABC-5U- than in the papain-digested group (Fig. 2, exemplary flexion-extension).

Discussion: The ROM increase and loss of disc height, as well as cavity formation in the papain-treated group indicate a similar behavior as described for human discs with cavities, e.g., due to disc herniation or nucleotomy³. This allows the targeted simulation of such pathologies. ChABC more closely mimics human degeneration occurring without cavities. The lower concentration of ChABC led to little effects and could mimic mild degeneration, whereas the higher concentration is suitable to simulate progressed degeneration. Both ChABC-5U and papain allowed standardized hydrogel injections and testing. However, differences in hydrogel distribution and injectable volume could be noticed. We hypothesize that the specific digestion of glycosaminoglycans by ChABC may lead to different structural defects than papain. These results have improved our overall understanding of the biomechanical effects (especially ROM) of IVD tissue digestion with ChABC and papain, and suggest that hydrogels can be investigated with these models.

Acknowledgments: iPSpine (825925).

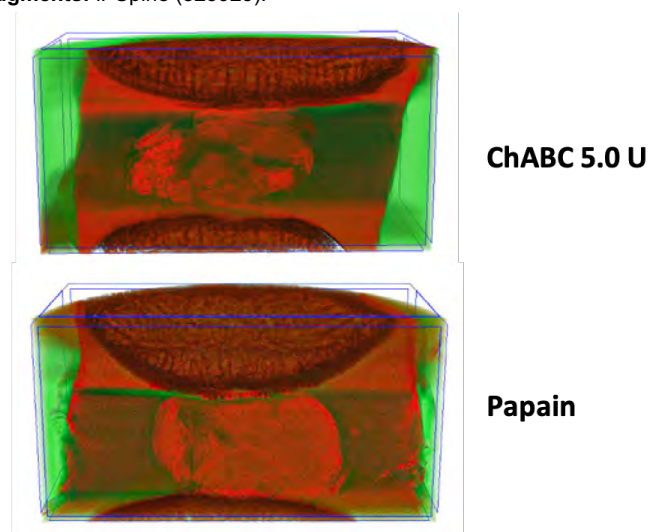


Fig. 1: Exemplary μ CTs show Albugel distribution after injection

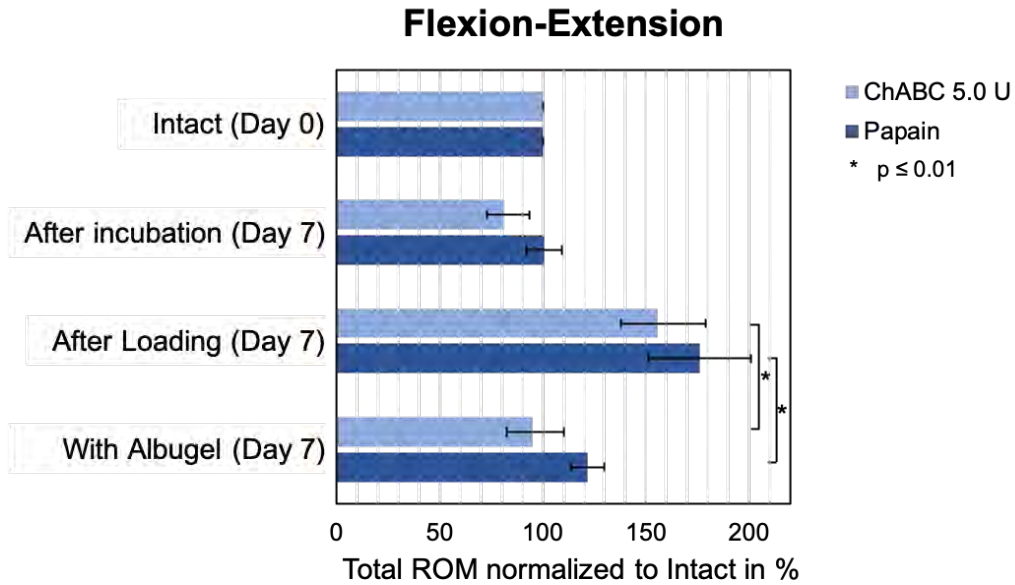


Fig. 2: Range of motion (ROM) for Flexion/Extension at different time points. No loading after Albugel injection; biomechanical characterization 60min after injection.

1. Teixeira, G.Q., et al., A Degenerative/Proinflammatory Intervertebral Disc Organ Culture: An Ex Vivo Model for Anti-inflammatory Drug and Cell Therapy. *Tissue Eng Part C Methods*, 2016. 22(1): p. 8-19.
2. Zheng, K. and D. Du, Recent advances of hydrogel-based biomaterials for intervertebral disc tissue treatment: A literature review. *J Tissue Eng Regen Med*, 2021. 15(4): p. 299-321.
3. Wilke, H.J., et al., Can prevention of a reherniation be investigated? Establishment of a herniation model and experiments with an annular closure device. *Spine (Phila Pa 1976)*, 2013. 38(10): p. E587-93.

Chimera Decoy Oligodeoxynucleotide Attenuated Intervertebral Disc Degeneration in the Rabbit Anular-puncture Model and Degenerated Disc-induced Pain Generation in the Rat Xenograft Radiculopathy Model

Koichi Masuda¹, Daisuke Fukui^{2,1}, Stephanie Y Adachi¹, Rikiya Baba¹, Natsuko Arimoto¹, Pei-Chen Choo¹, Mary Esparza¹, Julian J Garcia¹, Mamoru Kawakami³, Hiroshi Yamada²

1. Department of Orthopaedic Surgery, University of California, San Diego, San Diego, California, United States

2. Department of Orthopaedic Surgery, Wakayama Medical University, Wakayama, Japan

3. Department of Orthopaedic Surgery, Saiseikai Wakayama Hospital, Wakayama city, Wakayama, Japan

INTRODUCTION: The newly developed chimera decoy oligodeoxynucleotide (CDODN) improves on the NF- κ B decoy oligodeoxynucleotide (NDODN), with binding sequences for two transcription factors, NF- κ B and STAT-6, which are associated with the gene expression of inflammatory cytokines. In this study, we hypothesized that CDODN would inhibit the inflammatory response of intervertebral disc (IVD) degeneration. First, the short-term (4 weeks) and long-term (12 weeks) effects of a CDODN injection in IVDs in the rabbit anular-puncture model were characterized. The recovered nucleus pulposus (NP) tissues from the 4-week group were transplanted on nude rat dorsal root ganglion (DRG) as a xenograft transplant to assess potency for pain generation; pain generation was assessed by behavioral testing.

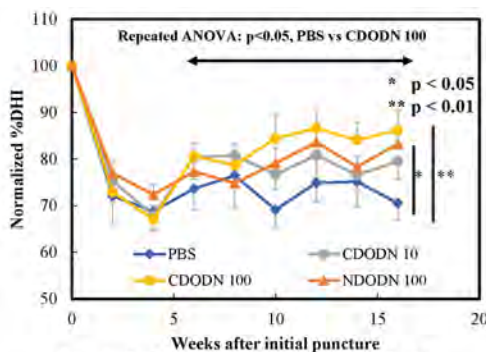


Fig. 1 %Normalized Disc Height Index

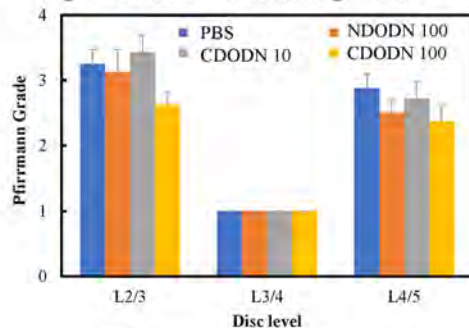


Fig. 2 MRI – Pfirrmann Grade

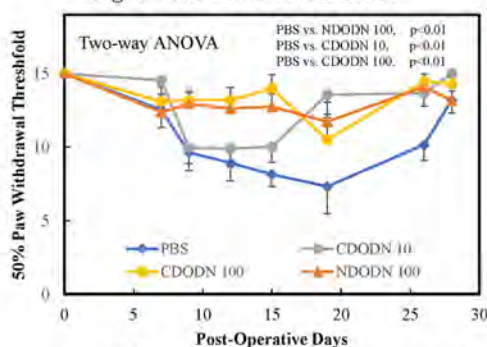


Fig. 3 Mechanical Allodynia (Von Frey Test)

METHODS:

Rabbit anular-puncture and injection of CDODN: Five-month-old female NZW rabbits (n=64) received anular-puncture in two non-consecutive lumbar IVDs (L2/3 and L4/5). Four weeks later, 10 μ l of either phosphate-buffered saline (PBS), NDODN (100 μ g in PBS), or CDODN (10 or 100 μ g in PBS) was injected into the punctured IVDs. Rabbits were euthanized at eight weeks or 16 weeks after the initial anular-puncture.

Radiographic analysis of Disc Height Index: IVD height was expressed as disc height index (DHI) from lateral radiographs of the lumbar spine obtained at two-week intervals, up to 16 weeks, after the initial puncture. The average percent change in DHI of injected IVDs was calculated for each postoperative disc as a ratio to its preoperative DHI and then further normalized to the unpunctured L3/4 IVD (normalized %DHI).

Magnetic Resonance Imaging Analyses: The average degeneration of the injected IVDs were calculated by the Pfirrmann grade using T2 weighted sagittal images obtained from MRI examinations on post-sacrifice isolated spine segments.

Nude rat disc xenograft radiculopathy model: Degenerated NP tissue from the injected IVDs of the anular-punctured rabbits were placed on the L5 right DRGs of female nude rats (n=32) as xenografts to assess pain induction.

Mechanical allodynia: Mechanical allodynia was evaluated in nude rats using the 50% paw withdrawal threshold response to mechanical stimulation by Von Frey hair filaments for both hind paws.

RESULTS:

Radiographic analysis of normalized %DHI: (Fig 1): Two-way ANOVA analysis for normalized %DHI showed a significant difference between the CDODN and PBS group ($p < 0.05$). At 16 weeks post-puncture, the NDODN 100 μ g and CDODN 100 μ g groups showed significantly higher normalized % DHI than the PBS group ($p < 0.05$).

MRI Analyses: (Fig 2): The Pfirrmann scoring showed lower tendency (less degeneration) in the CDODN 10 and 100 μ g groups compared to the PBS group ($p = 0.094$, $p = 0.088$, respectively).

Mechanical allodynia: (Fig 3): Rats transplanted with NDODN 100 μ g, CDODN 10, and 100 μ g-treated rabbit degenerated rabbit NPs exhibited reduced mechanical allodynia compared to rats transplanted with PBS-treated rabbit degenerated NPs ($p < 0.01$).

DISCUSSION: A CDODN intradiscal injection showed a significant improvement in IVD height preservation and tendency to be different in MRI scoring and indicates that the suppression of both NF- κ B and STAT 6 may attenuate disc degeneration. The decreased inflammation also

corresponded with less pain generation in the nude rat radiculopathy model.

TLR-2 Signaling Leads to the Dysregulation of miR-100-5p and miR-155-5p in Intervertebral Disc Degeneration

Petra Cazzanelli¹, Mikkael Lamoca¹, Oliver Nic Hausmann^{2,3}, Addisu Mesfin⁴, Karin Wuertz-Kozak^{1,5}

1. Rochester Institute of Technology, Rochester, NY, United States

2. Neuro- and Spine Center, Hirslanden Klinik St. Anna, Lucerne, Switzerland

3. Neurosurgical Department, University of Berne, Berne, Switzerland

4. Department of Orthopedics and Rehabilitation, University of Rochester Medical Center, Rochester, NY, USA

5. Spine Center, Schoen Clinic Munich Harlaching, Munich, Germany

INTRODUCTION: Inflammation is one of the hallmarks of intervertebral disc (IVD) degeneration. Next to other characteristics of IVD degeneration, such as extracellular matrix (ECM) degradation and cell loss, inflammation is of particular relevance since it can lead to innervation and the development of pain, hence making IVD degeneration one of the major contributors to low back pain. Toll-like receptors (TLRs) are well-known regulators of inflammation and amongst the numerous TLRs present in human IVD cells, TLR-2 is of specific relevance in the degenerative process. It has been shown that its expression correlates with increasing degrees of disc degeneration [1] and that TLR-2 can be activated by damage-associated molecular patterns, inflammatory mediators accumulating in the IVD tissue due to ECM degradation [2]. MicroRNAs (miRNAs) play a crucial role in regulating gene expression and intracellular signaling, being very strong post-transcriptional regulators. Multiple pathologies have been associated with the dysregulation of miRNAs, including degenerative diseases such as IVD degeneration [3]. However, the role of miRNAs in TLR signaling in the IVD is still poorly understood and was hence investigated in this study.

METHODS: TLR-2 signaling was activated in human *Nucleus pulposus* (*hNP*) and *Annulus fibrosus* (*hAF*) cells (n=5) isolated from degenerated IVDs (Pfirman grade: 3-4) with the TLR-2/6 agonist PAM2CSK4 (100 ng/mL for 6 hours) and TLR-2 knockdown (siRNA) cells served as a control. MiRNA and mRNA were isolated for Illumina small RNA sequencing and RT-qPCR analysis, respectively. Furthermore, cell supernatants were used to analyze proinflammatory cytokine secretion with enzyme-linked immunosorbent assay. Differentially expressed microRNAs identified by next-generation sequencing (NGS) were validated in *hNP* (n=5) and *hAF* (n=4). Target and pathway prediction of miRNAs was performed with the miRabel prediction tool (<http://bioinfo.univ-rouen.fr/mirabel/>). Statistical analysis was conducted by performing Kolmogorov-Smirnov test and a two-tailed Student's t-test, as well as Shapiro-Wilk test for normality and one-way ANOVA using GraphPad Prism version 9.0.2 for Windows (GraphPad Software).

RESULTS: The activation of the TLR-2 signaling pathway resulted in significant changes in the miRNA profile of human IVD cells. We identified 10 differentially expressed miRNAs by NGS (Figure 1). TLR-2 activation was confirmed by detecting a significant increase in protein secretion of IL-6 (30.5±8.1pg/mL) and IL-8 (28.9±5.4pg/mL) compared to untreated cells. TLR-2 knockdown was confirmed by RT-qPCR (77.7±3.5%). Amongst the miRNAs identified, the differential expression of miR-100-5p and miR-155-5p was confirmed with RT-qPCR showing the most significant TLR-2 dependent decrease and increase, respectively (Figure 2-3). These effects were fully or partially reversed in TLR-2 knockdown cells. Pathway prediction of these miRNA shows their involvement in signaling pathways downstream of TLR-2 such as MAPK, Wnt, and NF-κB signaling, as well as other inflammation and mechanosensing related pathways (Figure 4).

DISCUSSION: The TLR-2 associated dysregulation of miR-100-5p and miR-155-5p presents a link between TLR signaling and other inflammatory cell signaling pathways as well as multiple signaling pathways relevant to the degenerative process in the IVD. Ongoing experiments will further elucidate the functional role of these miRNAs in IVD pathophysiology, with a specific focus on inflammatory cell response and mechanoregulation.

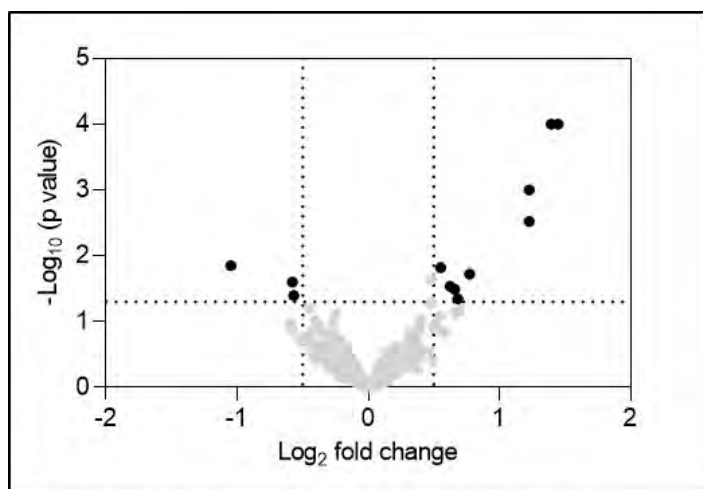


Figure 1: Volcano blot showing 10 significantly differently expressed miRNAs upon TLR-2 activation in *hNP* and *hAF* (n=5) identified by small RNA sequencing ($p < 0.05$ and \log_2 fold change $> \pm 0.5$)

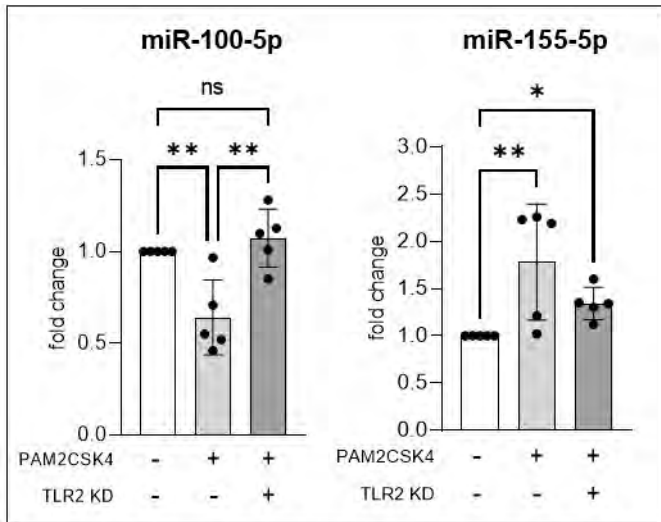


Figure 2: Differential expression of miR-100-5p and miR-155-5p in *hNP* (n=5) following treatment with Pam2CSK4. TLR-2 knockdown (KD) cells served as an additional control. * p<0.05; ** p<0.01

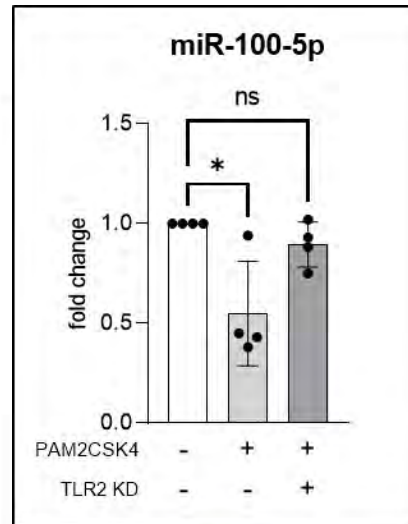


Figure 3: Differential expression of miR-100-5p in *hAF* (n=4) following treatment with Pam2CSK4. TLR-2 knockdown (KD) cells served as an additional control. * p<0.05

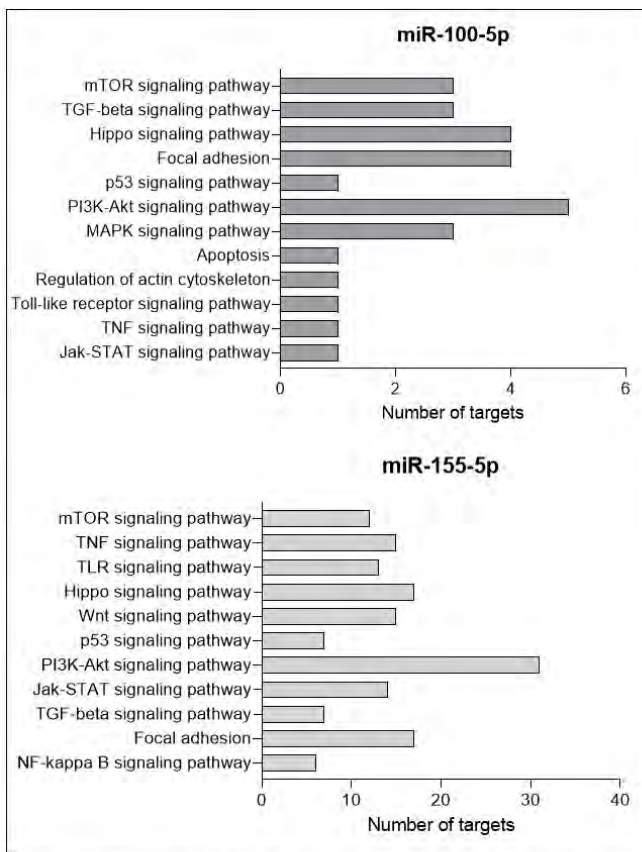


Figure 4: Pathway prediction of miR-100-5p and miR-155-5p based on the miRabel prediction tool.

- [1] Klawitter M., et al., "Expression and regulation of toll-like receptors (TLRs) in human intervertebral disc cells", *Eur Spine J.* 2014.
- [2] Krock E., et al., "Toll-like Receptor Activation Induces Degeneration of Human Intervertebral Discs", *Sci rep.* 2017
- [3] Cazzanelli P., Wuertz-Kozak K., "MicroRNAs in Intervertebral Disc Degeneration, Apoptosis, Inflammation, and Mechanobiology", *Int J Mol Sci.* 2020

Development of a Robust Intervertebral Disc Degeneration Model in-vitro Using Surgical Disc Specimen

Jennifer Gansau¹, Andrew C Hecht¹, Saad Chaudhary¹, James C Iatridis¹

1. Icahn School of Medicine at Mount Sinai, New York, NY, United States

INTRODUCTION: Chronic inflammation is a major feature of intervertebral disc degeneration (IVDD)¹ that contributes to back pain. TNF α , a key regulator of pro-inflammatory cytokines is increased in IVDD and often used to initiate the painful IVDD degenerative conditions in various models.^{1,2} However, TNF α alone underrepresents the cocktail of cytokines released from degenerated IVDs which are not well-characterized.^{1,3,4} This study quantified inflammatory cytokines in IVD tissues isolated from surgical patients, and then developed an in-vitro human AF cell culture model that recapitulates the clinical IVDD conditions by treating target AF cells with conditioned media (CM) generated from anterior discectomy and fusion (ADF) surgical IVD tissues as compared to TNF α . We hypothesized that CM is comprised of multiple pro-inflammatory cytokines that will initiate a robust IVDD phenotype in-vitro.

METHODS: IVD specimen collected from ADF patients were cultured to generate conditioned media (ADF-CM), which was analyzed using a 48-Plex inflammatory cytokine array. Human AF cells isolated from these subjects were divided into groups with the following conditions: i) Basal ii) TNF α supplementation (TNF) and iii) CM and analyzed for cell proliferation/morphology, metabolic activity and gene expression. Statistical differences were analyzed using ONE-WAY ANOVA with Tukey's post-hoc test ($p \leq 0.05$).

RESULTS: CM had significantly higher levels of several IVDD and pain related cytokines including TNF α , RANTES, IL-6 and the angiogenic marker VEGF) (**Fig. 1**) as well as 26 additional inflammation-related cytokines (not shown). CM challenged AF cells showed substantially reduced cell numbers and formation of long stress fibers and debris from dead cells within the media (**Fig. 2A**). MTT quantified these findings by showing a significantly reduced optical density (OD) of AF cells in CM indicating greatly reduced cellular metabolic activity, and consistent with cell damage and death observed on imaging (**Fig. 2B**). AF cells cultured in CM showed a significant downregulated expression of *Col1a1* and an upregulation of *Acan* (**Fig 3A**) and somewhat increased pro-inflammatory cytokines *IL-1 β* ($p=0.0872$), *IL-6* ($p=0.1160$) and *Tnf α* ($p=0.1065$) compared to basal (**Fig 3B**).

DISCUSSION: This study demonstrates that ADF-CM contains a cocktail of cytokines related to IVDD and pain. ADF-CM induces significant changes in cell proliferation, metabolic activity and gene expression on challenged AF cells that were substantially larger than TNF α alone and may more closely mimics IVDD microenvironment conditions. Therefore, many more factors than TNF α need to be considered when trying to mimic IVDD. The significantly reduced relative OD, elongated stress fibers and cellular debris demonstrates cell death from ADF-CM indicated that target AF cells are unlikely to recover after 3 days of CM treatment and suggests this human IVDD culture model can be titrated down to have lower duration and/or concentration. Importantly, AF cells from ADF tissue, once isolated were able to recover in basal conditions, suggesting rescue of these native AF cells may be possible if the challenge of these multiple cytokines can be managed. In conclusion, we established an in-vitro model using surgical ADF-CM that promotes a robust IVDD phenotype on target cells for prevention screening or treatment screening after optimizing severity of the model

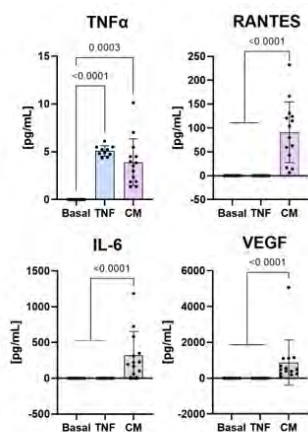


Fig. 1: Media analysis showing higher levels of inflammatory cytokines in CM

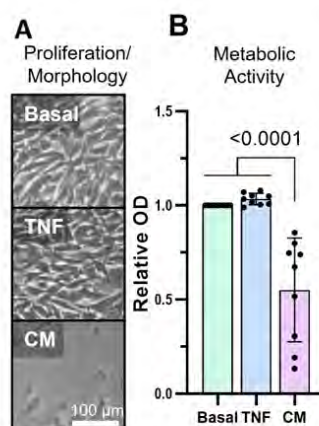


Fig. 2: Assessment of (A) cell proliferation and morphology (B) metabolic activity using MTT.

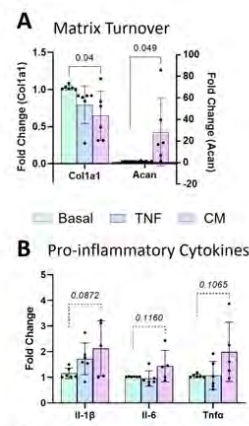


Fig. 3: Gene expression analysis of genes related to (A) matrix turnover and (B) Pro-inflammation

1. Risbud+ Nat Rev Rheumatol. 2014,
2. Lai+ J Orthop Res. 2015
3. Purmessur+ Arthritis Res Ther. 2008
4. Khan+ Ann N Y Acad Sci. 2017

Protective roles of Atg5-dependent autophagy against human and rat disc cellular apoptosis and senescence: an *in-vitro* and *in-vivo* loss-of-function study

Yoshiki Takeoka¹, Yutaro Kanda¹, Takashi Yurube¹, Masaaki Ito¹, Ryu Tsujimoto¹, Yuji Kakiuchi¹, Kunihiro Miyazaki¹, Hiroki Ohnishi¹, Tomoya Matsuo¹, Masao Ryu¹, Zhongying Zhang¹, Ryosuke Kuroda¹, Kenichiro Kakutani¹

1. Orthopaedic Surgery, Kobe University Graduate School of Medicine, Kobe, Hyogo, Japan

INTRODUCTION: The intervertebral disc is the largest avascular, low nutrient organ. Autophagy is an important cell survival mechanism by self-digestion and recycling damaged components under stress, primarily nutrient deprivation. We hence hypothesized that resident cells would utilize autophagy to cope with the harsh disc environment. However, pharmacological autophagy inhibitors elicit effects through modulating intracellular signaling or lysosomal acidification, thereby including multiple confounders. Our objective was to clarify specific roles of autophagy in *in-vitro* human and *in-vivo* rat disc homeostasis through RNA interference (RNAi)-mediated knockdown of autophagy-related gene 5 (Atg5), essential for autophagy.

METHODS: In human disc nucleus pulposus cells collected during lumbar interbody fusion surgery ($n = 25$: age, 63.0 ± 5.3 years old; 8 males and 17 females; Pfirrmann degeneration grade, 3.4 ± 0.2), autophagy inhibition by RNAi of Atg5 was tested. Cell viability with levels of autophagy including Atg5 expression, apoptosis, and senescence was assessed under serum starvation and/or pro-inflammatory interleukin-1 beta (IL-1 β) stimulation. In rat tail disc tissues ($n = 28$, 12 weeks old, all males), autophagy was monitored following Alexa Fluor® 555-labeled Atg5-small interfering RNA (siRNA) injection. Furthermore, radiographical and histological disruption with the incidence of apoptosis and senescence induced by 24-h temporary static compression at 1.3 MPa was observed for 56-d time-course. The paired *t*-test or one-way repeated measures or two-way analysis of variance with the Tukey–Kramer post-hoc test was used.

RESULTS: [In-vitro study] In human disc cells, Western blotting showed that serum deprivation and IL-1 β stimulation increased autophagy marker LC3-II and decreased autophagy substrate p62/SQSTM1, indicating enhanced autophagy. Then, multiple Atg5 siRNAs with different sequences consistently suppressed autophagy through decreases in Atg5 protein (26.8–27.4%, $P < 0.0001$). Cell viability was kept by Atg5 RNAi in serum-supplemented media (95.5%, $P = 0.28$) but reduced in serum-free media (80.4%, $P = 0.0013$) with IL-1 β (69.9%, $P = 0.0008$). Moreover, Atg5 RNAi accelerated IL-1 β -induced increases in expression of apoptosis and senescence markers in Western blotting, TUNEL staining, and SA- β -gal staining. Meanwhile, Atg5 RNAi less affected IL-1 β -induced catabolic MMP-3 and MMP-13 release, down-regulated anabolic *aggrecan* and *Col2a1* gene expression, and MAPK-pathway activation. [In-vivo study] In rat tail discs, immunofluorescence detected intradiscal signals for the Alexa Fluor® 555-labeled Atg5 siRNA at 2-d, 28-d, and even 56-d post-injection. Western blotting also found 2-d, 28-d, and 56-d autophagy suppression with Atg5 knockdown ($P = 0.003$ – 0.03). Under 24-h temporary static compression, Atg5 siRNA-injected loaded discs presented up to 56 d radiographic height loss ($P = 0.001$ – 0.03), histomorphological damage ($P = 0.0003$ – 0.002), and increased immunofluorescent positivity for apoptotic TUNEL and senescent p16/INK4a ($P < 0.0001$).

DISCUSSION: This *in-vitro* and *in-vivo* loss-of-function study findings suggests that Atg5-dependent autophagy primarily protects against human and rat disc cellular apoptosis and senescence rather than extracellular matrix catabolism. Then secondarily, enhanced cell survival by autophagy could favorably contribute to the maintenance of disc homeostasis under long-term stress conditions. Autophagy is thus a potent new molecular therapeutic target for intervertebral disc disease.

Is there any association between preoperative MRI disc characteristics and back pain at 1-year follow up in surgically treated lumbar disc herniation patients?

Kerstin Lagerstrand^{1,2}, Emil cedergardh¹, Christian Waldenberg^{1,2}, Hanna Hebelka^{1,3}, Helena Brisby^{1,4}

1. Inst. of Clinical Sciences, Sahlgrenska Academy, Gothenburg University, Gothenburg, Sweden

2. Dept. of Radiation Physics, Sahlgrenska University Hospital, Gothenburg, Sweden

3. Dept. of Radiology, Sahlgrenska University Hospital, Gothenburg, Sweden

4. Dept. of Orthopaedics, Sahlgrenska University Hospital, Gothenburg, Sweden

Introduction

Lumbar disc herniation (LDH) is a common condition with considerable impact on individual's everyday life. In general, surgical treatment of disc herniation leads to fast leg pain-relief and a majority (75%) of the patients are satisfied with the surgical outcome (1). However, some patients experience continuous back pain and later undergo surgical procedures for their back pain problem, as fusion or disc prosthesis surgery. Our hypothesis was that preoperative characteristics on magnetic resonance imaging (MRI) representing a more degenerated disc would be associated with poorer outcome after surgery. The aim here therefore was to study if there was any association between preoperative IVD characteristics on MRI and back pain and back pain related disability 1-year postoperatively.



Figure 1: Semi-automated segmentation of a disc with a herniation (L5-S1) on T2-weighted magnetic resonance images, using MATLAB software R206a

Methods

A total of 375 patients that had undergone lumbar disc herniation surgery at one hospital and been registered in the Swedish national spine surgery register (Swespine) 2012-2017 were identified. All patients with registered 1 year follow-up patient reported outcome measure (PROM) questionnaires (NRS, ODI, Global assessment (GA)) in Swespine and where the preop MRI could be localized were included in the study, n=218. Based on each of the 1-year reported PROM's patients were divided into two groups: "unsuccessful" or "successful" PROM's. On the MRI each herniated IVD was outlined on three consecutive T2-weighted midsagittal slices using semi-automated segmentation (Fig 1) and the mean signal intensity (MSI), standard deviation of signal intensity (SDSI) and SDSI/MSI of the midsagittal part of the IVD were calculated for the groups of patients. Further, to evaluate regional characteristics, each IVD was divided into 5 equally sized subregions, region of interest (ROI), based on the total midsagittal length of the IVD, ranging from 1 (anterior) to 5 (posterior). The different signal intensity measures between patients with "successful" versus "unsuccessful" surgical outcome were compared.

Results

The study population (n=218) had a mean age of 42.4 years at the time of surgery and consisted of 51.8% women. At 1-year follow-up they reported mean NRS back 2.9 (SD 2.7), and mean ODI 21.6 (SD 19.6). Descriptive statistics of the dichotomized groups based on PROM's are described in Table 1. No statistically significant differences in signal intensity measures of the midsagittal part of the IVDs were found between the 1-year PROM outcome groups. The distribution of signal intensity measures (MSI, SDSI and SDSI/MSI) of the whole midsagittal part of the IVDs for the different groups are displayed in 2. For the subregion's (ROI 1-5), no significant difference was found, except for SDSI in ROI 4 (p=0.045) comparing the NRS outcome groups.

Discussion

This study could not prove any relationship between IVD characteristics and surgical outcome for most of the measurements. The only association found was for the SDSI of ROI 4 in the NRS back outcome group, where a small, but significant difference was detected. Based on the findings, the hypothesis could not be proven, implying that the disc characteristics measured here are not detailed enough and/or that experiencing continuous back pain after LDH surgery are multifactorial.

Table 1: Baseline characteristics of “successful” (Group 0), and “unsuccessful” (Group 1) surgery outcome groups based on; Numeric Pain Rating Scale (NRS) back, Global Assessment (GA) and Oswestry Disability Index (ODI).

		NRS back 1-year outcome		GA 1-year outcome		ODI 1-year outcome	
		Group 0	Group 1	Group 0	Group 1	Group 0	Group 1
		NRS ≤2	NRS >2	GA ≤2	GA >2	ODI ≤ 20	ODI > 20
Number of Patients		116	102	149	68	120	92
Age	Mean	43	42	43	41	41	43
	SD	16	15	17	14	16	15
Sex	Men (%)	56.0%	39.2%	49.7%	45.6%	55.8%	37.0%
	Woman (%)	44.0%	60.8%	50.3%	54.4%	44.2%	63.0%
Disc level*	L1-L2 (%)	0.9%	0.0%	0.7%	0.0%	0.8%	0.0%
	L2-L3 (%)	0.9%	1.0%	0.7%	1.5%	0.8%	1.1%
	L3-L4 (%)	6.0%	4.9%	7.4%	1.5%	7.5%	3.3%
	L4-L5 (%)	38.8%	45.1%	40.9%	42.6%	36.7%	47.8%
	L5-S1 (%)	53.4%	49.0%	50.3%	54.4%	54.2%	47.8%
BMI**	Mean	26.33	27.23	26.62	27.06	25.71	28.30
	SD	4.48	4.22	3.94	5.45	3.94	4.69
Smokers*** (%)		4.8%	16.7%	5.5%	21.7%	2.3%	18.8%

* Level of disc herniation.

** Body Mass Index (BMI) only reported in n=71 (33%) out of n=218 patients.

*** Smoking habits (at the time of surgery) only reported in n=78 (36%) out of n=218 patients.

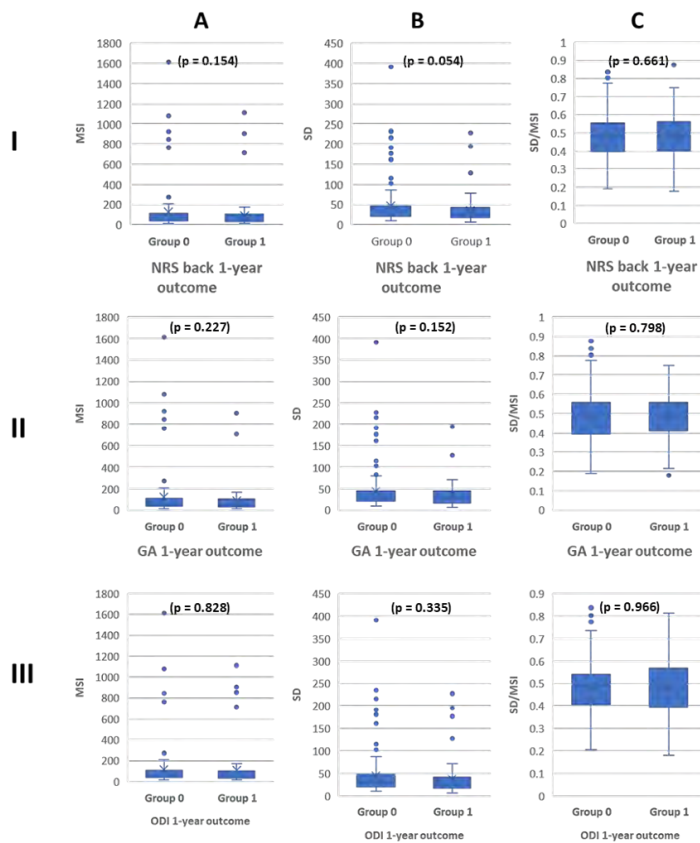


Figure 2: Boxplots showing the distribution of the measures; A - Mean signal intensity (MSI), B - Standard deviation of signal intensity (SDSI) and C- SDSI/MSI, and p-values between successful (Group 0), versus unsuccessful (Group 1) (Independent samples t-test), regarding (I) - Numeric Pain Rating Scale (NRS) back, (II) - Global Assessment (GA) and (III) - Oswestry disability index (ODI).

1. Fritzell P HO, Gerdhem P, Abbott A, Songsong A, Parai C, et al. 2018 Annual report - Follow up of spine surgery performed in Sweden in 2017. SWEDISH SOCIETY OF SPINAL SURGEONS. 2018.

Assessment of different nucleotomy techniques using ultra-high resolution MRI

Tamanna Rahman¹, Nicoleta Baxan¹, Robert T Murray¹, Saman Tavana¹, Thomas P Schaer², Nigel Smith³, Jonathan Bull⁴, Nicolas Newell¹

1. Imperial College London, London, United Kingdom

2. University of Pennsylvania School of Veterinary Medicine, Philadelphia

3. University College London, London, United Kingdom

4. BARTS Health NHS Trust, London, United Kingdom

Introduction

Nucleus pulposus replacement has the potential to be an early treatment for younger patients¹, who require a spinal surgery². The surgery involves removal (nucleotomy) and replacement of the native degenerated nucleus with a material designed to restore the segment's biomechanical properties. Multiple techniques have been considered for nucleotomy, but a detailed quantitative comparison of them is lacking. This study aims to compare three nucleotomy techniques: forceps, automated-shaver and laser.

Methods

Fifteen human (40 ± 13 years) vertebra-disc-vertebra lumbar specimens (Pfirrmann: 3 ± 1^3) were split into three groups of five, with each group assigned to a nucleotomy-technique. A posterolateral approach was used to insert 3mm-diameter forceps, an automated-shaver (Nucleotome®), and an 18G needle for laser-nucleotomy. The laser-nucleotomy followed methods reported in literature (1200J, 1s pulses at 10W). To compare changes in disc stiffness each specimen was axially compressed to 1kN (5 cycles at 1Hz) both when intact and after nucleotomy. T₂-weighted MRIs were acquired at 9.4T pre- and post-nucleotomy and used to quantify disc height change and volume of disc material removed.

Results

The automated-shaver group reported the largest reduction in disc height, with $13.15 \pm 1.63\%$ (9.13 ± 1.13 mm), compared to $6.57 \pm 1.23\%$ and $0.69 \pm 0.13\%$ from the forceps and laser groups, respectively. The automated-shaver and forceps removed similar volumes of disc material ($2.51 \pm 1.10\%$ and $2.76 \pm 1.39\%$, respectively), whilst the laser removed a considerably smaller volume ($0.12 \pm 0.07\%$). The automated shaver group had the smallest reduction in stiffness post-nucleotomy ($8.74 \pm 0.86\%$) while the forceps and laser groups had drops of $22.31 \pm 5.53\%$ and $15.93 \pm 4.49\%$, respectively. The automated-shaver removed the largest dry-nucleus mass, 0.25 ± 0.07 g compared to the 0.23 ± 0.01 g removed by the forceps, meanwhile, the laser removed 0.23 ± 0.04 g of wet-nucleus mass (dry-mass could not be calculated for this technique).

Discussion

The automated-shaver created more homogeneous cavities compared to forceps. Conversely, laser ablation formed localized cavities (Fig.1). The small volume of material removed, suggests that the laser-parameters used in this study are not suitable to ablate the large volumes that are required for nucleus-replacements without causing severe thermal damage. Optimising parameters such as power and frequency may however render the technique suitable. The damage to the annulus could not be fully quantified using the MRIs therefore, the change in disc stiffness was used as a marker to assess this effect^{4,5}. The automated-shaver removed similar masses of nucleus as the forceps, with the advantage of a smaller annulus incision and change in stiffness, suggesting that it may be the most appropriate technique to achieve nucleotomy for nucleus replacement surgery.

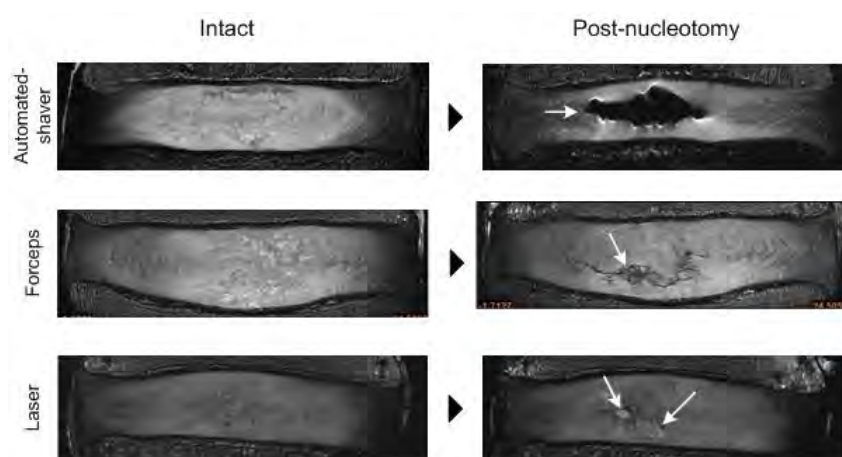


Figure 1. Left column shows intact MRI, and right column shows post nucleotomy MRIs. White arrows have been added to facilitate the identification of cavities

1. Coric et al., Neurosurgery Spine-8, 115–120 (2008).
2. Dang et al., Musculoskeletal Disorder-8, 1–4 (2007).
3. Pfirrmann et al., Spine-26, 1873–1878 (2001).
4. Iatridis et al., Biomechanics-38, 557–565 (2005).
5. Bezci et al., Biomechanical Engineering-137, 1–8 (2015).

Long-Term Nucleus Pulposus Replacement Mitigates Disc Degeneration in a Caprine Model

Rachel Hilliard¹, Harrah Newman², Adriana Barba¹, Leslie Brewer¹, Erik Brewer^{3,4}, Zachary Brown^{3,4}, Pete Wilson^{3,4}, Anthony Lowman^{3,4}, Dawn M Elliott², Thomas P Schaefer¹

1. New Bolton Center, University of Pennsylvania, Kennett Square, PENNSYLVANIA, United States

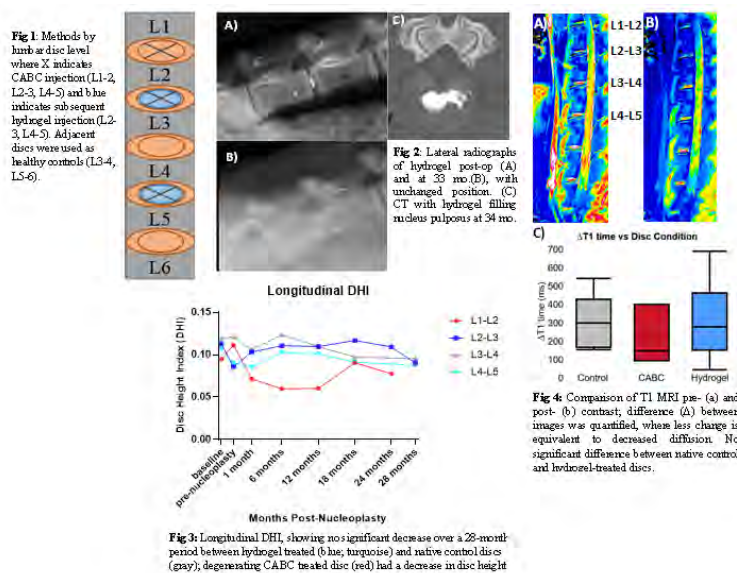
2. Biomedical Engineering, University of Delaware, Newark, DE, United States

3. College of Engineering, Rowan University, Glassboro, NJ, United States

4. ReGelTech Inc, Baltimore, MD, United States

Introduction: Lumbar intervertebral disc degeneration (IVDD) impacts up to 90% of the aged population, with > 25% of Americans reporting low back pain (1, 2). Early degenerative changes typically occur in the central nucleus pulposus (NP), where progressive dehydration from proteoglycan loss compromises mechanical function. Our team has developed a non-crosslinked injectable NP replacement hydrogel based upon a polyvinyl alcohol and polyvinyl pyrrolidone co-polymer, treated with polyethylene glycol to yield a thermally processible hydrogel with 59-66% water. The objective of this study was to use chondroitinase ABC (CABC) to induce IVDD through degradation of NP proteoglycans (4) and then treat with our injectable hydrogel.

Methods: Three adult goats (50-80kg) underwent intradiscal injection of 1.5U CABC to induce IVDD at levels L1-2, L2-3, and L4-5(4). Two weeks later, the degenerated NP was replaced with injectable hydrogel under fluoroscopic guidance (Fig. 1) in levels L2-3 and L4-5; level L1-2 served as an untreated degenerated control (CABC) and level L3-4 served as a native negative control. All animals recovered uneventfully and were maintained in a 20x30ft pen for 2.5-3-years. Animals were evaluated daily for pain, lameness, and neurologic deficits. Monthly standing lateral radiographs were used to calculate disc height index (DHI) through MatLab (5). After 2.5-3 years, contrast-enhanced MRI at 3T was performed to obtain T1 maps before and 30 minutes post-administration of 0.1 mmol/kg gadodiamide to assess trans-endplate small molecule diffusion, which is shown to be reduced with progressive end plate ossification seen in IVDD (6,7).



Results: After a minimum of 2.5 years, 4 of 6 hydrogels injected remained in the IVD (Fig. 2). In one animal, delivery assembly malfunction during injection caused dorsal rupture of the annulus fibrosus (AF) and hydrogel leakage into the vertebral canal. One hydrogel migrated laterally into the surrounding soft tissue at 20 months post-operatively. No lameness or neurologic deficits were observed. Longitudinal DHI showed hydrogel-treated discs maintained the same height as non-degenerated discs (Fig. 3). Contrast-enhanced T1 MRI revealed no difference in end-plate diffusion between hydrogel-treated and native discs. However, there was a reduction in T1 relaxation time change from pre- to post- contrast injection when comparing native discs to CABC only discs, suggesting that small molecule trans-endplate diffusion was reduced in untreated degenerating discs (Fig. 4).

Discussion: Taken together, our clinical findings demonstrate that hydrogel NP replacement mitigates disc degeneration and end-plate changes in an animal model of IVDD. These results are promising in support of minimally invasive injectable therapies for hydrogel-augmentation in early-onset human IVDD. This study has a small sample size, making statistical differences difficult to detect given the heterogeneity of measurements. Ongoing work is focused on increasing sample size and performing correlations across quantitative measures of native, hydrogel treated, and untreated degenerating discs (CABC).

1. Cheung+ Spine 2009
2. Deyo+ Spine 2006
3. Shankar+ Tech. Reg. Anesth. Pain Manag. 2009
4. Gullbrand+ Osteoarthr. Cartil. 2017
5. Akeda+ BMC Musculoskelet. Disord. 2015
6. Ashinsky+JBMR, 2020
7. Moore Eur. Spine J. 2006

Machine learning analysis of spinal movements to differentiate chronic low back pain

Spencer Baker¹, Kelsey Clark², Anton Bowden¹, Ulrike Mitchell², David Fullwood¹

1. Mechanical Engineering, Brigham Young University, Provo, Utah, United States

2. Exercise Science, Brigham Young University, Provo, Utah, United States

Introduction: Low back pain is prevalent and severe, yet difficult to treat. Chronic low back pain (cLBP) – is particularly challenging, in that both the source of the pain, as well as its severity may be multifactorial and patient-specific, depending on various aspects of the patient's psychological and social status, biological factors, and previous injury history [2]. One promising area of research is the use of changes in patient motion patterns to biomechanically phenotype different sources of low back pain. To this end, previous studies have attempted to differentiate between subjects with and without cLBP through quantitative analyses of spinal motion with promising results. The eventual goal of this study is to apply the same process to differentiate more specific motion characteristics, likely at the segmental level, and then to objectively track treatment progress by means of return to healthy biomechanical function. The purpose of this research is to continue the analysis of healthy and symptomatic spinal motion by including additional features of interest and a broader range of functional movements to determine which features statistically differ between healthy and cLBP subjects and how well those features detect cLBP.

Methods: Data were collected from 25 subjects (10 healthy and 15 with cLBP) as they performed a variety of single planar and functional movements with inertial measurement units (IMUs). The IMUs were placed on the sacrum, L4 spinous process, and C7 spinous process to record the subjects' angular velocity, acceleration, and jerk (the rate of change of acceleration) at each of these spinal levels. The motion features from each level for each movement were grouped by health status (healthy and cLBP) and tested for statistical significance differences between group means using t-tests analyses (a p-value of 0.05 or less was considered statically significant). Additionally, a classification machine learning model was developed using a k-nearest neighbor algorithm to predict subject health status.

Results: The t-tests revealed statistically significant differences between the healthy and cLBP motion features during several functions, especially for the L4 spinous process velocity and jerk. Figure 1 shows example data for a single activity (Flexion+Left Axial Rotation). The machine-learning model was able to predict subject health with 76% accuracy. The model was evaluated with a 10-fold cross validation using an optimized k-value of 5. Additional subject data will be useful for further model refinement and testing.

Discussion: Our results indicate that spinal kinematic information, specifically velocity and jerk during functional movements, clearly differentiates between healthy and cLBP subjects. We hypothesize that with a higher sample size and more detailed phenotyping information, kinematic information may also be used to identify specific sources of pain and treatment paradigms for cLBP patients.

Acknowledgements: This research was supported by NIH grant UH3AR076723.

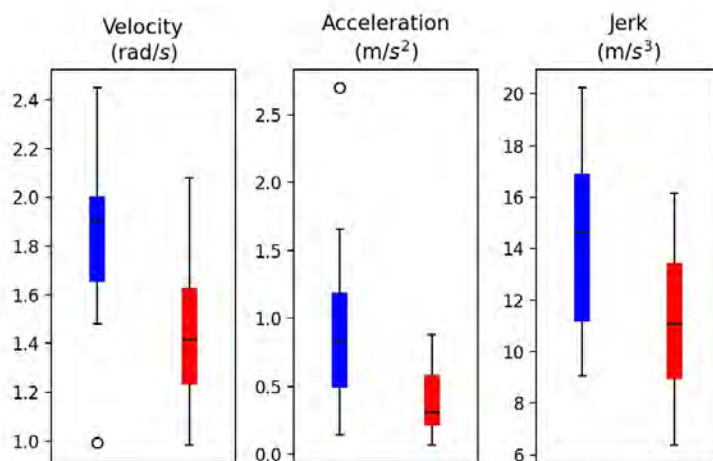


Figure 1: Summary of the maximum velocity, acceleration, and jerk data collected from the C7 spinous process during the Flexion Left functional movement. Blue plots represent data collected from healthy subjects; red plots represent data collected from cLBP subjects.

1. G.B.J. Anderson, "Epidemiological features of chronic low-back pain," *The Lancet*.
2. W.S. Marras et al., "The quantification of low back pain disorder using motion measures: Methodology and validation" *Spine*
3. G. Christie et al., "Multi-segment analysis of spinal kinematics during sit-to-stand in patients with chronic low back pain" *J. of Biomechanics*

Validation of an automated, artificial-intelligence-based system for grading radiological features of degeneration on MRIs of the lumbar spine

Alexandra Grob¹, Markus Loibl¹, Amir Jamaludin², Jeremy CT Fairbank³, Sebastian Winklhofer⁴, Tamas F Fekete¹, Daniel Haschtmann¹, Frank S Kleinstück¹, Dezső Jeszenszky¹, Francois Porchet¹, Anne F Mannion¹

1. *Schulthess Klinik, Zürich, Switzerland*

2. *Department of Engineering Science, University of Oxford, Oxford, UK*

3. *Nuffield Department of Rheumatology, Orthopaedics and Musculoskeletal Sciences, University of Oxford, , Oxford, United Kingdom*

4. *Department of Neuroradiology, Clinical Neuroscience Center, University Hospital Zurich, Zurich, Switzerland*

INTRODUCTION Magnetic resonance imaging (MRI) is used to detect degenerative changes of the lumbar spine. SpineNet (SN), a computer vision-based system, performs an automated analysis of degenerative features in MRI scans aiming to provide high accuracy, consistency and objectivity (1). This study aimed to externally validate SN's ratings against those of an expert radiologist.

METHODS MRIs of 882 patients (mean age, 72 ± 8.8 years) with degenerative spinal disorders from two previous trials carried out in our spine center between 2011 and 2019, were analyzed by an expert radiologist. Lumbar segments (L1/2 – L5/S1) were graded for Pfirrmann Grading (PG), Spondylolisthesis (SL) and Central Canal Stenosis (CCS). SN's analysis for the equivalent parameters was generated. Inter-rater agreement was analyzed using kappa coefficients and Spearman correlation (Rho) coefficients and class average accuracy (CAA).

RESULTS 4410 lumbar segments were analyzed. Depending on the vertebral level in question, kappa statistics showed moderate to substantial agreement between the radiologist and SN for **PG** (range for kappa, 0.63-0.77 (all vertebral levels together, 0.72), CAA 45-68% (all levels together, 55%), Rho 0.64-0.79 (all levels together, 0.72)); slight to substantial agreement for **SL** (kappa 0.07-0.60 (all levels together, 0.63), CAA 47-57% (all levels together, 56%), Rho 0.13-0.64 (all levels together, 0.36)); and slight to substantial agreement for **CCS** (kappa 0.17-0.57 (all levels together, 0.60), CAA 35-41% (all levels together, 43%), Rho 0.32-0.74 (all levels together, 0.57). Considering all vertebral levels together, SN indicated more severe disc degeneration (PG) but less severe SL and CCS than did the radiologist ($p < 0.01$).

DISCUSSION SN would appear to be a robust and reliable tool with the ability to grade degenerative features such as PG, SL or CCS in lumbar MRIs with moderate to substantial agreement compared to the current gold-standard, the radiologist, and with kappa values for agreement comparable to those reported in the literature for interrater reliability between any two radiologists. It represents an effective and efficient alternative for analyzing MRIs from large cohorts for diagnostic and research purposes.

(1) Jamaludin, A., et al., ISSLS PRIZE IN BIOENGINEERING SCIENCE 2017: Automation of reading of radiological features from magnetic resonance images (MRIs) of the lumbar spine without human intervention is comparable with an expert radiologist. *Eur Spine J*, 2017. 26(5): p. 1374-1383.

A fresh look at the three-dimensional spinal alignment: an AI-based *big data* retrospective analysis

Fabio Galbusera^{2,1}, Tito Bassani², Andrea Cina²

1. Schulthess Clinic, Zurich, Switzerland

2. IRCCS Istituto Ortopedico Galeazzi, Milan

Introduction. The analysis of the spinal alignment in the standing posture has gained wide attention in the last years. Among the large available body of literature, several studies investigated the spinal alignment of cohorts of patients with adult spine deformities (ASD) as well as of young subjects suffering from adolescent idiopathic scoliosis (AIS). Biplanar radiography is the state-of-the-art imaging technique for such investigations, but its use in large studies is restricted by the substantial manual labour required for the three-dimensional reconstruction of the spinal anatomy necessary to calculate the radiographic parameters. Therefore, most studies tend to be limited to relatively small cohorts. The aim of this study is to analyze a large dataset of biplanar radiographs of 9823 non-operated subjects by employing an automated tool based on artificial intelligence, rather the labour-intensive manual reconstruction.

Methods. A deep learning model based on a convolutional neural network using a Differentiable Spatial to Numerical Transform (DSNT) top layer has been developed and used to determine the coordinates of 10 vertebral landmarks in the T1-sacrum region, as well as the hip centers. The model was used to process biplanar radiographs in standing of the full trunk of 9823 consecutive patients acquired between 2015 and 2018 and stored in the local imaging database of the institute. The coordinates of the landmarks were then used to calculate the value of several radiographic parameters (Cobb angle of scoliosis, spinopelvic parameters, lumbar lordosis, thoracic kyphosis, sagittal vertical axis, apex rotation in the transverse plane) and to perform a descriptive statistics analysis after stratifying the subjects based on the type of deformity (no deformity, AIS, ASD) and on age groups.

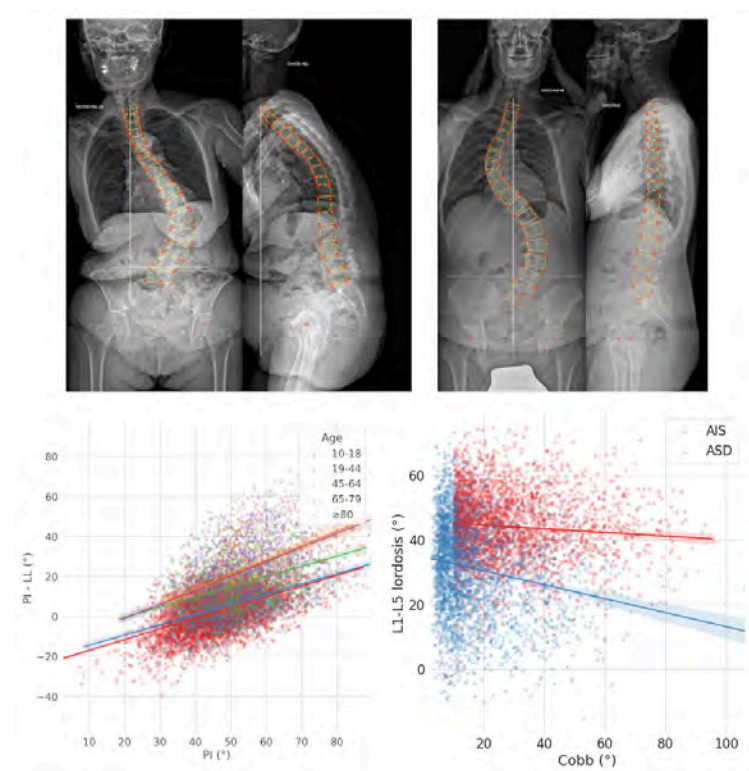


Figure caption. Biplanar radiographs of two exemplary patients with the corresponding vertebral landmarks detected by the automated deep learning tool (top); scatter and regression plots showing the correlations between pelvic incidence and the pelvic incidence–lumbar lordosis mismatch (bottom left) and those between the Cobb angle of scoliosis and the lumbar lordosis (bottom right).

Results. Among the 9823 patients, 3018 suffered from AIS, 2865 from ASD, and 3940 had no spinal deformities. The descriptive statistical analysis highlighted several findings not observed in previous smaller studies; for example, it could be shown that the pelvic incidence–lumbar lordosis mismatch clearly depends on the pelvic incidence itself regardless of the type and severity of spinal deformity, and that the lumbar lordosis decreases with increasing Cobb angles in both AIS and ASD patients, but more markedly in the latter case (Figure).

Discussion. The deep learning model allowed analyzing a very large database of biplanar spine radiographs, permitting for the first time a large-scale three-dimensional investigation of spinal deformities. Among the limitations of the study, it should be noted that information about the clinical indication for imaging was not available, and that the images were acquired in a raised-arm posture which may influence the radiographic parameters. In summary, the use of deep learning for large-scale studies has the potential to reveal clinically relevant information that does not emerge when smaller cohorts are investigated.

Augmented Reality-Assisted Spine Surgery: An Early Experience Demonstrating Safety and Accuracy with 218 screws

Fenil Bhatt¹, Lindsay Orosz², Anant Tewari², Rita Roy², Christopher Good¹, Thomas Schuler¹, Colin Haines¹, Ehsan Jazini¹

1. *Virginia Spine Institute, Reston, VA, United States*

2. *National Spine Health Foundation, Reston, VA*

Introduction: In spine surgery, screw guidance techniques continue to improve safety and accuracy while providing minimally invasive options and improved outcomes. Augmented reality (AR) is a novel technology to assist in screw placement and has shown promising results in early cadaveric and feasibility studies. This study aims to contribute an initial experience to the limited in vivo studies available by demonstrating safety and accuracy in the largest cohort of patients to date using ahead-mounted device (HMD) AR system.

Methods: Consecutive adult patients undergoing AR-assisted thoracolumbar fusion surgery between 2020-2021 with a minimum of 2 week follow-up were included in this multi-surgeon, single center prospective cohort study. Preoperative, intraoperative, and postoperative data were collected to include demographics, complications, revision surgeries, and AR performance. Intraoperative 3D imaging was used to assess screw accuracy using the Gertzbein and Robbins (G-R) grading scale.

Results: 32 patients (40.6% male) were included giving a total of 222 screws executed with the FDA approved HMD-AR system. Intraoperatively, 4 (1.8%) were deemed misplaced, and replaced freehand. The remaining 218 (98.2%) screws were placed accurately, there were no intraoperative adverse events or complications, and AR was not abandoned. Of the 208 AR-placed screws with 3D imaging intraoperatively, 97.1% were considered clinically accurate (91.8% Grade A, 5.3% Grade B). There were no postoperative surgical complications or revision surgeries during the 2 week follow-up.

Discussion: This early experience study demonstrated that HMD-AR assisted spine surgery is a safe and accurate method of placing pedicle, cortical, and pelvic fixation. An accuracy rate of 97.1% among all 3 surgeons novice to AR technology suggests ease of integration into the surgical workflow and minimal learning curve. Larger studies are needed to continue support this compelling evolution in spine surgery.

Detection intervertebral disc fissures in conventional MRI for clinical decision support using a combination of AI methods

Hanna Hebelka^{1,2}, Christian Waldenberg^{3,1}, Stefanie Eriksson^{3,1}, Helena Brisby^{1,4}, Kerstin Lagerstrand^{3,1}

1. Institute of Clinical Sciences, Sahlgrenska Academy, University of Gothenburg, Gothenburg, Sweden

2. Dept. of Radiology, Sahlgrenska University Hospital, Gothenburg, Sweden

3. Dept. of Radiation Physics, Sahlgrenska Academy, University of Gothenburg, Sweden, Gothenburg, Sweden

4. Dept. of Orthopaedics, Sahlgrenska University Hospital, Gothenburg, Sweden

Introduction Low back pain (LBP) is one of the most costly disorders worldwide [1]. Intervertebral disc (IVD) fissures in the outer annulus fibrosus (AF) are believed to be closely related to non-specific LBP [2]. Unfortunately, only a minority of these potentially painful fissures are identified in clinical routine magnetic resonance (MR) images [3]. New non-invasive methods for the detection of fissures have been developed, however, application of these in clinical settings is limited since they are restricted to in vitro measurements or high-field scanners and lack validation against rigorous reference standards [3-6]. This study aims to develop a clinically applicable method capable of determining the occurrence and position of annular fissures using only conventional MR images and artificial intelligence (AI) based techniques.

Methods A total of 123 IVDs in 43 patients (age 25-63 years, 19 male) suffering from chronic LBP were examined with T1- and T2-weighted conventional MR imaging, low-pressure discography and computed tomography (CT). Using textural features calculated from the MR images, an artificial neural network (ANN) classification model and a method for attention mapping of fissures were developed to identify the occurrence and position of fissures reaching the outer AF. The extension of the fissures was graded according to the Dallas Discogram Description (DDD) [7] using the CT-discograms. Since fissures in the outer AF have been suggested to be markers of LBP [8], IVDs with fissures extending to the outer AF (DDD=2 and 3) were sorted into one group and IVDs with no fissures or fissures not extending to the outer AF (DDD=0 and 1) were sorted into the second group.

Results The AI-based classifier correctly identified the occurrence of annular fissures in 122 of 123 IVDs (98.9% sensitivity/100% specificity) (Fig. 1). A receiver operating characteristic (ROC) analysis displayed an area under the curve (AUC) of 0.9996, indicating outstanding discriminating ability. The true position of the fissures was determined in 87% of the IVDs (Fig. 2). Inaccurately localized fissures were diffuse and/or non-delimitable fissures and, in the majority of cases, localized within noticeably degenerated IVDs.

Discussion: This is the first study utilizing a combination of texture analysis, ANNs and attention mapping to add invisible but important information within diagnostics. This classifier displayed outstanding discriminating ability and the vast majority of the attention maps determined the true location of the fissures but struggled with noticeably degenerated IVD with several fissures in both the posterior and anterior AF. However, IVDs in the late stages of degeneration have lost their biomechanical properties and viability and are considered more stable with impaired micro-mobility and, thus, less likely to give rise to pain sensations based on direct disc pathology. The novel method shows great promise and can be easily implemented to confidently detect the occurrence and position of potential painful fissures in conventional MR images. As such, it can be used to obtain unique insights into pathology, increase the diagnostic accuracy and allow for new non-invasive research in the clinical setting, both regarding spinal pathology and likely also within other images-based diagnostic areas.

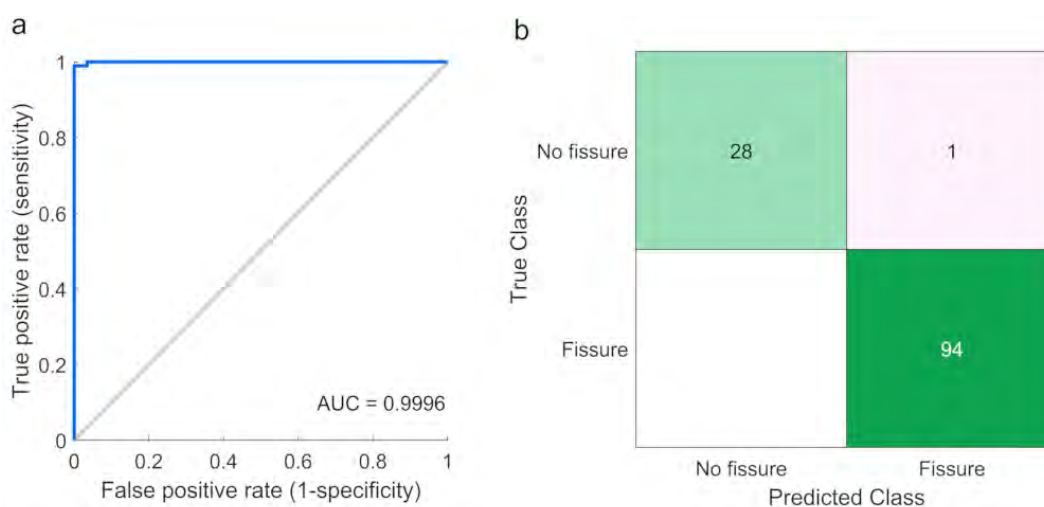


Fig. 1. a) Receiver operating characteristic (ROC) by logistic regression. Area under curve (AUC) value of 0.9996 was reached, indicating accurate diagnostic capability. b) Confusion matrix displaying the number of true positives (bottom right), true negatives (top left), false positives (top right) and false negatives (bottom left).

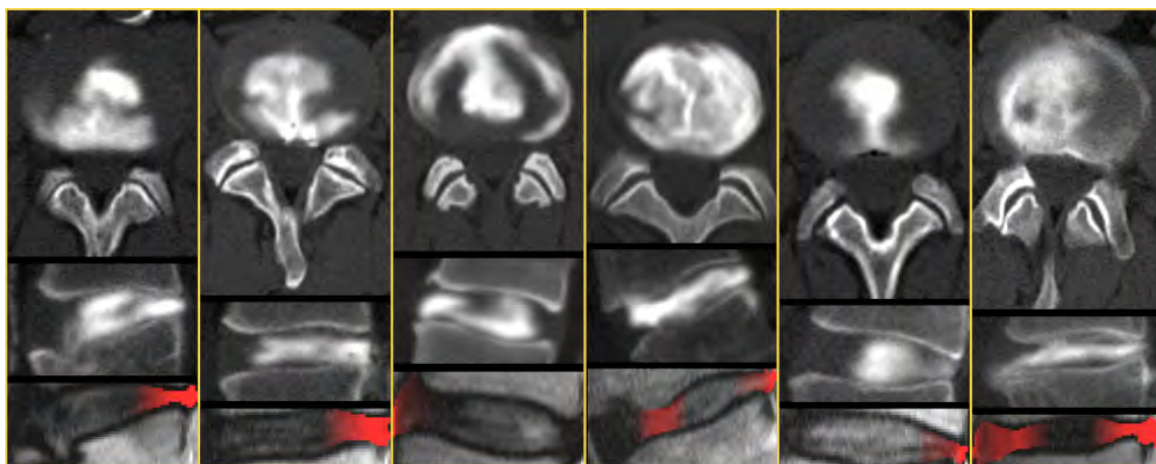


Fig.2. Representative examples of CT-discograms (top and middle) and the corresponding attention maps overlaid on a sagittal T2W MR image (bottom). The sagittal images display the posterior IVD on the right side. The figure displays instances where the attention maps correctly identify all outer annular fissures. The contrast media, injected into the NP (visible in white), spreads through annular fissures and their location is determined in the T2W MR image and highlighted in red.

1. Hoy, D., et al., The global burden of low back pain: estimates from the Global Burden of Disease 2010 study. *Ann Rheum Dis*, 2014. 73(6): p. 968-74.
2. DePalma, M.J., J.M. Ketchum, and T. Saullo, What Is the Source of Chronic Low Back Pain and Does Age Play a Role? *Pain Medicine*, 2011. 12(2): p. 224-233.
3. Berger-Roscher, N., et al., Intervertebral disc lesions: visualisation with ultra-high field MRI at 11.7 T. *European spine journal*, 2015. 24(11): p. 2488-2495.
4. Eldaya, R.W., et al., Evaluating the effect of a post-processing algorithm in detection of annular fissure on MR imaging. *European Spine Journal*, 2021.
5. Raudner, M., et al., Clinical implementation of accelerated T2 mapping: Quantitative magnetic resonance imaging as a biomarker for annular tear and lumbar disc herniation. *European Radiology*, 2021. 31(6): p. 3590-3599.
6. Deneuille, J.-P., et al., Quantitative MRI to Characterize the Nucleus Pulposus Morphological and Biomechanical Variation According to Sagittal Bending Load and Radial Fissure, an ex vivo Ovine Specimen Proof-of-Concept Study. *Frontiers in Bioengineering and Biotechnology*, 2021. 9(489).
7. Sachs, B.L., et al., Dallas discogram description. A new classification of CT/discography in low-back disorders. *Spine (Phila Pa 1976)*, 1987. 12(3): p. 287-94.
8. Peng, B., et al., The pathogenesis and clinical significance of a high-intensity zone (HIZ) of lumbar intervertebral disc on MR imaging in the patient with discogenic low back pain. *European Spine Journal*, 2006. 15(5): p. 583-587.

A 2-year longitudinal study of skeletal muscle mass in women over 40 years of age with degenerative lumbar scoliosis

Masaya Mizutani¹, Yawara Eguchi¹, Toyoguchi Toru², Sumihisa Orita¹, Kazuhide Inage¹, Yasuhiro Shiga¹, Seiji Ohtori¹

1. Orthopedic, Chiba University, Chiba

2. Orthopedic, Chiba Qiball Clinic, Chiba

[Purpose] Degenerative Lumbar Scoliosis (DLS) is increasing rapidly with aging. There are many cross-sectional studies showing the relationship between skeletal muscle loss and DLS, but there are no longitudinal studies. In this study, we investigated changes in skeletal muscle mass and bone mineral density in DLS patients during 2-year follow-up.

[Method] Of the 1596 women aged 40 and over (mean age 74 years, range 40-99) who underwent standing lumbar x-ray with measurement of body composition and bone mineral density, 418 women who could be observed for more than one year are included in this study. The study was divided into 50 patients in the DLS group (mean 76 years) and 368 patients in the control group (mean 73 years). The diagnosis of DLS was lumbar Cobb angle: 10 ° or more and SVA: 50 mm or more. Whole-body skeletal muscle mass was measured using a Bioelectrical impedance analyzer (BIA). Bone mineral density (BMD) was measured using DXA. Skin autofluorescence (SFA) was measured using a spectroscope AGE reader. Spinal alignment, skeletal muscle mass, BMD, grip strength, and SFA were examined in both groups, and the amount of change in Follow up (f/o) 1 year and 2 years from the initial examination for each item was compared in both groups.

[Results] Compared with the control group, the height, body fat mass, grip strength, upper limb muscle mass, and trunk muscle mass were significantly decreased, and the lumbar spine bone mineral density was significantly increased ($p < 0.05$). There was no significant difference in spinal alignment for 2 years at f / o in the DLS group ($p > 0.05$).

On the other hand, regarding the amount of change in each parameters during f/o 2 years between the two groups, the height decreased significantly in the DLS group (-0.9%) compared to the control group (-0.3%) in the f/o 2 years ($p < 0.05$). Trunk muscle mass decreased significantly in the DLS group (-2.8%) compared to the control group (-1.1%) at f/o 2 years ($p < 0.05$).

[Discussion] It has been reported that DLS has a high rate of sarcopenia and low trunk muscle mass is an age-independent risk factor. However, this is a cross-sectional study, and the mechanism of skeletal muscle loss and DLS progression is unclear. From this study, it was shown that the trunk muscle mass in the DLS group decreased significantly by about 2.5 times in 2 years compared with the control group. In DLS, trunk muscle atrophy is progressing due to a decrease in activity associated with kyphoscoliosis, and there is a possibility that a vicious cycle of kyphoscoliosis has occurred. In the future, it may be possible to clarify the mechanism of kyphoscoliosis progression by continuing large-scale longitudinal studies.

The cortical trajectory fixation versus traditional pedicle screw fixation in the treatment of lumbar degenerative patients with osteoporosis: a prospective randomized controlled trial

Hongtao Ding¹, Yuzeng Liu¹, Yong Hai¹

1. Beijing Chaoyang Hospital, Capital Medical University, Beijing, China

Objective

To elucidate the clinical and radiographic outcomes and complications of cortical bone trajectory (CBT) screw fixation in patients with osteoporosis at 24 months follow-up and to compare the results with those after transforaminal lumbar interbody fusion (TLIF) using traditional pedicle screw (PS) fixation.

Methods

We enrolled 124 patients and randomly assigned them to 2 groups (each group had 62 participants). The primary outcome: fusion rate, secondary outcome measures include 1) clinical outcomes: visual analog scale (VAS), Oswestry Disability Index (ODI), and Japanese Orthopaedic Association Score (JOA); 2) surgical parameters: operating duration, incision length, estimated blood loss, and drainage volume; 3) radiologic outcomes; 4) complications.

Results

At the 6- and 12-month follow-up points, similar fusion rate was observed based on CT scan in both groups ($p=0.583$ and 0.583). According to the clinical outcome, CBT provided significant better short-term functional status at 3 months post-operation regarding ODI and JOA score ($p=0.012$ and 0.000), and similar improvements in pain intensity and functional status at other follow-up point. In addition, CBT resulted in significantly better surgical characteristic. Notably, CBT fixation led to lower incidence of screw loosening in osteoporotic population ($p=0.006$).

Conclusions

The CBT screw fixation for single-level lumbar fusion in patients with osteoporosis provided improvement of clinical symptoms comparable to that of TLIF using PS fixation. In addition, statistically significant lumbar stability was found in the CBT group. Since the present study, we suggest CBT screw fixation to be a reasonable and superior alternative to PS in TLIF for osteoporotic population.

Trial registration number: ChiCTR1900022658

Date of registration: 2019/4/20

Innovative Percutaneous Endoscopic Transforaminal Lumbar Interbody Fusion of Lumbar Spinal Stenosis with Degenerative Instability: A non-randomized clinical trial

haifeng Gao¹, Jincai Yang¹, Yong Hai¹, Peng Yin¹

1. Orthopaedics, Beijing Chao-Yang Hospital, China Capital Medical University, Beijing, China

Purpose: Lumbar spinal stenosis (LSS) with instability is most common lumbar degenerative diseases for people with low back pain. The objective of this study was to compared the clinical effects for the treatment of Lumbar spinal stenosis (LSS) with degenerative instability between the innovative percutaneous endoscopic transforaminal lumbar interbody fusion (PE-TLIF) technique and posterior lumbar interbody fusion (PLIF) technique.

Patients and methods: Between April 2019 and April 2020, 114 patients with single-segment LSS were prospectively included in our study (ChiCTR1900022492). Visual Analogue Scale (VAS) on lumbar and leg pain (VAS-LBP, VAS-LP), Oswestry Disability Index (ODI), serum Creatine Kinase (CK), the maximal cross-sectional area of multifidus muscle (Max-CSA) and the peak intensity of Sulphur hexafluoride microbubble contrast agent (PI) around the surgical incision by contrast-enhanced ultrasonography were evaluated preoperatively, post-operatively and at regular follow-up.

Results: All patients were followed up. The VAS-LBP, VAS-LP, ODI after operation were improved significantly compared to these data before operation in all the patients ($P < 0.05$). The VAS-LBP at 1 weeks, 3 months after operation in PE-TLIF group were significantly lower than these in PLIF group ($P < 0.05$). The injury degree of multifidus muscle evaluated by MAX-CSA and PI was significantly less in PE-TLIF group after operation ($P < 0.05$). There was no significant difference on the complication rate between these two groups ($P > 0.05$).

Conclusion: Our results presented PE-TLIF technique could obtain comparable effective outcomes as conventional PLIF for the treatment of LSS with degenerative instability. The Patients with PE-TLIF had less muscle injury, less pain and quicker postoperative rehabilitation.

Keywords: pain, minimally invasive surgery; percutaneous; spinal endoscope; transforaminal lumbar interbody fusion; lumbar spinal stenosis.

Prevalence of lumbar scoliosis and its association with clinical symptoms -A large scale general population survey-: The Wakayama Spine Study-

Satoshi S.A Stashi Arita¹, Yuyu Y.Y Ishimoto¹, Hiroshi H.H Hashizume¹, Keiji K.N Nagata¹, Shigeyuki S.M Muraki², Hiroyuki H.O Oka³, Masanari M.T Takami¹, Shunji S.T Tsutsui¹, Hiroshi H.I Iwasaki¹, Yasutsugu Y.Y Yukawa¹, Toru T.A Akune⁴, Hiroshi H.K Kawaguchi⁵, Sakae S.T Tanaka⁶, Kozo K.N Nakamura⁷, Munehito M.Y Yoshida⁸, Noriko N.Y Yoshimura², Hiroshi H.Y Yamada¹

1. Department of Orthopaedic Surgery, Wakayama Medical University, Kimiidera, Wakayama City, Wakayama, Japan
2. Department of Preventive Medicine for Locomotive Organ Disorders, 22nd Century Medical and Research Centre, Faculty of Medicine, The University of Tokyo, Hongo, Bunkyo-ku, Tokyo, Japan
3. Department of Medical Research and Management for Musculoskeletal Pain, 22nd Century Medical and Research Center, Faculty of Medicine, The University of Tokyo, Hongo, Bunkyo-ku, Tokyo, Japan
4. Rehabilitation Services Bureau, National Rehabilitation Center for Persons With Disabilities, Tokorozawa City, Saitama, Japan
5. Department of Orthopaedics and Spine, Tokyo Neurological Center, Toranomon, Minato-ku, Tokyo, Japan
6. Department of Orthopaedic Surgery, Faculty of Medicine, The University of Tokyo Hospital, Hongo, Bunkyo-ku, Tokyo, Japan
7. Department of Orthopaedic Surgery, Towa Hospital, Towa Adachi-ku, Tokyo, Japan
8. Department of Orthopaedic Surgery, Sumiya Orthopaedic Hospital, Wakayama City, Wakayama, Japan

Objective

This study aimed to investigate the prevalence of radiographic lumbar scoliosis (LS) and its association with low back pain (LBP), leg symptoms, and quality of life (QOL) in the general population.

Methods

We used the baseline data of the Wakayama Spine Study performed in 2008-2013. LS was defined based on the presence of coronal curvature with a lumbar spine Cobb angle $\geq 10^\circ$ using radiographic anteroposterior X-ray analysis of T10-L5 spine in the standing position. Patients under 40 years of age. Those who had previously undergone lumbar surgery in the past were excluded from the study.

Results

Complete data of a total of 938 patients (307 male and 631 female, mean age 67.3 ± 12.4 years) were readily available. The prevalence of LS was estimated to be 23.9% among all patients, 14.4% in men, and 28.4% in women ($p < 0.001$). On the other hand, overall prevalence of LBP was found to be 39.6% among all patients, 48.0% in LS patients and 37.2% in non-LS patients ($p = 0.004$). Prevalence of leg symptoms were found to be 8.9% among all patients, 14.4% in LS patients, and 7.2% in non-LS patients ($p = 0.001$). Logistic regression analysis adjusted for age, sex, and body mass index (BMI) demonstrated significant correlation between LS and LBP (LS: odds ratio [OR], 1.43; 95% CI: 1.04–1.97). Logistic regression analysis adjusted for age, sex, and BMI demonstrated that LS was also significantly associated with leg symptoms (LBP: OR, 1.92; 95% CI: 1.16–3.15). Furthermore, the average ODI was estimated to be 15.0% in LS patients and 12.1% in non-LS patients, corresponding to a significant difference ($p = 0.011$). In addition, a significant difference in ODI was found between LS and non-LS groups (Q2; $p = 0.01$, Q3; $p = 0.03$, Q4; $p = 0.01$, Q6; $p = 0.01$, Q9; $p = 0.001$).

Conclusion

Based on this general population study, radiographic LS showed significant correlation with LBP, leg symptoms, and the ODI.

Facet joint osteoarthritis and low back pain: an epidemiological study in the community

Kenji Kobayashi¹, Koji Otani¹, Miho Sekiguchi¹, Ryoji Tominaga², Takehiro Watanabe¹, Shin-Ichi Konno¹

1. Orthopaedic Surgery, Fukushima Medical University, Fukushima City, Fukushima, Japan

2. Orthopaedic Surgery, Fukushima Medical University Aizu Medical Center, Fukuishima, Japan

【Introduction】

There are few detailed reports of facet joint osteoarthritis (FJOA) in epidemiological studies. The aim of this study was to evaluate the characteristics of individuals with FJOA and their association with low back pain (LBP) and LBP-related QOL using epidemiological data.

【Methods】

The subjects were 437 community residents (142 males and 295 females, mean age 65.0 years) who underwent lumbar spine MRI. FJOA from L1-L to L5-S using the Weishaupt classification (4 grades from 0-3) was evaluated and grade ≥ 2 was defined as FJOA. Furthermore, subjects underwent blood and urine sampling, blood pressure measurement to assess for hypertension, diabetes, hepatic and renal dysfunction. Arteriosclerosis was assessed by cardio-ankle vascular index (CAVI) and osteoarthritis (OA) of the hip and knee joints were evaluated by the ARA classification (Altman 1986, 1991). LBP was assessed with a self-administered questionnaire and defined as pain requiring treatment lasting at least 1 month. The Roland-Morris Disability Questionnaire (RDQ) was assessed with a norm-based score, and subjects with score less than 50 were considered to have low LBP-related QOL compared to national norm. We compared age, gender, BMI, prevalence of comorbidities, LBP, and RDQ <50 between the FJOA (+) and (-) groups. Chi-square test, Mann-Whitney U test, and multiple logistic regression analysis were used for statistical examination, and a p-value $< 5\%$ was considered statistically significant.

【Results】

A total of 225 subjects were enrolled, excluding those with compression fractures, scoliosis or degenerative spondylolisthesis. There were 179 (79.1%) subjects in the FJOA (+) group and 46 (20.9%) in the FJOA (-) group. Only age (66.6 ± 9.6 vs. 59.3 ± 14.7 , $p = 0.005$) was significantly different between the two groups. On the other hand, there were no significant differences in gender, BMI, or prevalence of any comorbidity: gender (male/female 0.62 vs 0.35 $p=0.12$), BMI (23.3 ± 3.1 vs 23.4 ± 3.5 , $p=0.84$) hypertension (53.6% vs 56.5%, $p=0.73$), diabetes (5.6% vs 0.0%, $p=0.10$), hepatic (34.6% vs 34.8%, $p=0.741$) and renal dysfunction (38.5% vs 41.3%, $p=0.99$), arteriosclerosis (33.6% vs 23.1%, $p=0.21$), and osteoarthritis of the knee (33.5% vs 26.7%, $p=0.38$) and hip (5.6% vs 8.7%, $p=0.442$). Finally, multiple logistic regression analysis adjusted for age, gender, and BMI showed no significant differences between FJOA and LBP (OR= 1.09, 95%CI: 0.37-3.15, $p=0.88$), RDQ <50 (OR=0.51, 95%CI: 0.24-1.12, $p=0.09$).

【Discussion】

In the present study, there was no association between FJOA and comorbidities, suggesting that FJOA may be an aging process or secondary to mechanical stress. Additionally, we found no association between FJOA and LBP or LBP-related QOL. Further evaluation of other spinal degenerative findings including intervertebral discs and longitudinal studies are needed to validate these results.

Natural history of the lumbar facet joint angle and onset of spondylolisthesis over 10 years

Takehiro Watanabe¹, Koji Otani¹, Kenji Kobayashi¹, Miho Sekiguchi¹, Shinichi Konno¹

1. Fukushima medical university, Fukushima City, FUKUSHIMA, Japan

INTRODUCTION

Sagittalization of the facet joints angle (FJA) has been suggested to be related to aging and lumbar spondylolisthesis by cross sectional studies. However, there have been no reports of long-term follow-up study for sagittalization of FJA evaluated by MRI in the community residents.

METHODS

This study included 294 participants (91 men, 203 women, mean age 64 years) with an age ranged from 28 to 91 years old in local residents in 2004. 120 of 294 patients received follow-up MRI in 2015. FAJ was measured in the axial image at each intervertebral disc level (L1/2-L5/S). Spondylolisthesis was defined as a vertebral body slipping more than 3mm on mid-line sagittal image. Statistical analysis was performed by Mann-Whitney U test and p values less than 0.05 were statistically significant difference.

RESULT

1. In 2004, the FJA tended to be larger in the lower intervertebral disc level and tended to be smaller at each intervertebral disc level with age. In the group with spondylolisthesis (n=57), FJA of slipped intervertebral disc level tended to be smaller than that of the same disc level in the group without spondylolisthesis (n=237).
2. In 2015, 27 patients (23%) (31 intervertebral disc level) showed the development of spondylolisthesis (L1/2: 1, L2/3: 3, L3/4: 7, L4/5: 15, L5/S1: 5). In the development of spondylolisthesis group, the average of FJA tended to increase in L1/2 and L2/3, and decrease in L3/4, L4/5 and L5/S compared with FJA in 2004, but there were no statistically significant differences.
3. In the new spondylolisthesis onset subjects, 13 intervertebral disc levels (42%) had remarkably decreased FJA ($\Delta FJA < -5^\circ$), while 7 joints (23%) had increased FJA ($\Delta FJA > 5^\circ$). These 7 intervertebral disc levels showed severe facet OA.

DISCUSSION

This study was the first to report the long-term course of FTJ. In this study, it was found that sagittalization of the facet joint progresses with age, regardless of the development of spondylolisthesis. Decreased FJA, which means sagittalization of the FJA, generally is thought to be essential for the development of spondylolisthesis, however, 23% of subjects with the development of spondylolisthesis showed increased FJA. This finding means that other factors except for sagittalization of FJA might have a strong influence on the development of spondylolisthesis. Further study is needed to determine the factors of the development of spondylolisthesis.

CONCLUSION

A tendency for sagittalization of FJA was observed over 10 years. However, in some cases with the development of spondylolisthesis, sagittalization was decreasing.

Central sensitization is a significant risk factor for the chronic low back pain

Hiroshi Hashizume^{1,2}, **Hiroyuki Oka**³, **Shingo Inoue**¹, **Seiji Kanno**¹, **Yuki Matsuyama**¹, **Takeru Ueno**¹, **Akimasa Murata**¹, **Yuusuke Kido**¹, **Mayumi Sonekatsu**¹, **Hidenobu Tamai**¹, **Takashi Shimoe**¹, **Ryo Taiji**¹, **Shizumasa Murata**¹, **Takuhei Kozaki**¹, **Masatoshi Teraguchi**⁴, **YOSHIO ENYO**⁴, **Yukihiro Nakagawa**⁴, **Nobuyuki Miyai**², **Hiroshi Yamada**¹

1. Dept. of Orthopaedic Surgery, Wakayama Medical University, Wakayama City, Wakayama, Japan

2. School of Health and Nursing Science, Wakayama Medical University, Wakayama, Japan

3. 22nd Century Medical and Research Center, The University of Tokyo Hospital, Tokyo, Japan

4. Spine Care Center, Wakayama Medical University Kihoku Hospital, Katsuragi, Wakayama, Japan

Purpose: To clarify the relationship between central sensitization and chronic low back pain (CLBP), we conducted a longitudinal survey under the spread of COVID-19 infection in Japan.

Methods: Invitations were sent to 771 people who participated in the baseline survey in July 2019 before the spread of the COVID-19 infection in rural areas in Wakayama prefecture, and 227 people (79 men, 148 women, average age at baseline 68.5 ± 9.5 years) who participated in the follow-up survey in October 2020 were included in the analysis. The main evaluation items were (1) presence or absence of CLBP (definition: low back pain that lasts for 3 months or more), (2) central sensitization screening tool: Central Sensitization Inventory (CSI). At the time of follow-up survey, we also asked about whether or not to refrain from going out due to the spread of COVID-19 infection.

Statistics: First, we observed changes in the prevalence of CLBP and CSI scores through the observation period. Second, the participants were divided into the following four groups and the baseline characteristics were compared among the groups; (1) "None group" did not have CLBP through the observation period, (2) "De novo group" did not have CLBP at baseline while it had CLBP at follow-up, (3) "Continued group" had CLBP through the observation period, (4) "Improved group" had CLBP at the baseline while it did not have CLBP at the follow-up. Third, a multiple logistic regression analysis was conducted to elucidate risk factors for the development of CLBP on 167 patients who did not have CLBP at baseline.

Results: The prevalence of CLBP were 59/227 (26%) at baseline and 71/227 (32%) at follow-up. The CSI score was 16.9 at baseline and 17.1 at follow-up. There were 131 participants (60%) in the None group, 32 (15%) in the De novo group, 39 (18%) in the Continued group, and 15 (7%) in the Improved group. There were no significant differences in gender, age, BMI at baseline, and whether or not to refrain from going out among the four groups. The baseline CSI score (mean) was 14.2 in the None group, 17.9 points in the De novo group, 22 points in the Continued group, and 20 points in the Continued group- a significant difference was observed between the None group and the Continued group. The multiple logistic regression analysis revealed that higher baseline CSI scores were a significant risk factor for the development of CLBP.

Conclusion: (1) After the spread of COVID-19 infection, the prevalence of CLBP increased. (2) Higher CSI score was a significant risk factor for the development of CLBP.

Sensory innervation by NETRIN1 from osteoclasts mediates spinal pain hypersensitivity in lumbar endplate Modic changes

Bao Huang^{1,2}, Zhi Shan^{1,2}, Fengdong Zhao^{1,2}

1. Department of Orthopaedics, Sir Run Run Shaw Hospital, Zhejiang University School of Medicine, Hangzhou, Zhejiang Province, China

2. Key Laboratory of Musculoskeletal System Degeneration and Regeneration Translational Research of Zhejiang Province, Sir Run Run Shaw Hospital, Zhejiang University School of Medicine, Hangzhou, Zhejiang Province, China

Introduction: Modic changes are usually associated with degenerative disc diseases (DDD) and vertebral endplate subchondral changes, which can be the major cause of discogenic low back pain. However, the sensory innervation, spinal hypersensitivity and underlying mechanisms remain still unclear. The presence and association of osteoclast and NETRIN1 in the endplate changes has not been well studied.

Methods: Firstly, we detected the osteoclasts, the expression of NETRIN1, and nerve ingrowth in the specimens from the human lumbar endplate Modic changes and *P. acnes*-induced rat lumbar. Secondly, to clarify *P. acnes*-associated pain, calcium imaging and flux was used to show the neuronal calcium traces from dorsal root neurons (DRGs) exposed to *P. acnes*. We then investigated whether NETRIN1 was derived from the osteoclasts by ELISA, Western Blot and immunofluorescence (IF) in vitro and in vivo. Further, we detected the calcitonin gene-related peptide (CGRP) or substance P-positive nerve fibers in lumbar endplates, and the c-Fos-positive neurons in lumbar DRGs in the *P. acnes*-induced animal model in vivo. Finally, by the subcutaneous injection of denosumab (5mg/kg), we examined the formation of osteoclasts and proceeded the pain assessment to observe the pain sensation in the *P. acnes*-induced model in vivo.

Results: By TRAP staining and IF assays, we firstly found the increased osteoclasts and NETRIN1 in *P. acnes*-induced rat lumbar and the human lumbar endplate Modic changes, especially type I Modic changes. Western blot and IF data showed that osteoclasts could secrete a large amount of NETRIN1 rather than NETRIN2 or NETRIN3, and TRAP/NETRIN1 were co-localized in vivo, indicating that NETRIN1 was derived from osteoclasts. By the co-culture system (20% conditioned medium), we clarified that osteoclast-derived NETRIN1 promoted the axon elongation of DRGs in vitro. Secondly, we detected the increased calcium and influx in the DRGs exposed to *P. acnes*, implying that *P. acnes* were positively associated with pain. Then, we discovered the increasing CGRP-positive nerve fibers in lumbar endplates and the c-Fos-positive neurons in lumbar DRGs in the *P. acnes*-induced animal model in vivo, compared to the control group. Further, we inhibited the in vivo formation of osteoclasts and revealed the less pain in the *P. acnes*-induced animal model with denosumab treatment. Finally, by IF assay, the CGRP or substance P-positive nerve fibers in lumbar endplates and the c-Fos-positive neurons in lumbar DRGs were decreased in the *P. acnes*-induced animal model with denosumab treatment. Sensory innervation by NETRIN1 from osteoclasts mediates spinal hypersensitivity in lumbar endplate Modic changes.

Discussion: Modic changes are strongly related with low back pain, especially type I Modic changes. Many researches showed the increased sensory innervation in lumbar endplate region, whereas its precise mechanism remained unknown. We showed the NETRIN1 from osteoclasts in lumbar endplate guided the axon elongation of DRGs to mediate spinal pain hypersensitivity. By denosumab management, CGRP-positive nerve fibers were suppressed in lumbar endplates. Meanwhile, c-Fos-positive neurons were reduced in lumbar DRGs. These data indicated that osteoclast might be the therapeutic target for lumbar endplate Modic changes.

Microbiome and bone marrow metabolism dysbiosis in Low Back Pain

Wentian Li¹, Ashish Diwan¹, Zhaomin Zheng¹, Abhirup Das¹

1. UNSW, Sydney, NSW, Australia

Introduction

Low back pain (LBP), a widely prevalent and costly disease around the world, is mainly caused by intervertebral disc (IVD) degeneration (IDD). Numerous factors may trigger this degenerative process, for example, aging, inflammation, genetic susceptibility and trauma. Modic changes (MCs) is one of disc degeneration. Research have found Modic changes were present in 46% of patients with chronic low back pain compared with only 6% of the general population. The pathological alteration of microbiome composition, also known as dysbiosis, has been associated with diseases linked to damaged bone metabolic disorders such as osteoarthritis, rheumatoid arthritis (RA), ankylosing spondylitis (AS), adolescent idiopathic scoliosis (AIS) and osteoporosis. However, the connection between the microbiome and MCs has not been well understood but is believed to happen through translocation of the bacteria across the gut epithelial barrier, regulation of the mucosal and systemic immune system, and regulation of nutrient absorption, metabolites formation at the gut epithelium. We believe that the microbiome has the potential to serve as a biomarker of IDD and a target for LBP treatment.

Methods

We performed a case–control study to compare the faecal microbiome of LBP with/without patients and healthy control by 16S ribosomal RNA (rRNA) sequencing and metagenomics. The overwhelming mass of research supports gut microbiome could produce some end products of fermentation, these products may enter our circulation system by blood and cause some influence on our physiology. The serum metabolome can provide the functional redout of the gut microbiome. So to address the causative relationship between gut dysbiosis and LBP, we also use the untargeted metabolomic methods to detect the serum metabolome.

Results

We identified 3 bacterial species showing notable differences in abundance between MDD patients and healthy controls (HCs). Patients with LBP+MCs were mainly characterized by increased abundance of the species are Erysipelotrichaceae bacterium and Eubacterium bioforme and decreased abundance of the species Ruminococcus torque. Besides, the metabolomics enriched 7 pathways, including Valine, leucine and isoleucine degradation, Nicotinate and nicotinamide metabolism, Sphingolipid metabolism, Amino sugar and nucleotide sugar metabolism, Neomycin, kanamycin and gentamicin biosynthesis, Porphyrin and chlorophyll metabolism, Drug metabolism - cytochrome P450. Disturbed microbial genes and serum metabolites were consistently mapped to Valine, leucine and isoleucine degradation metabolism. Our findings provide a deep insight into understanding of the roles of disturbed gut ecosystem in LBP with MCs.

Discussion

This study suggests that the gut microbiome of patients with LBP is dysbiotic and contributes to disease pathogenesis. More invitro works need to do for detecting the mechanism about microbiome and the development of MCs

Integrating 2D radiographs and 1D clinical data in the AI prediction of adolescent idiopathic scoliosis progression

Kenneth Chu¹, Jason Pui Yin Cheung¹

1. Department of Orthopedics and Traumatology, The University of Hong Kong, Hong Kong

INTRODUCTION

Adolescent idiopathic scoliosis (AIS) is the most common form of scoliosis, attributing to about 70% of all cases, and is usually diagnosed during puberty [1-3]. One can imagine a curved spine can detrimentally affect the patient's daily activities, quality of life and even cardiopulmonary function [4]. The progressive nature of AIS warrants an early diagnosis and treatment to prevent progression as soon as possible and to save the patient from more aggressive interventions. Many studies have investigated how structural deformity parameters, and even biomarkers, may contribute to the likelihood of AIS progression. [5-7] But no study has been done so far that utilizes a convolutional neural network (CNN) to combine information from raw two-dimensional (2D) radiographs and one-dimensional (1D) clinical parameters in the research of AIS progression prediction. Thus, **by using capsule network as a backbone [8], this study aims to develop a CNN model that is able to predict the probability of AIS progression at the patient's first visit by integrating 2D radiological images with 1D clinical data.**

METHODS

A total of 513 patients have been recruited with the exclusion of 43 patients due to lack of followup. Clinical parameters were recorded at specialist clinics and bi-planar radiographs of the full body were scanned with the EOS system.

Three different crops of the original radiographs are generated -- (1) whole-spine crop, (2) upper end vertebra crop of major curvature, and (3) lower end vertebra crop of major curvature, all of which are used as the 2D inputs of the CNN model.

The clinical parameters used in this study include sex, age, weight, sitting height, standing height, arm span, risser sign, ulna maturity and distal radius maturity. Categorical data are represented as 1D unit vectors, whereas numerical data are normalized to a number between 0 and 1. The processed vector then serves as the 1D input of the CNN model.

The presence of AIS progression is defined by a minimum increase of 5 degrees in the Cobb angle of the major curve, which can happen as soon as 2 months after the initial consultation. This definition is used to verify the predicted outputs from the CNN model.

RESULTS

The CNN model achieved a 92.6% sensitivity and 90.6% negative predictive value (NPV) with an overall accuracy of 72.8%. In addition, it also achieved 56.9% specificity and 63.3% positive predictive value (PPV). The ROC AUC is 0.76.

DISCUSSION

The high sensitivity and NPV make this AI model a great *screening* tool to exclude those without the risk of AIS progression. With a negative risk predicted by the model, treatment resources can then be spared and reassurance can be given to the patient. With a positive predicted progression risk, the specialist can decide to more closely monitor AIS progression of the patient by increasing the frequency of follow ups to significantly speed up the diagnosis and management of AIS progression and further optimize appropriate allocation of healthcare resources. Limitations of this study include a small data size and occasional missing clinical data.

Novel ultrasound applications for the characterization of adult lumbar intervertebral disc

Priscilla Galinié¹, Wafa Skalli¹, Camille Eyssartier¹, Christophe Sauret¹, Mickael Tordjman², Marie-Line Pissonnier², Robert Carlier², Claudio Vergari¹

1. Institut de Biomécanique Humaine Georges Charpak, Arts et Métiers ParisTech, Paris, France

2. Medical Imaging Department, Raymond Poincaré Hospital, Garches, France

Introduction

Ultrasound-based applications were recently developed to measure intervertebral disc (IVD) mechanical properties and its microstructure *in vivo* (Langlais et al., 2019; Vergari et al 2014). These are complementary evaluations to magnetic resonance imaging, which is the golden standard to assess IVD as it allows to quantify disc morphology and hydration, in addition to recent *in vitro* applications to determine IVD mechanical properties. However, ultrasound methods were limited to children because of poor ultrasound penetration in adult's abdominal region. Nevertheless, such non-invasive and fast evaluation in adults could allow defining novel biomarkers for early disc degeneration. In this work, feasibility and reliability of IVD characterization by ultrasound in adults were explored, which were made possible by the continuous development of ultrasound technology.

Methods

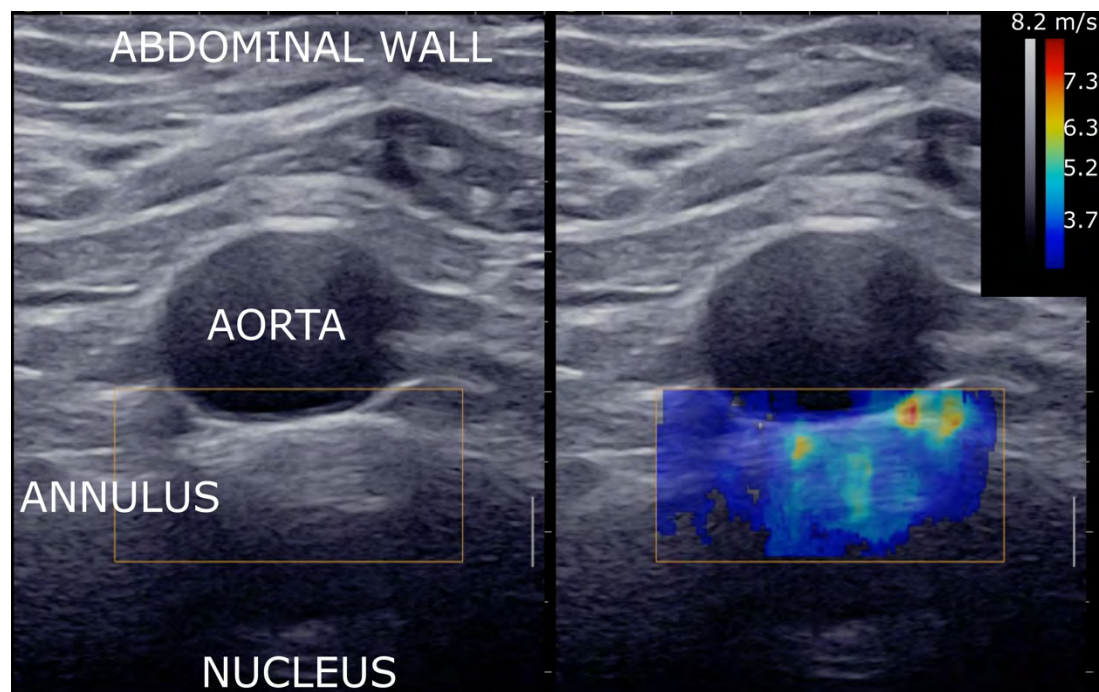
Conventional ultrasound images and SWE (Figure 1) were acquired at the L3-L4, L4-L5 and L5-S1 IVD of 28 asymptomatic adults (13 women and 15 men, age range: 22-67 years). Images were acquired with an abdominal approach with a Mach30 (Supersonic imagine, Aix-en-Provence). Shear wave speed (SWS) and lamellar thickness were measured in the outer annulus with previously described protocols (Langlais et al., 2019; Vergari et al 2014). SWS was measured at all disc levels, while lamellar thickness only at L3-L4. Three operators, one with a 7-year experience and two with a one-day training, repeated the measurements on L3-L4 IVD of 8 subjects to determine measurement reproducibility. Results are reported as median [75% confidence interval], and uncertainty is reported as standard deviation. Non-parametric statistical tests were used ($p < 0.05$).

Results

Inter-operator uncertainty of SWS was 8.7% (0.55 m/s), while uncertainty of lamellar thickness was 10% (24.7 μ m). SWS was similar at the L3-L4 and L4-L5 levels (4.0 m/s [3.5-4.3]) and significantly lower at L5-S1 (3.4 m/s [3.2-3.6]). Median lamellar thickness at L3-L4 level was 253 μ m \pm [245-269]. Lamellar thickness was significantly correlated to SWS at the same disc level ($p < 0.001$, Spearman's rho = 0.75).

Discussion

A measurement protocol which was previously limited to application in children, was successfully applied to assess lumbar discs in adults. Results are promising, showing good reproducibility in the assessment of IVD mechanical and microstructural properties. Indeed, SWS is directly related to disc material stiffness, and there results suggest a correlation between disc microstructure and mechanical properties. This provides complementary information to other imaging modalities to characterize the IVD. Further research is underway to study the aging and degeneration of IVD by ultrasound.



C. Vergari et al.(2014). Non-invasive biomechanical characterization of intervertebral disc by shear wave elastography. *European Radiology*, 24(12), 3210–3216.

1. T. Langlais et al. (2019). Microstructural characterization of annulus fibrosus by ultrasonography: a feasibility study with an *in vivo* and *in vitro* approach. *Biomechanics and Modeling in Mechanobiology*, 18, 1979–1986.

A novel technique for in vivo deformation and strain measurements in human lumbar intervertebral discs using 3T clinical MRIs

Saman Tavana¹, Julian Leong², Brett Freedman³, Nicolas Newell¹

1. Imperial College London, London, UK

2. Royal National Orthopaedic Hospital, London, UK

3. Mayo Clinic, Rochester, USA

Introduction: The intervertebral disc (IVD) transmits 80-90% of axial loads within the spinal column¹. The mechanical response of the IVD to load is an important indicator of the IVD health and pathology². In vivo evaluation of the IVD strains is crucial to better understand normal and pathological IVD mechanics, to investigate the effect of injuries on the mechanics of the IVD, and to evaluate the effectiveness of treatments. However, in vivo characterisation of IVD strains remained largely unexplored, likely due to the lack of a reliable and non-invasive strain measurement technique. The aim of this study was 1) to develop a novel in vivo technique based on 3T MRI and digital volume correlation (DVC) for non-invasive strain measurement within human IVDs and 2) to use this technique to resolve 3D strains within lumbar IVDs during extension.

Methods: This study included 20 lumbar IVDs from four healthy subjects (M/F: 2/2, average age 30 years, range: 27-34 years). In order to find an optimal MR sequence to minimise DVC measurement errors, one subject was scanned two times using 3T MRI with four different sequences: CISS, T1 VIBE, T2 SPACE, and T2 TSE. DVC errors were quantified by conducting zero-strain tests³ (two repeated unloaded scans). Based on the DVC measured errors, the optimal MRI sequence was selected. To assess the repeatability of the strain measurements in spines with different anatomical variations and compositions all subjects (n=4) were scanned two times with the optimal sequence, and accuracy and precision of the strain measurements were quantified. In addition, to calculate 3D strains during lumbar extension, MR Images were acquired from subjects in both the neutral position (Figure 1(a)), and after full extension (Figure 1(b)).

Results: DVC strain measurement errors were notably lower for the T2 TSE (0.33 %) in comparison with the CISS, T1 VIBE, and T2 SPACE (6.13, 6.98, and 2.05 %, respectively). The result of the repeatability study identified that DVC in combination with T2 TSE MRI is able to measure internal IVD strains with a precision of 0.33 ± 0.10 % and accuracy of 0.48 ± 0.11 % for a measurement spatial resolution of 4.64 mm. During lumbar extension, the site of peak maximum 3D principal (tensile) and shear strains were commonly observed at the anterior annulus (Figure 1(c)). Level L2-L3 experienced the largest peak tensile and shear strains (16.8 ± 0.4 % and 16.2 ± 2.4 %, respectively), while the L5-S1 level experienced the lowest peak tensile and shear strains (3.5 ± 0.1 % and 3.9 ± 0.2 %, respectively).

Discussion: The findings of this study establish clinical MRI based DVC (MRI-DVC) as a new tool for in vivo strain measurement within human IVDs. Medical imaging modalities that calculate tissue morphology alone cannot provide direct information regarding the biomechanics of the disc. MRI-DVC successfully provided internal strain distributions within IVDs and has great potential to be used for a wide range of clinical applications.

Acknowledgements: This work was supported by the EPSRC, New Investigator Award, EP/V029452/1.

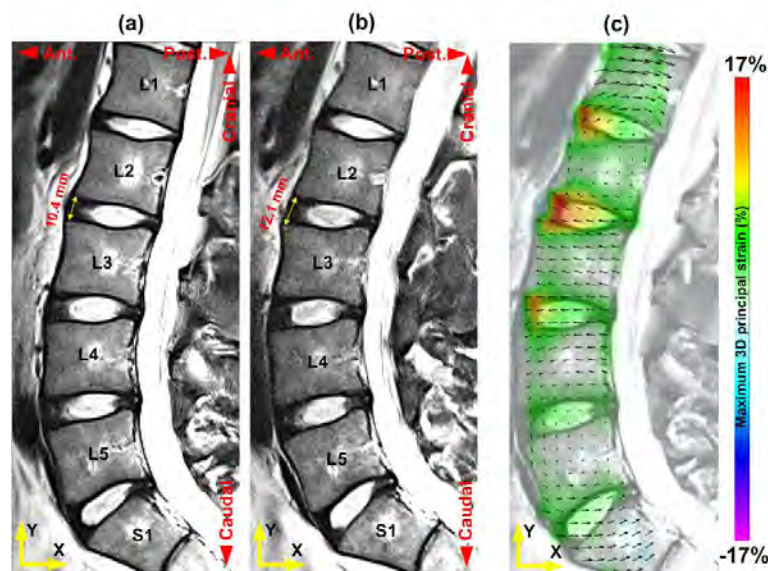


Figure 1 - The mid-sagittal MRI slice of a lumbar spine in a neutral (a), and extended (b) posture. The maximum range of lumbar spine motion that could be achieved comfortably within the MRI scanner was obtained using a T2 TSE sequence. The depicted images are from a 27-year-old male subject. The MRI slice, with superimposed maximum 3D principal strains during extension is shown in (c). Black vectors identify the total 3D displacement of different locations within the lumbar spine during neutral to extension movement.

1. Adams et al, J Bone Joint Surg Br, 62 (3), 358-62, 1980.
2. Tavana et al, Front. Bioeng. Biotechnol, 8:610907, 2021.
3. Liu et al, Journal of Biomechanics 40, 3516-3520, 2007.

Single-cell transcriptome profiling reveals multicellular ecosystem of nucleus pulposus during degeneration progression

Ashish Diwan¹, Ji Tu¹, Wentian Li¹, Jun Zou²

1. The University of New South Wales, Sydney, NSW, Australia

2. The First Affiliated Hospital of Soochow University, Soochow, China

Introduction: Low back pain is a major disabling health condition in humans, with a lifetime prevalence as high as 84%. IVDD is a widely recognized contributor to low back pain. The major constituents of the normal NP are type-II collagen and aggrecan proteoglycan. The loss of these extracellular matrix proteins occurs in IVDD. The current treatments of low back pain are limited to relieving back or leg symptoms. They do not focus on replenishing the NP loss and restoring the native disk structure. NPCs are the main cell type residing in the NP, and they are responsible for maintaining tissue homeostasis (8). NPCs proliferate slowly and lack self-regeneration capacity, adding to the intractability of the disease. Current studies on the pathophysiology of NPCs are usually supported by mRNA and epigenomic analyses. However, bulk-tissue level resolution masks the complexity of alterations across cells and within cell types. The uncharacterized cell types and markers residing in the NP raise interest in terms of unexplored cellular heterogeneity.

Methods: We aimed to provide a single-cell view of IVDD pathology, profiling 39,732 cells from NP tissues across eight individuals with different grades of progressive degeneration. Notably, we comprehensively characterized the transcriptome feature of NPCs and immune cells, and we decoded the cell percentage, the heterogeneity of cell subtypes during degeneration, providing a unique cellular-level insight into transcriptional alterations associated with IVDD pathology.

Results: Six novel human NP cell (NPCs) populations were identified by their distinct molecular signatures. The potential functional differences among NPC subpopulations were analyzed at the single-cell level. Predictive transcripts, transcriptional factors, and signal pathways with respect to degeneration grades were analyzed. We reported that fibroNPCs, one of our identified cell types, is the subpopulation for end-stage degeneration. CD90+NPCs were observed to be progenitor cells in degenerative NP tissues. NP-infiltrating immune cells comprise a previously unrecognized diversity of cell types, including granulocytic myeloid-derived suppressor cells (G-MDSCs). We uncovered integrin α M (CD11b) and oxidized low density lipoprotein receptor 1 (OLR1) as surface markers of NP-derived G-MDSCs. The G MDSCs were also found to be enriched in mildly degenerated (grade II and III) NP tissues compared to severely degenerated (grade IV and V) NP tissues. Their immunosuppressive function and alleviation effects on NPCs' matrix degradation were revealed in vitro.

Discussion: These findings might aid the understanding of molecular complexity and cellular heterogeneity in intervertebral disc degeneration. The IVDs have been identified as immune privilege organs; the steady-state of immune privilege is fundamental to organ homeostasis. This single-cell study also showed there are multiple immune cell lines inside the NP, which may play a role in IVDD progression.